

Pipe Wall Damage Morphology Measurement Methodology Development
for Flow Assisted Corrosion Evaluation

by

Julio Cesar Ferreira Rangel

B.S. Naval Architecture and Marine Engineering
University of Sao Paulo, Brazil (1991)

SUBMITTED TO THE DEPARTMENT OF NUCLEAR ENGINEERING
IN PARTIAL FULFILLMENT OF THE REQUIREMENTS
FOR THE DEGREES OF

NUCLEAR ENGINEERING
and


MASTER OF SCIENCE IN MATERIALS SCIENCE AND ENGINEERING

at the


MASSACHUSETTS INSTITUTE OF TECHNOLOGY
February, 1999

© 1999 Massachusetts Institute of Technology
All rights reserved

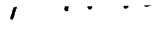
Signature of the Author _____

 _____
Department of Nuclear Engineering
January 15, 1999


Certified by _____

 _____
Ronald G. Ballinger
Associate Professor of Nuclear Engineering
Thesis Supervisor


Certified by _____

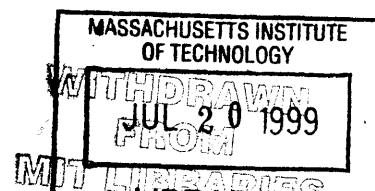
 _____
Ronald M. Latanision
Professor of Materials Science and Engineering
Thesis Reader

Accepted by _____

 _____
Lawrence Lidsky
Chairman, Department Committee on Graduate Students

Accepted by _____

 _____
Linn W. Hobbs
John F. Elliott Professor of Materials
Chairman, Departmental Committee on Graduate Students



Science

Pipe Wall Damage Morphology Measurement Methodology Development for Flow Assisted Corrosion Evaluation

by

Julio Cesar Ferreira Rangel

Submitted to the Department of Nuclear Engineering on January 15, 1999 in partial fulfillment of the requirements for the degrees of Nuclear Engineering and Master of Science in Materials Science and Engineering.

ABSTRACT

A new methodology has been developed that allows the evaluation of real-time local pipe thickness. The methodology was developed for application in the power generation industry where flow assisted corrosion (FAC) of carbon steel piping is a significant cause of increased maintenance and plant shut down time. The methodology is non-intrusive and remote reading and requires only that probes be attached to the outside on the pipe surface.

Local pipe thickness is determined by attaching probe wires to the outside of a piping section in a regular array. DC current is then passed through the pipe and the potential field is measured. The measured potential data is then operated on using the methods developed in this work to produce a thickness map for the inside wall of the pipe.

The pipe thickness measurement methodology development was carried out in two major phases. In the first phase the analytical solution was developed for the case where a known defect was present in a pipe section. The analytical solution to this "forward" problem was then verified using measurements taken from plate and then piping samples containing machined-in defects. In the second phase the analytical solution for the case where one starts only with the potential field data was developed. The solution to this "inverse" problem was obtained for plate and then piping sections with machined-in defects. Based on these results an algorithm was developed for pipe thickness mapping. In all cases the machined-in defects were such that 2D morphology was obtained.

The pipe thickness measurement method that has been developed is capable of detecting wall thickness reductions of 5% of nominal for a two-dimensional damage pattern. The methodology was then applied to the case where a three dimensional defect was present. In this case the defect was easily detected and localized within the piping. The error in minimum pipe wall thickness was less than 5% (relative) but defect morphology (shape) detection was significantly degraded. Further expansion of the analytical solution to 3D has been done but not tested.

Thesis Supervisor: Ronald G. Ballinger
Title: Associate Professor of Nuclear Engineering

ACKNOWLEDGEMENTS

I wish to express my sincere gratitude to Professor Ronald G. Ballinger for his technical guidance and patience throughout this work. I also would like to thank Professor Ronald M. Latanision who kindly accepted to be my thesis reader.

Special thanks are extended to Professor Jeffrey P. Freidberg for his restless and invaluable support in the math development.

I also would like to thank Engineer Pete Sthale for his assistance with the instrumentation.

I am deeply grateful to the Brazilian Navy for having sponsored my studies at MIT.

Finally, I want to thank my parents for their irreplaceable guidance, my wife Helena for her patience, devotion, love and support and my children Paulo Neto, “Rambinho”, and Julia for bearing with me when spending time at the laboratory instead of on the playground.

TABLE OF CONTENTS

Abstract	2
Acknowledgments	3
Table of Contents	4
List of Figures	7
Chapter 1 Introduction	
1.1 Flow Assisted Corrosion	10
1.2 Motivation	13
1.3 Objective	15
1.4 Solution Path	16
Chapter 2 Potential Drop Technique	18
Chapter 3 Experimental Procedure	23
Chapter 4 Results and Discussion	
4.1 Solution to the forward problem	
4.1.1 Numeric solution for an infinite plate with slot defect	28
4.1.2 Numeric solution for a semi-infinite plate without defect	31
4.1.3 Analytic solution for a semi-infinite plate without defect	35
4.1.4 Analytic solution for a semi-infinite plate with slot defect	38
4.1.5 Analytic solution for a semi-infinite plate with smooth defect	46
4.1.6 Correction for the cylindrical geometry	52

4.1.7 Three-dimensional solution for a pipe with a non-symmetric defect ...	56
4.2 Solution to the inverse problem	
4.2.1 Solution for a 2D symmetric defect	62
4.2.2 Alternative approach for the 2D symmetric defect	67
4.2.3 Solution for a 3D cylindrical non-symmetric defect	70
4.3 Forward problem for a semi-infinite plate without defect	76
4.4 Forward problem for a semi-infinite plate with slot defect	78
4.5 Forward problem for a semi-infinite plate with ramp defect	82
4.6 Forward problem for a semi-infinite pipe without defect	84
4.7 Inverse problem for a semi-infinite plate with slot defect	86
4.8 Inverse problem for a semi-infinite plate with ramp defect	93
4.9 Inverse problem for a semi-infinite plate with smooth defect	96
4.10 Inverse problem for a semi-infinite pipe with circular defect	97
Conclusion	101
Future Work	102
References	103
Appendix A	111
Appendix B	119
Appendix C	132
Appendix D	145
Appendix E	151
Appendix F	164
Appendix G	175

Appendix H	182
Appendix I	186
Appendix J	198
Appendix K	207
Appendix L	210
Appendix M	217
Appendix N	223
Appendix O	230
Appendix P	243

LIST OF FIGURES

2.1	DC electrical field distribution for an edge crack specimen	19
2.2	General features of an AC field injected into a flat plate	20
3.1	DCPD System Schematic Diagram	23
3.2	Photograph of the Experimental Apparatus	24
3.3	Plate with slot defect used during experiments	25
3.4	Plate with ramp defect used during experiments	26
3.5	Pipe without defect used during experiments	26
4.1	Schematic model for analysis (2D)	29
4.2	Schematic view of a semi-infinite plate without defect	31
4.3	Periodicity of the potential function	32
4.4	Schematic view of a semi-infinite plate with symmetric defect	38
4.5	Schematic view of a semi-infinite plate with slot defect	40
4.6	Comparison between the potential functions for a plate with slot defect ...	43
4.7	Comparison between the potential functions for a plate with slot defect ... using new B.C at Δ_0	45
4.8	Schematic view of a semi-infinite plate with smooth defect	46
4.9	Smooth defect given by Equation 4.59	50
4.10	Analytic potential functions for a plate with smooth defect	51
4.11	Schematic view of a semi-infinite pipe without defect	52
4.12	Schematic view of a pipe with a non-symmetric defect	56

4.13	Schematic view of a semi-infinite plate with symmetric defect	62
4.14	Comparison between experimental and analytical results for a no defect rectangular plate	77
4.15	Comparison between experimental and analytical results for a 2mm-height slot defect plate	79
4.16	Comparison between experimental and analytical results for a 4mm-height slot defect plate	80
4.17	Comparison between experimental and analytical results for a 6.3mm-height slot defect plate	81
4.18	Ramp defect function	82
4.19	Comparison between experimental and analytical results for a ramp defect plate	...	83
4.20	Comparison between experimental and analytical solution without correction for a pipe with no defect	84
4.21	Comparison between experimental and analytical solution with correction for a pipe with no defect	85
4.22	Thickness contour plot for a slot defect in a plate	87
4.23	2D defect solved for a slot plate ($\lambda = 50.8mm, h = 6.3mm$) using experimental data	...	88
4.24	2D defect solved for a slot plate ($\lambda = 50.8mm, h = 6.3mm$) using “analytical data”	...	89
4.25	2D defect solved for a slot plate ($\lambda = 400mm, h = 6.3mm$) using “analytical data”	...	90

4.26	2D defect solved for a slot plate ($\lambda = 50.8mm, h = 2mm$) using experimental data	...	91
4.27	2D defect solved for a slot plate ($\lambda = 50.8mm, h = 2mm$) using “analytical data”	...	92
4.28	2D defect solved for a ramp plate using experimental data and first order approximation	...	93
4.29	2D defect solved for a ramp plate using experimental data and second order approximation	...	94
4.30	Comparison between first and the second order solutions for a ramp defect	...	95
4.31	Inverse problem for a smooth defect given by Equation 4.59	96
4.32	AUTOCAD reproduction of a circular defect machined in the pipe	...	97
4.33	Thickness contour plot for a circular defect in a pipe	99
4.34	2D defect solved for a pipe using experimental data	100

CHAPTER 1

INTRODUCTION

1.1 Flow Assisted Corrosion

Flow assisted corrosion (FAC) is a process where the normal protective oxide layer on carbon steel or low-alloy steel dissolves into a stream of flowing water or water-steam mixture. As the oxide layer becomes thinner and less protective, the corrosion rate is increased (Chexal *et. al.*, 1996). The phenomenon is more common at elbows, turbines, pumps, tube constrictions, and other structural features that alter flow direction or velocity and increase turbulence. FAC causes a reduction of the pipe wall thickness unlike forms of local attack, such as droplet impingement. FAC occurs under both single and two-phase flow conditions. Since water is necessary to remove the oxide layer, the phenomenon is not observed in superheating conditions.

The main factors influencing FAC are fluid velocity, void fraction and quality, geometry, fluid temperature, water chemistry and piping material (Cragolino *et. al.*, 1988). Susceptibility to FAC depends on the interaction of these variables. The fluid velocity plays a vital in determining the mass transfer of iron oxide into the fluid stream. FAC rates increase with increasing fluid velocity and turbulence. There is no practical threshold velocity below which FAC cannot occur (Chexal *et. al.*, 1996). In two-phase flow conditions void fraction and steam quality play an important role in determining the FAC rates. Component geometry also has a direct influence on the

fluid velocity and mass transfer rate. FAC is more common in components with a geometry that increases fluid velocity and turbulence. Nonetheless, FAC is encountered in straight piping, especially when the fluid velocity is high.

Water chemistry has been shown to be an important variable influencing the stability and solubility of the oxide layer and thus the FAC rate (Cragolino *et. al.*, 1988). In Boiling Water Reactors (BWR) no poison is added to control pH and the oxygen concentration drives the rate of flow accelerated corrosion. Increasing the oxygen concentration in the water tends to stabilize the oxide layer and, therefore, decreases the rate of FAC. On the other hand, in Pressurized Water Reactors (PWR), amines are added to control the pH. The lower the pH, the greater the rate of flow accelerated corrosion.

Temperature influences the rate of the oxidation and reduction reactions. The mass transfer rate is a function of temperature and pH.

The chemical composition of the steel has a major effect on the resistance to FAC in high temperature water or wet steam. Whereas plain carbon steels are extremely susceptible to FAC, austenitic stainless steels are essentially immune (Cragolino *et. al.*, 1988). Many authors have reported that the addition of chromium to steel has a profound beneficial effect on the resistance to FAC under both single and two-phase flow conditions. Even at chromium content as low as 1%, the FAC rate can be reduced by more than one order of magnitude in comparison to plain carbon steels (Bignold *et. al.*, 1983).

Since FAC results in degradation of the internal pipe wall, it is necessary to monitor the pipe wall thickness during the plant life. Often, a layer of insulation

covers most of the susceptible pipeline, at high pressure and temperature. A monitoring program, using a conventional technique such as ultrasound, can only be done by shutting down the plant. In this thesis a new measurement technique based on the direct current (DC) potential drop method is proposed to evaluate the pipe wall damage in real time without the need to shut down the plant.

1.2 Motivation

Flow Assisted Corrosion is a phenomenon that results in metal loss from piping, vessels and equipment made of carbon steel. FAC occurs only under certain conditions of flow, chemistry, geometry and material. Unfortunately, these conditions are common in much of the nuclear and fossil-fueled power plants. Undetected, FAC may cause leaks and ruptures. Consequently, FAC has become an important issue, particularly for nuclear power plants.

Although major failures are rare, the consequences can be severe. In 1986, a high-pressure condensate line in Virginia Power's Surry nuclear power plant suddenly burst and caused the death of four men (Chexal *et. al.*, 1996). In 1995 and 1996, two failures at two different fossil-fired plants caused four fatalities (Chexal *et. al.*, 1996). In addition to concerns about personnel safety, a major FAC failure can force a plant to shut down and purchase replacement power at a price approaching a million dollars per day.

A great deal of time and money has been spent developing the technology to predict, detect, and mitigate FAC in order to prevent catastrophic failures. Plant personnel conduct inspections in order to prevent an unexpected failure or unplanned shutdown like the case of the Surry plant. The objective of these inspections is to obtain a measured value of the wall thickness and to compare it with previous values. With many forms of degradation, there are several non-destructive evaluation (NDE) methods such as an ultrasonic test (UT), a radiography test (RT) and an eddy current test (ECT). The examination process for these methods includes removal of insulation, the layout of an inspection grid, acquisition of thickness measurement, and input of the data into

evaluation programs for predicting repair, maintenance and corrective action. Insulation removal, disposal and replacement can account for higher costs than the actual NDE, particularly where asbestos insulation is used. The elimination of insulation removal and/or of a grid production on components prior to examination for FAC can reduce the cost of inspection by more than 50% (Walker, S.M., 1998). There is a need for appropriate NDE inspection techniques that can detect corrosion damage without the extended downtime and expense that occurs during insulation removal and replacement.

A new method of NDE involves the use of the potential drop technique. It was developed originally for measurement of crack growth in material, but it can be used for measurements of wall thickness, especially as a practical method for continuous measurement of thickness. This technique reduces the cost of monitoring piping systems associated with the removal of insulation, provides a continuous time history that makes it possible to develop reliable models of corrosion evaluation and does not require space around the component to be inspected.

1.3 Objective

The objective of this thesis is to develop an on-line methodology to predict the pipe wall damage morphology based on the direct current potential drop (DCPD) technique.

1.4 Solution Path

Using the direct current potential drop (DCPD) technique the goal was to develop a new methodology to measure the thickness morphology in a pipe. This method involves applying a constant direct current (DC) through the pipe, measuring the resulting potential drop between the voltage probes on the external surface of the pipe, and then using these data to construct an algorithm to map the pipe wall thickness. First several experiments were carried out using plates with symmetric defect on the bottom. Then experiments using pipes with a more likely defect caused by FAC were performed.

The analytic solution is divided into two parts. The first part, called the forward problem, involves solving the Laplace equation for the electrical potential field of a plate with a well-defined defect present. Then, a correction term due to the cylindrical geometry of the pipe is added to this solution. In this problem, one specifies the (experimentally known) normal current density on the outer measurement surface and assumes the shape of the inner “corroded” surface is known. Mathematically the forward problem is a classic linear well-posed problem.

The second part, called the inverse problem, takes measured potential drop data from a pipe with unknown damage. In this case, the boundary conditions specify the normal current distribution and the potential distribution over the outer surface, both known from experimental measurements. The goal of the theory is to then predict the morphology of the inner corroded surface. Mathematically, although the basic equation for the potential function is linear, the problem itself is highly nonlinear because of the transcendental manner in which the basic unknown, the shape of the inner surface, enters

the equations. Furthermore, specifying two boundary conditions on a single surface for the Laplacian operator makes the problem ill-conditioned. Small errors in either of the boundary conditions grow exponentially moving away from the measurement surface. Therefore, a good deal of care is needed in designing an algorithm that gives stable results. The inverse calculation is based on the forward calculation; the better the forward calculations agrees with the actual measurements, the better our inversion will be.

CHAPTER 2

POTENTIAL DROP TECHNIQUE

Potential drop is a widely used and successful technique that involves measuring the changes in electrical potential at probes placed across a material containing a defect to which a direct current (DC) or an alternating current (AC) is applied. This method has been used to measure crack length during fracture toughness tests, fatigue, stress corrosion cracking, etc (Dover *et. al.*, 1980). Another more recent application is called Electrical Impedance Tomography (EIT), which is a relatively new medical imaging modality that produces images by computing electrical properties within the human body.

The potential drop technique can be used with either DC or AC. The DC potential drop (DCPD) method of crack length measurement is a convenient and well-established technique (Halliday *et. al.*, 1980). A constant current is passed along the specimen perpendicular to the crack growth direction and a potential drop is measured using probes placed on either side of the crack. Figure 2.1 illustrates this technique for a plate with an edge crack (Dover *et. al.*, 1980). It is assumed that the current connections are on plane remote from the defect so that a uniform field is set up in the plate. Adjacent to the crack the field is perturbed and its measurements in this region must be interpreted in terms of crack depth. For this application, as the crack propagates the resistance, and hence the measured potential drop, increases due to reduction in uncracked cross sectional area of the specimen. A potential drop V_a across a crack is compared with a reference potential

drop, V_0 , across an uncracked part of the same material. The ratio V_a/V_0 can be correlated to the crack length.

The major advantages of the DC method are that it does not rely on advanced electronics and for certain specimen size and geometry it is a well-known, established technique. However, it does have the disadvantages of a complex relationship between potential drop and crack length and the problems inherent in handling low level (millivolt to microvolt) DC signals including difficulties arising from thermal effects (Watt, K.R., 1980). These thermoelectric voltages can be a substantial fraction of the total measured voltage. Since the thermoelectric effect is present even without the input current, it is possible to account for it by subtracting voltage measurements taken with the current off from the measurements made with the current on.

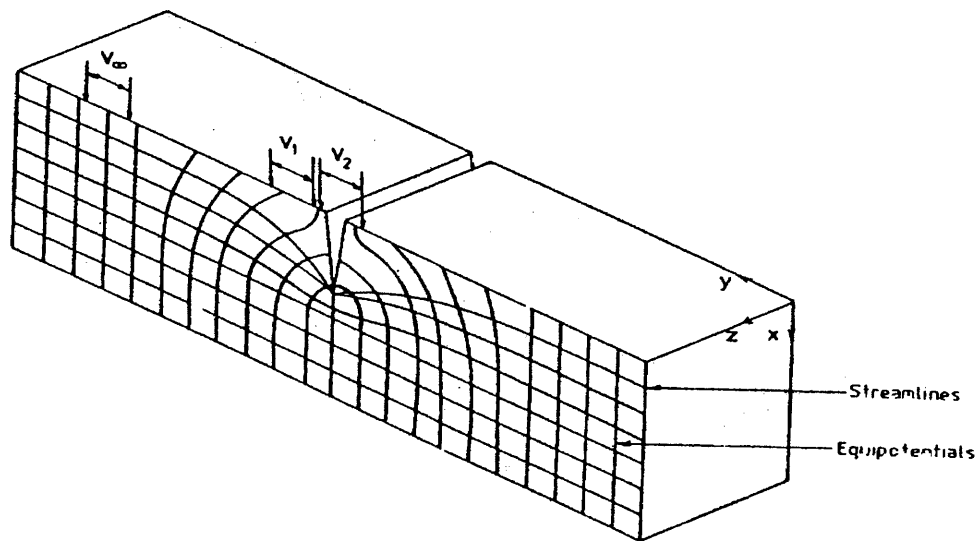


Figure 2.1 – DC electrical field distribution for an edge crack specimen (Dover, *et. al.*, 1980).

Using AC produces several advantages that can be enjoyed only if the practical problems of measuring small AC voltages are overcome. The most important difference between AC and DC is that for the former the current is carried only in a thin layer at the metal surface. This phenomenon is known as the “skin effect”. Figure 2.2 shows that it is possible to arrange the AC connections so that the field is uniform in the region adjacent to the crack (Charlesworth and Dover, 1982).

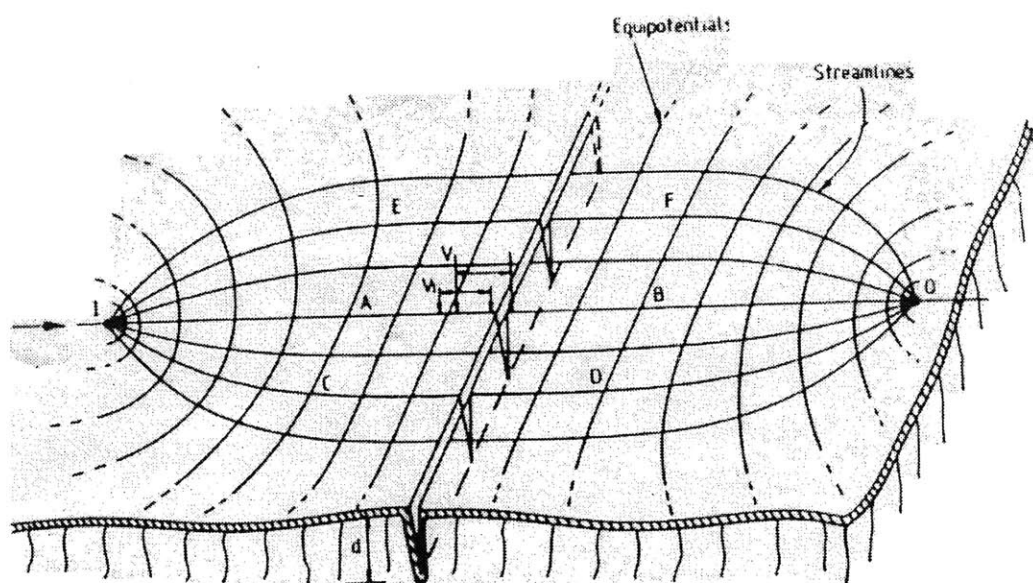


Figure 2.2 – General features of an AC field injected into a flat plate (Charlesworth and Dover, 1982).

In this case the measured potential difference, between any two points parallel to the current flow direction, is a linear function of the distance between the points. Thus the potential is linearly related to the path length between the contact points. The current required to produce a given field strength at the surface is much less than for DC as the resistance is higher (the effective cross section carrying the current is much less in the

case of AC). The skin thickness (δ) depends on several material properties and can be calculated from the following equation (Dover *et. al.*, 1980)

$$\delta = (\mu \mu_0 \sigma \pi f)^{-1/2}, \quad (2.1)$$

where μ is the relative permeability of conductor, μ_0 is the permeability of free space, σ is the conductivity of conductor and f is the frequency of AC.

The major advantages of the AC technique are the ease of calibration for different specimen geometries and the lack of size dependence of the technique, coupled with the ease of amplification of the input signal. The main problems with the technique are those of lead interaction and electronic stability (Watt, K.R., 1980).

The decision whether to use the AC or DC technique in any particular case requires careful consideration. However, if the specimen size and geometry are such that the DC technique is well established, there is no advantage in changing to the AC method. On the other hand, the AC technique does offer considerable advantages in some circumstance. The inherently linear response of the method together with a lack of sensitivity to specimen geometry or size means that crack detection and crack monitoring can be carried out much more easily on an increased range of specimens.

The EIT is a more recent application using this method. It is a technique for producing an image of the electrical resistivity profile within a body from measurements made on the body's exterior. To make these measurements, an array of electrodes is attached to the surface of the body. Sets of current patterns are applied through these electrodes, and the voltages needed to maintain these specified currents are measured and recorded. These applied currents and measured voltages are then used in a reconstruction algorithm to produce images that represent approximations to the electrical resistivity

distribution in the interior of the body. The mathematical models are well described in several works, especially in those published by Margaret Cheney and David Isaacson (Cheney *et. al.*, 1990).

For the purpose of monitoring specimen thickness the DCPD method can be used. A constant direct current (DC) is passed through a specimen and the potential drop between probes on either side of a defect is measured. The basis of the method is that in a current carrying body there will be a disturbance in the electrical potential field about any discontinuity in that body. Therefore, for this application, a constant DC results in a potential drop across the defected region. Considering a uniform current distribution in the specimen, Ohm's law can be used to calculate the potential drop between two points:

$$V = R \cdot I = \frac{\rho l}{A} I, \quad (2.2)$$

where I is the current (Amp), ρ is the resistivity of the material ($\Omega \cdot m$), l is the probe spacing (m) and A is the cross section area (m^2).

For the case of uniform wall thinning Equation 2.2 completely defines the system. Once the current is known, the potential difference between any two points is sufficient to calculate the pipe wall thickness. This is called forward problem and can be solved not only analytically but also using a finite element method. On the other hand, the presence of a localized defect causes a perturbation in the potential field and a more accurate analysis must be done. This problem is called inverse problem since, like in the EIT problem, we are given a set of measurements and need to know the defect morphology.

CHAPTER 3

EXPERIMENTAL PROCEDURE

A Direct Current Potential Drop (DCPD) system has been developed and used for experiments. Figure 3.1 shows a schematic diagram of this system. The major components of the system are as follows: a DC Power Supply as a constant current driver (model HP6259B, Hewlett Packard), Non-Reversing contactors as alternating DC producer (model LC1D3210G6, Telemecanique), a Switch/Control Unit (model HP3488A, Hewlett Packard) as relay set controller, a Multimeter (model HP3457A, Hewlett Packard) as a data acquisition system and a PC Computer. Figure 3.2 shows a picture with the experimental apparatus.

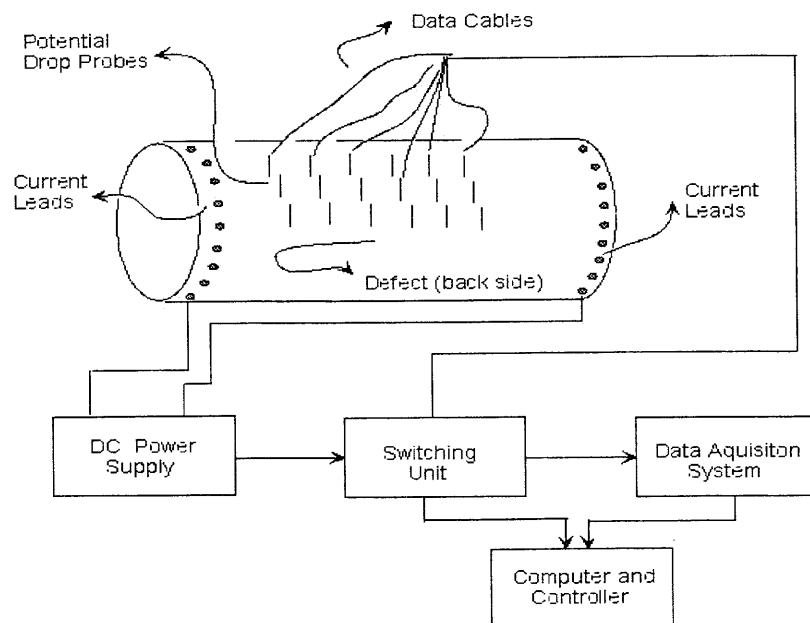


Figure 3.1 – DCPD System Schematic Diagram

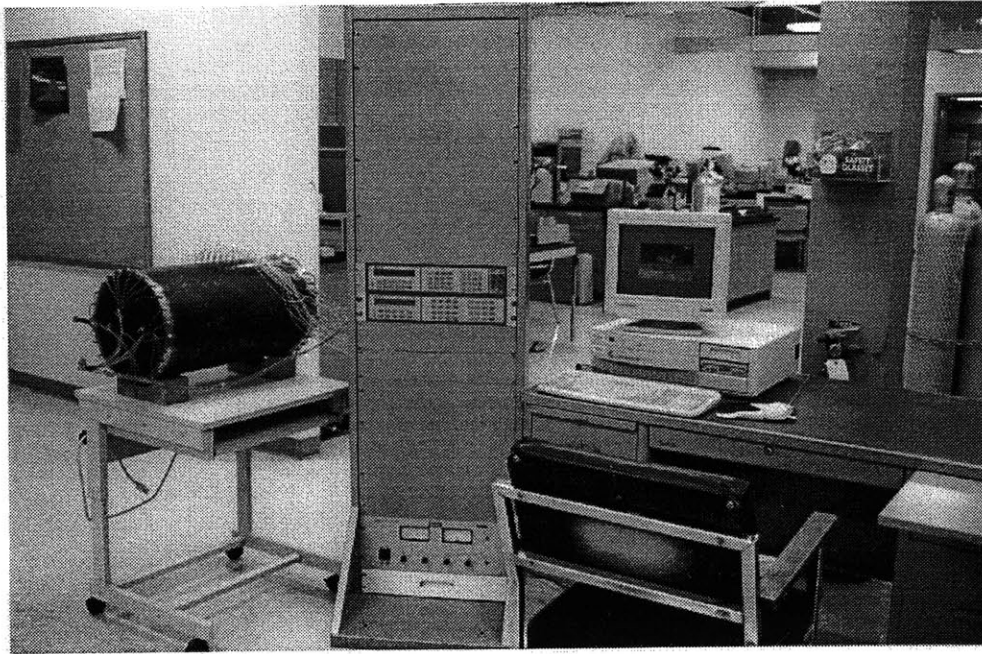


Figure 3.2 – Photograph of the Experimental Apparatus. From the bottom to the top of the rack: DC power supply, switch/control unit and multimeter.

For the experiments using plates, a total current of 10Amp was applied throughout 15 points on the border of the plate. All current wires were connected to a common bar in order to ensure an equal distribution of current in each wire. Figure 3.3 shows a picture of one plate used in the experiments. A row of probes 12.7mm (0.5 inch) apart was arranged along the plate. The potential drop between points is measured for one polarity of applied current. The polarity is then reversed and the potential drops between probes measured again. The average of the potential is then computed. In this way voltages generated due to thermoelectric effects are normalized out. First, a plate 304.8mm (12 inches) long by 203.2mm (8 inches) wide and 19.05mm ($\frac{3}{4}$ inch) thick without defect was used. Then, a slot defect 101.6mm (4 inches) wide (measured from the center of the plate) and 2 mm high was machined in the same plate. Finally, the same slot was increased to 4 mm and 6.3 mm deep and new measurements were carried out.

After these experiments the 6.3mm-height slot defect was modified to a ramp defect.

Figure 3.4 shows a picture of the plate with a ramp defect. In this experiment the total current used was 20Amp.

For a pipe specimen of 326.4mm (12.85 inches) external diameter and 12.7mm ($\frac{1}{2}$ inch) wall thickness a current of 35Amp was applied to the ends of the pipe test section in such a manner as to ensure that a uniform current distribution is achieved around the circumference of the pipe. Figure 3.5 shows one of the pipes used in the experiments. The current was applied at 26 taps around the circumference of the pipe. The potential probes were arranged in a one inch-array on the outside of the pipe opposite the defect, which was located inside the pipe. First, a pipe without defect was used. Then, new measurements were carried out on an identical pipe with some circular defects on the inside of the pipe.

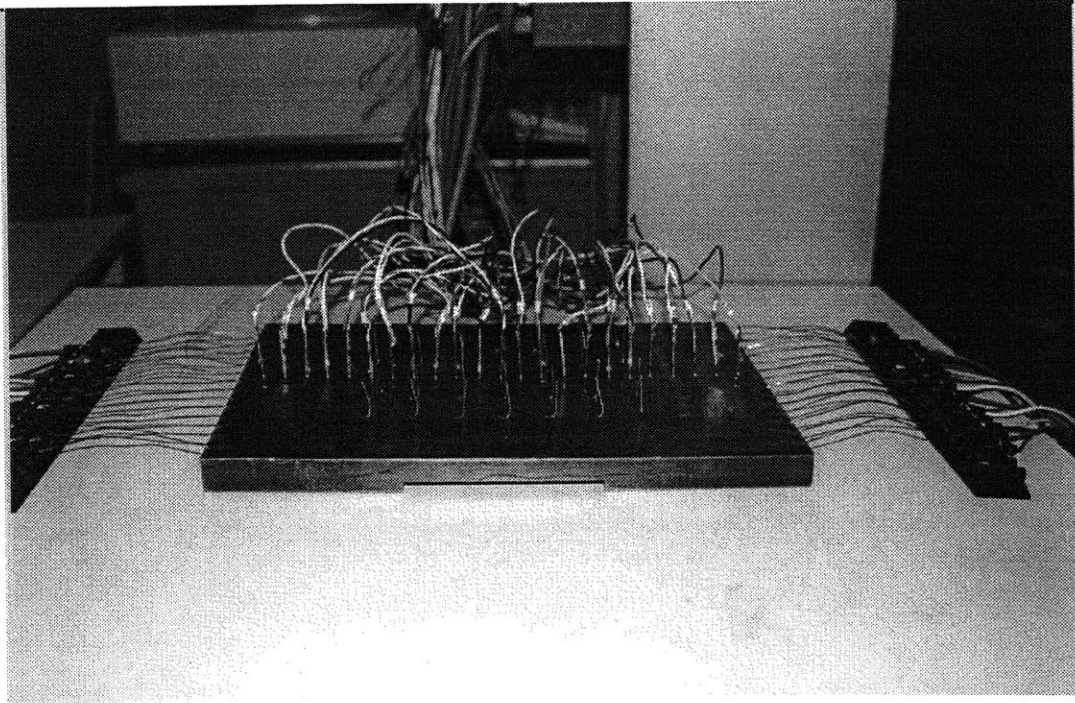


Figure 3.3 – Plate with slot defect used during experiments.

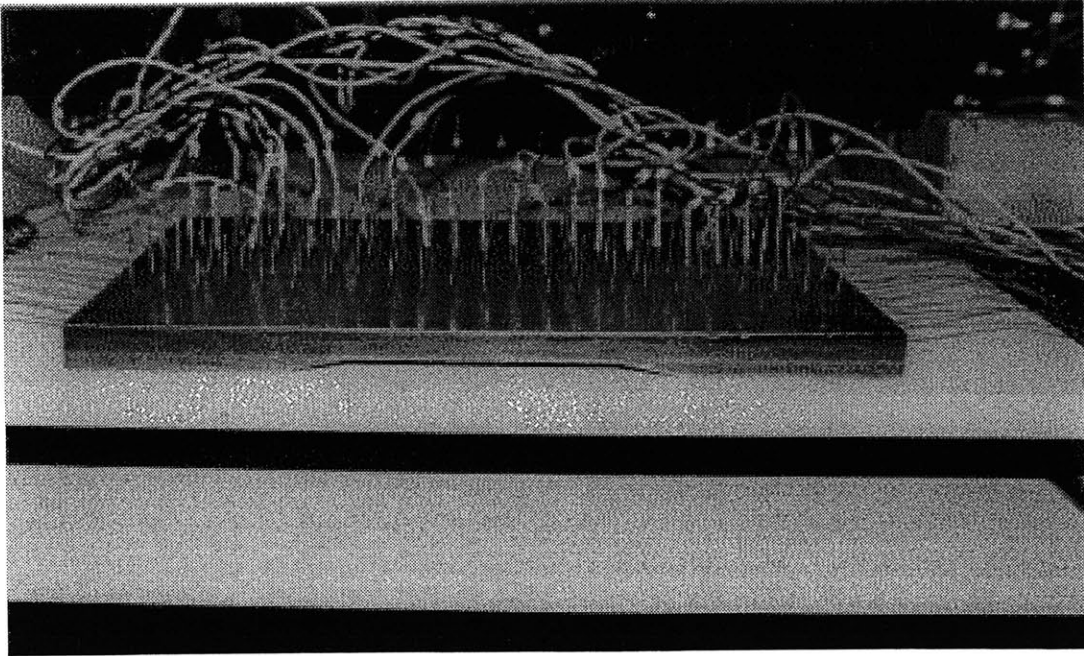


Figure 3.4 - Plate with ramp defect used during experiments.

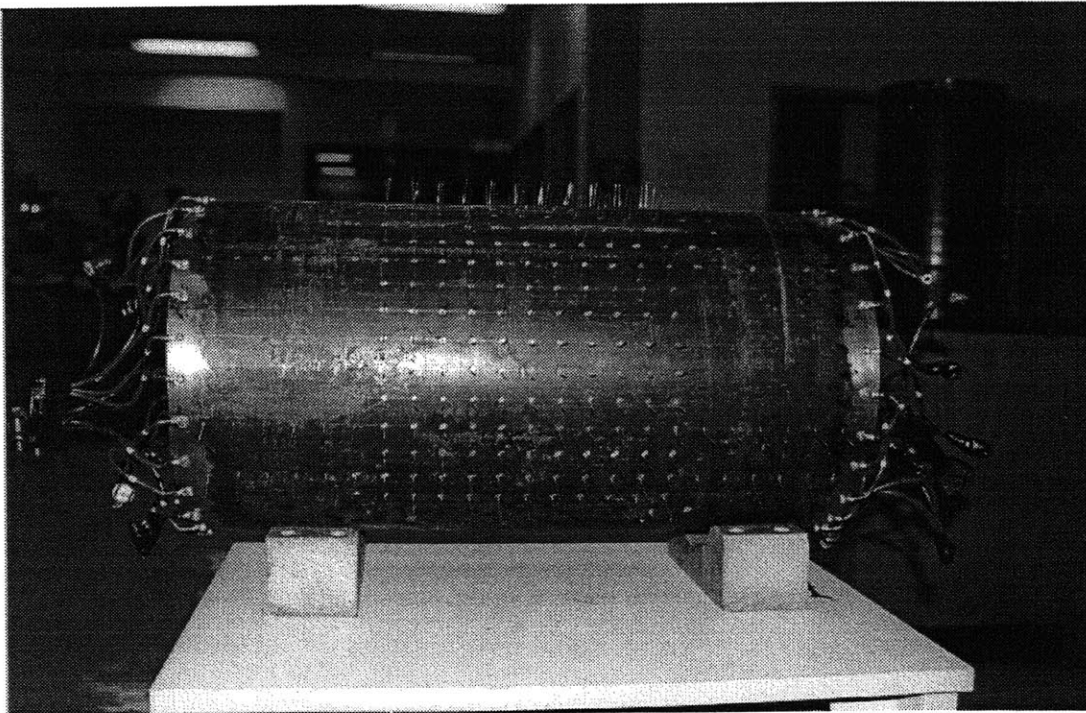


Figure 3.5 – Pipe without defect used during experiments.

The data acquisition was carried out using Hewlett Packard devices. A program in HP Basic language was developed to acquire the data. The data were acquired for a specific time, for example one minute at each channel and then averaged. A filter was introduced in order to reject the data that deviated by more than half of a standard deviation from the average. Appendix A is a listing of the code called “pipe thinning” that makes the data acquisition.

CHAPTER 4

RESULTS AND DISCUSSION

This chapter contains a description of the algorithm developed to predict the pipe wall damage morphology and the experiment results. First, a solution to the forward problem for plates with symmetric defect on the bottom is developed. Then a correction term for the cylindrical geometry is added to the slab solution. The results are compared with the experimental ones. A three-dimension solution is also developed for a pipe with a non-symmetric defect.

Another section of this chapter describes the solution to the inverse problem. The results for two-dimensional symmetric defect cases are compared with the experimental ones. A solution is also developed for a 3D cylindrical non-symmetric defect.

4.1 Solution to the forward problem

4.1.1 Numeric Solution for an infinite plate with slot defect

A general analysis for the electrical field involves a solution of Maxwell's equations. The presence of a defect can be modeled as a two-dimensional problem as illustrated in Figure 4.1.

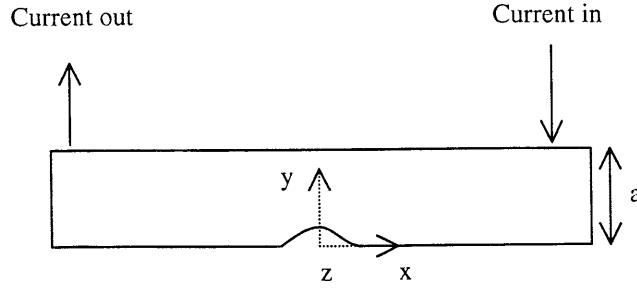


Figure 4.1 – Schematic model for analysis (2D)

When current flows through a defected material, the electrical field and potential distribution will reflect the locations and shapes of the defects. The electrical field (\underline{E}) is defined as the gradient of the scalar potential (φ),

$$\underline{E} = -\text{grad } \varphi = -\nabla \varphi, \quad (4.1)$$

$$\underline{J} = \sigma \cdot \underline{E}, \quad (4.2)$$

$$\text{div } \underline{J} = \nabla \cdot \underline{J} = 0, \quad (4.3)$$

where \underline{J} is the current density and σ is the conductivity of the material $(\Omega - m)^{-1}$. Thus,

$$\text{curl } \underline{E} = \nabla \times \underline{E} = 0, \quad (4.4)$$

and the Laplace equation is satisfied:

$$\nabla^2 \varphi(x, y, z) = 0. \quad (4.5)$$

The boundary conditions for this problem are:

$$\text{at } y = a: \quad \underline{n} \cdot \underline{J} = \sigma \cdot \frac{\partial \varphi}{\partial y} = S(x, z), \quad (4.6)$$

$$\text{at } y = 0: \quad \underline{n} \cdot \underline{J} = \sigma \cdot \frac{\partial \varphi}{\partial y} = P(x, z), \quad (4.7)$$

where \underline{n} is the normal vector, a is the thickness of the plate, $S(x, z)$ and $P(x, z)$ are the current source and perturbation functions, respectively. Appendix B shows a detailed description of these functions.

The voltage difference between two points can be calculated from the potential function as

$$V(x, y, z) = \varphi(x, y, z) - \varphi(-x, y, z). \quad (4.8)$$

In order to get the analytical expression for voltage measurements it is necessary to find the potential function from the Laplace equation. This function can be found using Fourier transformation. The final solution to this problem is given by:

$$V(x) = \frac{4S_0\rho}{\pi} \sum_{m=-\infty}^{\infty} \int_0^{\infty} \frac{dk}{\tanh ka} \frac{J_1(kr)}{kr} [J_0(k\sqrt{(x-l)^2 + m^2c^2}) - J_0(k\sqrt{(x+l)^2 + m^2c^2})] - \frac{P_0\lambda^2\rho}{\pi 2^{3/2}} \int_0^{\infty} dk_x \frac{\sin k_x x}{\sinh(k_x a)} e^{-\frac{k_x^2 z^2}{4}}, \quad (4.9)$$

where J_0 is the zeroth order Bessel function, J_1 is the first order Bessel function, l is the distance between the current wire and the center of the plate and c is the spacing between the current wires at the border of the plate.

Appendix B shows a detailed derivation of Equation 4.9. This equation works well for an infinite plate (both in the x and z directions). It is necessary to change the boundary conditions of the problem in order to account for the finite boundaries and compare the analytical results with the experimental ones.

4.1.2 Numeric Solution for a semi-infinite plate without defect

Consider a plate with finite dimensions in the z and y directions. Figure 4.2 shows a schematic view of the slab without defect that has been modeled (assume the dimension in the x direction is infinite).

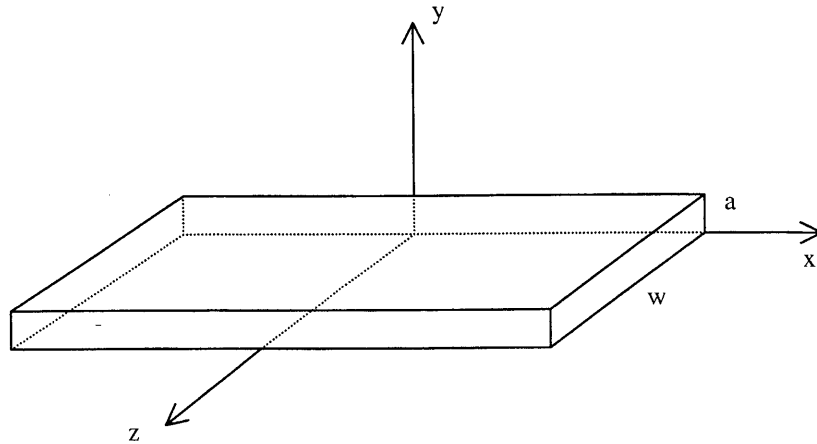


Figure 4.2 – Schematic view of a semi-infinite plate without defect (assume infinite in the x direction).

The new boundary conditions will be:

$$\begin{aligned} \varphi|_{x=\pm\infty} &= 0, & \frac{\partial\varphi}{\partial y}\Big|_{y=0} &= 0, \\ \frac{\partial\varphi}{\partial z}\Big|_{z=0,w} &= 0, & \frac{\partial\varphi}{\partial y}\Big|_{y=a} &= \rho S(x,z), \end{aligned}$$

where w is the width of the plate.

Figure 4.3 shows the condition for periodicity of the potential function. Since the boundary conditions in z require $\frac{\partial\varphi}{\partial z}\Big|_{z=0,w} = 0$, the potential function has a semi-period

between $[0,w]$. In order to use Fourier analysis it is convenient to build a mirror image of φ to make it periodic in the interval $[0,2w]$.

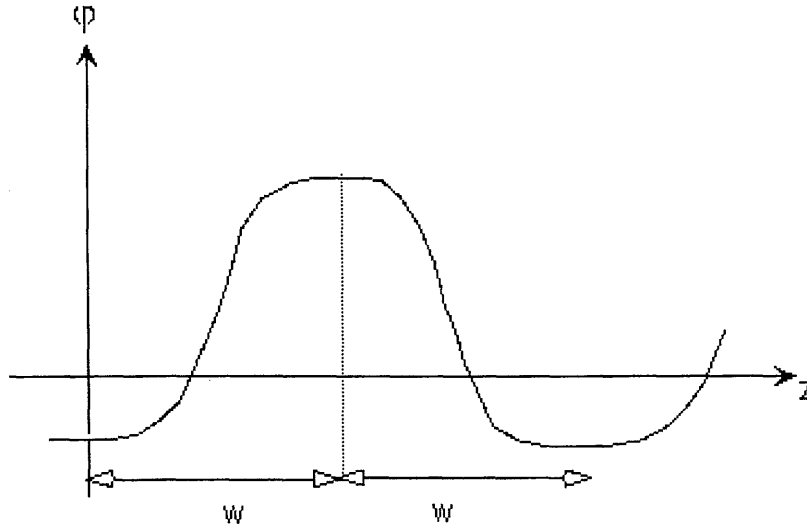


Figure 4.3 – Periodicity of the potential function

Expanding $\varphi(x, y, z)$ as a Fourier series in the z direction and Fourier transformation in the x direction gives

$$\varphi(x, y, z) = \frac{1}{\sqrt{2\pi}} \sum_{n=0}^{\infty} \int_{-\infty}^{\infty} e^{ikx} \cos\left(\frac{n\pi z}{w}\right) \hat{\varphi}_n(k, y) dk, \quad (4.10)$$

which automatically satisfies the boundary conditions at $z=0$ and $z=w$.

Applying Fourier transformation to the Laplace equation and the new boundary conditions results in

$$\varphi(x, y, z) = -\frac{2i\rho S_0}{\pi w} \sum_{m=0}^{\infty} \int_{-\infty}^{\infty} e^{ik'x} \cos\left(\frac{m\pi z}{w}\right) \frac{\cos\left(\frac{m\pi z_k}{w}\right) \sin(k'l)}{k_m \sigma_m \sinh(k_m a)} \cosh(k_m y) dk', \quad (4.11)$$

where l is the distance from the center of the plate to the current wires at the border of the plate, z_k is the position at the border of the plate of the current wire, $\sigma_m = 1$ if $m \neq 0$ and $\sigma_m = 2$ if $m = 0$.

The voltage difference along the centerline of the plate ($z = \frac{w}{2}$) can be evaluated using

Equation 4.8. Thus,

$$V(x) = \varphi(x, y = a, z = \frac{w}{2}) - \varphi(-x, y = a, z = \frac{w}{2}),$$

$$V(x) = \frac{4\rho S_0}{\pi w} \sum_{m=0}^{\infty} \int_{-\infty}^{\infty} \frac{\sin(k'x) \sin(k'l)}{k_m \sigma_m \tanh(k_m a)} \cos\left(\frac{m\pi}{2}\right) \cos\left(\frac{m\pi z_k}{w}\right) dk'. \quad (4.12)$$

In the case of multiple current wires it is necessary to sum all contributions. Thus,

$$V(x) = \frac{4\rho S_0 a}{\pi w} \sum_{m=0}^{\infty} \sum_{k=1}^{N_w} \int_{-\infty}^{\infty} \frac{\sin(k'x) \sin(k'l)}{k_m a \sigma_m \tanh(k_m a)} \cos\left(\frac{m\pi}{2}\right) \cos\left(\frac{m\pi z_k}{w}\right) dk', \quad (4.13)$$

where N_w is the total number of current wires.

The integral of the Equation 4.13 can be solved using complex analysis and this equation can be rewritten as

$$V(x) = \frac{4\rho S_0}{wa} \sum_{m=0}^{\infty} \sum_{k=1}^{N_w} \frac{\cos\left(\frac{m\pi}{2}\right) \cos\left(\frac{m\pi z_k}{w}\right)}{\sigma_m} \sum_{n=0}^{\infty} \frac{e^{-y_{mn}(l-x)} - e^{-y_{mn}(l+x)}}{\sigma_n y_{mn}}, \quad (4.14)$$

where $y_{mn} = \sqrt{\frac{m^2 \pi^2}{w^2} + \frac{n^2 \pi^2}{a^2}}$, $\sigma_n = 1$ if $n \neq 0$ and $\sigma_n = 2$ if $n = 0$.

To validate this analysis a numerical evaluation and comparison with the experimental results becomes necessary. The evaluation of the system was carried out

using Mathcad (Mathcad7 User's Guide, 1997). The dominant term of this equation holds for $m = n = 0$, which gives

$$V(x) = \frac{4\rho S_0}{wa} \frac{N_w}{2} x. \quad (4.15)$$

Equation 4.15 essentially shows that the resistivity for the plate is $\frac{2\rho}{wa} x$, which confirms the expected result. Appendix C shows detailed derivation of equations 4.11 and 4.14.

4.1.3 Analytic Solution for a semi-infinite plate without defect

The problem discussed previously can be interpreted as a two-dimensional one if the current is considered to be applied uniformly along the z-direction as shown in Figure 3.3. In this case, the current source can be expressed as

$$S(x) = \frac{S_0}{w} [\delta(x-l) - \delta(x+l)]. \quad (4.16)$$

The potential function will be

$$\varphi(x, y) = \int_{-\infty}^{\infty} e^{ikx} \hat{\varphi}(k, y) dk, \text{ and} \quad (4.17)$$

$$\hat{\varphi}(k, y) = \frac{1}{2\pi} \int_{-\infty}^{\infty} e^{-ikx} \varphi(x, y) dx, \quad (4.18)$$

where $\hat{\varphi}(k, y)$ is the Fourier transform of $\varphi(x, y)$.

The Laplace equation will be

$$\frac{\partial^2 \hat{\varphi}}{\partial y^2} - k^2 \hat{\varphi} = 0, \quad (4.19)$$

and the boundary conditions can be written as

$$\left. \frac{\partial \hat{\varphi}}{\partial y} \right|_{y=0} = 0, \quad (4.20)$$

$$\left. \frac{\partial \hat{\varphi}}{\partial y} \right|_{y=a} = \frac{\rho}{2\pi} \int_{-\infty}^{\infty} e^{-ikx} S(x) dx. \quad (4.21)$$

Solving the Laplace equation with the boundary conditions above results in

$$\varphi(x, y) = -\frac{i\rho S_0}{\pi w} \int_{-\infty}^{\infty} e^{ikx} \frac{\sin kl}{k \sinh ka} \cosh(ky) dk. \quad (4.22)$$

The potential difference between two points at the surface can be calculated as

$$V(x) = \varphi(x, a) - \varphi(-x, a). \quad (4.23)$$

Therefore,

$$V(x) = -\frac{i\rho S_0}{\pi w} \int_{-\infty}^{\infty} (e^{ikx} - e^{-ikx}) \frac{\sin kl}{k \sinh ka} \cosh(ka) dk.$$

This integral can be solved using complex analysis. The final result is given by the equation below:

$$V(x) = \frac{2\rho S_0}{w} \left[\frac{x}{a} - \frac{1}{\pi} \ln \frac{1 - e^{-\frac{(l-x)\pi}{a}}}{1 - e^{-\frac{(l+x)\pi}{a}}} \right]. \quad (4.24)$$

Equation 4.24 is an analytic expression for the potential difference between two points at the surface of a plate without defect. Since the potential is an odd function gives

$$\varphi(-x) = -\varphi(x),$$

$$\varphi(x) = \frac{\rho S_0}{w} \left[\frac{x}{a} - \frac{1}{\pi} \ln \frac{1 - e^{-\frac{(l-x)\pi}{a}}}{1 - e^{-\frac{(l+x)\pi}{a}}} \right]. \quad (4.25)$$

Another way to find an analytic expression for the potential function is using a table of integrals. Consider Equation 4.22:

$$\varphi(x, y) = -\frac{i\rho S_0}{\pi w} \int_{-\infty}^{\infty} e^{ikx} \frac{\sin kl}{k \sinh ka} \cosh(ky) dk.$$

Appendix D describes how an expression for the potential function can be derived using a table of integrals. The final results is

$$\varphi(x, y) = \frac{\rho S_0}{2\pi w} \ln \frac{\cosh \frac{\pi(l+x)}{a} + \cos \frac{\pi y}{a}}{\cosh \frac{\pi(l-x)}{a} + \cos \frac{\pi y}{a}}. \quad (4.26)$$

This equation is the two-dimensional potential function for a plate without defect. At the surface of the plate ($y = a$) results in

$$\varphi(x) = \frac{\rho S_0}{2\pi w} \ln \frac{\cosh \frac{\pi(l+x)}{a} - 1}{\cosh \frac{\pi(l-x)}{a} - 1}. \quad (4.27)$$

This equation is similar to Equation 4.25 and it provides the potential at the surface of a plate without defect. Appendix D presents a detailed derivation of equations 4.22, 4.24 and 4.26.

4.1.4 Analytic Solution for a semi-infinite plate with slot defect

Since a formula for the voltage difference on a no defect region has been developed, the next step is to consider the case of a defect located on the bottom of the specimen. Figure 4.4 shows schematically a view of a defected plate.

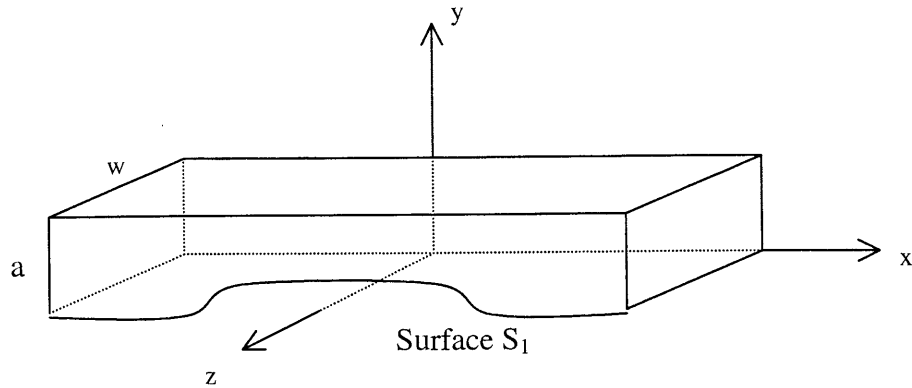


Figure 4.4 – Schematic view of a semi-infinite plate with symmetric defect (assume infinite in the x direction).

Considering that the current is applied uniformly along the z direction and that the defect is symmetric, such as a slot, the problem can be treated as a two-dimensional one.

The new boundary conditions for this problem will be:

$$\varphi|_{x=\pm\infty} = 0, \quad \frac{\partial \varphi}{\partial y} \Big|_{y=a} = \rho S(x),$$

$$\underline{n} \cdot \nabla \varphi|_{S_1} = 0.$$

The surface S_1 can be defined as $S_1(x, y) \equiv y - \Delta(x) = 0$, where $\Delta(x)$ represents the defect amplitude, and its normal vector as

$$\underline{n} = \frac{(e_y - \Delta' e_x)}{(1 + \Delta'^2)^{1/2}},$$

where $\Delta' = \frac{d\Delta}{dx}$.

The boundary condition on the surface will be $\underline{n} \cdot \nabla \varphi|_{S_1} = \left(\frac{\partial \varphi}{\partial y} - \Delta' \frac{\partial \varphi}{\partial x} \right)_{S_1} = 0$. Assuming a small defect amplitude compared to the thickness, that is, $\Delta \ll a$, perturbation theory can be used and the potential function can be written as $\varphi = \varphi_0 + \varphi_1$, where φ_0 and φ_1 are the potential functions that account for the non-defect region and the defect region, respectively.

The Laplace equation holds for each potential function, therefore,

$$\nabla^2 \varphi_0(x, y) = 0,$$

$$\nabla^2 \varphi_1(x, y) = 0.$$

The first problem has the boundary conditions

$$\left. \frac{\partial \varphi_0}{\partial y} \right|_{y=a} = \rho \cdot S(x),$$

$$\left. \frac{\partial \varphi_0}{\partial y} \right|_{y=0} = 0,$$

and has been solved previously. Equation 4.27 gives the solution for the potential function φ_0 . Thus

$$\varphi_0(x) = \frac{\rho S_0}{2\pi w} \ln \frac{\cosh \frac{\pi(l+x)}{a} - 1}{\cosh \frac{\pi(l-x)}{a} - 1}. \quad (4.28)$$

Since the potential is an odd function the voltage difference at the surface can be given as

$$V_0(x) = \frac{\rho S_0}{\pi w} \ln \frac{\cosh \frac{\pi(l+x)}{a} - 1}{\cosh \frac{\pi(l-x)}{a} - 1}, \quad (4.29)$$

which is another way to write Equation 4.24.

The second problem has the boundary condition

$$\left. \frac{\partial \phi_1}{\partial y} \right|_{y=a} = 0, \quad (4.30)$$

and from the boundary condition at the surface S_1 gives

$$\left(\frac{\partial \phi}{\partial y} - \Delta \frac{\partial \phi}{\partial x} \right)_{S_1} = 0. \quad (4.31)$$

Expanding this boundary condition about $y = 0$ and considering only the first order approximation gives

$$\left(\frac{\partial \phi_1}{\partial y} + \Delta \frac{\partial^2 \phi_0}{\partial y^2} - \Delta \frac{\partial \phi_0}{\partial x} \right)_{y=0} = 0. \quad (4.32)$$

Consider a rectangular slot with dimensions as shown in Figure 4.5.

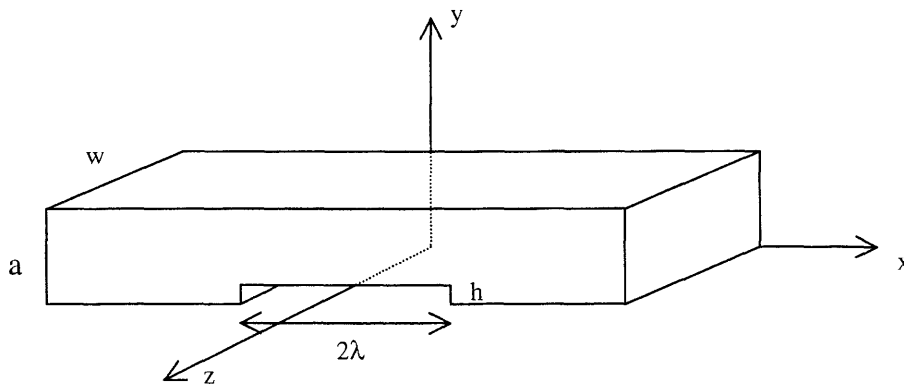


Figure 4.5 – Schematic view of a semi-infinite plate with slot defect (assume infinite in the x direction).

The slot defect function can be defined as a sum of two step functions with amplitude h .

Therefore,

$$\Delta(x) = h[U(x + \lambda) - U(x - \lambda)],$$

$$\frac{d\Delta}{dx} = h[\delta(x + \lambda) - \delta(x - \lambda)],$$

where λ is the half-width of the slot and h is the height of the slot.

The potential function that accounts for the defect region using the first order approximation can be written similarly to Equation 4.17. So,

$$\varphi_1(x, y) = \int_{-\infty}^{\infty} e^{ikx} \hat{\varphi}_1(k, y) dk, \text{ and} \quad (4.33)$$

$$\hat{\varphi}_1(k, y) = \frac{1}{2\pi} \int_{-\infty}^{\infty} e^{-ikx} \varphi_1(x, y) dx, \quad (4.34)$$

where $\hat{\varphi}_1(k, y)$ is the Fourier transform of $\varphi_1(x, y)$.

Taking the Fourier transformation of the Laplace equation and solving for the boundary conditions of equations 4.30 and 4.32 gives

$$\varphi_1(x, y) = -\frac{i\rho S_0 h}{\pi^2 w} \int_{-\infty}^{\infty} \int_{-\infty}^{\infty} dk' dk \frac{\sin k'l}{\sinh k'a} \frac{\sin(k' - k)\lambda}{(k' - k)} \frac{\cosh k(y - a) e^{ikx}}{\sinh ka}. \quad (4.35)$$

The potential difference may be calculated as

$$V_1(x) = \varphi_1(x, a) - \varphi_1(-x, a),$$

$$V_1(x) = \frac{2\rho S_0 h}{\pi^2 w} \int_{-\infty}^{\infty} \int_{-\infty}^{\infty} dk' dk \frac{\sin k'l}{\sinh k'a} \frac{\sin(k' - k)\lambda}{(k' - k)} \frac{\sin kx}{\sinh ka}. \quad (4.36)$$

Solving the double integral above results in

$$V_1(x) = -\frac{\rho S_0 h}{\pi a w} \left[\coth \frac{\pi}{2a} (l-x) \ln \frac{\cosh \frac{\pi}{2a} (l+\lambda) \cosh \frac{\pi}{2a} (\lambda-x)}{\cosh \frac{\pi}{2a} (x+\lambda) \cosh \frac{\pi}{2a} (\lambda-l)} - \coth \frac{\pi}{2a} (l+x) \ln \frac{\cosh \frac{\pi}{2a} (\lambda+x) \cosh \frac{\pi}{2a} (\lambda+l)}{\cosh \frac{\pi}{2a} (\lambda-l) \cosh \frac{\pi}{2a} (\lambda-x)} \right] \quad (4.37)$$

The total voltage difference is given by the sum of equations 4.29 and 4.37. Therefore,

$$V(x) = V_0(x) + V_1(x),$$

$$V(x) = \frac{\rho S_0}{\pi w} \ln \frac{\cosh \frac{\pi(l+x)}{a} - 1}{\cosh \frac{\pi(l-x)}{a} - 1} - \frac{\rho S_0 h}{\pi a w} \left[\coth \frac{\pi}{2a} (l-x) \ln \frac{\cosh \frac{\pi}{2a} (l+\lambda) \cosh \frac{\pi}{2a} (\lambda-x)}{\cosh \frac{\pi}{2a} (x+\lambda) \cosh \frac{\pi}{2a} (\lambda-l)} - \coth \frac{\pi}{2a} (l+x) \ln \frac{\cosh \frac{\pi}{2a} (\lambda+x) \cosh \frac{\pi}{2a} (\lambda+l)}{\cosh \frac{\pi}{2a} (\lambda-l) \cosh \frac{\pi}{2a} (\lambda-x)} \right] \quad (4.38)$$

This equation gives an analytical solution for the potential difference between two points at the top surface of the plate shown in Figure 4.5 in the presence of a defect on the back of the plate. It was developed for a defect with a small slot height compared to the thickness of the plate ($h \ll a$) and, therefore, is linear with the slot height (h). Appendix E shows a detailed derivation of equations 4.32, 4.35, 4.37.

Since the potential is an odd function with respect to the x direction the potential function $\varphi_1(x)$ can be written as

$$\varphi_1(x) = \frac{\rho S_0 h}{2\pi a w} \left[\coth \frac{\pi}{2a} (l-x) \ln \frac{\cosh \frac{\pi}{2a} (l+\lambda) \cosh \frac{\pi}{2a} (\lambda-x)}{\cosh \frac{\pi}{2a} (x+\lambda) \cosh \frac{\pi}{2a} (\lambda-l)} - \coth \frac{\pi}{2a} (l+x) \ln \frac{\cosh \frac{\pi}{2a} (\lambda+x) \cosh \frac{\pi}{2a} (\lambda+l)}{\cosh \frac{\pi}{2a} (\lambda-l) \cosh \frac{\pi}{2a} (\lambda-x)} \right]$$

Figure 4.6 shows a plot of the potential functions φ , φ_0 and φ_1 for a particular slot defect ($h = 6.3mm$ and $\lambda = 50.8mm$).

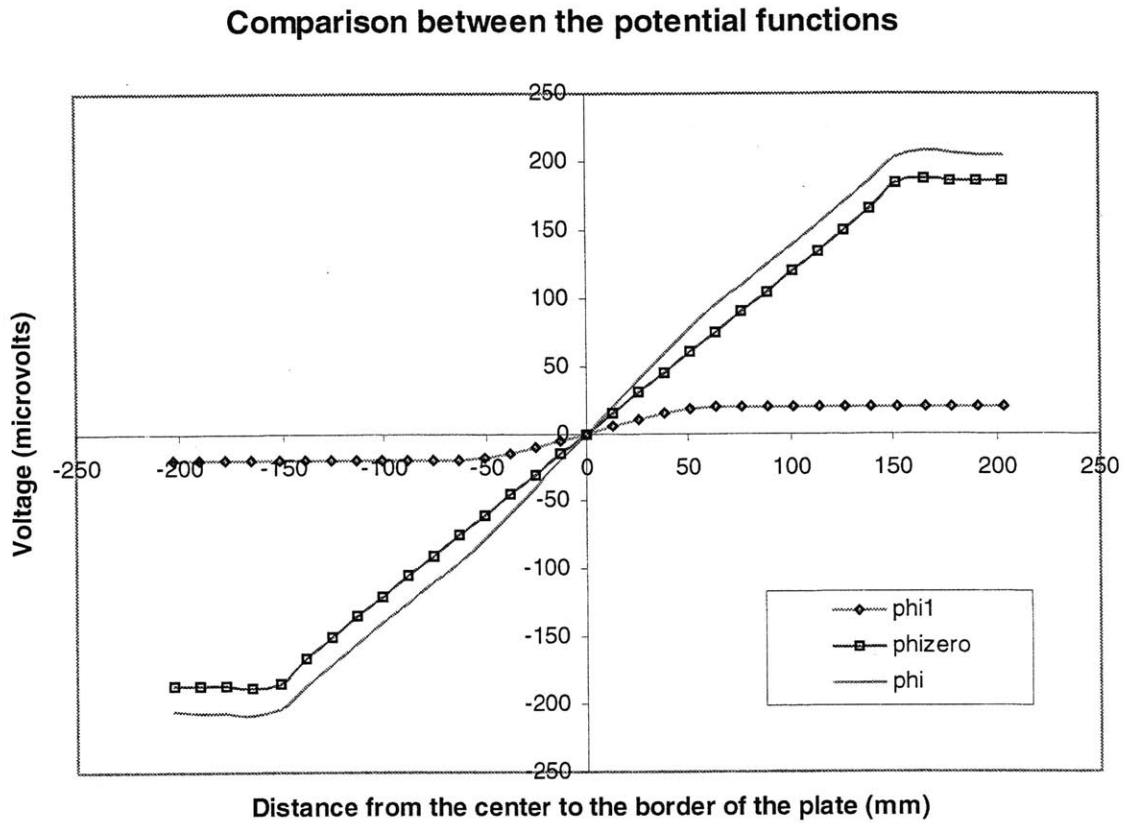


Figure 4.6 – Comparison between the potential functions for a plate with slot defect ($h = 6.3mm$ and $\lambda = 50.8mm$).

For large values of x (outside of the current probes region) the electrical field vanishes and a constant potential function φ was expected. Nevertheless, the potential function φ_1 does not go to zero at large values of x . In order to force the potential function φ_1 to zero

the boundary condition at the bottom surface of the plate must be changed. Assume, for a symmetric defect, that

$$\left. \frac{\partial \varphi_0}{\partial y} \right|_{y=\Delta_0} = 0, \quad (4.39)$$

where Δ_0 is a parameter ($0 < \Delta_0 < a$) chosen such that $(\varphi - \varphi_0^{new}) \Big|_{\substack{x=\pm\infty \\ y=a}} = 0$. This means that at infinity the plate is seen as without defect and with a thickness of $(a - \Delta_0)$.

In this case the new potential function φ_0^{new} will be

$$\varphi_0^{new}(x, y) = -\frac{i\rho S_0}{\pi w} \int_{-\infty}^{\infty} e^{ikx} \frac{\sin kl}{k \sinh k(a - \Delta_0)} \cosh k(y - \Delta_0) dk, \quad (4.40)$$

$$\varphi_0^{new}(x, y) = \frac{\rho S_0}{2\pi w} \ln \frac{\cosh \frac{\pi(l+x)}{(a-\Delta_0)} + \cos \frac{\pi(y-\Delta_0)}{(a-\Delta_0)}}{\cosh \frac{\pi(l-x)}{(a-\Delta_0)} + \cos \frac{\pi(y-\Delta_0)}{(a-\Delta_0)}}. \quad (4.41)$$

The potential function may be written as $\varphi = \varphi_0 + \varphi_1$ and, therefore,

$$\varphi_1^{new} = \varphi_0 + \varphi_1 - \varphi_0^{new}.$$

The parameter Δ_0 may be estimated as

$$\Delta_0 \approx \frac{h\lambda}{l}. \quad (4.42)$$

A detailed discussion of this is provided in Appendix E. Figure 4.7 shows the potential functions considering the new boundary condition at Δ_0 . It can be observed that this new boundary condition fixed the potential function φ_1 at large values of x .

Comparison between the potential functions for the new B.C.

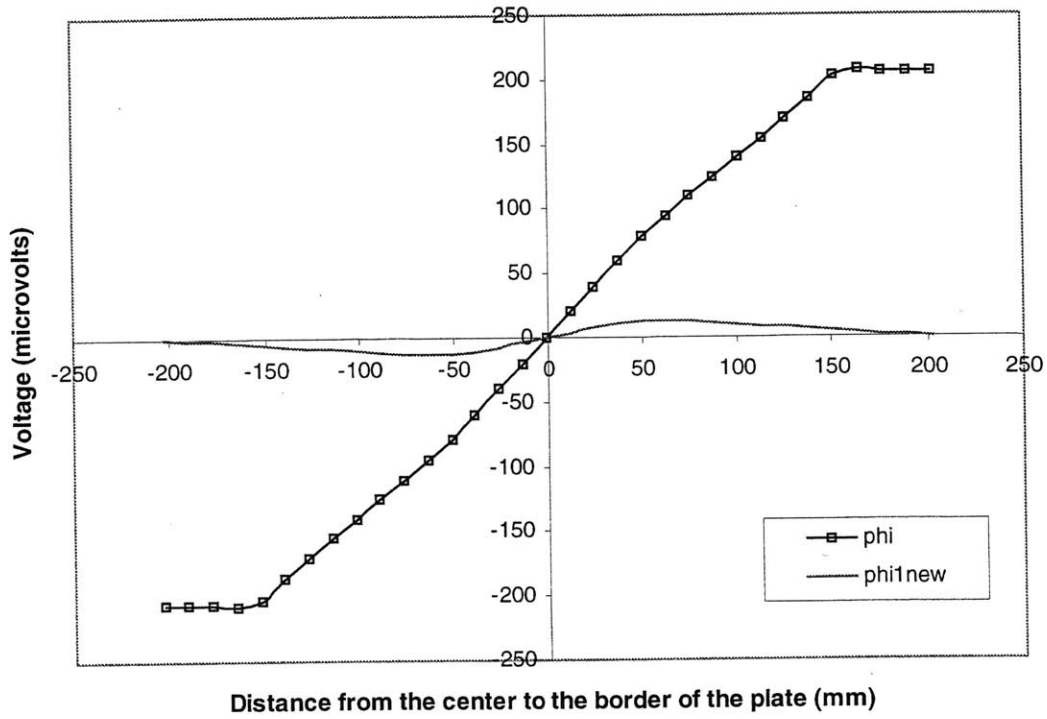


Figure 4.7 - Comparison between the potential functions for a plate with slot defect

($h = 6.3mm$ and $\lambda = 50.8mm$) using new B.C at Δ_0 .

4.1.5 Analytic Solution for a semi-infinite plate with smooth defect

Consider a plate with a defect as shown schematically in Figure 4.8. This is a more likely defect caused by flow-accelerated corrosion, which is called here a “smooth defect”.

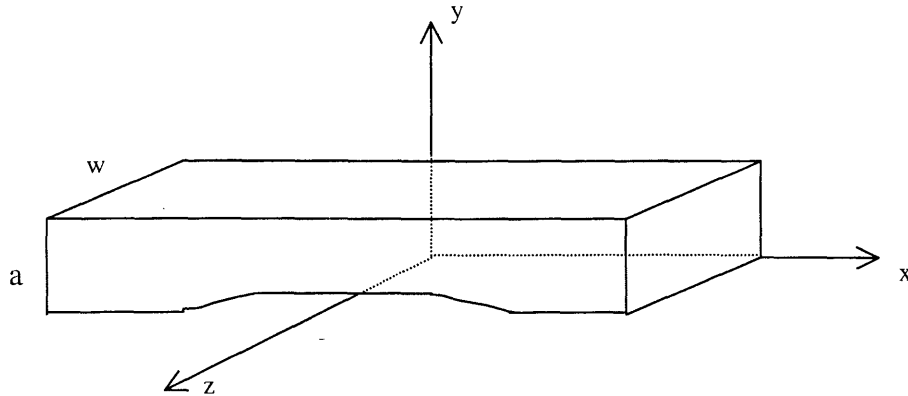


Figure 4.8 – Schematic view of a semi-infinite plate with smooth defect
(assume infinite in the x direction).

In two dimensions, the general problem can be described by the following equations:

$$\nabla^2 \varphi(x, y) = 0,$$

$$\left. \frac{\partial \varphi}{\partial y} \right|_{y=a} = \frac{\rho S_0}{w} [\delta(x-l) - \delta(x+l)],$$

$$\underline{n} \cdot \nabla \varphi|_{S_1} = \left(\frac{\partial \varphi}{\partial y} - \Delta, \frac{\partial \varphi}{\partial x} \right)_{S_1} = 0,$$

$$\varphi|_{x=\pm\infty} = 0.$$

The surface S_1 can be defined as $S_1(x, y) \equiv y - \Delta(x) = 0$, where $\Delta(x)$ represents the defect amplitude, and its normal vector as

$$\underline{n} = \frac{(e_y - \Delta' e_x)}{(1 + \Delta'^2)^{1/2}},$$

where $\Delta' = \frac{d\Delta}{dx}$.

The potential function can be written as $\varphi = \varphi_0 + \varphi_1 + \varphi_2$, where φ_0 is the potential function for a plate without defect, and φ_1 and φ_2 are the potential functions that consider first and second order solution for the defect, respectively.

The solution to the potential function φ_0 is given by Equation 4.26:

$$\varphi_0(x, y) = \frac{\rho S_0}{2\pi w} \ln \frac{\cosh \frac{\pi(l+x)}{a} + \cos \frac{\pi y}{a}}{\cosh \frac{\pi(l-x)}{a} + \cos \frac{\pi y}{a}}. \quad (4.43)$$

The next step is to find a solution for the potential function φ_1 . The Laplace equation and the boundary conditions are

$$\nabla^2 \varphi_1(x, y) = 0, \quad (4.44)$$

$$\left. \frac{\partial \varphi_1}{\partial y} \right|_{y=a} = 0, \quad (4.45)$$

$$\left(\frac{\partial \varphi}{\partial y} - \Delta' \frac{\partial \varphi}{\partial x} \right) \Big|_{S_1} = 0.$$

Expanding the last boundary condition about $y = 0$ yields to Equation 4.32:

$$\left(\frac{\partial \varphi_1}{\partial y} + \Delta \frac{\partial^2 \varphi_0}{\partial y^2} - \Delta' \frac{\partial \varphi_0}{\partial x} \right) \Big|_{y=0} = 0, \text{ or}$$

$$\left. \frac{\partial \varphi_1}{\partial y} \right|_{y=0} = \frac{\partial}{\partial x} \left(\Delta \frac{\partial \varphi_0}{\partial x} \right) \Big|_{y=0}. \quad (4.46)$$

Equations 4.33 and 4.34 give the potential function φ_1 and its Fourier transform $\hat{\varphi}_1$:

$$\varphi_1(x, y) = \int_{-\infty}^{\infty} e^{ikx} \hat{\varphi}_1(k, y) dk, \text{ and}$$

$$\hat{\varphi}_1(k, y) = \frac{1}{2\pi} \int_{-\infty}^{\infty} e^{-ikx} \varphi_1(x, y) dx.$$

Applying the Fourier transformation to equations 4.44, 4.45 and 4.46 and solving for the potential function φ_1 results in

$$\varphi_1(x, y) = -\frac{1}{2\pi} \int_0^{\infty} dx' \left. \frac{\partial}{\partial x'} \left(\Delta \frac{\partial \varphi_0}{\partial x'} \right) \right|_{y=0} \ln \left[\frac{\cosh \frac{\pi(x+x')}{a} + \cos \frac{\pi(y-a)}{a}}{\cosh \frac{\pi(x'-x)}{a} + \cos \frac{\pi(y-a)}{a}} \right]. \quad (4.47)$$

Evaluating this potential function at the surface of the plate ($y = a$) gives

$$\varphi_1(x) \Big|_{y=a} = -\frac{1}{2\pi} \int_0^{\infty} dx' \left. \frac{\partial}{\partial x'} \left(\Delta \frac{\partial \varphi_0}{\partial x'} \right) \right|_{y=0} \ln \left[\frac{\cosh \frac{\pi(x+x')}{a} + 1}{\cosh \frac{\pi(x'-x)}{a} + 1} \right].$$

Using trigonometric identity and integration by parts this equation can be simplified to

$$\varphi_1(x) \Big|_{y=a} = \frac{\rho S_0}{4a^2 w_0} \int_0^{\infty} \Delta(x') \left[\tanh \frac{\pi(l+x)}{2a} + \tanh \frac{\pi(l-x)}{2a} \right] \left[\tanh \frac{\pi(x'+x)}{2a} + \tanh \frac{\pi(x-x')}{2a} \right] dx'. \quad (4.48)$$

The final step is to find a solution for the potential function φ_2 . The Laplace equation and the boundary conditions are

$$\nabla^2 \varphi_2(x, y) = 0, \quad (4.49)$$

$$\left. \frac{\partial \varphi_2}{\partial y} \right|_{y=a} = 0, \quad (4.50)$$

$$\left(\frac{\partial \varphi}{\partial y} - \Delta, \frac{\partial \varphi}{\partial x} \right)_{S_1} = 0. \quad (4.51)$$

Expanding the last boundary condition and considering the second order term gives

$$\left. \frac{\partial \varphi_2}{\partial y} \right|_{y=0} = \frac{\partial}{\partial x} \left(\Delta \frac{\partial \varphi_1}{\partial x} \right)_{y=0}. \quad (4.52)$$

The potential function φ_2 and its Fourier transform $\hat{\varphi}_2$ are given, by definition, as

$$\varphi_2(x, y) = \int_{-\infty}^{\infty} e^{ikx} \hat{\varphi}_2(k, y) dk, \text{ and} \quad (4.53)$$

$$\hat{\varphi}_2(k, y) = \frac{1}{2\pi} \int_{-\infty}^{\infty} e^{-ikx} \varphi_2(x, y) dx. \quad (4.54)$$

Taking the Fourier transformation of equations 4.49, 4.50 and 4.52 and solving for the potential function φ_2 gives

$$\varphi_2(x, y) = -\frac{1}{2\pi} \int_0^{\infty} dx' \frac{\partial}{\partial x'} \left(\Delta \frac{\partial \varphi_1}{\partial x'} \right)_{y=0} \ln \left[\frac{\cosh \frac{\pi(x+x')}{a} + \cos \frac{\pi(y-a)}{a}}{\cosh \frac{\pi(x'-x)}{a} + \cos \frac{\pi(y-a)}{a}} \right]. \quad (4.55)$$

Evaluating this potential function at the surface of the plate ($y = a$) produces

$$\varphi_2(x) \Big|_{y=a} = \frac{1}{2a} \int_0^{\infty} dx' \Delta(x') \frac{\partial \varphi_1}{\partial x'} \Big|_{y=0} \left[\tanh \frac{\pi(x'+x)}{2a} + \tanh \frac{\pi(x-x')}{2a} \right]. \quad (4.56)$$

The term $\frac{\partial \varphi_1}{\partial x'} \Big|_{y=0}$ can be evaluated as

$$\frac{\partial \varphi_1}{\partial x'} \Big|_{y=0} = \frac{1}{2\pi} \int_0^{\infty} dx'' \left[\Delta \frac{\partial^3 \varphi_0}{\partial x''^3} + 2 \frac{d\Delta}{dx''} \frac{\partial^2 \varphi_0}{\partial x''^2} + \frac{d^2 \Delta}{dx''^2} \frac{\partial \varphi_0}{\partial x''} \right]_{y=0} \ln \left[\cosh \frac{\pi x''}{a} - \cosh \frac{\pi x'}{a} \right]^2. \quad (4.57)$$

The details of this derivation are presented in Appendix F. The integrand has a logarithmic singularity when $x' = x''$, but this singularity is integrable if Δ and φ_0 are sufficiently smooth. In this case, at the singularity $x' = x''$ Equation 4.57 becomes

$$\frac{\partial \varphi_1}{\partial x'} \Big|_{y=0} \approx \frac{\delta x}{\pi} \left[\Delta \frac{\partial^3 \varphi_0}{\partial x'^3} + 2 \frac{d\Delta}{dx''} \frac{\partial^2 \varphi_0}{\partial x''^2} + \frac{d^2 \Delta}{dx''^2} \frac{\partial \varphi_0}{\partial x''} \right]_{y=0} \left[\ln \left(\frac{\pi \delta x}{a} \sinh \frac{\pi x'}{a} \right)^2 - 2 \right], \quad (4.58)$$

where δx is a small increment about the singularity point. The details of this analysis are shown in Appendix F. Suppose we have a smooth defect given by the equation below:

$$\Delta(x) = h \left[\frac{\tanh \frac{(c+x)}{s} + \tanh \frac{(c-x)}{s}}{2 \tanh(c/s)} \right], \quad (4.59)$$

where h , c and s are parameters shown in Figure 4.9. In this case the parameters are $c = 101.6 \text{ mm}$, $s = 50.8 \text{ mm}$ and $h = 6.3 \text{ mm}$.

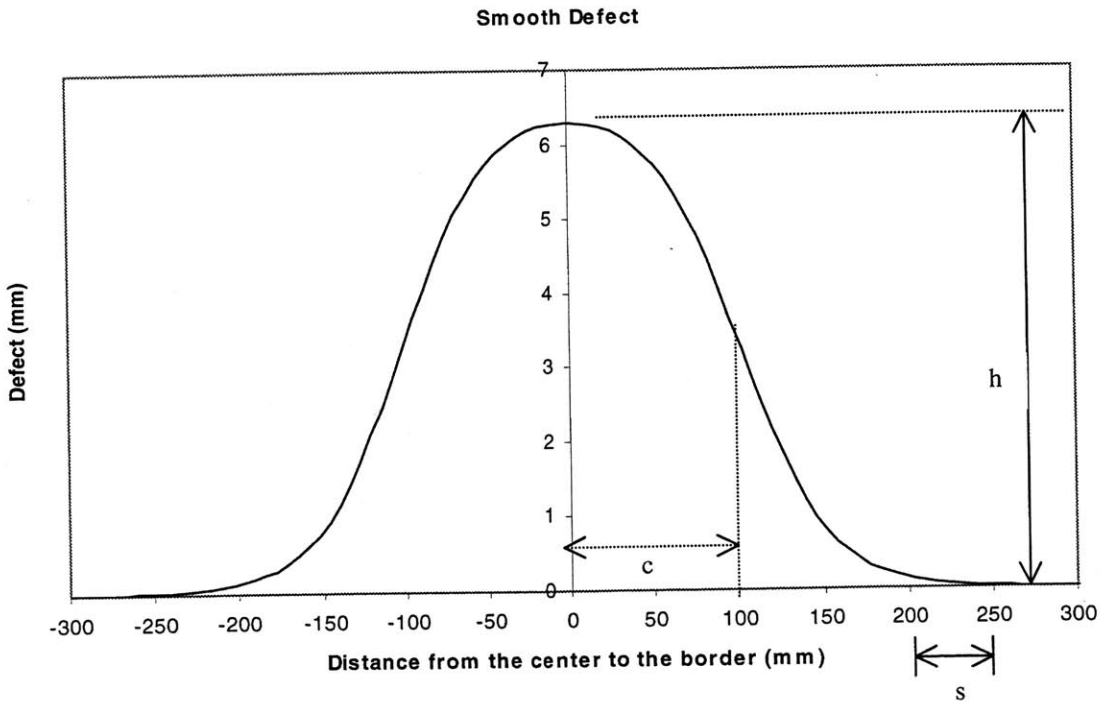


Figure 4.9 – Smooth defect given by Equation 4.59.

Evaluating the first and second derivatives of this function with respect to x , as well as the derivatives of the potential function φ_0 with respect to x , the potential function φ_2 evaluated at $y = a$ may be calculated, which is given by Equation 4.56. This result added to the potential functions $\varphi_0|_{y=a}$ and $\varphi_1|_{y=a}$ gives the solution to the forward problem for a smooth defect given by Equation 4.59. Appendix F shows the derivations of equations 4.47, 4.48, 4.52, 4.55 and 4.56.

A program in MATLAB was developed to solve this problem. Appendix G has a listing of this code called “forward_smooth”. Figure 4.10 shows the result of this analysis for the defect shown in Figure 4.9. An experimental result to compare with the analytic one was not performed.

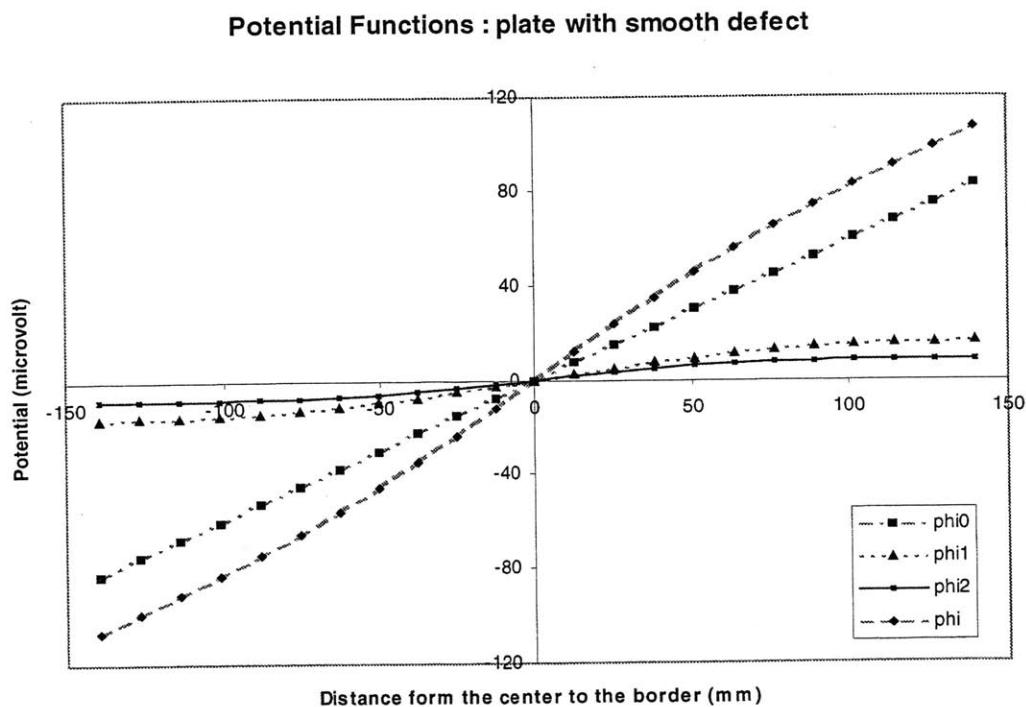


Figure 4.10 – Analytic potential functions for a plate with smooth defect

4.1.6 Correction for the cylindrical geometry

Consider a pipe without defect, which is infinitely long in the z-direction, as shown in Figure 4.11. The Laplace equation can be rewritten in cylindrical coordinates as

$$\begin{aligned}\nabla^2 \varphi(r, \theta, Z) &= 0, \\ \frac{1}{r} \frac{\partial}{\partial r} r \frac{\partial \varphi}{\partial r} + \frac{1}{r^2} \frac{\partial^2 \varphi}{\partial \theta^2} + \frac{\partial^2 \varphi}{\partial Z^2} &= 0, \\ \frac{\partial^2 \varphi}{\partial r^2} + \frac{1}{r} \frac{\partial \varphi}{\partial r} + \frac{1}{r^2} \frac{\partial^2 \varphi}{\partial \theta^2} + \frac{\partial^2 \varphi}{\partial Z^2} &= 0.\end{aligned}\tag{4.60}$$

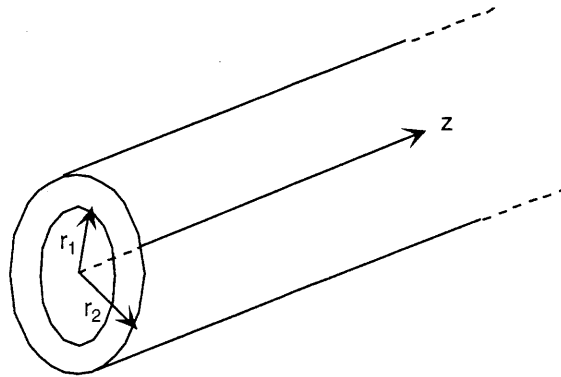


Figure 4.11 – Schematic view of a semi-infinite pipe without defect

Consider the variables below

$$r_0 = \frac{r_1 + r_2}{2} \quad (\text{mean radius of the pipe}), \text{ and}$$

$$a = r_2 - r_1 \quad (\text{wall thickness of the pipe}).$$

Making the following change of variables, the pipe may be approximated as a plate and a correction term for the cylindrical geometry can be calculated:

$$r = r_0 + y - \frac{a}{2},$$

$$\theta = \frac{z}{r_0},$$

$$Z = x.$$

Equation 4.60 becomes

$$\frac{\partial^2 \varphi}{\partial y^2} + \frac{1}{r_0 + y - \frac{a}{2}} \frac{\partial \varphi}{\partial y} + \frac{r_0^2}{(r_0 + y - \frac{a}{2})^2} \frac{\partial^2 \varphi}{\partial z^2} + \frac{\partial^2 \varphi}{\partial x^2} = 0.$$

Assuming a small wall thickness compared to the mean radius of the pipe, that is

$y - \frac{a}{2} \ll r_0$, the equation above can be approximated as

$$\frac{\partial^2 \varphi}{\partial y^2} + \frac{\partial^2 \varphi}{\partial z^2} + \frac{\partial^2 \varphi}{\partial x^2} \approx -\frac{1}{r_0} \frac{\partial \varphi}{\partial y} + \frac{2(y - \frac{a}{2})}{r_0} \frac{\partial^2 \varphi}{\partial z^2}. \quad (4.61)$$

Expanding the potential function to find the cylindrical correction the solution can be written as

$$\varphi(x, y, z) \approx \varphi_0(x, y) + \varphi_c(x, y, z), \quad (4.62)$$

where $\varphi_0(x, y)$ is the potential function for a non-defect region and $\varphi_c(x, y, z)$ is the correction term for cylindrical geometry. Considering first order approximations, the problem can be stated as

$$\frac{\partial^2 \varphi_0}{\partial x^2} + \frac{\partial^2 \varphi_0}{\partial y^2} = 0,$$

$$\frac{\partial^2 \varphi_c}{\partial x^2} + \frac{\partial^2 \varphi_c}{\partial y^2} + \frac{\partial^2 \varphi_c}{\partial z^2} = -\frac{1}{r_0} \frac{\partial \varphi_0}{\partial y},$$

with the boundary conditions

$$\left. \frac{\partial \varphi_0}{\partial y} \right|_{y=a} = \frac{S_0 \rho}{w} [\delta(x-l) - \delta(x+l)],$$

$$\left. \frac{\partial \varphi_0}{\partial y} \right|_{y=\Delta_0} = 0,$$

$$\left. \frac{\partial \varphi_c}{\partial y} \right|_{y=a} = 0,$$

$$\left. \frac{\partial \varphi_c}{\partial y} \right|_{y=\Delta_0} = 0,$$

where $w = 2\pi r_0$.

The solution for the non-defect region has already been calculated. From Equation 4.40

$$\varphi_0(x, y) = -\frac{i\rho S_0}{\pi w} \int_{-\infty}^{\infty} e^{ikx} \frac{\sin kl}{k \sinh k(a - \Delta_0)} \cosh k(y - \Delta_0) dk,$$

$$\varphi_0(x, y) = \frac{\rho S_0}{2\pi w} \ln \frac{\cosh \frac{\pi(l+x)}{(a - \Delta_0)} + \cos \frac{\pi(y - \Delta_0)}{(a - \Delta_0)}}{\cosh \frac{\pi(l-x)}{(a - \Delta_0)} + \cos \frac{\pi(y - \Delta_0)}{(a - \Delta_0)}}.$$

For a uniform slot defect the correction term is not a function of z , therefore the problem can be stated as

$$\frac{\partial^2 \varphi_c}{\partial x^2} + \frac{\partial^2 \varphi_c}{\partial y^2} = -\frac{1}{r_0} \frac{\partial \varphi_0}{\partial y},$$

$$\left. \frac{\partial \varphi_c}{\partial y} \right|_{y=a} = 0,$$

$$\left. \frac{\partial \varphi_c}{\partial y} \right|_{y=\Delta_0} = 0.$$

Solving this system for the potential function φ_c gives

$$\varphi_c(x, a) = \frac{\rho S_0}{4 w r_0} [|l+x| - |l-x|]. \quad (4.63)$$

Appendix H shows the derivation of this equation. From Equation 4.62

$$\varphi(x, a) = \varphi_0(x, a) + \varphi_c(x, a),$$

$$\varphi(x, a) = \frac{\rho S_0}{4 w} \left\{ \frac{1}{r_0} [|l+x| - |l-x|] + \frac{2}{\pi} \ln \frac{\cosh \frac{\pi(l+x)}{(a-\Delta_0)} + \cos \frac{\pi(a-\Delta_0)}{(a-\Delta_0)}}{\cosh \frac{\pi(l-x)}{(a-\Delta_0)} + \cos \frac{\pi(a-\Delta_0)}{(a-\Delta_0)}} \right\}. \quad (4.64)$$

This equation gives the potential function at the surface of a pipe without defect. It was calculated approximating a pipe as a plate and then making a correction for the cylindrical geometry. It is valid for pipes with a large ratio between the external radius and the wall thickness ($r_2 \gg a$).

4.1.7 Three-dimensional solution for a pipe with a non-symmetric defect

Consider a pipe similar to that shown in Figure 4.11, but with a non-symmetric defect in its inner surface. Figure 4.12 shows a schematic view of this pipe.

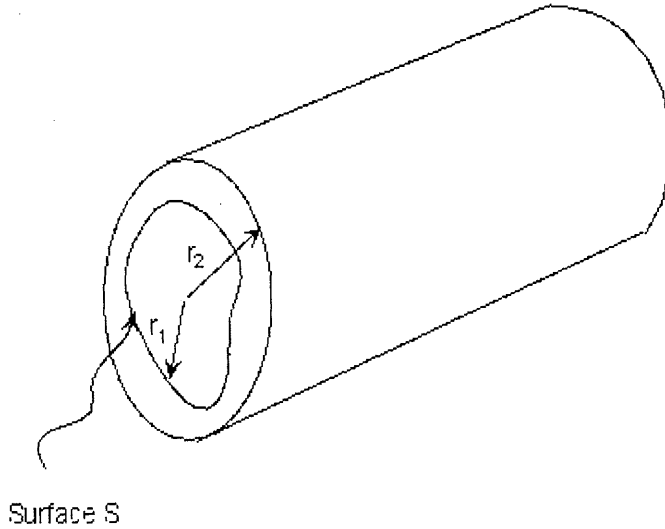


Figure 4.12 – Schematic view of a pipe with a non-symmetric defect.

Assuming a small wall thickness compared to the mean radius of the pipe, the Laplace equation is written as

$$\frac{\partial^2 \varphi}{\partial y^2} + \frac{\partial^2 \varphi}{\partial z^2} + \frac{\partial^2 \varphi}{\partial x^2} \approx -\frac{1}{r_0} \frac{\partial \varphi}{\partial y} + \frac{2(y - a/2)}{r_0} \frac{\partial^2 \varphi}{\partial z^2}.$$

The potential function can be expressed as

$$\varphi(x, y, z) \approx \varphi_0(x, y) + \varphi_1(x, y, z) + \varphi_2(x, y, z) + \varphi_c(x, y, z), \quad (4.65)$$

where $\varphi_0(x, y)$ is the potential function for a non-defect region, $\varphi_1(x, y, z)$ and $\varphi_2(x, y, z)$ are the potential functions that account for the defect region, and $\varphi_c(x, y, z)$ is the correction term for cylindrical geometry.

The basic equations are

$$\frac{\partial^2 \varphi_0}{\partial x^2} + \frac{\partial^2 \varphi_0}{\partial y^2} = 0, \quad (4.66)$$

$$\frac{\partial^2 \varphi_1}{\partial x^2} + \frac{\partial^2 \varphi_1}{\partial y^2} + \frac{\partial^2 \varphi_1}{\partial z^2} = 0, \quad (4.67)$$

$$\frac{\partial^2 \varphi_2}{\partial x^2} + \frac{\partial^2 \varphi_2}{\partial y^2} + \frac{\partial^2 \varphi_2}{\partial z^2} = 0, \text{ and} \quad (4.68)$$

$$\frac{\partial^2 \varphi_c}{\partial x^2} + \frac{\partial^2 \varphi_c}{\partial y^2} + \frac{\partial^2 \varphi_c}{\partial z^2} = -\frac{1}{r_0} \frac{\partial \varphi_0}{\partial y}. \quad (4.69)$$

The surface S can be defined as $S(R, \theta, Z) \equiv R - F(\theta, Z) = 0$, where $F(\theta, Z)$ represents the defect amplitude. The boundary condition at the surface S is

$$J_n = \underline{n} \cdot \nabla \varphi|_S = 0,$$

where $\underline{n} \propto \underline{e}_R - \frac{1}{R} \frac{\partial F}{\partial \theta} \underline{e}_\theta - \frac{\partial F}{\partial Z} \underline{e}_z$. Thus,

$$\left(\frac{\partial \varphi}{\partial R} - \frac{1}{R^2} \frac{\partial F}{\partial \theta} \frac{\partial \varphi}{\partial \theta} - \frac{\partial F}{\partial Z} \frac{\partial \varphi}{\partial Z} \right)_S = 0.$$

Writing the equation above in slab coordinates gives

$$\left[\frac{\partial \varphi}{\partial y} - \frac{r_0^2}{(r_0 + y - \frac{a}{2})^2} \frac{\partial \varphi}{\partial z} \frac{\partial F}{\partial z} - \frac{\partial \varphi}{\partial x} \frac{\partial F}{\partial x} \right]_S = 0. \quad (4.70)$$

The defect $\Delta(x, z)$ can be defined as

$$\Delta(x, z) = F(\theta, Z) - r_0 + \frac{a}{2},$$

therefore Equation 4.70 can be rewritten as

$$\left[\frac{\partial \phi}{\partial y} - \frac{r_0^2}{(r_0 + y - \frac{a}{2})^2} \frac{\partial \phi}{\partial z} \frac{\partial \Delta}{\partial z} - \frac{\partial \phi}{\partial x} \frac{\partial \Delta}{\partial x} \right]_{\Delta} = 0. \quad (4.71)$$

Expanding this equation about $\Delta = 0$ produces, for each order of magnitude indicated as a superscript index, the following equations:

$$\Delta^{(0)} : \left. \frac{\partial \phi_0}{\partial y} \right|_{y=0} = 0, \quad (4.72)$$

$$\Delta^{(1)} : \left[\frac{\partial \phi_1}{\partial y} - \frac{\partial}{\partial x} \left(\Delta \frac{\partial \phi_0}{\partial x} \right) \right]_{y=0} = 0, \quad (4.73)$$

$$\Delta^{(2)} : \left. \frac{\partial \phi_c}{\partial y} \right|_{y=0} = 0, \quad (4.74)$$

$$\left[\frac{\partial \phi_2}{\partial y} - \frac{\partial}{\partial x} \left(\Delta \frac{\partial \phi_1}{\partial x} \right) - \frac{\partial}{\partial z} \left(\Delta \frac{\partial \phi_1}{\partial z} \right) \right]_{y=0} = 0. \quad (4.75)$$

Appendix I shows how these equations are derived. The boundary conditions at the external surface of the pipe ($y = a$) are

$$\left. \frac{\partial \phi_0}{\partial y} \right|_{y=a} = \frac{S_0 \rho}{w} [\delta(x-l) - \delta(x+l)], \quad (4.76)$$

$$\left. \frac{\partial \phi_1}{\partial y} \right|_{y=a} = 0, \quad (4.77)$$

$$\left. \frac{\partial \phi_2}{\partial y} \right|_{y=a} = 0, \quad (4.78)$$

$$\left. \frac{\partial \varphi_c}{\partial y} \right|_{y=a} = 0. \quad (4.79)$$

The potential function φ_0 can be calculated using equations 4.66, 4.72 and 4.76. It has been solved previously and the solution is given by Equation 4.26. Thus,

$$\varphi_0(x, y) = \frac{\rho S_0}{2\pi w} \ln \frac{\cosh \frac{\pi(l+x)}{a} + \cos \frac{\pi y}{a}}{\cosh \frac{\pi(l-x)}{a} + \cos \frac{\pi y}{a}}.$$

The potential function φ_c can be calculated using the equations 4.69, 4.74 and 4.79. It also has been solved previously and the solution is given by Equation 4.63. Therefore,

$$\varphi_c(x, a) = \frac{\rho S_0}{4 w r_0} [|l+x| - |l-x|].$$

Equations 4.67, 4.73 and 4.77 provide the solution to the potential function φ_1 . By definition,

$$\begin{aligned} \varphi_1(x, y, z) &= \sum_{n=-\infty}^{\infty} e^{i \frac{2\pi n z}{w}} \varphi_{1n}(x, y), \\ \varphi_1(x, y, z) &= \sum_{n=-\infty}^{\infty} e^{i \frac{2\pi n z}{w}} \int_{-\infty}^{\infty} e^{ikx} \hat{\varphi}_{1n}(k, y) dk, \end{aligned} \quad (4.80)$$

where $\hat{\varphi}_{1n}(k, y)$ is the Fourier transform of $\varphi_{1n}(x, y)$.

Applying the Fourier transformation to the Laplace equation and its boundary conditions and solving for $\varphi_{1n}(x, y)$ gives

$$\varphi_{1n}(x) \Big|_{y=a} = \frac{1}{2\pi} \int_{-\infty}^{\infty} dk \int_{-\infty}^{\infty} dx' \frac{k \sin k(x-x')}{k_n \sinh k_n a} \Delta_n(x') \left. \frac{\partial \varphi_0}{\partial x'} \right|_{y=0}, \quad (4.81)$$

where $k_n = k^2 + \left(\frac{2\pi n}{w}\right)^2$ and $\Delta(x, z) = \sum_{n=-\infty}^{\infty} \Delta_n(x) e^{i \frac{2\pi n z}{w}}$.

Appendix I shows the derivation of this equation. An analogous approach can be followed for the potential function φ_2 using equations 4.68, 4.75 and 4.78. Appendix I also shows that

$$\varphi_{2m}(x)|_{y=a} = \frac{1}{2\pi} \sum_{n=-\infty}^{\infty} \int_{-\infty}^{\infty} dk \int_{-\infty}^{\infty} dx' \frac{\Delta_{m-n}(x')}{k_m \sinh k_m a} [k \sin k(x-x') \frac{\partial \varphi_{1n}}{\partial x} + (\frac{2\pi}{w})^2 m n \cos k(x-x') \varphi_{1n}]_{y=0} \quad (4.82)$$

Appendix J shows that equations 4.81 and 4.82 can be written in a more convenient form.

Therefore, the potential function $\varphi_1(x, y, z)$ can be calculated using the following equations:

$$\begin{aligned} \varphi_1(x, z)|_{y=a} &= \sum_{m=-\infty}^{\infty} e^{i\frac{2\pi mz}{w}} \varphi_{1m}(x), \\ \varphi_{1m}(x) &= \frac{1}{\pi} \int_{-\infty}^{\infty} dx' \Delta(x') \frac{\partial \varphi_0}{\partial x} \Big|_{y=0} S_m(x, x'), \\ S_m(x, x') &= \begin{cases} \int_0^{\infty} dk \frac{k \sin k(x-x')}{k_m \sinh k_m a}, & \text{for } m \neq 0 \\ \frac{\pi}{2a} \tanh \frac{\pi(x-x')}{2a}, & \text{for } m = 0 \end{cases} \end{aligned}$$

In addition, the potential function $\varphi_2(x, y, z)$ may be calculated using the equations below:

$$\begin{aligned} \varphi_2(x, z)|_{y=a} &= \sum_{m=-\infty}^{\infty} e^{i\frac{2\pi mz}{w}} \varphi_{2m}(x), \\ \varphi_{2m}(x) &= -\frac{1}{\pi^2} \sum_{n=-\infty}^{\infty} \int_{-\infty}^{\infty} dx' \int_{-\infty}^{\infty} dx'' \Delta_{m-n}(x') G_n \left[S_m \left(\frac{\partial^2}{\partial x''^2} \Delta_n(x'') \frac{\partial \varphi_0}{\partial x} \right) \Big|_{y=0} + \frac{2n\pi}{w} C_m \left(\frac{\partial}{\partial x''} \Delta_n(x'') \frac{\partial \varphi_0}{\partial x} \right) \Big|_{y=0} \right] \\ C_m(x, x') &= \begin{cases} \frac{2m\pi}{w} \int_0^{\infty} dk \frac{\cos k(x-x')}{k_m \sinh k_m a}, & \text{for } m \neq 0 \\ 0, & \text{for } m = 0 \end{cases} \end{aligned}$$

$$G_n(x', x'') = \begin{cases} K_0 \left(\left| \frac{2n\pi(x' - x'')}{w} \right| \right) + \int_0^\infty dk \cdot \frac{e^{-k_n a} \cos k'(x' - x'')}{k_n \sinh k_n a}, & \text{for } n \neq 0 \\ -\frac{1}{2} \ln \left[\sinh^2 \frac{\pi(x' - x'')}{2a} \right], & \text{for } n = 0 \end{cases}$$

4.2 Solution to the inverse problem

4.2.1 Solution for a 2D symmetric defect

Consider a semi-infinite plate with defect as shown in Figure 4.13.

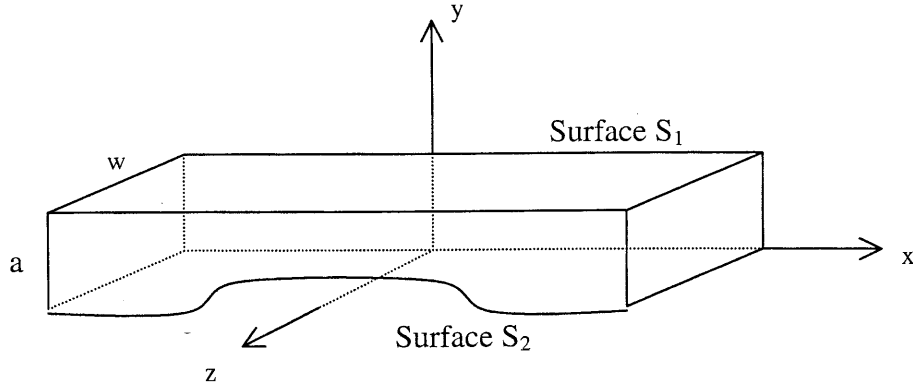


Figure 4.13 – Schematic view of a semi-infinite plate with symmetric defect (assume infinite in the x direction).

The surface S_1 is the top surface where the current is applied and the surface S_2 , defined as $y = \Delta(x, z)$, is the bottom surface with defect. Equations 4.1 through 4.5 are valid and the potential function can be written as $\varphi(x, y, z) = \varphi_0(x, y) + \varphi_1(x, y, z)$, where φ_0 and φ_1 are the potential functions that account for the non-defect region of the plate and the defect region of the plate, respectively. In this problem, $\varphi|_{S_1}$ as well as $\underline{n} \cdot \nabla \varphi|_{S_1}$ are given and we desire to find the contours of $\underline{n} \cdot \nabla \varphi = 0$, or in the other words, the surfaces where the normal current density (J_n) is zero.

Summarizing, this problem is described by the following equations:

$$\nabla^2 \varphi(x, y, z) = 0, \quad (4.83)$$

$$\left. \frac{\partial \varphi}{\partial y} \right|_{y=a} = \frac{S_0 \rho}{w} [\delta(x-l) - \delta(x+l)], \quad (4.84)$$

$$\varphi \Big|_{y=a} = \varphi_m(x, z), \quad (4.85)$$

where $\varphi_m(x, z)$ is the potential given by measurements.

The problem is to find $\Delta(x, z)$ so that $J_n = \underline{n} \cdot \nabla \varphi \Big|_{S_2} = 0$, where $\underline{n} \propto \underline{e}_y - \frac{\partial \Delta}{\partial x} \underline{e}_x - \frac{\partial \Delta}{\partial z} \underline{e}_z$.

Thus,

$$\left(\frac{\partial \varphi}{\partial y} - \frac{\partial \Delta}{\partial x} \frac{\partial \varphi}{\partial x} - \frac{\partial \Delta}{\partial z} \frac{\partial \varphi}{\partial z} \right) \Big|_{S_2} = 0. \quad (4.86)$$

The first part of this problem, which is the Laplace equation $\nabla^2 \varphi_0(x, y) = 0$ with boundary conditions $\underline{n} \cdot \nabla \varphi_0 \Big|_{S_1} = \rho S(x, z)$ and $\underline{n} \cdot \nabla \varphi_0 \Big|_{S_2} = 0$ has already been solved previously. The solution is given by Equation 4.41:

$$\varphi_0(x, y) = \frac{\rho S_0}{2\pi w} \ln \frac{\cosh \frac{\pi(l+x)}{(a-\Delta_0)} + \cos \frac{\pi(y-\Delta_0)}{(a-\Delta_0)}}{\cosh \frac{\pi(l-x)}{(a-\Delta_0)} + \cos \frac{\pi(y-\Delta_0)}{(a-\Delta_0)}}. \quad (4.87)$$

For a two-dimensional case, the second part of the problem can be stated as

$$\nabla^2 \varphi_1(x, y) = 0, \quad (4.88)$$

with boundary conditions

$$\underline{n} \cdot \nabla \varphi_1 \Big|_{y=a} = \frac{\partial \varphi_1}{\partial y} \Big|_{y=a} = 0, \text{ and} \quad (4.89)$$

$$\varphi_1 \Big|_{y=a} = \varphi_m(x) - \varphi_0(x, y=a) = \varphi_s(x). \quad (4.90)$$

Consider a small defect compared to the thickness ($\Delta \ll a$). The defect can be modeled as sum of the first and second order terms, which is

$$\Delta(x) \approx \Delta_1(x) + \Delta_2(x). \quad (4.91)$$

In a two-dimensional case, Equation 4.86 can be rewritten as

$$\left(\frac{\partial \varphi}{\partial y} - \frac{\partial \Delta}{\partial x} \frac{\partial \varphi}{\partial x} \right) \Big|_{S_2} = 0. \quad (4.92)$$

Expanding the equation above as a Taylor series about $y = \Delta_0$ gives

$$\Delta_1(x) = \Delta_0 + \frac{\int_{-\infty}^x \frac{\partial \varphi_1}{\partial y} \Big|_{y=\Delta_0} dx}{\frac{\partial \varphi_0}{\partial x} \Big|_{y=\Delta_0}}, \quad (4.93)$$

$$\Delta_2(x) = -(\Delta_1 - \Delta_0) \frac{\frac{\partial \varphi_1}{\partial x} \Big|_{y=\Delta_0}}{\frac{\partial \varphi_0}{\partial x} \Big|_{y=\Delta_0}}. \quad (4.94)$$

Equations 4.93 and 4.94 are derived in Appendix K.

From equations 4.33 and 4.34

$$\varphi_1(x, y) = \int_{-\infty}^{\infty} e^{ikx} \hat{\varphi}_1(k, y) dk, \text{ and} \quad (4.95)$$

$$\hat{\varphi}_1(k, y) = \frac{1}{2\pi} \int_{-\infty}^{\infty} e^{-ikx} \varphi_1(x, y) dx, \quad (4.96)$$

where $\hat{\varphi}_1(k, y)$ is the Fourier transform of $\varphi_1(x, y)$.

Applying the Fourier transformation to the Laplace equation and to the boundary condition of Equation 4.89 gives

$$\frac{\partial^2 \hat{\varphi}_1}{\partial y^2} - k^2 \hat{\varphi}_1 = 0, \quad (4.97)$$

$$\left. \frac{\partial \hat{\phi}_1}{\partial y} \right|_{y=a} = 0. \quad (4.98)$$

The general solution to the Equation 4.97 with the boundary condition above is

$$\hat{\phi}_1(k, y) = B(k) \cosh k(y - a).$$

Substituting this solution into Equation 4.95 results in

$$\phi_1(x, y) = \int_{-\infty}^{\infty} e^{ikx} B(k) \cosh k(y - a) dk. \quad (4.99)$$

Thus,

$$\left. \frac{\partial \phi_1}{\partial y} \right|_{y=\Delta_0} = \int_{-\infty}^{\infty} e^{ikx} B(k) k \sinh k(\Delta_0 - a) dk. \quad (4.100)$$

The coefficient $B(k)$ can be defined as

$$B(k) = \hat{\phi}_1(k, a),$$

$$B(k) = \frac{1}{2\pi} \int_{-\infty}^{\infty} e^{-ikx} \phi_1(x, a) dx.$$

The boundary condition defined by Equation 4.90 is

$$\phi_1|_{y=a} = \phi_m(x) - \phi_0(x) = \phi_s(x),$$

thus

$$B(k) = \frac{1}{2\pi} \int_{-\infty}^{\infty} e^{-ikx} \phi_s(x) dx. \quad (4.101)$$

Since the potential measurement ϕ_m is given by a set of data, Equation 4.101 has to be calculated numerically. Basically, the problem consists of solving Equation 4.101, plugging the result into Equation 4.100 and then calculating the defect solution by solving Equation 4.93. A program in MATLAB was developed to numerically solve this

system of integrals. Appendix L has a description of the integrals and a listing of this code, entitled “inverse _first_data”.

4.2.2 Alternative approach for the 2D inverse problem

The previous solution used the parameter Δ_0 to correct the boundary condition at infinity. Although this approach provides a good result, it introduces a new parameter that needs to be evaluated iteratively. A solution can also be developed without using the parameter Δ_0 .

Expanding the boundary condition of Equation 4.92 about $y = 0$, the following equations are obtained for a 2D case:

$$\Delta_1(x) = \frac{\int_{-\infty}^x \left. \frac{\partial \varphi_1}{\partial y} \right|_{y=0} dx'}{\left. \frac{\partial \varphi_0}{\partial x} \right|_{y=0}}, \quad (4.102)$$

$$\Delta_2(x) = -\Delta_1(x) \frac{\left. \frac{\partial \varphi_1}{\partial x} \right|_{y=0}}{\left. \frac{\partial \varphi_0}{\partial x} \right|_{y=0}}. \quad (4.103)$$

The potential function φ_0 is given by Equation 4.26. Therefore,

$$\varphi_0(x, y) = \frac{\rho S_0}{2\pi w} \ln \frac{\cosh \frac{\pi(l+x)}{a} + \cos \frac{\pi y}{a}}{\cosh \frac{\pi(l-x)}{a} + \cos \frac{\pi y}{a}}.$$

From this equation the denominator of equations 4.102 and 4.103 can be evaluated. Thus,

$$\left. \frac{\partial \varphi_0}{\partial x} \right|_{y=0} = \frac{\rho S_0}{2wa} \left[\tanh \frac{\pi(l+x)}{2a} + \tanh \frac{\pi(l-x)}{2a} \right]. \quad (4.104)$$

The potential function φ_1 can be defined as

$$\varphi_1(x, y) = \tilde{\varphi}_1(x, y) + \varphi_\infty \tanh \frac{\pi x}{2a}, \quad (4.105)$$

where $\varphi_\infty = (\varphi_m - \varphi_0|_{y=a})_{x \rightarrow \infty}$ is defined so that $\tilde{\varphi}_1|_a = 0$ as $|x| \rightarrow \infty$.

The function $\tilde{\varphi}_1(x, y)$ satisfies

$$\nabla^2 \tilde{\varphi}_1 = -\varphi_\infty \nabla^2 \tanh \frac{\pi x}{2a}, \quad (4.106)$$

$$\left. \frac{\partial \tilde{\varphi}_1}{\partial y} \right|_{y=a} = 0, \quad (4.107)$$

$$\tilde{\varphi}_1|_{y=a} = \varphi_m - \varphi_0|_a - \varphi_\infty \tanh \frac{\pi x}{2a}. \quad (4.108)$$

By definition,

$$\tilde{\varphi}_1(x, y) = \int_{-\infty}^{\infty} e^{ikx} \hat{\tilde{\varphi}}_1(k, y) dk, \text{ and}$$

$$\hat{\tilde{\varphi}}_1(k, y) = \frac{1}{2\pi} \int_{-\infty}^{\infty} e^{-ikx} \tilde{\varphi}_1(x, y) dx.$$

Taking the Fourier transformation of equations 4.106, 4.107 and 4.108 and solving for

the function $\hat{\tilde{\varphi}}_1(k, y)$ gives

$$\hat{\tilde{\varphi}}_1 = i \left\{ \frac{\varphi_\infty a}{\pi} \frac{1}{\sinh ka} + \left[\delta\hat{\varphi} - \frac{\varphi_\infty a}{\pi} \frac{1}{\sinh ka} \right] \cosh k(y-a) \right\}, \quad (4.109)$$

where

$$\delta\hat{\varphi} = -\frac{1}{\pi} \int_0^{\infty} \sin kx \left[\varphi_m - \varphi_0|_a - \varphi_\infty \tanh \frac{\pi x}{2a} \right] dx. \quad (4.110)$$

Equation 4.109 is derived in Appendix M.

In order to avoid the ill-conditioned part of this solution the short wavelengths must be suppressed. This can be done introducing a damping factor to the solution above.

Consider

$$\hat{\varphi}_1 = i \left\{ \frac{\varphi_\infty a}{\pi} \frac{1}{\sinh ka} + \left[\delta\hat{\varphi} - \frac{\varphi_\infty a}{\pi} \frac{1}{\sinh ka} \right] \cosh k(y-a) e^{-\frac{k^2}{k_m^2}} \right\}, \quad (4.111)$$

where k_m is a damping parameter.

Appendix M also shows that the numerator of the Equation 4.102, called $Num(x)$, can be evaluated as

$$Num(x) = \frac{\varphi_\infty a k_m}{\sqrt{\pi}} e^{-\frac{k_m^2 x^2}{4}} - 2 \int_0^\infty dk \cos kx (\delta\hat{\varphi} \sinh ka) e^{-\frac{k^2}{k_m^2}}. \quad (4.112)$$

Equations 4.104, 4.110 and 4.112 are used to calculate the first order approximation of the defect given by Equation 4.102.

In order to calculate the second order approximation of the defect given by Equation

4.103 the term $\left. \frac{\partial \varphi_1}{\partial x} \right|_{y=0}$ must be determined. Appendix M shows that this term is given by

$$\left. \frac{\partial \varphi_1}{\partial x} \right|_{y=0} = -2 \int_0^\infty dk k \cos kx \left[\delta\hat{\varphi} - \frac{\varphi_\infty a}{\pi \sinh ka} \right] \cosh ka e^{-\frac{k^2}{k_m^2}}. \quad (4.113)$$

Equations 4.113 and 4.104 are used to calculate $\Delta_2(x)$ given by Equation 4.103. A

MATLAB code called “inverse_second” was developed to numerically solve these integrals and calculate the defect to a second order of approximation. Appendix N has a listing of this code.

4.2.3 Solution for a 3D cylindrical non-symmetric defect

Consider a pipe as shown in Figure 4.12. The surface S can be defined as

$S(R, \theta, Z) \equiv R - F(\theta, Z) = 0$, where $F(\theta, Z)$ represents the defect amplitude. In slab coordinates the defect amplitude may be defined as $\Delta(x, z) = F(\theta, Z) - r_0 + \frac{a}{2}$. The

potential function can be expanded as

$$\varphi(x, y, z) \approx \varphi_0(x, y) + \varphi_1(x, y, z) + \varphi_c(x, y, z). \quad (4.114)$$

The problem is described by the following equations:

$$\frac{\partial^2 \varphi}{\partial y^2} + \frac{\partial^2 \varphi}{\partial z^2} + \frac{\partial^2 \varphi}{\partial x^2} \approx -\frac{1}{r_0} \frac{\partial \varphi}{\partial y} + \frac{2(y - a/2)}{r_0} \frac{\partial^2 \varphi}{\partial z^2}, \quad (4.115)$$

$$\left. \frac{\partial \varphi}{\partial y} \right|_{y=a} = \frac{S_0 \rho}{w} [\delta(x-l) - \delta(x+l)], \quad (4.116)$$

$$\varphi|_{y=a} = \varphi_m(x, z), \quad (4.117)$$

where $w = 2\pi r_0$ and $\varphi_m(x, z)$ is the potential given by measurements.

The problem is to find $\Delta(x, z)$ so that $J_n = \underline{n} \cdot \nabla \varphi|_S = 0$,

where $\underline{n} \propto \underline{e}_R - \frac{1}{R} \frac{\partial F}{\partial \theta} \underline{e}_\theta - \frac{\partial F}{\partial Z} \underline{e}_z$. Thus,

$$\left(\frac{\partial \varphi}{\partial R} - \frac{1}{R^2} \frac{\partial F}{\partial \theta} \frac{\partial \varphi}{\partial \theta} - \frac{\partial F}{\partial Z} \frac{\partial \varphi}{\partial Z} \right)_S = 0.$$

Writing the equation above in slab coordinates gives

$$\left[\frac{\partial \varphi}{\partial y} - \frac{r_0^2}{(r_0 + y - \frac{a}{2})^2} \frac{\partial \varphi}{\partial z} \frac{\partial F}{\partial z} - \frac{\partial \varphi}{\partial x} \frac{\partial F}{\partial x} \right]_S = 0,$$

$$\left[\frac{\partial \varphi}{\partial y} - \frac{r_0^2}{(r_0 + y - \frac{a}{2})^2} \frac{\partial \varphi}{\partial z} \frac{\partial \Delta}{\partial z} - \frac{\partial \varphi}{\partial x} \frac{\partial \Delta}{\partial x} \right]_{\Delta} = 0. \quad (4.118)$$

The first part of this problem, which is the Laplace equation $\nabla^2 \varphi_0(x, y) = 0$ with boundary conditions $\underline{n} \cdot \nabla \varphi_0|_{y=a} = \rho S(x, z)$ and $\underline{n} \cdot \nabla \varphi_0|_S = 0$ has already been solved previously. The solution is given by Equation 4.26:

$$\varphi_0(x, y) = \frac{\rho S_0}{2\pi w} \ln \frac{\cosh \frac{\pi(l+x)}{a} + \cos \frac{\pi y}{a}}{\cosh \frac{\pi(l-x)}{a} + \cos \frac{\pi y}{a}}.$$

The second part of the problem can be stated as

$$\nabla^2 \varphi_1(x, y, z) = 0, \quad (4.119)$$

$$\underline{n} \cdot \nabla \varphi_1|_{y=a} = \frac{\partial \varphi_1}{\partial y}|_{y=a} = 0, \quad (4.120)$$

$$\varphi_1|_{y=a} = \varphi_m(x, z) - \varphi_0(x, a) - \varphi_c(x, a). \quad (4.121)$$

Consider a small defect compared to the thickness ($\Delta \ll a$). The defect can be written as sum of the first and second order terms, which is

$$\Delta(x, z) \approx \Delta_1(x, z) + \Delta_2(x, z).$$

Expanding Equation 4.118 as a Taylor series about $y = 0$ gives

$$\left[\frac{\partial \varphi_1}{\partial y} - \frac{\partial}{\partial x} \left(\Delta_1 \frac{\partial \varphi_0}{\partial x} \right) \right]_{y=0} = 0, \quad (4.122)$$

$$\left[\frac{\partial}{\partial x} \left(\Delta_2 \frac{\partial \varphi_0}{\partial x} + \Delta_1 \frac{\partial \varphi_1}{\partial x} \right) + \frac{\partial}{\partial z} \left(\Delta_1 \frac{\partial \varphi_1}{\partial z} \right) \right]_{y=0} = 0. \quad (4.123)$$

Appendix O shows the derivation of equations 4.122 and 4.123. One can see that from

Equation 4.122

$$\Delta_1(x, z) = \frac{\int_{-\infty}^x \frac{\partial \varphi_1}{\partial y} \Big|_{y=0} dx'}{\frac{\partial \varphi_0}{\partial x} \Big|_{y=0}}, \quad (4.124)$$

and from Equation 4.123

$$\left[\Delta_2 \frac{\partial \varphi_0}{\partial x} + \Delta_1 \frac{\partial \varphi_1}{\partial x} + \int_{-\infty}^x dx' \frac{\partial}{\partial z} \left(\Delta_1 \frac{\partial \varphi_1}{\partial z} \right) \right]_{y=0} = 0. \quad (4.125)$$

The potential function φ_1 can be defined as

$$\varphi_1(x, y, z) = \tilde{\varphi}_1(x, y, z) + \sigma + \delta \tanh \frac{\pi x}{2a}, \quad (4.126)$$

$$\text{where } \sigma = \frac{1}{2} [\varphi(\infty) + \varphi(-\infty)], \quad (4.127)$$

$$\delta = \frac{1}{2} [\varphi(\infty) - \varphi(-\infty)], \quad (4.128)$$

$$\varphi(\infty) = \left[\varphi_m - \frac{\rho S_0 l}{wa} - \frac{\rho S_0 l}{2r_0 w} \right]_{x \rightarrow \infty}, \quad (4.129)$$

$$\varphi(-\infty) = \left[\varphi_m + \frac{\rho S_0 l}{wa} + \frac{\rho S_0 l}{2r_0 w} \right]_{x \rightarrow -\infty}, \quad (4.130)$$

are defined so that $\tilde{\varphi}_1|_{y=a} = 0$ as $|x| \rightarrow \infty$.

The function $\tilde{\varphi}_1(x, y, z)$ satisfies

$$\nabla^2 \tilde{\varphi}_1 = -\delta \nabla^2 \tanh \frac{\pi x}{2a}, \quad (4.131)$$

$$\left. \frac{\partial \tilde{\varphi}_1}{\partial y} \right|_{y=a} = 0, \quad (4.132)$$

$$\tilde{\varphi}_1|_{y=a} = \varphi_m - \varphi_0|_a - \frac{\rho S_0}{4 w r_0} [|l+x| - |l-x|] - \sigma - \delta \tanh \frac{\pi x}{2a}. \quad (4.133)$$

By definition,

$$\tilde{\varphi}_1(x, y, z) = \sum_{n=-\infty}^{\infty} e^{i \frac{2\pi n z}{w}} \varphi_{1n}(x, y), \quad (4.134)$$

$$\varphi_{1n}(x, y) = \int_{-\infty}^{\infty} e^{ikx} \hat{\varphi}_{1n}(k, y) dk, \quad (4.135)$$

$$\hat{\varphi}_{1n}(k, y) = \frac{1}{2\pi} \int_{-\infty}^{\infty} e^{-ikx} \varphi_{1n}(x, y) dx. \quad (4.136)$$

Taking the Fourier transformation of equations 4.131, 4.132 and 4.133 and solving for the function $\hat{\varphi}_{1n}(k, y)$ gives

$$\hat{\varphi}_{1m} = i \left\{ \delta_m \frac{\delta a}{\pi k_m^2} \frac{k^2}{\sinh ka} + \left[\hat{\Psi}_m - \delta_m \frac{\delta a}{\pi k_m^2} \frac{k^2}{\sinh ka} \right] \cosh k_m (y-a) \right\}, \quad (4.137)$$

where

$$k_m = \sqrt{k^2 + \left(\frac{2\pi m}{w} \right)^2}, \quad (4.138)$$

$$\hat{\Psi}_m(k) = \frac{1}{2\pi i w} \int_{-\infty}^{\infty} dx \int_0^w dz e^{i \frac{2\pi m z}{w}} e^{-ikx} \left\{ \varphi_m - \varphi_0|_a - \frac{\rho S_0}{4 w r_0} [|l+x| - |l-x|] - \sigma - \delta \tanh \frac{\pi x}{2a} \right\}, \quad (4.139)$$

$$\delta_m = \frac{1}{w} \int_0^w dz e^{-i \frac{2\pi m}{w} z} = \begin{cases} 1, & \text{if } m = 0 \\ 0, & \text{if } m \neq 0 \end{cases}. \quad (4.140)$$

Equation 4.137 is derived in Appendix O.

In order to avoid the ill-conditioned part of this solution the short wavelengths must be suppressed. This can be done introducing a damping factor to the solution above.

Consider

$$\hat{\phi}_{1m} = i \left\{ \frac{\delta_m}{\pi} \frac{\delta a}{\sinh ka} + \left[\hat{\Psi}_m - \frac{\delta_m}{\pi} \frac{\delta a}{\sinh ka} \right] \cosh k_m (y - a) e^{-\frac{k_m^2}{k_{\max}^2}} \right\}, \quad (4.141)$$

where k_{\max} is a damping parameter.

Assume

$$\Delta_1(x, z) = \sum_m \Delta_{1m}(x) e^{i \frac{2\pi m}{w} z}, \text{ and} \quad (4.142)$$

$$\Delta_{1m}(x) = \frac{\int_{-\infty}^x \frac{\partial \phi_{1m}}{\partial y} \Big|_{y=0} dx}{\frac{\partial \phi_0}{\partial x} \Big|_{y=0}}. \quad (4.143)$$

The term $\int_{-\infty}^x dx \frac{\partial \phi_{1m}}{\partial y} \Big|_{y=0}$ is given by

$$\int_{-\infty}^x dx \frac{\partial \phi_{1m}}{\partial y} \Big|_{y=0} = - \int_{-\infty}^{\infty} dk e^{\left(ikx - \frac{k_m^2}{k_{\max}^2} \right)} \hat{\Psi}_m \frac{k_m \sinh k_m a}{k} + \delta_m \frac{\delta a}{\sqrt{\pi}} k_{\max} e^{\left(\frac{k_{\max}^2 x^2}{4} \right)}. \quad (4.144)$$

The details of this derivation are presented in Appendix O. Equations 4.142 through 4.144 can be used to calculate the first order approximation of the defect given by Equation 4.124.

Assume

$$\Delta_2(x, z) = \sum_p \Delta_{2p}(x) e^{i \frac{2\pi p}{w} z}. \quad (4.145)$$

The second order approximation of the defect can be calculated applying Fourier analysis to Equation 4.125. Appendix O shows that

$$\Delta_{2p}(x) = \frac{1}{\left. \frac{\partial \varphi_0}{\partial x} \right|_{y=0}} \left\{ \begin{aligned} & \sum_n \int_{-\infty}^{\infty} dk k e^{ikx} \Delta_{1(p-n)} \hat{\Psi}_n \cosh k_n a e^{-\frac{k_n^2}{k_{\max}^2}} \\ & - \frac{\delta a}{\pi} \Delta_{1p} \int_{-\infty}^{\infty} dk k \cos kx \frac{\cosh ka}{\sinh ka} e^{-\frac{k^2}{k_{\max}^2}} \\ & + i \sum_n \frac{2\pi n}{w} \frac{2\pi p}{w} \int_{-\infty}^x dx' \int_{-\infty}^{\infty} dk e^{ikx'} \Delta_{1(p-n)} \hat{\Psi}_n \cosh k_n a e^{-\frac{k_n^2}{k_{\max}^2}} \end{aligned} \right\}. \quad (4.146)$$

4.3 Forward problem for a semi-infinite plate without defect

Two expressions were developed that give the voltage difference between two points at the surface of a plate without defect:

$$V(x) = \frac{4\rho S_0}{wa} \sum_{m=0}^{\infty} \sum_{k=1}^{N_w} \frac{\cos\left(\frac{m\pi}{2}\right) \cos\left(\frac{m\pi z_k}{w}\right)}{\sigma_m} \sum_{n=0}^{\infty} \frac{e^{-y_{mn}(l-x)} - e^{-y_{mn}(l+x)}}{\sigma_n y_{mn}}, \text{ and}$$

$$V(x) = \frac{\rho S_0}{\pi w} \ln \frac{\cosh \frac{\pi(l+x)}{a} - 1}{\cosh \frac{\pi(l-x)}{a} - 1}.$$

These equations are essentially identical. The first one is a numerical expression and the second equation is an analytical function. The results of these equations were compared with those obtained experimentally. Figure 4.14 shows the comparison between the experimental and analytical results for a rectangular plate (12 inches x 8 inches x 3/4 inch). As shown in Figure 3.3 the voltage probes were spaced at 12.7mm (1/2 inch) intervals and 15 input current wires (total current of 10 Amp) were attached at the plate ends, equally spaced 12.7mm (1/2 inch) apart.

Potential Difference - plate 3/4" no defect

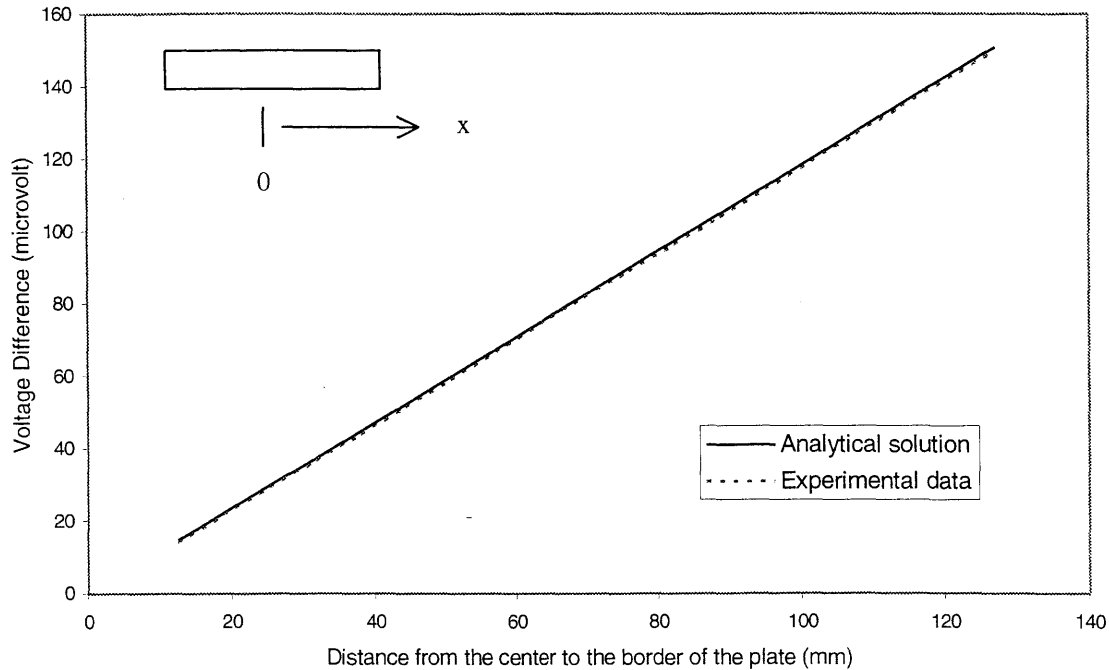


Figure 4.14 - Comparison between experimental and analytical results for a no-defect rectangular plate.

It can be seen that the theoretical result is extremely close to the experimental one. Although the model assumes a semi-infinite plate, experimentally no end effects were observed. The uniform current distribution throughout the wires contributed to the good agreement between the results. The difference between the analytical and experimental result is mostly due to measurement uncertainties.

4.4 Forward problem for a semi-infinite plate with a slot defect

When a slot defect, such as the one showed in Figure 4.5, is introduced in the plate a new term is added to Equation 4.27 in order to consider this defect. Equation 4.38 is the analytical solution for the potential difference between two points on the surface of a slot-defective plate:

$$V(x) = \frac{\rho S_0}{\pi w} \ln \frac{\cosh \frac{\pi(l+x)}{a} - 1}{\cosh \frac{\pi(l-x)}{a} - 1} - \frac{\rho S_0 h}{\pi a w} \left[\coth \frac{\pi}{2a} (l-x) \ln \frac{\cosh \frac{\pi}{2a} (l+\lambda) \cosh \frac{\pi}{2a} (\lambda-x)}{\cosh \frac{\pi}{2a} (x+\lambda) \cosh \frac{\pi}{2a} (\lambda-l)} - \coth \frac{\pi}{2a} (l+x) \ln \frac{\cosh \frac{\pi}{2a} (\lambda+x) \cosh \frac{\pi}{2a} (\lambda+l)}{\cosh \frac{\pi}{2a} (\lambda-l) \cosh \frac{\pi}{2a} (\lambda-x)} \right]$$

Several experiments were carried out on a rectangular plate with 304.8mm x 203.2mm x 19.05mm (12 in x 8 in x ¾ in). A groove, as described in Figure 4.5, with dimensions $\lambda = 50.8$ mm and $h = 2$ mm was machined in the bottom of the plate. Figure 4.15 shows the experimental data and the analytical result using Equation 4.38. Again, 15 current wires were used, equally spaced at 12.7mm (½ inch) at the ends of the plate. The total current was 10 Amp. It can be seen that the analytical result was very close to the experimental data.

Equation 4.38 was developed considering a small slot height defect compared to the thickness of the plate ($h \ll a$) and shows a linear dependence of the potential difference with the height of the slot defect (h). For a 2mm-height slot defect (approximately 10.5 % of the plate thickness) Equation 4.38 predicts a good result compared to the experimental data. A change in the slope of the curve for distances

greater than 50.8 mm (2 inches), which is the half slot length, points out a change in the resistance of the plate and therefore the presence of a defect.

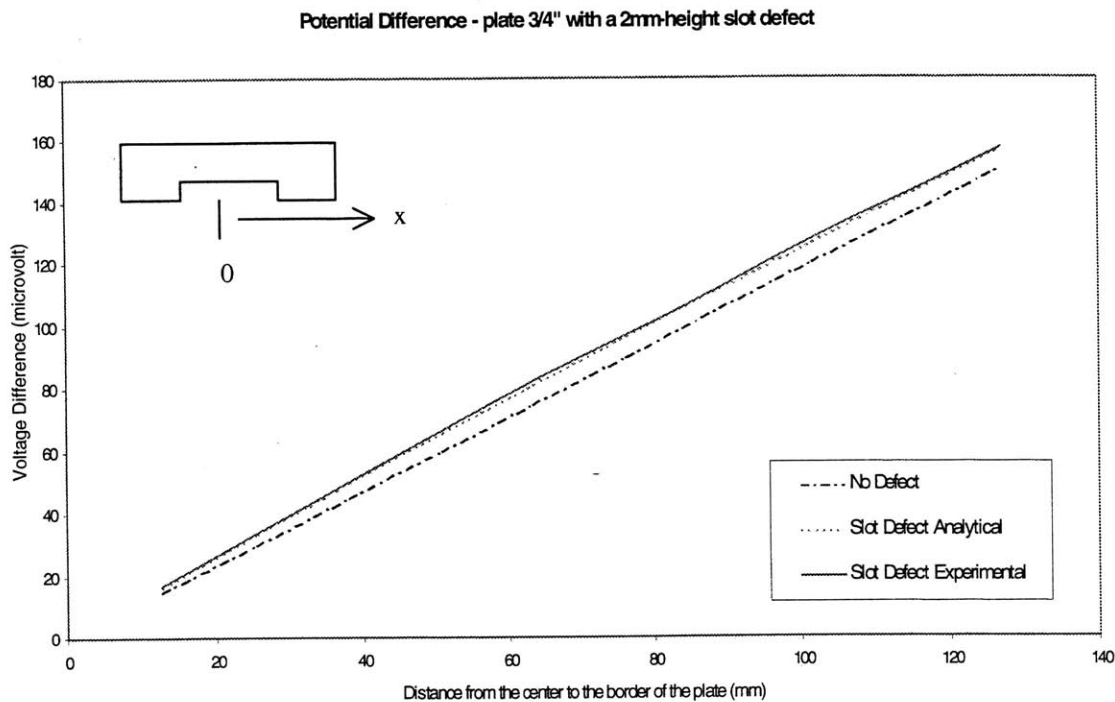


Figure 4.15 – Comparison between experimental and analytical results for a 2mm-height slot defect plate.

Figure 4.16 shows the results for a plate with a 4 mm-height slot defect. For this case, where the depth of the slot was about 21% of the thickness of the plate, the linear correction for the potential difference given by Equation 4.38 is not enough. The experimental data are about 3% to 6% greater than the results given by the analytical solution. It turns out that a second order term correction is necessary to improve the analytical solution. The changing of the slope for distances greater than 50.8 mm (2

inches) is more visible since there is a relatively larger decrease in the resistance of the plate, as compared to Figure 4.15.

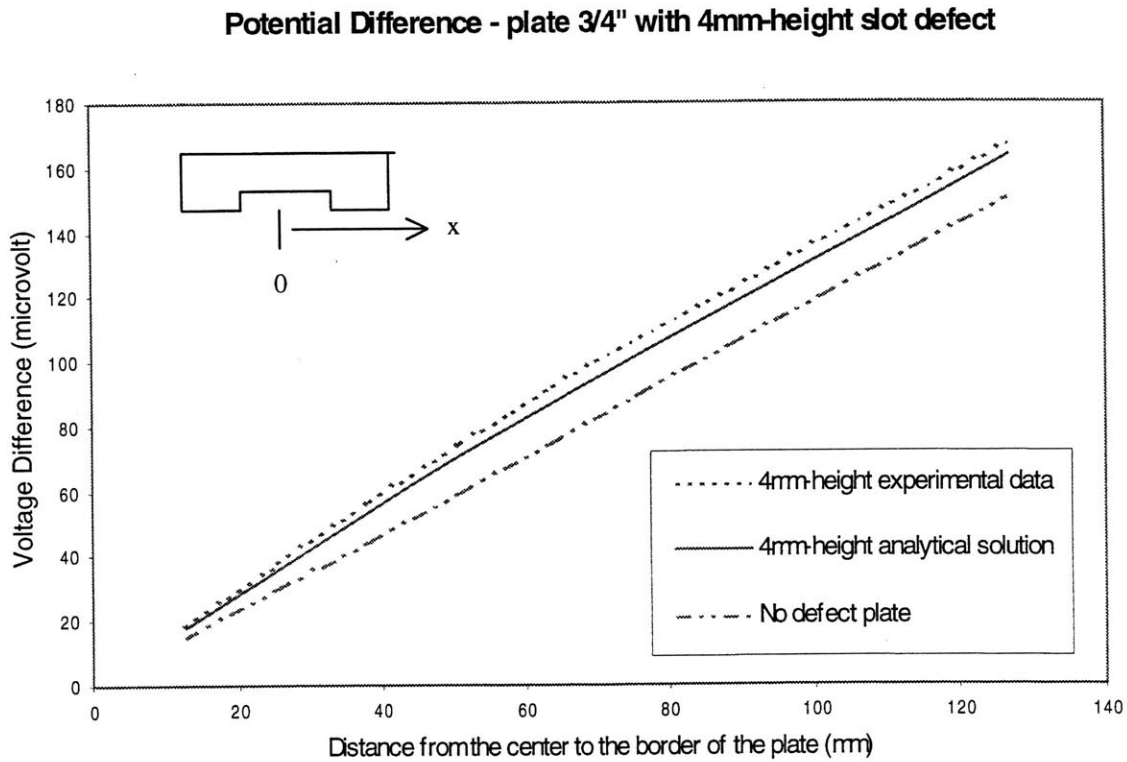


Figure 4.16 - Comparison between experimental and analytical results for a 4mm-height slot defect plate.

Finally, a slot with 6.3mm of depth was machined in the plate. Figure 4.17 shows the comparison between the analytical solution given by Equation 4.38 and the experimental data. In this case the slot depth is more than 32% of the thickness of the plate and, therefore, a good agreement between experimental and analytical results was

not expected. The difference between the experimental data and the analytical solution varies from 7% to 12%. In this case a second order term correction for the potential function becomes necessary. The bigger the depth of the slot defect, the greater the difference between the experimental data and the analytic solution given by Equation 4.38.

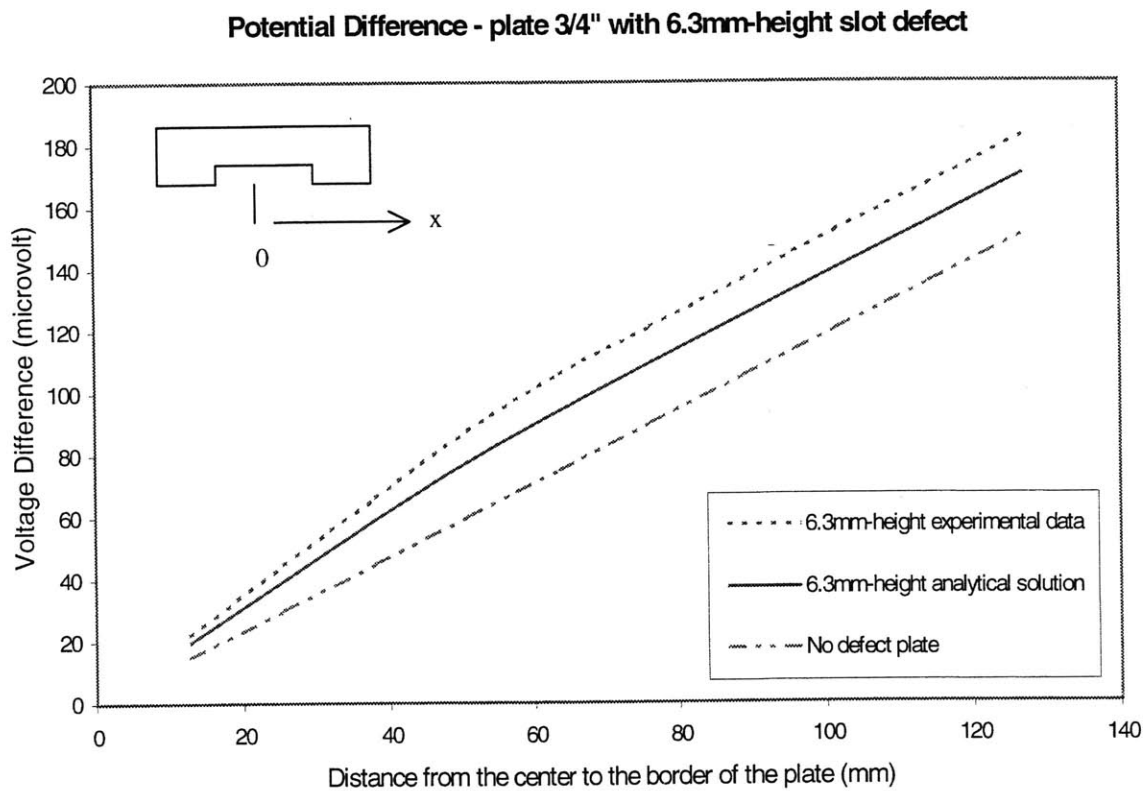


Figure 4.17 - Comparison between experimental and analytical results for a 6.3mm-height slot defect plate.

4.5 Forward problem for a semi-infinite plate with a ramp defect

Consider a plate with a ramp defect as shown in the Figure 3.4. The plate has dimensions of 304.8mm x 203.2mm x 19.05mm (12 in x 8 in x ¾ in). The total current applied was 20 Amp and 15 current wires were used, equally spaced at 12.7mm (½ inch) at the end of the plate and. In two dimensions this defect can be represented by the following equations:

$$\begin{aligned}
 \Delta(x) &= h && \text{for } -c \leq x \leq c, \\
 \Delta(x) &= \frac{h}{s}(c+s-x) && \text{for } c < x < c+s, \\
 \Delta(x) &= \frac{h}{s}(c+s+x) && \text{for } -c-s < x < -c, \\
 \Delta(x) &= 0 && \text{else.}
 \end{aligned}
 \tag{4.147}$$

Figure 4.18 shows a schematic view of the function above. The first derivative of this function can be easily calculated and the second derivative vanishes for all points. Equation 4.147 replaces Equation 4.59 in the analytic solution for a semi-infinite plate with a smooth defect. A code called “forward_ramp” was developed to calculate the potential at the surface of the plate for this ramp geometry.

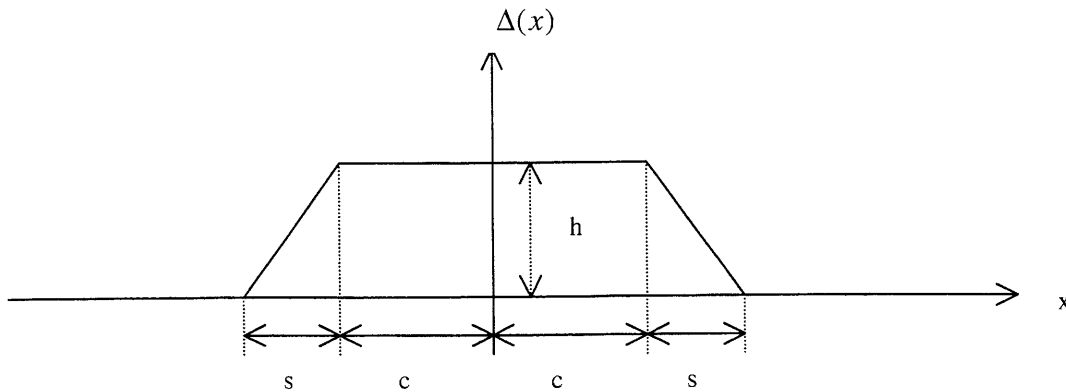


Figure 4.18 – Ramp defect function given by Equation 4.114.

Figure 4.19 shows a comparison between the experimental data and the analytic result given by the code "forward_ramp". The parameters described in the Figure 4.18 for this experiment are $h = 6.3\text{mm}$, $c = 50.8\text{mm}$ and $s = 24.6\text{mm}$. Although the defect depth is more than 32% of the thickness of the plate the agreement between the two curves is good. The reason for this better behavior compared to that obtained in Figure 4.17 is not only because defect is smoother but also because a second order term was considered for the potential function.

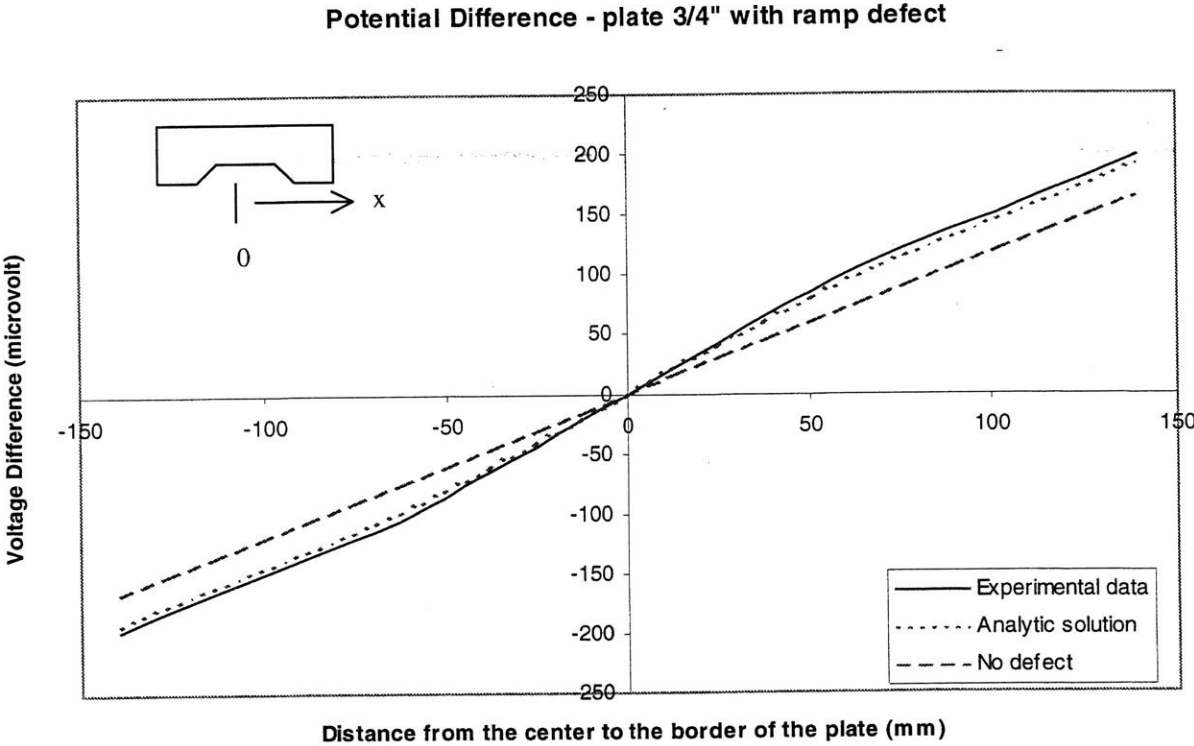


Figure 4.19 – Comparison between experimental and analytical results for a ramp defect plate.

4.6 Forward problem for a semi-infinite pipe without defect

The pipes used during the experiments had a large diameter compared to the wall thickness, therefore the cylinder was approximated as a plate and Equation 4.28 was used to estimate the analytic solution. Several experiments were carried out in a pipe with an external diameter of 326.4mm (12.85 inches), a wall thickness of 12.7mm (0.5 inch) and 609.6mm (24 inches) in length. The total current applied was 35 Amp and 26 current wires were used at each end of the plate. Figure 3.5 shows a picture of this pipe. Figure 4.20 gives a comparison between the experimental results and the approximated analytic solution given by Equation 4.28. An average radius was assumed for the calculation.

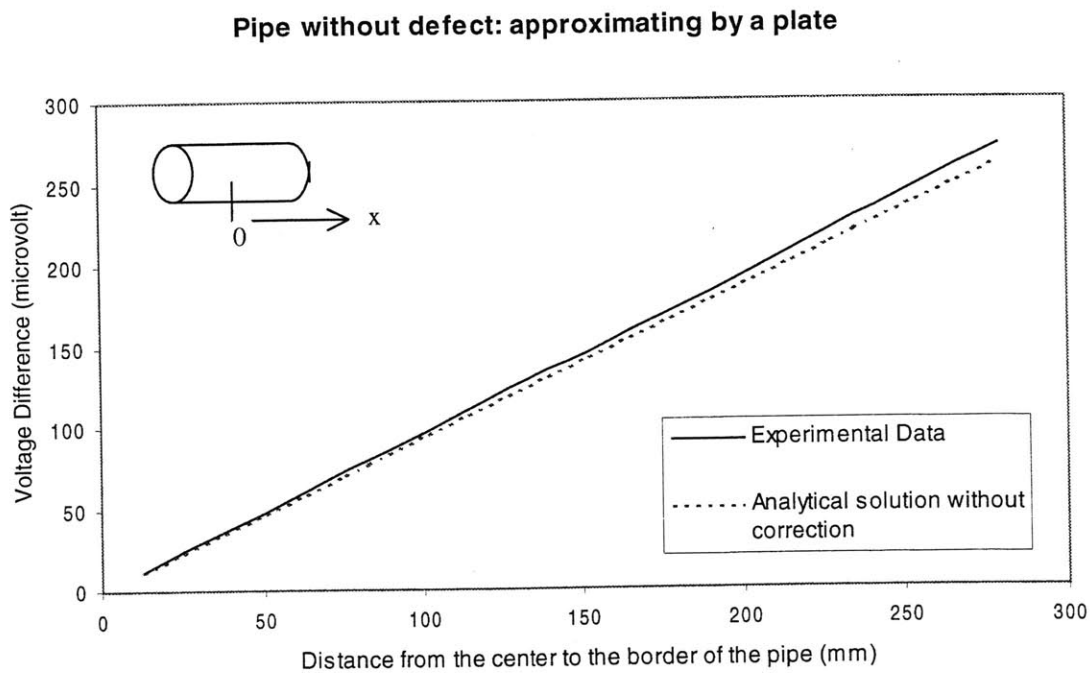


Figure 4.20 – Comparison between experimental and analytical solution without correction for a pipe with no defect.

The analytic solution matches well the experimental data only in the center of the pipe, where the effect of the geometry is less evident. For large distances from the center of the pipe the difference between the experimental and analytical results can be reduced using the correction term for the cylindrical geometry given by Equation 4.63.

Equation 4.64 gives the potential function at the surface of a pipe without defect using the correction term for the cylindrical geometry. It is valid since the pipe has a large external radius compared to the wall thickness ($r_2 \gg a$). Figure 4.21 shows a good agreement between the experimental data and the analytical result given by Equation 4.64.

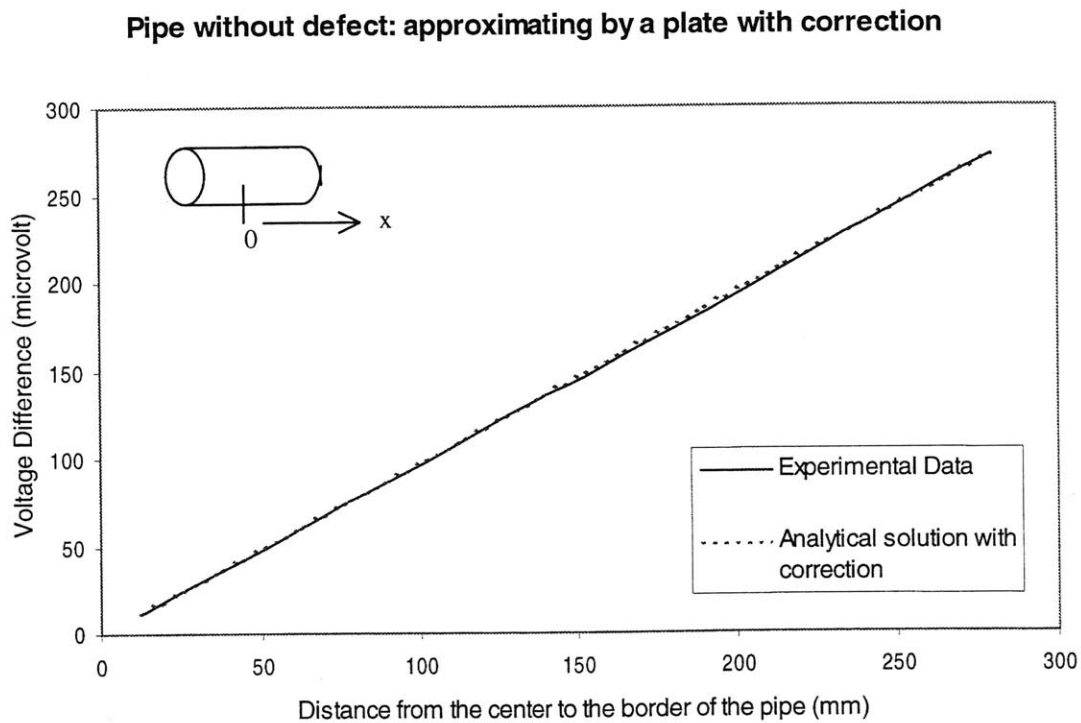


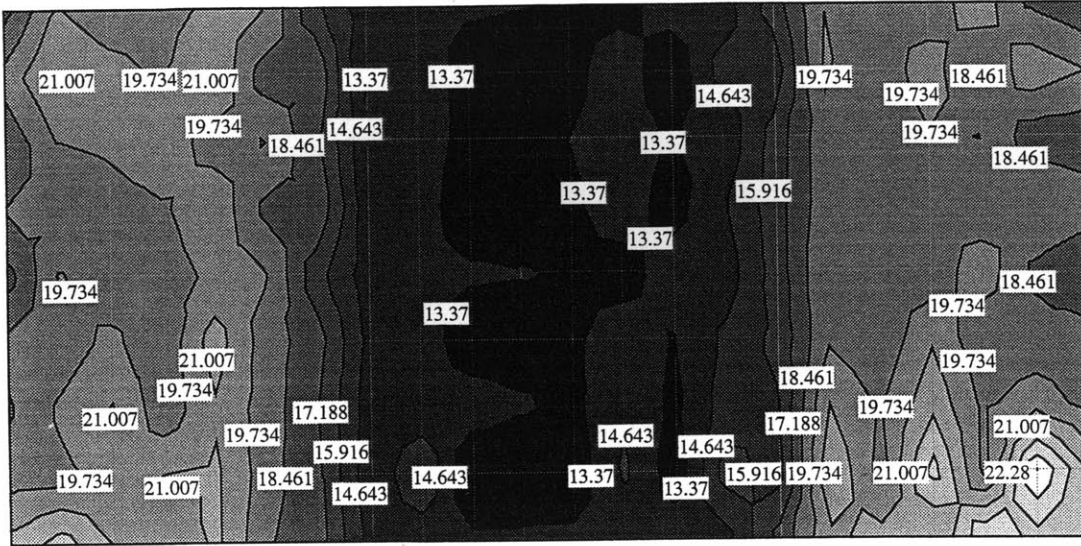
Figure 4.21 - Comparison between experimental and analytical solution with correction for a pipe with no defect.

4.7 Inverse problem for a semi-infinite plate with a slot defect

Consider the plate with a slot defect as shown in Figure 3.3. The DCPD measurements can be used to calculate a series of contour plots of constant plate thickness. These thickness measurements were derived from Equation 2.2. Figure 4.22 shows these contour plots in two sections. The upper part of the figure shows the contour plot as experimentally determined. The numbers denote the plate thickness (in millimeters) for that contour and the thinner the wall, the darker the shading. The lower portion shows the contour plot with the defect drawn in. Although the depth of the defect is not well predicted, the presence of the defect is clearly identified in the top figure.

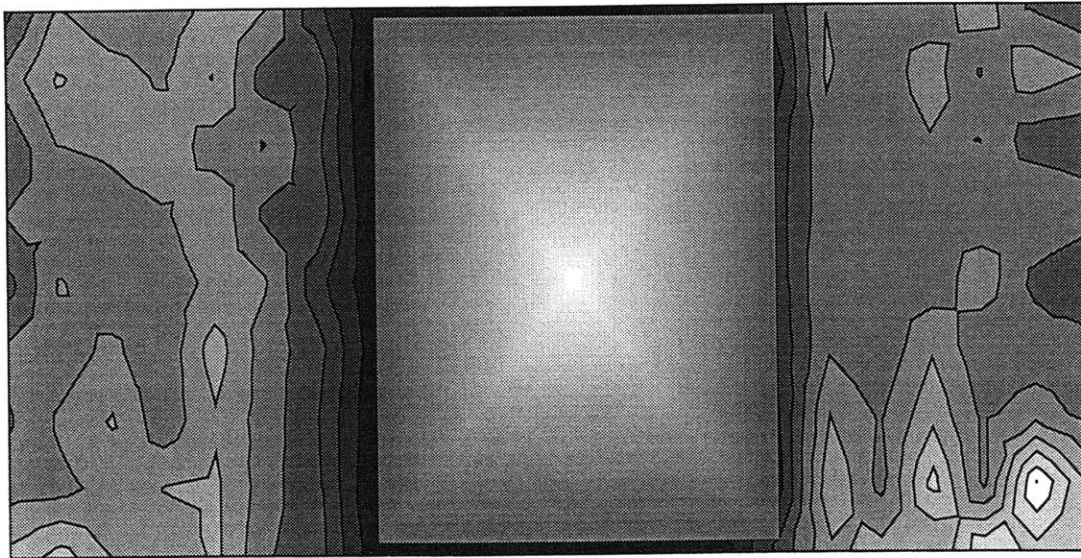
Equation 4.93 calculates the first order of the defect considering a two-dimension case. A MATLAB code described in Appendix L was developed to solve the equation. Figure 4.23 shows the two-dimension solution from the measurements acquired along the centerline of the plate. It can be seen that the solution given by the model predicts a height about 17% greater than the actual value, which represents a plate thickness of 11.7mm. It is a more conservative prediction compared to the thickness shown in the contour plot. The sharp edges cannot be predicted mathematically but do not represent a likely defect caused by flow accelerated corrosion. The potential data were collected only between the current probes.

Thickness contour plot for a slot defect



thic

Thickness contour plot for a slot defect



thic

Figure 4.22 – Thickness contour plot for a slot defect in a plate.

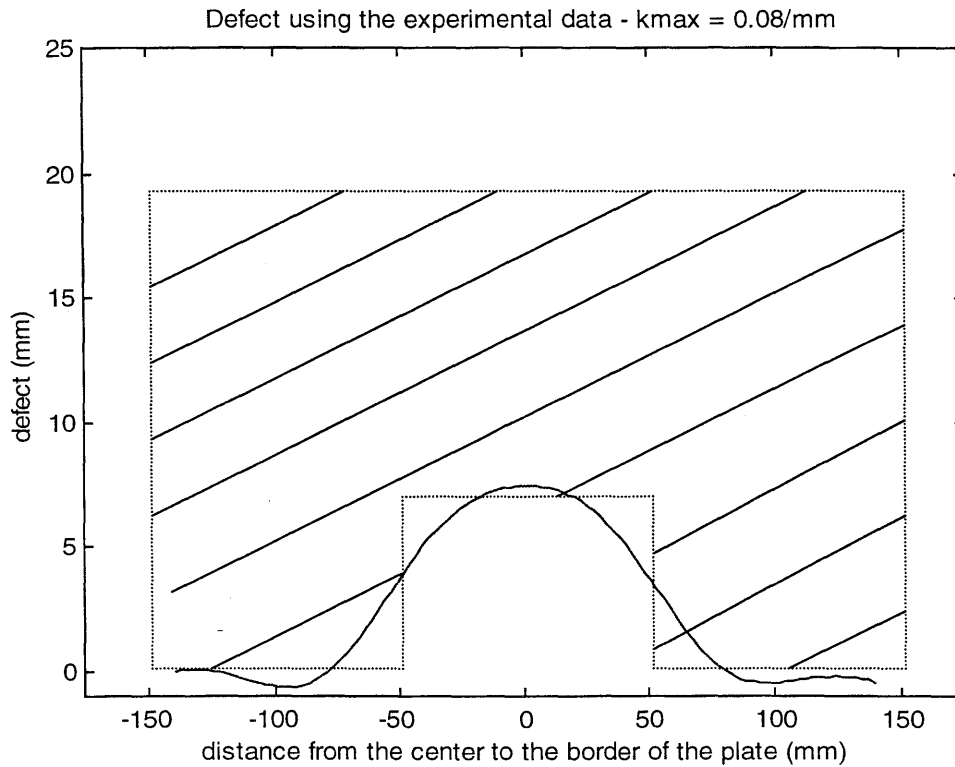


Figure 4.23 – 2D defect solved for a slot plate ($\lambda = 50.8\text{mm}$, $h = 6.3\text{mm}$) using experimental data.

Since the analytical solution has been determined for the potential function at the surface of the plate, “analytical data” can be generated for any slot. These “virtual” data can be used, instead of the potential measurements, to solve the inverse problem.

Appendix P describes the code used to solve the inverse problem using “analytical data”.

Figure 4.24 shows the output of this code for a slot defect with the same dimensions

($h = 6.3\text{mm}$ and $\lambda = 50.8\text{mm}$).

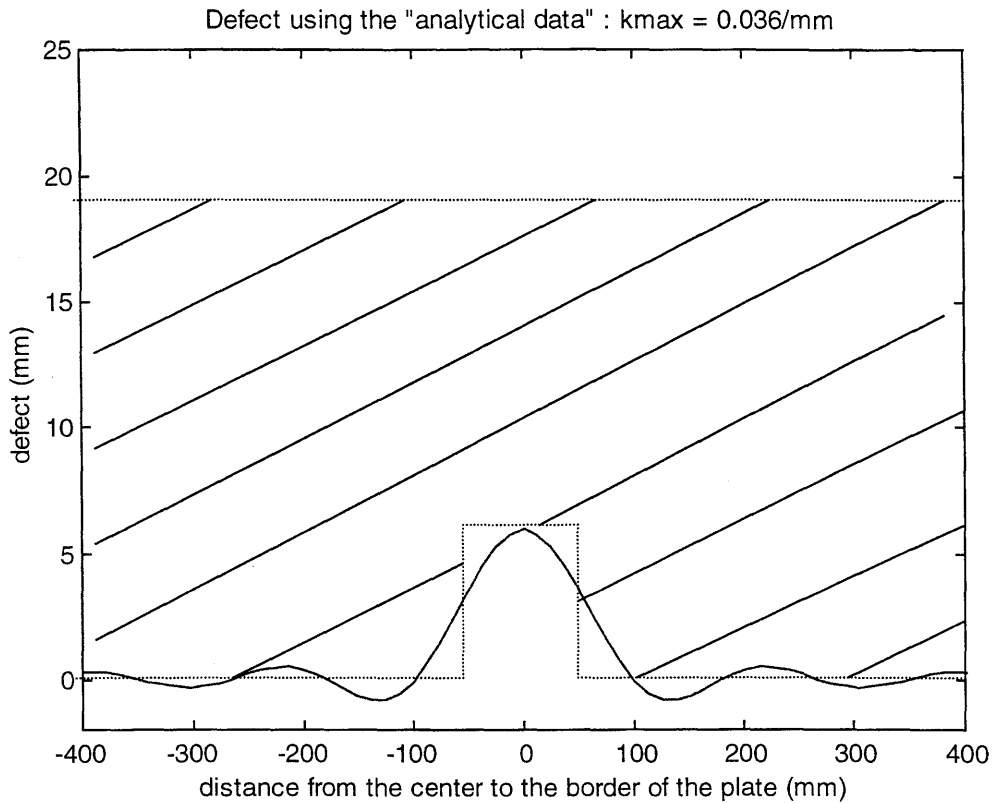


Figure 4.24 - 2D defect solved for a slot plate ($\lambda = 50.8mm$, $h = 6.3mm$) using “analytical data”.

Using the forward problem “analytical data” was generated for long distances from the current probes where the electrical field vanishes and the potential function φ_1 goes to zero. The model results predict a defect of 6.1mm in height, which is very close to the real value of 6.3mm.

“Analytical data” can also be produced for a wider slot. Figure 4.25 shows the solution for a plate with slot defect with $h = 6.3mm$ and $\lambda = 400mm$ compared to the real defect.

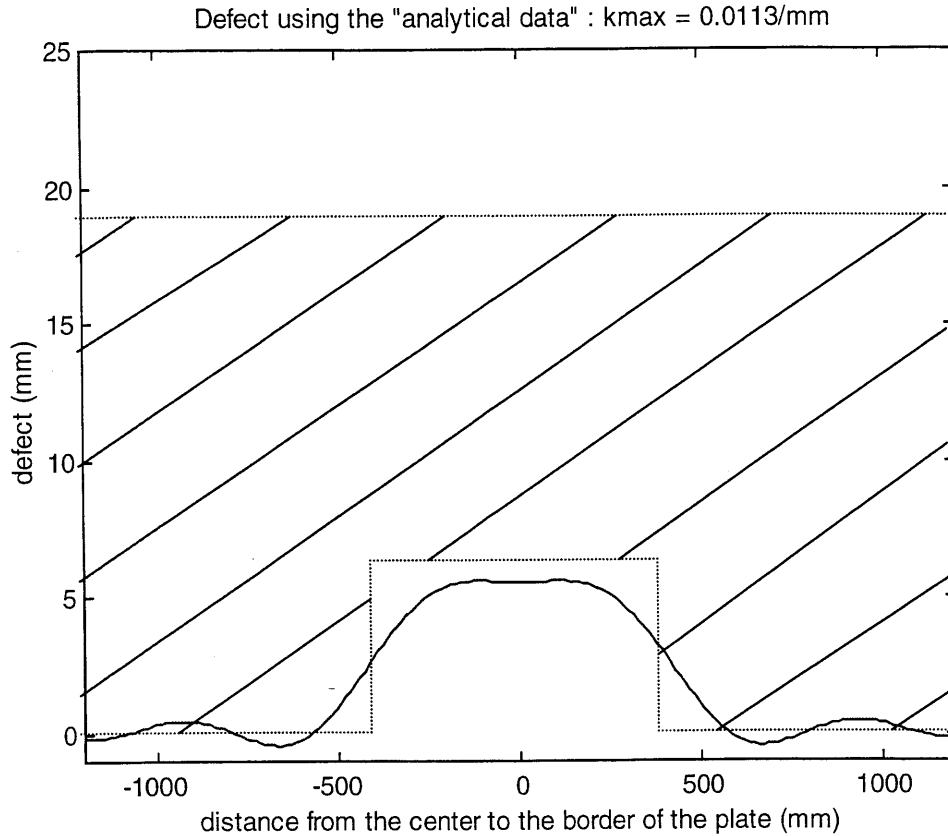


Figure 4.25 - 2D defect solved for a slot plate ($\lambda = 400mm$, $h = 6.3mm$) using “analytical data”.

The solution predicts a defect with about 5.6mm of height and a better resolution of the flat part of the defect. The inverse problem was solved considering only the first order approximation, which means that the height of the defect could be more accurate if a second order term were added to the solution.

Figure 4.26 shows the output of the code for a slot defect with $h = 2mm$ and $\lambda = 50.8mm$.

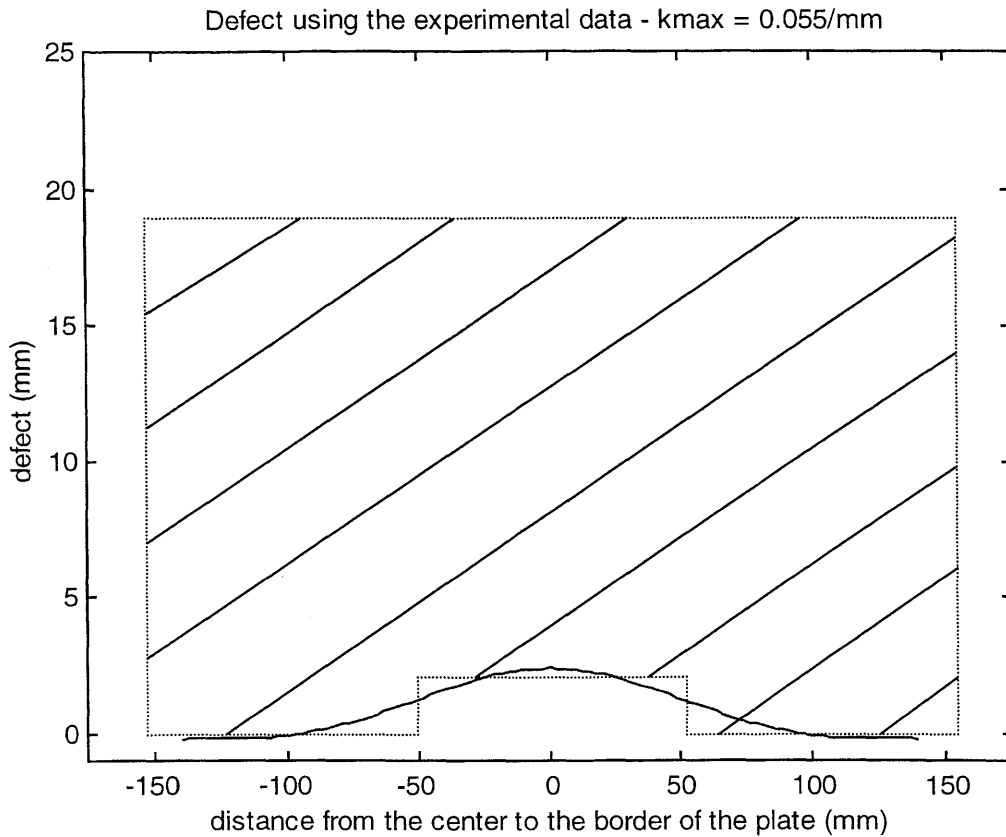


Figure 4.26 - 2D defect solved for a slot plate ($\lambda = 50.8\text{mm}$, $h = 2\text{mm}$) using experimental data.

This figure shows a predicted defect with a height about 19% greater than the actual value. It is a good prediction considering that the plate was 12 inches in length and no data was acquired outside of the current probes.

“Analytical data” can also be produced for this defect slot and compared to the solution of the real defect. Figure 4.27 shows the solution to be in excellent agreement with the actual height of the defect.

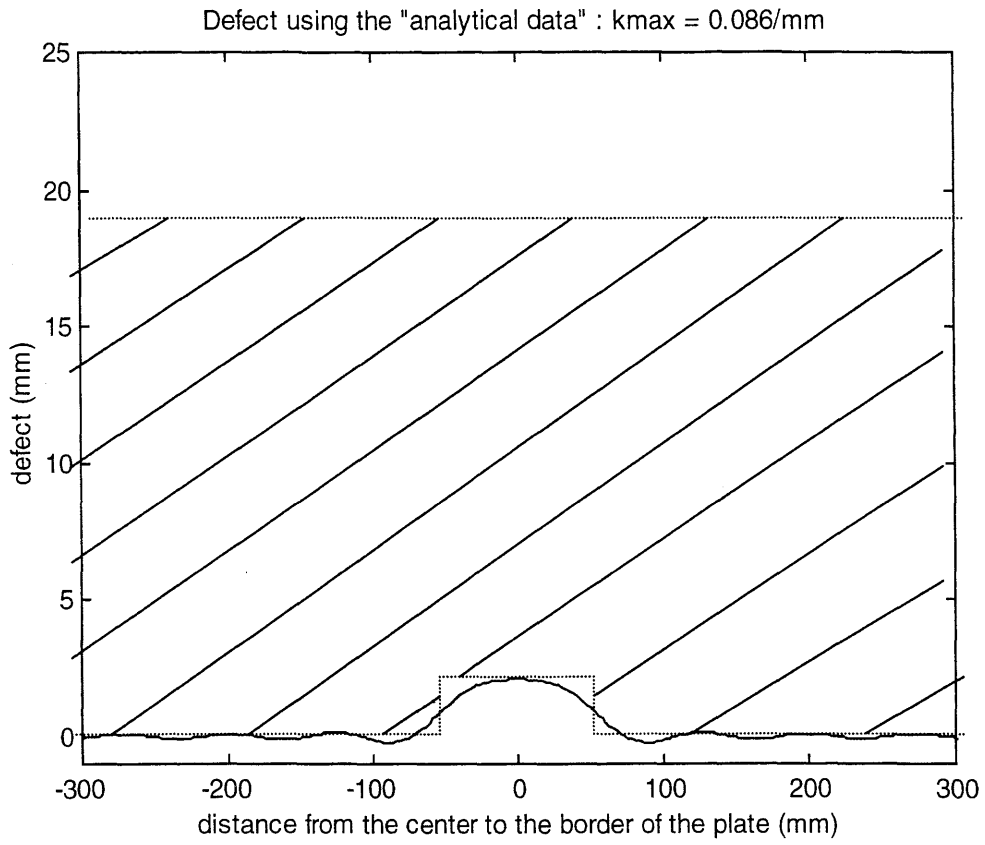


Figure 4.27 - 2D defect solved for a slot plate ($\lambda = 50.8mm$, $h = 2mm$) using “analytical data”.

4.8 Inverse problem for a semi-infinite plate with a ramp defect

Consider the plate with a ramp defect as shown in Figure 3.4. Equation 4.93 calculates the first order defect considering a two-dimensional case. A MATLAB code described in Appendix L was developed to solve the equation. Figure 4.28 shows the output of this code for a plate with a ramp defect given by Equation 4.114 with parameters $h = 6.3\text{mm}$, $c = 50.8\text{mm}$ and $s = 24.6\text{mm}$.

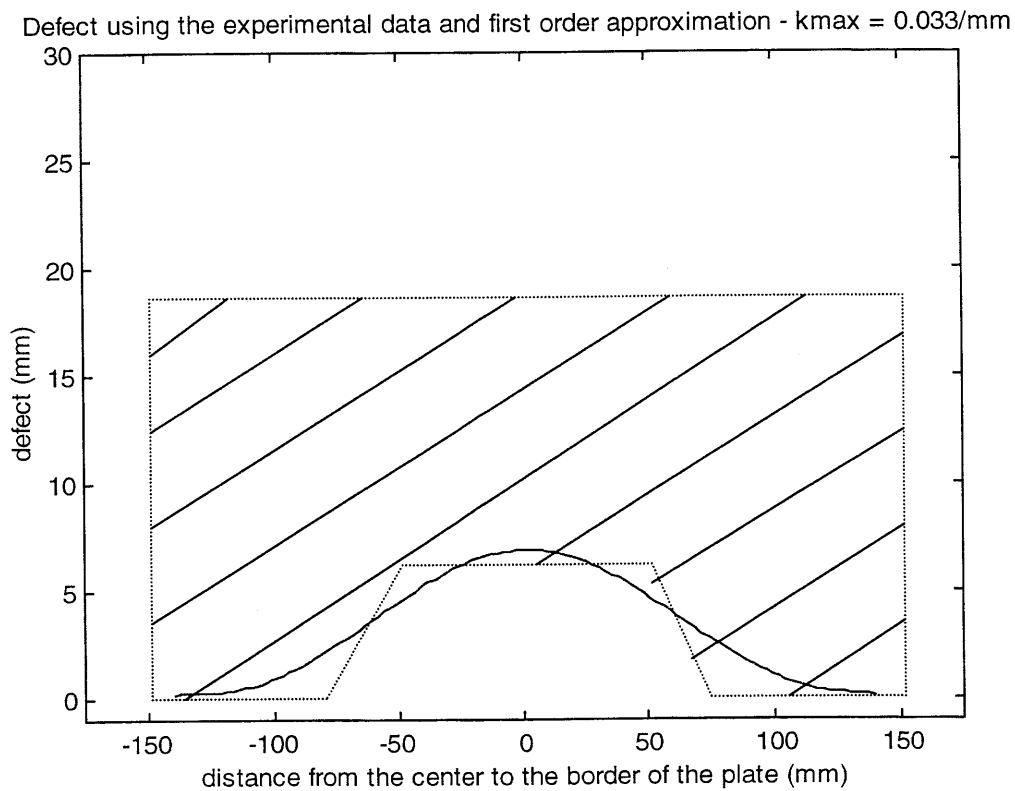


Figure 4.28 - 2D defect solved for a ramp plate using experimental data and first order approximation.

Equation 4.103 calculates the defect considering the second order approximation for the two-dimension case. A MATLAB code described in Appendix N was developed to solve the equation. Figure 4.29 shows the output of this code for a plate with a ramp defect given by Equation 4.114 with parameters $h = 6.3\text{mm}$, $c = 50.8\text{mm}$ and $s = 24.6\text{mm}$. The defect height calculated was about 5% less than the actual one. Since the depth of the defect represents 33% of the thickness of the plate, the model and real defect are in good agreement.

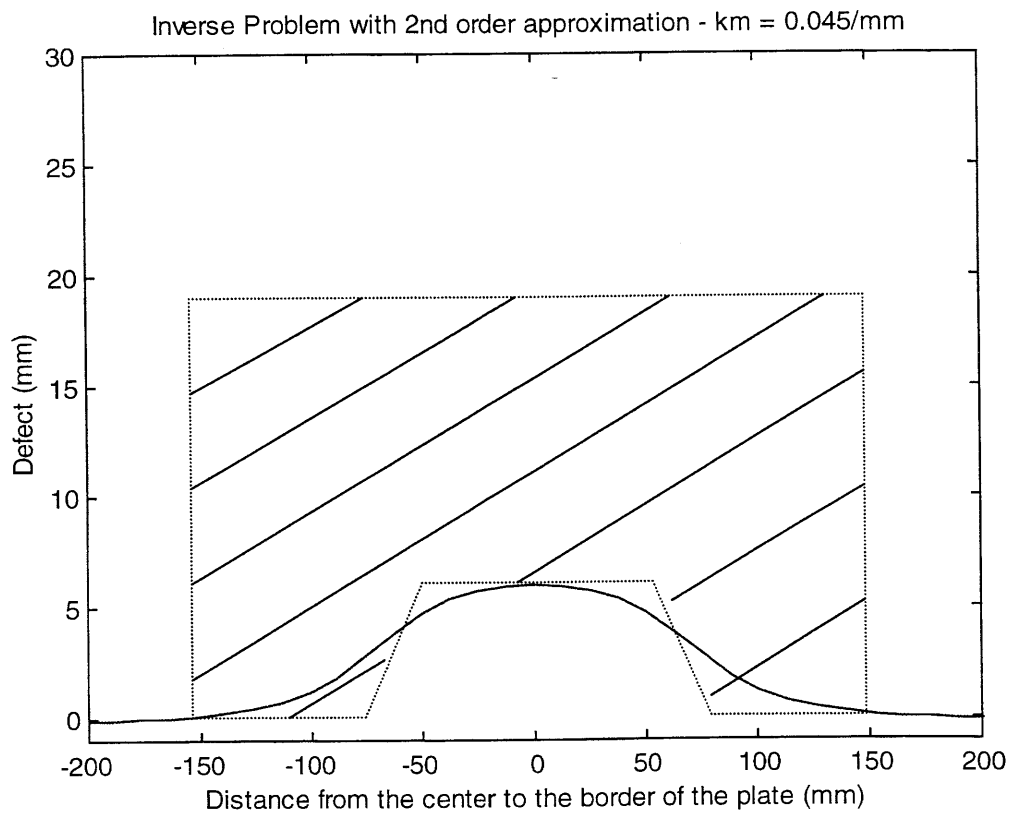


Figure 4.29 - 2D defect solved for a ramp plate using experimental data and second order approximation.

Figure 4.30 shows a comparison of the defect solution using the first and the second order approximation. It can be seen that by considering the second order term in the calculation of the defect, the solution better approximates the actual value.

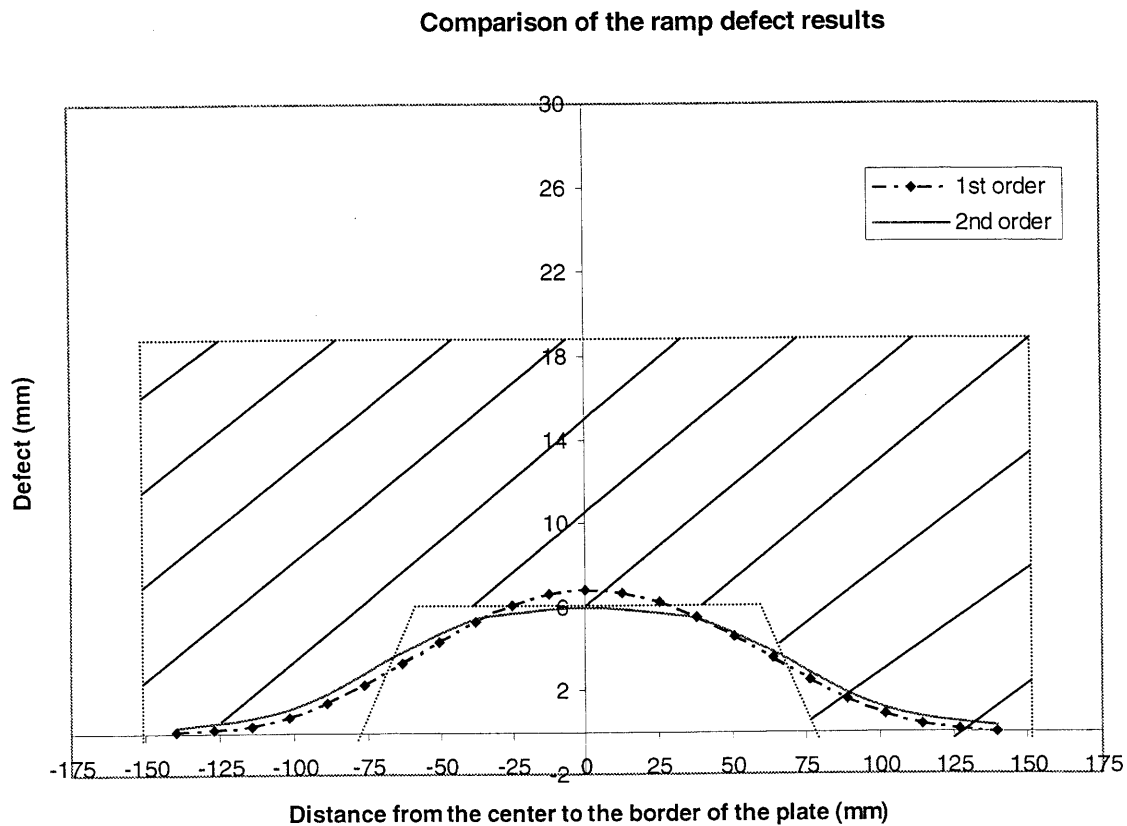


Figure 4.30 – Comparison between first and the second order solutions for a ramp defect.

4.9 Inverse problem for a semi-infinite plate with a smooth defect

Consider a plate with a smooth defect as shown in Figure 4.9. Using the “analytic data” calculated by the code “forward_smooth”, as presented in Figure 4.10, the inverse problem can be solved for this defect. Figure 4.31 shows a comparison between the result calculated using first and second order approximation and the real defect shown in Figure 4.9. The analytic result gives a good estimate of the depth of the defect. The model also predicts a better width of the defect compared to the slot and ramp defect cases.

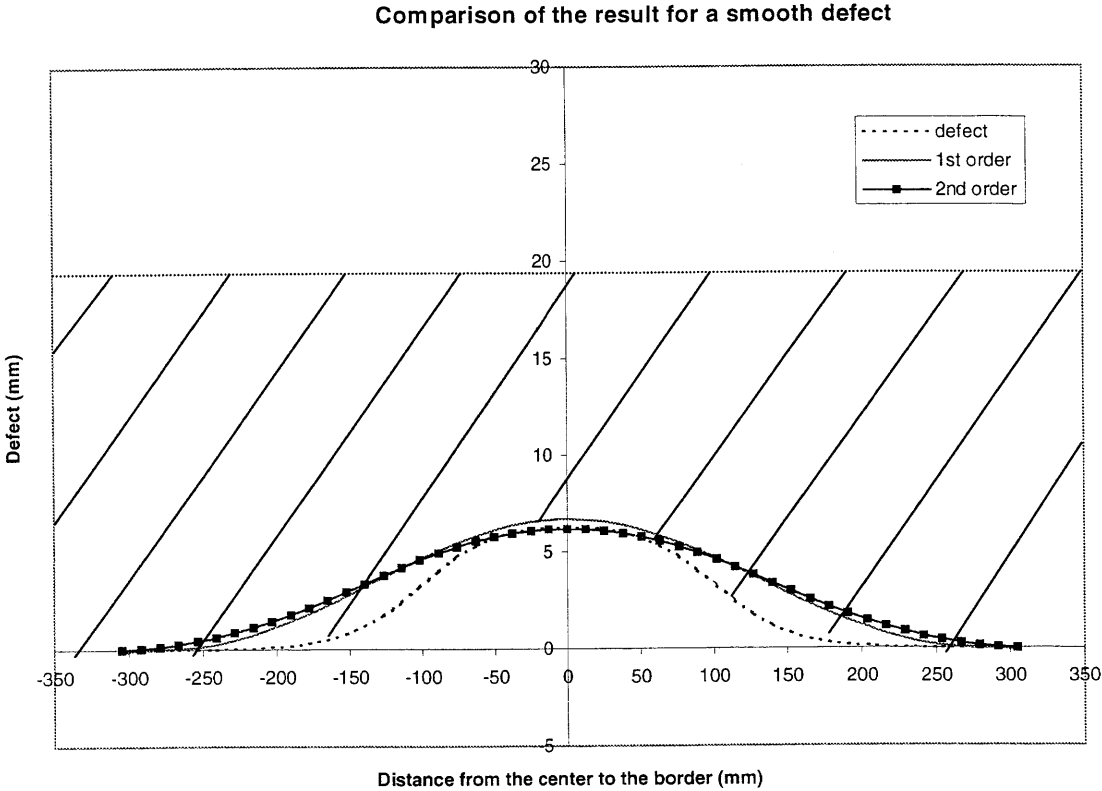


Figure 4.31 – Inverse problem for a smooth defect given by Equation 4.59.

4.10 Inverse problem for a pipe with a circular defect

Consider a pipe similar to the one shown in Figure 3.5 with a circular defect on its inner surface. The original thickness of the pipe wall was 12.7mm ($\frac{1}{2}$ inch). The defect was 101.6mm (4 inches) in total diameter with a 76.2mm (3 inches) diameter region having a constant depth of 6.35mm ($\frac{1}{4}$ inch), as shown in Figure 4.32. This is a more likely type of defect that resulting from flow-accelerated corrosion phenomena.

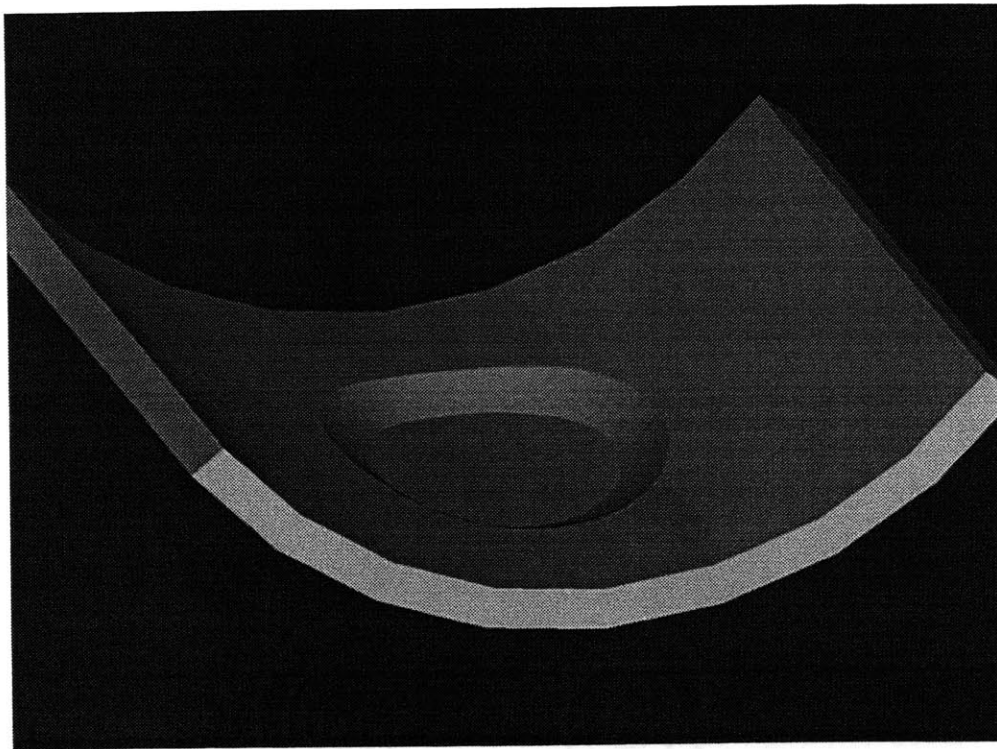
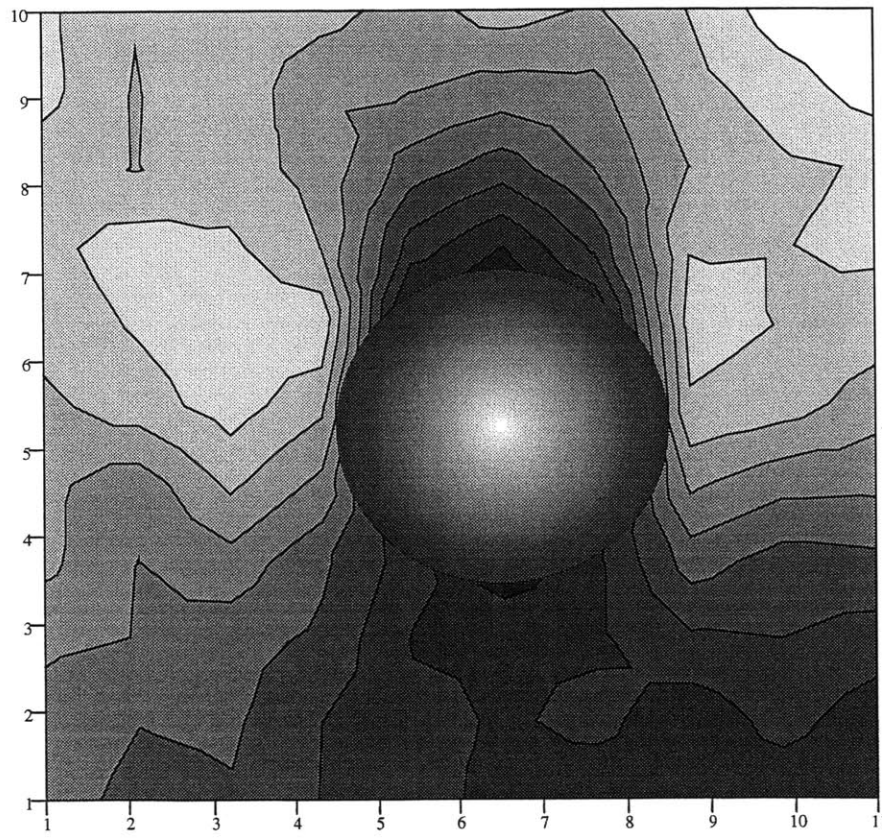
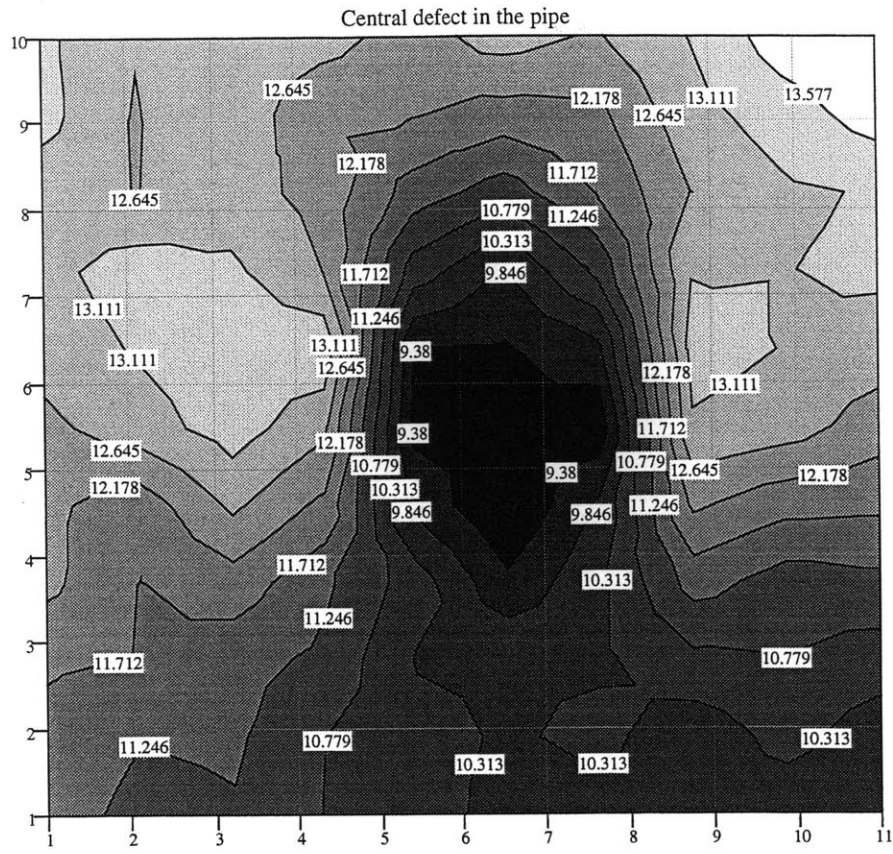


Figure 4.32 – AUTOCAD reproduction of a circular defect machined in the pipe.

Figure 4.33 shows the contour plots of constant pipe thickness using the DCPD measurements. The upper part of the figure shows the contour plot by itself. The lower portion shows the contour plot with the defect draw in. A current density of 0.28 Amp/cm² (35Amp total) was used in this experiment. Although the assumption of constant current density is a weak one, the presence of the defect is clearly identified by the dark shaded region in the top figure.

The depth of the defect is not well predicted by these contour plots. Solving the inverse problem from the DCPD measurements can refine this result. Figure 4.34 shows a two-dimension solution from the measurements acquired along the centerline of the circular defect. Although the evaluation of the depth of the defect is better, the solution is not as good as to that shown for the ramp-defect case in Figure 4.30. In the slot and ramp defects, the defects were independent of the z direction. However, in this case the defect is no longer independent of the z direction. A three-dimensional solution for the pipe defect is required to obtain better resolution of the defect morphology. Nevertheless, the application of the methodology developed in this work allows for a significant refinement and improvement of predicted pipe thickness.



tnew

Figure 4.33 – Thickness contour plot for a circular defect in a pipe.

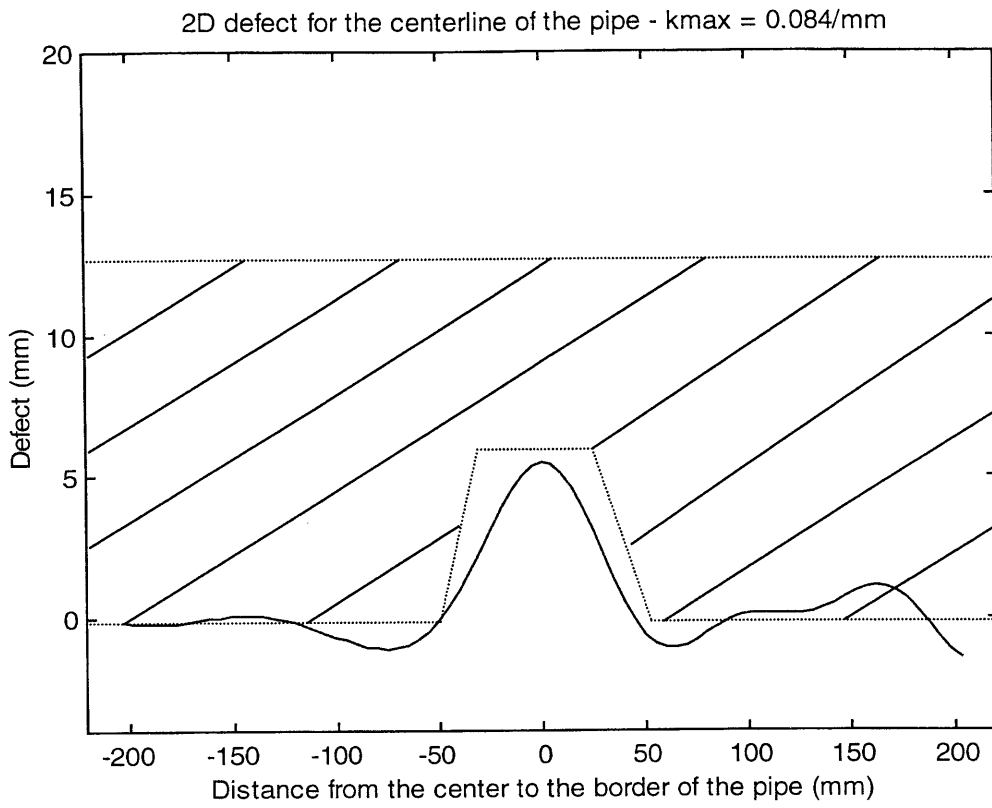


Figure 4.34 – 2D defect solved for the pipe using experimental data.

CONCLUSION

A new methodology, based on the direct current potential drop technique, has been developed to measure the pipe wall damage morphology caused by flow assisted corrosion or any other phenomenon that results in wall thinning. The methodology has been confirmed using plate and pipe with a well-defined defect present.

This new non-destructive evaluation technique allows the real-time determination of the evolution of pipe wall thickness and damage morphology. In the actual field the data will be in the form of the potential drop measurements for an array of probes placed on the outside diameter of the pipe. First, the algorithm determines the presence of a defect and then, assuming that a defect is detected, it develops the morphology of the defect. The method is capable of detecting wall loss greater than 5% of nominal wall thickness of the pipe.

FUTURE WORK

The methodology developed was tested in two-dimensional cases for a well-defined defect. Although the algorithm for three-dimensional evaluation has been developed it was not tested. Interesting future work, then, would be testing this algorithm for the circular defect that was shown in the pipe. Then, the algorithm can be used to evaluate the pipe wall thickness and damage morphology for a real defect caused by flow assisted corrosion (FAC).

Because FAC is common in components with geometry that increases fluid velocity and turbulence, it is recommended to develop similar methodology for other geometries than pipes. Building algorithm for elbows, for example, would be a valuable addition.

Finally significant computer work must be done to present the results. For applications in the field conversion of all codes to FORTRAN and developing an interface for the data acquisition is necessary. Moreover, a graphical user interface using Visual Basic could be developed to show the wall damage morphology.

REFERENCES

- Alessandrini, G. and Rosset, E. "The inverse conductivity problem with one measurement: bounds on the size of the unknown object. *SIAM Journal on Applied Mathematical*, vol 58 (1998), n° 4, pp. 1060-1071.
- Aparicio, N.D. and Pidcock, M.K. "On a class of free boundary problems for the Laplace equation in two dimensions. *Inverse Problems* 14 (1998) 9-18.
- Bridgeman, J. and Shankar, R. "Erosion/corrosion data handling for reliable NDE". *Nuclear Engineering and Design* 131 (1991) 285-297.
- Carriveau, G.W. and Austin, R. "Nondestructive evaluation of corrosion through insulation". *Review of Progress in Quantitative Nondestructive Evaluation*, vol 15B, 1996, pp. 1741-1746.
- Charlesworth, F.D.W. and Dover, W.D. "Some aspects of crack detection and sizing using a.c. field measurements". *Advances in Crack Length Measurement*. Engineering Materials Advisory Services Ltd., London, 1982, pp. 253-276.
- Cheney, M. "An introduction to inverse problems". *Proceedings of symposia in applied mathematics*, vol 48, 1994, pp. 21-42.
- Cheney, M. and Isaacson, D. "An overview of inversion algorithms for impedance imaging". *Collection: Inverse scattering and applications*. *Contemporary Mathematics*, vol 122, pp. 29-39.

- Cheney, M and Isaacson, D. "Distinguishability in Impedance Imaging". IEEE Transactions on Biomedical Engineering, vol. 39, n° 8, August 1992.
- Cheney, M. and Isaacson, D. "Inverse problems for a perturbed dissipative half-space". Inverse Problems 11 (1995) 865-888.
- Cheney, M. et al. "NOSER: An algorithm for solving the inverse conductivity problem". International Journal of Imaging Systems and Technology, vol. 2, 66-75 (1990).
- Cheney, M.; Isaacson, D.; Somersalo, E. and Isaacson, E. "Layer stripping: a direct numerical method for impedance imaging". Inverse Problems 7 (1991) 899-926.
- Cheney, M.; Isaacson, D. and Isaacson, E. "Exact solutions to a linearized inverse boundary value problem". Inverse Problems 6 (1990) 923-934.
- Cheng, K.; Isaacson, D.; Newell, J.C. and Gisser, D.G. "Electrode models for electric current computed tomography". IEEE Transactions on Biomedical Engineering, vol. 36, n° 9, September 1989.
- Chexal, B., et al. "Flow-Accelerated Corrosion in Power Plants". EPRI TR-106611, 1996.
- Conolly, T.J. and Wall, D.J.N. "On an inverse problem, with boundary measurements, for the steady state diffusion equation". Inverse Problems 4 (1988) 995-1020.
- Courant, R. and Hilbert, D. "Methods of Mathematical Physics", vol. 2, Interscience Publishers, Inc., New York, 1953.
- Cragolino, G.; Czajkowski, C. and Schack, W.J. "Review of erosion-corrosion in single-phase flows. Argonne National Laboratory, Materials and Components Technology Division, report NUREG/CR-5156, ANL-88-25, April 1988.

- Dobson, D. and Santosa, F. "Resolution and stability analysis of an inverse problem in electrical impedance tomography: dependence on the input current patterns". *SIAM Journal on Applied Mathematical*, vol 54 (1994), n° 6, pp. 1542-1560.
- Dover, W.D. *et al.* "a.c. field measurement – theory and practice". *The Measurement of Crack Length and Shape during Fracture and Fatigue*. Engineering Materials Advisory Services Ltd., London, 1980, pp. 222-260.
- Druce, S.G. and Booth, G.S. "The effect of errors in the geometric and electrical measurements on crack length monitoring by the potential drop technique". *The Measurement of Crack Length and Shape during Fracture and Fatigue*. Engineering Materials Advisory Services Ltd., London, 1980, pp. 136-163.
- Eggleston, M.R.; Schwabe, R.J.; Isaacson, D. and Coffin, L.F. "The application of electric current computed tomography to defect imaging in metals". *Review of Progress in Quantitative Nondestructive Evaluation*, vol 9A, 1990, pp. 455-462.
- Gerber, T.L.; Deardorff, A.F.; Norris, D.M. and Lucas, W.F. "Acceptance criteria for structural evaluation of erosion-corrosion thinning in carbon steel piping". *Nuclear Engineering and Design* 133 (1992) 31-36.
- Gibson, G.P. "Evaluation of the a.c. potential drop method to determine J-crack resistance curves for a pressure vessel steel". *Engineering Fracture Mechanics*, vol. 32, n° 3, pp. 387-401, 1989.
- Gisser, D. G.; Isaacson, D. and Newell, J.C. "Electric current computed tomography and eigenvalues". *SIAM Journal on Applied Mathematical*, vol 50 (1990), n° 6, pp. 1623-1634.

- Glasko, V.B. "Inverse Problems of Mathematical Physics". American Institute of Physics Translation Series, 1988.
- Gradshteyn, I.S. and Ryzhik, I.M. "Table of Integrals, Series, and Products". Fifth Edition, Alan Jeffrey, Editor, 1994.
- Halliday, M.D. and Beever, C.J. "The d.c. electrical potential method for crack length measurement". The Measurement of Crack Length and Shape during Fracture and Fatigue. Engineering Materials Advisory Services Ltd., London, 1980, pp. 85-112.
- Hicks, M.A. and Pickard, A.C. "A comparison of theoretical and experimental methods of calibrating the electrical potential drop technique for crack length determination". International Journal of Fracture 20 (1982), pp. 91-101.
- Hildebrand, F.B. "Advanced Calculus for Applications". Second Edition, Prentice-Hall, Inc., 1976.
- Isaacson, D. and Cheney, M. "Effects of measurement precision and finite numbers of electrodes on linear impedance imaging algorithms". SIAM Journal on Applied Mathematical, vol 51 (1989), n° 6, pp. 1705-1731.
- Isaacson, D.; Cheney, M. and Newell, J. "Problems in impedance imaging". Inverse Problems in Mathematical Physics. Proceedings of the Lapland Conference on Inverse Problems, Saariselka, Finland, 1992, pp. 9-15.
- Iwamura, Y. and Miya, K. "Numerical approach to inverse problem of crack shape recognition based on the electrical potential method". IEEE Transactions on Magnetics, vol. 26, n° 2, March 1990.

- Krompholz, K. *et al.* "Application of the d.c P.D. technique in the high temperature regime". Advances in Crack Length Measurement. Engineering Materials Advisory Services Ltd., London, 1982, pp. 231-250.
- Lebowitz, C.A. and Brown, L.M. "Ultrasonic measurement of pipe thickness". Review of Progress in Quantitative Nondestructive Evaluation, vol 12B, 1993, pp. 1987-1994.
- Mathcad User's Guide. Mathsoft Inc., Cambridge, MA, 1997.
- McIver, M. "Inversion of voltage data to predict crack shape". Review of Progress in Quantitative Nondestructive Evaluation, vol 9A, 1990, pp. 367-373.
- Morel, A.R. and Reynes, L.J. "Short-term degradation mechanisms of piping". Nuclear Engineering and Design 133 (1992), pp. 37-40.
- Morse, P.M. and Feshbach, H. "Methods of Theoretical Physics". Parts I and II. McGraw-Hill Book Company, Inc. 1953.
- Mudge, P.J. and Lank, A.M. "Detection of Corrosion in Pipes and Pipelines". ANST International Chemical and Petroleum Industry Inspection Technology Topical Conference V, Houston, TX, 16-19 June 1997.
- Nachman, A.I. "Reconstruction from boundary measurements". Annals of Mathematics, 128 (1988), pp. 531-576.
- Nishimura, N. and Kobayashi, S. "A Boundary Integral Equation Method for an Inverse Problem Related to Crack Detection". International Journal for Numerical Methods in Engineering, vol. 32, 1991, pp. 1371-1387.
- Okada, H.; Zhao, W. and Atluri, S.N. "A computational approach to determining the depth of surface flaws by the ACPD technique". Engineering Fracture Mechanics, vol 43 (1992), n° 6, pp. 911-921.

- O'Neil, P.V. "Advanced Engineering Mathematics". Fourth Edition, Brooks/Cole Publishing Company, 1995.
- Pickard, A.C. and Hicks, M.A. "Crack length determination using the d.c. electrical p.d. technique – a comparison of calibration methods". Advances in Crack Length Measurement. Engineering Materials Advisory Services Ltd., London, 1982, pp. 97-113.
- Read, D.T. and Pfuff, M. "Potential drop in the center-cracked panel with asymmetric crack extension". International Journal of Fracture, 48 (1991), pp. 219-229.
- Remy, F.N. and Bouchacourt, M. "Flow-assisted corrosion: a method to avoid damage". Nuclear Engineering and Design 133 (1992) 23-30.
- Ritchie, R.O. and Bathe, K.J. "On the calibration of the electrical potential technique for monitoring crack growth using finite element methods". International Journal of Fracture, vol 15 (1979), n° 1, pp. 47-55.
- Ritter, M.A. and Ritchie, R.O. "On the calibration, optimization and use of d.c. electrical potential methods for monitoring mode III crack growth in torsionally-loaded samples". Fatigue of Engineering Materials and Fractures, vol. 5, n° 1, pp. 91-99, 1982.
- Romanov, V.G. "Inverse Problems of Mathematical Physics". VNU Science Press BV, 1987.
- Selby, G. "Development of Phased Array Ultrasonic Examination Applications at the EPRI NDE Center". Proceedings of the 6th International Conference on Nuclear Engineering, Paper n° 6041, May 10-14, 1998.

- Somersalo, E. and Cheney, M. "A linearized inverse boundary value problem for Maxwell's equations. *Journal of Computational and Applied Mathematics* 42 (1992) 123-136.
- Somersalo, E.; Cheney, M. and Isaacson, D. "Existence and uniqueness for electrode models for electric current computed tomography". *SIAM Journal on Applied Mathematical*, vol 52 (1992), n° 4, pp. 1023-1040.
- Strang, G. "Introduction to Applied Mathematics". Wellesley-Cambridge Press, 1986.
- Taylor, H.; Kilpatrick, I.M. and Jolley, G. "ACPD Measurements using four points probes". *Proceedings of the first International Conference of the Engineering Integrity Society*, Bournemouth, UK, pp. 17-20, March 1986.
- Taylor, H.; Kilpatrick, I.M. and Jolley, G. "Developments in a.c. potential-drop crack sizing". *British Journal of NDT*, pp. 88-90, March 1985.
- The Student Edition of Matlab: Version 5 User's Guide. The MathWorks, Inc., Natick, MA, 1997.
- Udpa, S.S. and Udpa, L. "Solution of inverse problems in eddy-current nondestructive evaluation (NDE)". *Journal of Nondestructive Evaluation* 7 (1988) 111-120.
- Vasatis, I.P. and Pelloux, R.M. "DC potential drop technique in creep stress rupture testing". *Journal of Metals*, October 1985.
- Walker, S.M. "New NDE Developments Support Rapid, Economical Screening for Flow-Accelerated Corrosion". *Proceedings of the 6th International Conference on Nuclear Engineering*, Paper n° 6044, May 10-14, 1998.

Watt, K.R. "A consideration of an a.c. potential drop method for crack length measurement". The Measurement of Crack Length and Shape during Fracture and Fatigue. Engineering Materials Advisory Services Ltd., London, 1980, pp. 202-221.

Wei, R.P and Brazill, R.L. " An a.c. potential system for crack length measurement". The Measurement of Crack Length and Shape during Fracture and Fatigue. Engineering Materials Advisory Services Ltd., London, 1980, pp. 190-201.

APPENDIX A

This appendix is a listing of the program "Pipe Thinning" developed in HP Basic for acquiring potential difference measurements. This program sets up the channels for voltage reading, assigns the switch controller to invert the current and filters the data to neglect a deviation by more than half standard deviation from the average.

```
5  ! Program Pipe Thinning
10 ! by
15 ! P. STAHL
20 !
25 OPTION BASE 1
26 DIM File$(20)
30 COM /Screen_data/Ht,Wd,Ih,Iw
35 COM /Devices/@Dvm
36 INPUT "ENTER FILE NAME",File$
37 CREATE File$,1
40 ASSIGN @F TO File$
45 INTEGER G(0:5)
50 GESCAPE CRT,3;G(*)
55 Ht=.75*G(3)
```

```

60 Wd=G(2)
65 CLEAR SCREEN
70 CLEAR 7
75 ASSIGN @Dvm TO 722    ! DIGITAL VOLT METER
80 ASSIGN @Swt TO 710    ! SWITCH CONTROLLER
85 !
90 ASSIGN @Main_panel TO WIDGET "PANEL";SET ("VISIBLE":0)
95 CALL Panel_build(@Main_panel,"Main Panel")
100 STATUS @Main_panel;RETURN ("INSIDE HEIGHT":Ih,"INSIDE WIDTH":Iw)
105 !
110 ON KEY 1 LABEL " HALT" GOTO Halt
115! ON KEY 2 LABEL " TAKE READING" GOTO Take_reading
120 !
125 ASSIGN @Cht TO WIDGET "STRIPCHART";PARENT @Main_panel
130 Chart_build(@Main_panel,@Cht,-1.E-5,-3.E-5,1,"", "")
135 CONTROL @Cht;SET ("CURRENT AXIS":"Y","AUTOSCALE":0)
140 CONTROL @Main_panel;SET ("VISIBLE":1)
145 CONTROL @Cht;SET ("CURRENT AXIS":"X","RANGE":2000)
150 OUTPUT @Swt;"SLIST200-209,300-309,400-409,500-509,0"
155 Nrows=10
160 !
165 Take_reading:!
170 !

```



```

175 Timer=60

180 !

185 OUTPUT @Dvm;"RESET"

190 OUTPUT @Dvm;"TERM REAR"

195 OUTPUT @Dvm;"NDIG 6"

200 OUTPUT @Dvm;"NPLC 100"

205 OUTPUT @Swt;"CLOSE 100"

210 Crnt$="POSITIVE"

215 FOR Chnl=1 TO 40!

220 GOSUB Monitor

225 OUTPUT @Swt;"STEP"

230 Volt=FNEnter_volts(Timer)

235 CONTROL @Cht;SET ("POINT LOCATION":TIMEDATE,"VALUE":Volt)

240 OUTPUT @F USING

"4(K, "", ""),K";DATES$(TIMEDATE),TIMES$(TIMEDATE),Volt,Chnl,Crnt$

245 DISP DATES$(TIMEDATE),TIMES$(TIMEDATE),Volt,Chnl,Crnt$

250 NEXT Chnl

255 OUTPUT @Swt;"STEP"

260 OUTPUT @Swt;"OPEN 100"

265 OUTPUT @Swt;"CLOSE 101"

270 Crnt$="NEGATIVE"

275 FOR Chnl=1 TO 40!

280 GOSUB Monitor

```

```

285 OUTPUT @Swt;"STEP"
290 Volt=FNEnter_volts(Timer)
295 CONTROL @Cht;SET ("POINT LOCATION":TIMEDATE,"VALUE":Volt)
300 OUTPUT @F USING
"4(K,"",""),K";DATES$(TIMEDATE),TIMES$(TIMEDATE),Volt,Chnl,Crnt$
305 DISP DATES$(TIMEDATE),TIMES$(TIMEDATE),Volt,Chnl,Crnt$
310 NEXT Chnl
315 OUTPUT @Swt;"RESET"
320 Halt: !
325 ASSIGN @F TO *
330 LOCAL 710
335 LOCAL 722
340 CLEAR 7
345 STOP
350 Monitor: !
355 SELECT Chnl
360 CASE 1
365 OUTPUT @Swt;"CMON 2"
370 CASE 11
375 OUTPUT @Swt;"CMON 3"
380 CASE 21
385 OUTPUT @Swt;"CMON 4"
390 CASE 31

```

```

395 OUTPUT @Swt;"CMON 5"
400 END SELECT
405 RETURN
410 The_end: END
415 !
420 SUB Time_delay(T)
425 T1=TIMEDATE
430 IF TIMEDATE-T1>T THEN
435 SUBEXIT
440 ELSE
445 GOTO 430
450 END IF
455 SUBEND
460 Chart_build: SUB Chart_build(@Charts,@W,REAL Yorg,Yrng,Traces,Titl$,Ylbl$)
465 OPTION BASE 1
470 INTEGER G(0:5)
475 GESCAPE CRT,3;G(*)
480 STATUS @Charts;RETURN ("INSIDE HEIGHT":G(3),"INSIDE WIDTH":G(2))
485 CONTROL @W;SET ("X":0,"Y":0)
490 CONTROL @W;SET ("WIDTH":G(2),"HEIGHT":G(3))
495 CONTROL @W;SET ("CURRENT AXIS":"X","DIGITS":5,"NUMBER
FORMAT":"CLOCK24")
500 CONTROL @W;SET ("ORIGIN":TIMEDATE,"RANGE":43200)

```

```

505 CONTROL @W;SET ("AXIS LABEL":"Time")
510 Crtid$=SYSTEM$("CRT ID")
515 IF Crtid$[7;7]="C" THEN
520     CONTROL @W;SET ("BACKGROUND":11,"TRACE BACKGROUND":1)
525 END IF
530 CONTROL @W;SET ("CURRENT TRACE":0,"POINT CAPACITY":1500)
535 CONTROL @W;SET ("SHARED X":1,"TRACE COUNT":Traces)
540 CONTROL @W;SET ("MINIMUM SCROLL":0)
545 CONTROL @W;SET ("CURRENT AXIS":"Y","ORIGIN":Yorg,"RANGE":Yrng)
550 CONTROL @W;SET ("AXIS LABEL":Ylbl$)
555 CONTROL @W;SET ("SHOW GRID":1)
560 SUBEND
565 !
570 !
575 SUB Panel_build(@P,A$)
580 OPTION BASE 1
585 COM /Screen_data/Ht,Wd,Ih,Iw
590 !
595 CONTROL @P;SET ("X":0,"Y":0)
600 CONTROL @P;SET ("WIDTH":Wd,"HEIGHT":Ht)
605 CONTROL @P;SET ("TITLE":A$)
610 SUBEND
615 !

```

```

620 !
625 ! CODE TO READ AND FILTER THE RESULTS
630 !
635 DEF FNEnter_volts(Timer)
640 COM /Devices/@Dvm
645 DIM V(100)
650 I=-1
655 T=TIMEDATE
660 LOOP
665 I=I+1
670 ENTER @Dvm;V(I)
675 EXIT IF TIMEDATE-T>Timer
680 END LOOP
685 CALL Filter(V(*),Vfiltered,I)
690 RETURN Vfiltered
695 FNEND
700 !
705 SUB Filter(X(*),X_filtered,N)
710 Mean=SUM(X)/N
715 Xsum=0.
720 FOR I=1 TO N
725 Xsum=Xsum+(X(I)-Mean)^2
730 NEXT I

```

```
735  Sigma=SQR(.1111111111*Xsum)
740  Test=.5*Sigma
745  Incr=.1*Sigma
750  Testing:~
755  Xsum=0.
760  Nsum=0
765  FOR I=1 TO N
770    IF ABS(X(I)-Mean)>Test THEN GOTO 785
775    Xsum=Xsum+X(I)
780    Nsum=Nsum+1
785  NEXT I
790  IF Nsum=0 THEN
795    Test=Test+Incr
800    GOTO Testing
805  END IF
810  X_filtered=Xsum/Nsum
815 SUBEND
```

APPENDIX B

This appendix describes the numerical solution for an infinite plate with slot defect using Fourier transformation. From equations 4.5, 4.6 and 4.7,

$$\nabla^2 \varphi(x, y, z) = 0 \quad (\text{B.1})$$

$$\left. \frac{\partial \varphi}{\partial y} \right|_{y=a} = \rho S(x, z), \quad (\text{B.2})$$

$$\left. \frac{\partial \varphi}{\partial y} \right|_{y=0} = \rho P(x, z). \quad (\text{B.3})$$

By definition,

$$\hat{\varphi}(k_x, k_z, y) = \frac{1}{2\pi} \int_{-\infty}^{\infty} \int_{-\infty}^{\infty} \varphi(x, y, z) e^{(ik_x x + ik_z z)} dz dx, \quad (\text{B.4})$$

$$\varphi(x, y, z) = \frac{1}{2\pi} \int_{-\infty}^{\infty} \int_{-\infty}^{\infty} \hat{\varphi}(k_x, k_z, y) e^{-(ik_x x + ik_z z)} dk_x dk_z, \quad (\text{B.5})$$

where $\hat{\varphi}$ is the Fourier transform of φ and k_x, k_z are the variables in the frequency domain.

Applying the Fourier transformation to Equation B.1 results in

$$\frac{\partial^2 \hat{\varphi}}{\partial y^2} - k^2 \hat{\varphi} = 0, \quad (\text{B.6})$$

where $k^2 = k_x^2 + k_z^2$.

Applying the Fourier transformation to equations B.2 and B.3, the boundary conditions change to

$$\text{at } y = a : \quad \frac{\partial \hat{\phi}}{\partial y} = \rho \hat{S}(k_x, k_z), \quad (\text{B.7})$$

$$\text{at } y = 0 : \quad \frac{\partial \hat{\phi}}{\partial y} = \rho \hat{P}(k_x, k_z), \quad (\text{B.8})$$

where \hat{S} and \hat{P} are the Fourier transform of $S(x, z)$ and $P(x, z)$, respectively.

The general solution for Equation B.6 is

$$\hat{\phi}(k, y) = A \cosh ky + B \sinh ky, \quad (\text{B.9})$$

and after applying the boundary conditions

$$\hat{\phi}(k, y) = \frac{\rho}{k \sinh ka} [\hat{S} \cosh ky - \hat{P} \cosh k(y - a)]. \quad (\text{B.10})$$

Plugging this equation into Equation B.5 results in

$$\varphi(x, y, z) = \frac{1}{2\pi} \int_{-\infty}^{\infty} \int_{-\infty}^{\infty} \frac{\rho}{k \sinh ka} [\hat{S} \cosh ky - \hat{P} \cosh k(y - a)] e^{-(ik_x x + ik_z z)} dk_x dk_z. \quad (\text{B.11})$$

To solve Equation B.11 it is necessary to find the functions \hat{S} and \hat{P} . Using the

definition of the current source function as $S(x, z) = \frac{S_0}{\pi r^2}$, the Fourier transform of S can

be found:

$$\hat{S} = \frac{1}{2\pi} \int_{-\infty}^{\infty} \int_{-\infty}^{\infty} S(x, z) e^{(ik_x x + ik_z z)} dx dz. \quad (\text{B.12})$$

Figure B.1 shows a schematic view of the wires attached to the plate. At this time, the problem is being modeled as one wire on each end of the plate.

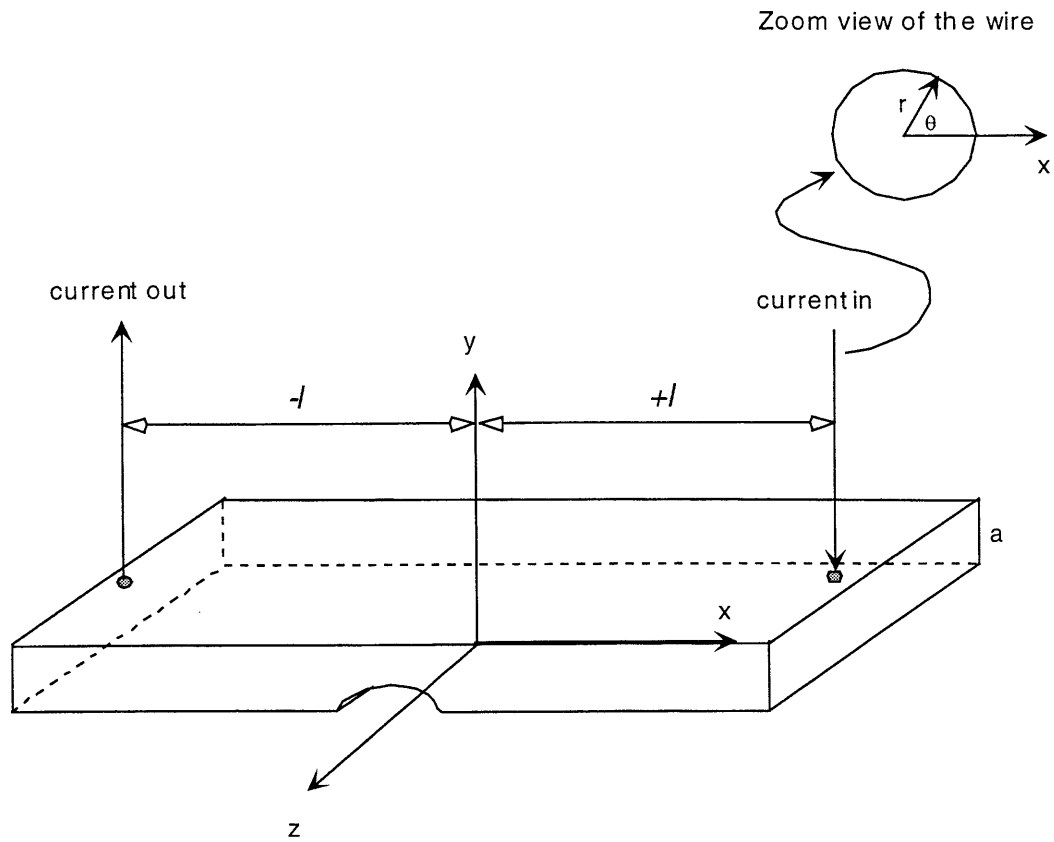


Figure B.1 – Schematic view of plate with the round wires.

Considering only the input current wire on the right border of the plate, the following change of variables is helpful:

$$x = l + \rho \cos \theta ,$$

$$z = \rho \sin \theta ,$$

$$dx dz = \rho d\rho d\theta ,$$

$$k_x = k \cos \alpha ,$$

$$k_z = k \sin \alpha ,$$

where l is the distance between the current wire and the center of the plate and r is the radius of the wire.

The argument of the exponential of Equation B.12 can be expressed as

$$\begin{aligned}
 i(k_x x + k_z z) &= i[k \cos \alpha (l + \rho \cos \theta) + k \sin \alpha (\rho \sin \theta)], \\
 i(k_x x + k_z z) &= i[kl \cos \alpha + k\rho (\cos \alpha \cos \theta + \sin \alpha \sin \theta)], \\
 i(k_x x + k_z z) &= i[kl \cos \alpha + k\rho \cos(\alpha - \theta)],
 \end{aligned} \tag{B.13}$$

and substituting Equation B.13 into Equation B.12 produces an expression for \hat{S} ,

considering only the current wire located on the right border of the plate:

$$\begin{aligned}
 \hat{S}_{right} &= \frac{1}{2\pi} \int_0^{2\pi r} \int_0^{S_0} \frac{S_0}{\pi r^2} e^{[ikl \cos \alpha + ik\rho \cos(\alpha - \theta)]} \rho d\rho d\theta, \\
 \hat{S}_{right} &= \frac{e^{ik_x l} S_0}{2\pi \cdot \pi r^2} \int_0^{2\pi r} \int_0^{S_0} e^{ik\rho \cos(\alpha - \theta)} \rho d\rho d\theta.
 \end{aligned} \tag{B.14}$$

Using the definition of the zero order Bessel function,

$$J_0(k\rho) = \frac{1}{2\pi} \int_0^{2\pi} e^{ik\rho \cos \theta} d\theta, \tag{B.15}$$

gives

$$\hat{S}_{right} = \frac{e^{ik_x l} S_0}{\pi r^2} \int_0^r J_0(k\rho) \rho d\rho. \tag{B.16}$$

Making another change of variables,

$$w = k\rho,$$

$$dw = k d\rho,$$

Equation B.16 can be expressed as

$$\hat{S}_{right} = \frac{e^{ik_x l} S_0}{\pi r^2 k^2} \int_0^{kr} J_0(w) w dw,$$

$$\hat{S}_{right} = \frac{S_0}{\pi} \frac{e^{ikl \cos \alpha}}{kr} J_1(kr), \quad (\text{B.17})$$

where J_1 is the first order Bessel function.

For the outlet current wire on the left border of the plate, a similar change of variables is necessary:

$$x = -(l + \rho \cos \theta),$$

$$z = \rho \sin \theta,$$

$$dx dz = -\rho d\rho d\theta.$$

With similar results:

$$\hat{S}_{left} = \frac{S_0}{\pi} \frac{e^{-ikl \cos \alpha}}{kr} J_1(kr), \quad (\text{B.18})$$

and therefore, the total source current function can be calculated as

$$\begin{aligned} \hat{S}_{total} &= \hat{S}_{right} - \hat{S}_{left}, \\ \hat{S}_{total} &= \frac{S_0}{\pi} \left[\frac{e^{ikl \cos \alpha}}{kr} - \frac{e^{-ikl \cos \alpha}}{kr} \right] J_1(kr), \\ \hat{S}_{total} &= 2i \frac{S_0}{\pi} \frac{\sin(kl \cos \alpha)}{kr} J_1(kr). \end{aligned} \quad (\text{B.19})$$

To find the function \hat{P} it was assumed the defect in the material is given by a

Gaussian distribution type with parameters P_0 and λ , that is, $P(x, z) = P_0 \frac{x}{\lambda} e^{-x^2/\lambda^2}$.

Using the Fourier transformation the function \hat{P} can be calculated as:

$$\hat{P} = \frac{1}{2\pi} \int_{-\infty}^{\infty} \int_{-\infty}^{\infty} P(x, z) e^{(ik_x x + ik_z z)} dx dz,$$

$$\hat{P} = \frac{1}{2\pi} \int_{-\infty}^{\infty} e^{ik_z z} dz \int_{-\infty}^{\infty} \frac{P_0}{\lambda} x e^{-x^2/\lambda^2} e^{ik_x x} dx,$$

$$\hat{P} = \frac{P_0 \sqrt{2\pi}}{2\pi} \delta(k_z) \int_{-\infty}^{\infty} \frac{x}{\lambda} e^{-\frac{x^2}{\lambda^2} + ik_x x} dx. \quad (\text{B.20})$$

Applying the following change of variables:

$$\zeta = \frac{x}{\lambda},$$

$$dx = \lambda d\zeta,$$

the \hat{P} function will be

$$\hat{P} = \frac{P_0 \sqrt{2\pi}}{2\pi} \delta(k_z) \int_{-\infty}^{\infty} \lambda \zeta e^{-\zeta^2 + ik_x \lambda \zeta} d\zeta,$$

$$\hat{P} = \frac{P_0 \sqrt{2\pi}}{2\pi} \delta(k_z) \lambda \int_{-\infty}^{\infty} \left(\zeta + i \frac{k_x \lambda}{2} - i \frac{k_x \lambda}{2} \right) e^{-(\zeta - i \frac{k_x \lambda}{2})^2} e^{-\frac{k_x^2 \lambda^2}{4}} d\zeta,$$

$$\hat{P} = \frac{P_0 \sqrt{2\pi}}{2\pi} \delta(k_z) \lambda e^{-\frac{k_x^2 \lambda^2}{4}} \int_{-\infty}^{\infty} \left(\zeta + i \frac{k_x \lambda}{2} - i \frac{k_x \lambda}{2} \right) e^{-(\zeta - i \frac{k_x \lambda}{2})^2} d\zeta. \quad (\text{B.21})$$

This integral can be simplified through another change of variables,

$$u = \zeta - i \frac{k_x \lambda}{2},$$

thus

$$\hat{P} = \frac{P_0 \sqrt{2\pi}}{2\pi} \delta(k_z) \lambda e^{-\frac{k_x^2 \lambda^2}{4}} \int_{-\infty}^{\infty} \left(u + i \frac{k_x \lambda}{2} \right) e^{-u^2} du,$$

$$\hat{P} = \frac{P_0 \sqrt{2\pi}}{2\pi} \delta(k_z) \lambda e^{-\frac{k_x^2 \lambda^2}{4}} \sqrt{\pi} i \frac{k_x \lambda}{2},$$

$$\hat{P} = i \frac{P_0}{2^{3/2}} \delta(k_z) e^{-\frac{k_x^2 \lambda^2}{4}} k_x \lambda^2. \quad (\text{B.22})$$

Now, the voltage difference between two probes can be calculated. Substituting equations B.19 and B.22 into Equation B.10 gives

$$\hat{\varphi}(k, y) = \frac{\rho}{k \sinh ka} \left[2i \frac{S_0}{\pi} \frac{\sin(kl \cos \alpha)}{kr} J_1(kr) \cosh ky - i \frac{P_0}{2^{3/2}} \delta(k_z) e^{-\frac{k_x^2 \lambda^2}{4}} k_x \lambda^2 \cosh k(y-a) \right].$$

Substituting this expression into Equation B.5 a general expression for the potential function can be calculated:

$$\varphi(x, y, z) = \frac{1}{2\pi} \int_{-\infty}^{\infty} \int_{-\infty}^{\infty} \frac{\rho}{k \sinh ka} \left[2i \frac{S_0}{\pi} \frac{\sin(kl \cos \alpha)}{kr} J_1(kr) \cosh ky - i \frac{P_0}{2^{3/2}} \delta(k_z) e^{-\frac{k_x^2 \lambda^2}{4}} k_x \lambda^2 \cosh k(y-a) \right] e^{-i(k_x x + ik_z z)} dk_x dk_z$$

Evaluating this function at the centerline of the plate ($z = 0$) and at the surface of the plate ($y = a$) results in

$$\varphi(x, y = a, z = 0) = \frac{i}{2\pi} \int_{-\infty}^{\infty} \int_{-\infty}^{\infty} \frac{\rho}{k \sinh ka} \left[2 \frac{S_0}{\pi} \frac{\sin(kl \cos \alpha)}{kr} J_1(kr) \cosh ka - \frac{P_0}{2^{3/2}} \delta(k_z) e^{-\frac{k_x^2 \lambda^2}{4}} k_x \lambda^2 \right] e^{-ik_x x} dk_x dk_z$$

Finally, recalling Equation 4.8 and substituting the expression above obtained for φ gives

$$V(x, y = a, z = 0) = V(x) = \varphi(x, y = a, z = 0) - \varphi(-x, y = a, z = 0), \quad (\text{B.23})$$

$$V(x) = \frac{\rho}{2\pi} \int_{-\infty}^{\infty} \int_{-\infty}^{\infty} dk_x dk_z \frac{(e^{-ik_x x} - e^{ik_x x})}{k \sinh ka} \left[\cosh ka \frac{2iS_0}{\pi} \sin(kl \cos \alpha) \frac{J_1(kr)}{kr} - i \frac{P_0}{2^{3/2}} \delta(k_z) e^{-\frac{k_x^2 \lambda^2}{4}} k_x \lambda^2 \right],$$

$$V(x) = \frac{\rho}{\pi} \int_{-\infty}^{\infty} \int_{-\infty}^{\infty} dk_x dk_z \frac{\sin k_x x}{k \sinh ka} \left[\cosh ka \frac{2S_0}{\pi} \sin(kl \cos \alpha) \frac{J_1(kr)}{kr} - \frac{P_0}{2^{3/2}} \delta(k_z) e^{-\frac{k_x^2 \lambda^2}{4}} k_x \lambda^2 \right]. \quad (\text{B.24})$$

This integral can be separated into two parts: the first part takes into account only the non-defected region of the specimen. The second part considers the effect of a defect

with a Gaussian distribution. These integrals will be represented as I1 and I2, respectively. Thus,

$$V(x) = I1 - I2. \quad (\text{B.25})$$

The first integral is

$$I1 = \frac{\rho}{\pi} \int_{-\infty}^{\infty} \int_{-\infty}^{\infty} dk_x dk_z \frac{\sin k_x x}{k \sinh ka} \cosh ka \frac{2S_0}{\pi} \sin(kl \cos \alpha) \frac{J_1(kr)}{kr},$$

$$I1 = \frac{2S_0 \rho}{\pi^2} \int_{-\infty}^{\infty} \int_{-\infty}^{\infty} dk_x dk_z \frac{\sin k_x x}{k \tanh ka} \sin(kl \cos \alpha) \frac{J_1(kr)}{kr}. \quad (\text{B.26})$$

If we change variables,

$$k_x = k \cos \alpha,$$

$$k_z = k \sin \alpha,$$

$$dk_x dk_z = k dk d\alpha,$$

the integral becomes

$$I1 = \frac{2S_0 \rho}{\pi^2} \int_0^{\infty} \int_{-\infty}^{\infty} dk d\alpha \frac{\sin(kx \cos \alpha) \sin(kl \cos \alpha)}{\tanh ka} \frac{J_1(kr)}{kr}. \quad (\text{B.27})$$

From trigonometric relations

$$\sin(a) \cdot \sin(b) = \frac{1}{2} [\cos(a-b) - \cos(a+b)], \text{ and}$$

$$\cos \beta = \frac{1}{2} (e^{i\beta} + e^{-i\beta}),$$

therefore,

$$I1 = \frac{S_0 \rho}{\pi^2} \int_0^{\infty} \int_{-\infty}^{\infty} dk d\alpha \frac{\cos[k \cos \alpha (x-l)] - \cos[k \cos \alpha (x+l)]}{\tanh ka} \frac{J_1(kr)}{kr},$$

$$I1 = \frac{2S_0\rho}{\pi^2} \int_0^{2\pi\infty} \int_0^\infty dk d\alpha \frac{\cos[k \cos \alpha(x-l)] - \cos[k \cos \alpha(x+l)]}{\tanh ka} \frac{J_1(kr)}{kr},$$

$$I1 = \frac{S_0\rho}{\pi^2} \int_0^{2\pi\infty} \int_0^\infty dk d\alpha \frac{[e^{ik \cos \alpha(x-l)} + e^{-ik \cos \alpha(x-l)} - e^{ik \cos \alpha(x+l)} - e^{-ik \cos \alpha(x+l)}]}{\tanh ka} \frac{J_1(kr)}{kr}. \quad (\text{B.28})$$

Recalling the definition of the zero order Bessel function in Equation B.15 $I1$ becomes

$$I1 = \frac{4S_0\rho}{\pi} \int_0^\infty \frac{dk}{\tanh ka} \frac{J_1(kr)}{kr} \{J_0[k(x-l)] - J_0[k(x+l)]\}. \quad (\text{B.29})$$

The second integral, represented by $I2$, is

$$I2 = \frac{\rho}{\pi} \int_{-\infty}^\infty \int_{-\infty}^\infty dk_x dk_z \frac{\sin k_x x}{k \sinh ka} \frac{P_0}{2^{3/2}} \delta(k_z) e^{-\frac{k_x^2 \lambda^2}{4}} k_x \lambda^2,$$

$$I2 = \frac{P_0 \lambda^2 \rho}{\pi 2^{3/2}} \int_{-\infty}^\infty \int_{-\infty}^\infty dk_x dk_z \frac{\sin k_x x}{k \sinh ka} \delta(k_z) e^{-\frac{k_x^2 \lambda^2}{4}} k_x. \quad (\text{B.30})$$

Recalling that

$$k = \sqrt{k_x^2 + k_z^2}, \text{ and by definition}$$

$$\int_{-\infty}^\infty f(k_z) \delta(k_z) dk_z = f(0),$$

the following expression for $I2$ is obtained:

$$I2 = \frac{P_0 \lambda^2 \rho}{\pi 2^{3/2}} \int_{-\infty}^\infty dk_x dk_z \frac{\sin k_x x}{|k_x| \sinh(|k_x|a)} e^{-\frac{k_x^2 \lambda^2}{4}} k_x,$$

$$I2 = \frac{P_0 \lambda^2 \rho}{\pi 2^{3/2}} \int_0^\infty dk_x \frac{\sin k_x x}{\sinh(k_x a)} e^{-\frac{k_x^2 \lambda^2}{4}}. \quad (\text{B.31})$$

Substituting equations B.29 and B.31 into Equation B.25 the final expression for voltage difference will be:

$$V(x) = \frac{4S_0\rho}{\pi} \int_0^{\infty} \frac{dk}{\tanh ka} \frac{J_1(kr)}{kr} \{J_0[k(x-l)] - J_0[k(x+l)]\} - \frac{P_0\lambda^2\rho}{\pi 2^{3/2}} \int_0^{\infty} dk_x \frac{\sin k_x x}{\sinh(k_x a)} e^{-\frac{k_x^2 \lambda^2}{4}}. \quad (\text{B.32})$$

This expression considers the current coming in for a single wire and coming out for another single wire, as shown in Figure B.1. The next step, in order to provide a more uniform current distribution along the plate, is to model the specimen with multiple wires. Figure B.2 shows a schematic view of this model.

Defining $z_m = mc$, where c is the spacing between current wires, the following change of variables will be necessary:

$$\begin{aligned} x &= l + \rho \cos \theta, \\ z &= z_m + \rho \sin \theta, \\ k_x &= k \cos \alpha, \\ k_z &= k \sin \alpha, \\ dx dz &= \rho d\rho d\theta, \end{aligned}$$

and the argument of the exponential of Equation B.12 can be written as

$$\begin{aligned} i(k_x x + k_z z) &= i[k \cos \alpha (l + \rho \cos \theta) + k \sin \alpha (z_m + \rho \sin \theta)], \\ i(k_x x + k_z z) &= i[kl \cos \alpha + k\rho \cos(\alpha - \theta) + (k \sin \alpha)z_m]. \end{aligned} \quad (\text{B.33})$$

Analogous to Equation B.14, the function \hat{S} considering only the current wires located on the right border of the plate (current coming in) will be:

$$\hat{S}_{right} = \frac{1}{2\pi} \sum_{m=-\infty}^{\infty} \int_0^{2\pi} \int_0^r \frac{S_0}{\pi r^2} e^{[ikl \cos \alpha + ik\rho \cos(\alpha - \theta) + ikz_m \sin \alpha]} \rho d\rho d\theta. \quad (\text{B.34})$$

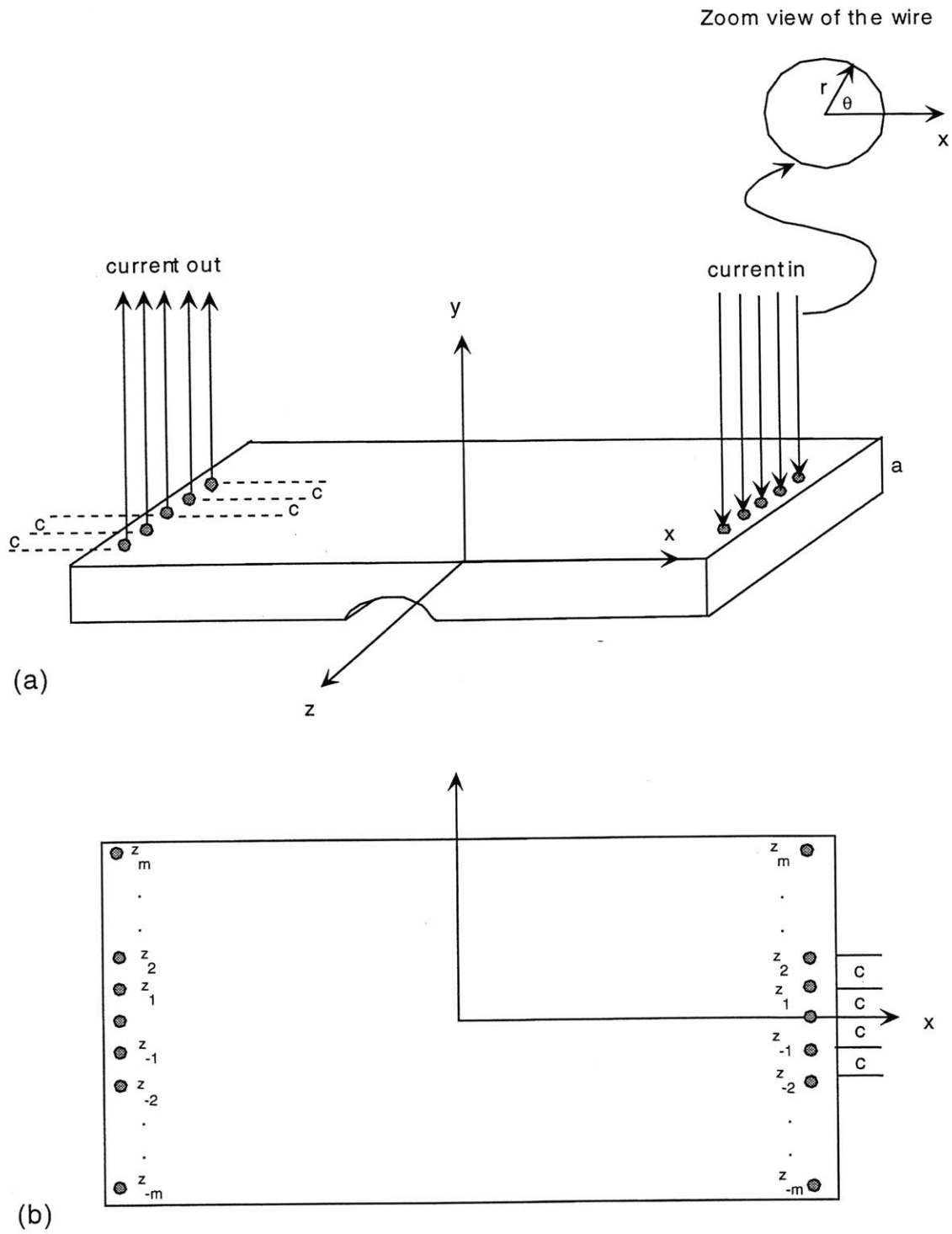


Figure B.2 – (a) Schematic view of the model with multiple wires;
 (b) top view of the plate.

Developing this equation in the same way as was done for the single current wire case an expression similar to Equation B.17 results:

$$\hat{S}_{right} = \frac{S_0}{\pi} \frac{e^{ikl \cos \alpha}}{kr} J_1(kr) \sum_{m=-\infty}^{\infty} e^{ikz_m \sin \alpha} . \quad (\text{B.35})$$

Finally, taking account of the current wires on the left border of the plate, where the current is coming out, gives

$$\hat{S}_{total} = 2i \frac{S_0}{\pi} \frac{\sin(kl \cos \alpha)}{kr} J_1(kr) \sum_{m=-\infty}^{\infty} e^{ikz_m \sin \alpha} . \quad (\text{B.36})$$

Since the model with multiple wires does not change Equation B.31, only the contribution of the non-defect region to the voltage difference measurements changes.

This term is represented by $V_0(x)$ and, similarly to Equation B.26, it can be expressed as

$$V_0(x) = \frac{2S_0\rho}{\pi^2} \sum_{m=-\infty}^{\infty} \int_{-\infty}^{\infty} \int_{-\infty}^{\infty} dk_x dk_z \frac{\sin k_x x}{k \tanh ka} \sin(kl \cos \alpha) \frac{J_1(kr)}{kr} e^{ikz_m \sin \alpha} . \quad (\text{B.37})$$

Making the same change of variables as before results in

$$V_0(x) = \frac{2S_0\rho}{\pi^2} \sum_{m=-\infty}^{\infty} \int_0^{2\pi} \int_{-\infty}^{\infty} dk d\alpha \frac{\sin(kx \cos \alpha)}{\tanh ka} \sin(kl \cos \alpha) \frac{J_1(kr)}{kr} e^{ikz_m \sin \alpha} . \quad (\text{B.38})$$

Using the same approach as Equation B.27 the equation above can be written as

$$V_0(x) = \frac{S_0\rho}{\pi^2} \sum_{m=-\infty}^{\infty} \int_0^{2\pi} \int_0^{\infty} dk d\alpha \frac{[e^{ik \cos \alpha(x-l)} + e^{-ik \cos \alpha(x-l)} - e^{ik \cos \alpha(x+l)} - e^{-ik \cos \alpha(x+l)}]}{\tanh ka} \frac{J_1(kr)}{kr} e^{ikz_m \sin \alpha} . \quad (\text{B.39})$$

The following change of variables simplifies the above expression:

$$\begin{aligned} a &= k(x-l) , \\ b &= kmc , \\ \gamma &= a \cos \alpha + b \sin \alpha . \end{aligned} \quad (\text{B.40})$$

Equation B.40 can be written as

$$\gamma = \sqrt{a^2 + b^2} \left(\frac{1}{\sqrt{1 + \frac{b^2}{a}}} \cos \alpha + \frac{1}{\sqrt{1 + \frac{a^2}{b}}} \sin \alpha \right),$$

and defining $\tan \phi_0 = \frac{b}{a}$ results in

$$\gamma = \sqrt{a^2 + b^2} \cos(\alpha + \phi_0), \quad (\text{B.41})$$

$$\gamma = \sqrt{k^2(x-l)^2 + k^2 m^2 c^2} \cos(\alpha + \phi_0).$$

Recalling the definition of the Bessel function in Equation B.15

$$J_0 \left(\sqrt{k^2(x-l)^2 + k^2 m^2 c^2} \right) = \frac{1}{2\pi} \int_0^{2\pi} e^{i \sqrt{k^2(x-l)^2 + k^2 m^2 c^2} \cos(\alpha + \phi_0)} d\alpha,$$

and finally the contribution of the non-defect region to the voltage difference

measurements can be expressed as

$$V_0(x) = \frac{4S_0\rho}{\pi} \sum_{m=-\infty}^{\infty} \int_0^{\infty} \frac{dk}{\tanh ka} \frac{J_1(kr)}{kr} [J_0(k\sqrt{(x-l)^2 + m^2 c^2}) - J_0(k\sqrt{(x+l)^2 + m^2 c^2})]. \quad (\text{B.42})$$

The total potential difference will be

$$V(x) = \frac{4S_0\rho}{\pi} \sum_{m=-\infty}^{\infty} \int_0^{\infty} \frac{dk}{\tanh ka} \frac{J_1(kr)}{kr} [J_0(k\sqrt{(x-l)^2 + m^2 c^2}) - J_0(k\sqrt{(x+l)^2 + m^2 c^2})] - \frac{P_0 \lambda^2 \rho}{\pi 2^{3/2}} \int_0^{\infty} dk_x \frac{\sin k_x x}{\sinh(k_x a)} e^{-\frac{k_x^2 \lambda^2}{4}},$$

which is the expression for Equation 4.9.

APPENDIX C

This appendix describes the numerical solution for a semi-infinite plate without defect using Fourier transformation. From Equation 4.10

$$\varphi(x, y, z) = \frac{1}{\sqrt{2\pi}} \sum_{n=0}^{\infty} \int_{-\infty}^{\infty} e^{ikx} \cos\left(\frac{n\pi z}{w}\right) \hat{\varphi}_n(k, y) dk. \quad (\text{C.1})$$

Taking the Fourier transform of the Laplace equation:

$$\frac{\partial^2 \hat{\varphi}_n}{\partial y^2} - \left(k^2 + \frac{n^2 \pi^2}{w^2} \right) \hat{\varphi}_n = 0 \quad (\text{C.2})$$

and calling $k_n^2 = k^2 + \frac{n^2 \pi^2}{w^2}$, the Laplace equation can be expressed as

$$\frac{\partial^2 \hat{\varphi}_n}{\partial y^2} - k_n^2 \hat{\varphi}_n = 0. \quad (\text{C.3})$$

The general solution to this equation is

$$\hat{\varphi}_n(k, y) = A_n \cosh(k_n y) + B_n \sinh(k_n y). \quad (\text{C.4})$$

The boundary conditions require

$$\left. \frac{\partial \hat{\varphi}}{\partial y} \right|_{y=0} = B_n k_n = 0 \rightarrow B_n = 0 \text{ and}$$

$$\left. \frac{\partial \hat{\varphi}}{\partial y} \right|_{y=a} = A_n k_n \sinh k_n a = \rho \hat{S}(k, y),$$

where $\hat{S}(k, y)$ is the Fourier transform of $S(x, z)$.

Equation C.1 can be written as

$$\varphi(x, y, z) = \frac{1}{\sqrt{2\pi}} \sum_{n=0}^{\infty} \int_{-\infty}^{\infty} e^{ikx} \cos\left(\frac{n\pi z}{w}\right) A_n \cosh(k_n y) dk. \quad (\text{C.5})$$

From the boundary condition

$$\left. \frac{\partial \varphi}{\partial y} \right)_{y=a} = \rho S(x, z), \text{ and}$$

from the Equation C.5

$$\left. \frac{\partial \varphi}{\partial y} \right)_{y=a} = \frac{1}{\sqrt{2\pi}} \sum_{n=0}^{\infty} \int_{-\infty}^{\infty} e^{ikx} \cos\left(\frac{n\pi z}{w}\right) A_n k_n \sinh(k_n a) dk.$$

These equations give

$$\frac{1}{\sqrt{2\pi}} \sum_{n=0}^{\infty} \int_{-\infty}^{\infty} e^{ikx} \cos\left(\frac{n\pi z}{w}\right) A_n k_n \sinh(k_n a) dk = \rho S(x, z). \quad (\text{C.6})$$

In order to calculate the coefficient A_n from the equation above, again apply

Fourier analysis. Multiplying both sides of Equation C.6 by

$$\int_0^{2w} \cos \frac{m\pi z}{w} dz \int_{-\infty}^{\infty} e^{-ikx} dx,$$

the left-hand side becomes

$$\begin{aligned} LHS &= \frac{1}{\sqrt{2\pi}} \sum_{n=0}^{\infty} \int_{-\infty}^{\infty} e^{ikx} \cos\left(\frac{n\pi z}{w}\right) A_n k_n \sinh(k_n a) dk \int_0^{2w} \cos \frac{m\pi z}{w} dz \int_{-\infty}^{\infty} e^{-ikx} dx, \\ LHS &= \frac{1}{\sqrt{2\pi}} \sum_{n=0}^{\infty} \int_{-\infty}^{\infty} A_n k_n \sinh(k_n a) dk \int_0^{2w} \cos\left(\frac{n\pi z}{w}\right) \cos \frac{m\pi z}{w} dz \int_{-\infty}^{\infty} e^{i(k-k')x} dx. \end{aligned} \quad (\text{C.7})$$

Observe that

$$I1 = \int_0^{2w} \cos \frac{m\pi z}{w} \cos \frac{n\pi z}{w} dz = \begin{cases} 2w & \text{if } n = m = 0 \\ w & \text{if } n = m \neq 0 \end{cases},$$

$$I1 = w \sigma_n \delta_{mn}, \quad (\text{C.8})$$

where δ_{mn} is the Kronecker delta and $\sigma_n = 1$ if $n \neq 0$ and $\sigma_n = 2$ if $n = 0$. The other integral is

$$I2 = \int_{-\infty}^{\infty} e^{-i(k-k')x} dx = 2\pi \delta(k-k'), \quad (C.9)$$

thus Equation C.7 can be rewritten as

$$LHS = \frac{1}{\sqrt{2\pi}} \sum_{n=0}^{\infty} \int_{-\infty}^{\infty} dk A_n k_n \sinh(k_n a) I1 I2,$$

and substituting equations C.8 and C.9 into the equation above results in

$$LHS = \frac{1}{\sqrt{2\pi}} \sum_{n=0}^{\infty} \int_{-\infty}^{\infty} A_n k_n \sinh(k_n a) 2\pi \delta(k-k') w \sigma_n \delta_{mn} dk,$$

$$LHS = \frac{1}{\sqrt{2\pi}} A_m k_m \sigma_m \sinh(k_m a) 2\pi w, \quad (C.10)$$

where $k_m^2 = k'^2 + \frac{m^2 \pi^2}{w^2}$.

In addition, the right hand side of Equation C.6 becomes

$$RHS = \rho \int_0^{2w} \cos \frac{m\pi z}{w} dz \int_{-\infty}^{\infty} e^{-ik'x} dx S(x, z). \quad (C.11)$$

Recalling that to make ϕ periodic a mirror image in the z direction was built, the current source can be expressed as

$$S_k(x, z) = S_0 [\delta(x-l)\delta(z-z_k) + \delta(x-l)\delta(z-2w+z_k) - \delta(x+l)\delta(z-z_k) - \delta(x+l)\delta(z-2w+z_k)].$$

The subscript k denotes one wire at position k . Rewriting Equation C.11 results in:

$$RHS = \rho \int_0^{2w} \int_{-\infty}^{\infty} S_k(x, z) \cos \frac{m\pi z}{w} e^{-ik'x} dx dz,$$

$$RHS = \rho S_0 [e^{-ik'l} \cos \frac{m\pi z_k}{w} + e^{-ik'l} \cos \frac{m\pi(2w-z_k)}{w} - e^{ik'l} \cos \frac{m\pi z_k}{w} - e^{ik'l} \cos \frac{m\pi(2w-z_k)}{w}],$$

and noting that $\cos \frac{m\pi(2w - z_k)}{w} = \cos[2m\pi - \frac{m\pi z_k}{w}] = \cos \frac{m\pi z_k}{w}$

gives

$$\begin{aligned} RHS &= \rho S_0 [2e^{-ik'l} \cos \frac{m\pi z_k}{w} - 2e^{ik'l} \cos \frac{m\pi z_k}{w}], \\ RHS &= -2\rho S_0 \cos \frac{m\pi z_k}{w} (e^{ik'l} - e^{-ik'l}), \\ RHS &= -4i\rho S_0 \cos \frac{m\pi z_k}{w} \sin(k'l). \end{aligned} \quad (C.12)$$

From equations C.10 and C.12 the coefficient A_m can be calculated:

$$A_m = \frac{-4i\rho S_0 \cos \frac{m\pi z_k}{w} \sin(k'l)}{\sqrt{2\pi} w k_m \sigma_m \sinh(k_m a)}. \quad (C.13)$$

Substituting Equation C.13 into Equation C.5 an expression for the potential function can be derived:

$$\begin{aligned} \varphi(x, y, z) &= -\frac{1}{\sqrt{2\pi}} \sum_{m=0}^{\infty} \int_{-\infty}^{\infty} e^{ik_x x} \cos\left(\frac{m\pi z}{w}\right) \frac{4i\rho S_0 \cos\left(\frac{m\pi z_k}{w}\right) \sin(k'l)}{\sqrt{2\pi} w k_m \sigma_m \sinh(k_m a)} \cosh(k_m y) dk', \\ \varphi(x, y, z) &= -\frac{2i\rho S_0}{\pi w} \sum_{m=0}^{\infty} \int_{-\infty}^{\infty} e^{ik_x x} \cos\left(\frac{m\pi z}{w}\right) \frac{\cos\left(\frac{m\pi z_k}{w}\right) \sin(k'l)}{k_m \sigma_m \sinh(k_m a)} \cosh(k_m y) dk', \end{aligned} \quad (C.14)$$

which is Equation 4.11.

Now the voltage difference along the centerline of the plate ($z = \frac{w}{2}$) can be evaluated as

$$\begin{aligned} V(x) &= \varphi(x, y = a, z = \frac{w}{2}) - \varphi(-x, y = a, z = \frac{w}{2}), \\ V(x) &= \frac{4\rho S_0}{\pi w} \sum_{m=0}^{\infty} \int_{-\infty}^{\infty} \frac{\sin(k'x) \sin(k'l)}{k_m \sigma_m \tanh(k_m a)} \cos\left(\frac{m\pi}{2}\right) \cos\left(\frac{m\pi z_k}{w}\right) dk'. \end{aligned} \quad (C.15)$$

In case of multiple current wires it is necessary to sum all contributions. Thus,

$$V(x) = \frac{4\rho S_0 a}{\pi w} \sum_{m=0}^{\infty} \sum_{k=1}^{N_w} \int_{-\infty}^{\infty} \frac{\sin(k'x) \sin(k'l)}{k_m a \sigma_m \tanh(k_m a)} \cos\left(\frac{m\pi}{2}\right) \cos\left(\frac{m\pi z_k}{w}\right) dk', \quad (\text{C.16})$$

where N_w is the total number of current wires.

The contribution of the current wires for the semi-infinite plate can be analyzed separately. From Equation C.16 for $m \neq 0$:

$$\sum_{k=1}^{N_w} \cos\left(\frac{m\pi z_k}{w}\right) = \frac{1}{2} \sum_{k=1}^{N_w} \left(e^{i\frac{m\pi z_k}{w}} + e^{-i\frac{m\pi z_k}{w}} \right). \quad (\text{C.17})$$

From a geometric progression:

$$\sum_{k=1}^K r^k = \frac{r^{K+1} - r}{r - 1},$$

and considering that $w = (N_w + 1)c$ and $z_k = kc$, where c is the spacing between the current wires, Equation C.17 can be written as

$$\sum_{k=1}^{N_w} \cos\left(\frac{m\pi z_k}{w}\right) = \frac{1}{2} \left(\frac{e^{im\pi} - e^{i\frac{m\pi c}{w}}}{e^{i\frac{m\pi c}{w}} - 1} + \frac{e^{-im\pi} - e^{-i\frac{m\pi c}{w}}}{e^{-i\frac{m\pi c}{w}} - 1} \right). \quad (\text{C.18})$$

Let $b = \frac{m\pi c}{w}$, so

$$\sum_{k=1}^{N_w} \cos\left(\frac{m\pi z_k}{w}\right) = \frac{1}{2} \left(\frac{e^{im\pi} - e^{ib}}{e^{ib} - 1} + \frac{e^{-im\pi} - e^{-ib}}{e^{-ib} - 1} \right),$$

$$\sum_{k=1}^{N_w} \cos\left(\frac{m\pi z_k}{w}\right) = \frac{1}{2} \left(\frac{e^{im\pi} - e^{ib}}{e^{ib} - 1} + \frac{e^{-im\pi} - e^{-ib}}{e^{-ib} - 1} \right),$$

$$\sum_{k=1}^{N_w} \cos\left(\frac{m\pi z_k}{w}\right) = \frac{1}{2} \left[\frac{2 \cos b - 2 - 2 \cos m\pi + 2 \cos(m\pi - b)}{2 - 2 \cos b} \right],$$

$$\sum_{k=1}^{N_w} \cos\left(\frac{m\pi z_k}{w}\right) = -\frac{1}{2}(1 + \cos m\pi). \quad (\text{C.19})$$

This equation is only valid for $\frac{m\pi c}{w} \neq 2\pi$. When $\frac{m\pi c}{w} = 2\pi$, that is $m = \frac{2w}{c}$, or $m = 0$

Equation C.17 becomes

$$\sum_{k=1}^{N_w} \cos\left(\frac{m\pi z_k}{w}\right) = \sum_{k=1}^{N_w} (e^{2\pi i})^k = N_w.$$

The next step is to focus on the integral of the Equation C.16. Rewriting that integral for $m = 0$ as

$$I = \int_{-\infty}^{\infty} dk \frac{\sin(kx) \sin(kl)}{ka \tanh ka},$$

$$I = 2 \int_0^{\infty} dk \frac{\sin(kx) \sin(kl)}{ka \tanh ka},$$

and letting $u = ka$,

$$I = \frac{2}{a} \int_0^{\infty} du \frac{\sin\left(\frac{u}{a}x\right) \sin\left(\frac{u}{a}l\right)}{u \tanh u}.$$

We can rewrite this integral as

$$I = \frac{2}{a} \int_0^{\infty} du \sin\left(\frac{u}{a}x\right) \sin\left(\frac{u}{a}l\right) \left[\frac{1}{u \tanh u} - \frac{1}{u^2} + \frac{1}{u^2} \right]. \quad (\text{C.20})$$

Consider

$$\hat{I} = \frac{2}{a} \int_0^{\infty} du \frac{\sin\left(\frac{u}{a}x\right) \sin\left(\frac{u}{a}l\right)}{u^2}, \quad (\text{C.21})$$

$$\tilde{I} = \frac{2}{a} \int_0^{\infty} du \sin\left(\frac{u}{a}x\right) \sin\left(\frac{u}{a}l\right) \left[\frac{1}{u \tanh u} - \frac{1}{u^2} \right], \quad (\text{C.22})$$

therefore, Equation C.20 can be rewritten as

$$I = \hat{I} + \tilde{I}. \quad (\text{C.23})$$

From tables (Gradshteyn and Ryzhik, 1994) Equation C.21 can be expressed as

$$\hat{I} = \frac{2}{a} \int_0^{\infty} du \frac{\sin(\frac{u}{a}x) \sin(\frac{u}{a}l)}{u^2} = \frac{2}{a} \frac{\pi x}{2a} = \frac{\pi x}{a^2}. \quad (\text{C.24})$$

Recalling that

$$\sin(kx) \cdot \sin(kl) = \frac{1}{2} [\cos k(l-x) - \cos k(l+x)],$$

gives

$$\tilde{I} = \frac{1}{a} \int_0^{\infty} du \left[\cos \frac{u}{a}(l-x) - \cos \frac{u}{a}(l+x) \right] \left[\frac{1}{u \tanh u} - \frac{1}{u^2} \right]. \quad (\text{C.25})$$

Making the following change of variables,

$$\alpha = \frac{l-x}{a}, \quad \beta = \frac{l+x}{a},$$

Equation C.25 can be expressed as

$$\tilde{I} = \frac{1}{a} \operatorname{Re} \int_0^{\infty} du (e^{i\alpha u} - e^{i\beta u}) \left[\frac{1}{u \tanh u} - \frac{1}{u^2} \right], \quad (\text{C.26})$$

where Re means the real part of a complex variable.

Let $u = y i$. Using the following relationships:

$$\sinh(iy) = i \cdot \frac{e^{iy} - e^{-iy}}{2i} = i \sin y,$$

$$\cosh(iy) = \frac{e^{iy} + e^{-iy}}{2} = \cos y,$$

$$\tanh(iy) = \frac{i \sin y}{\cos y} = i \tan y,$$

evaluating this integral along the dashed contour defined in Figure C.1 and using Cauchy's theorem gives

$$\tilde{I} = \frac{1}{a} \operatorname{Re} i \oint (e^{-\alpha y} - e^{-\beta y}) \left[\frac{1}{y \tan y} - \frac{1}{y^2} \right] dy. \quad (\text{C.27})$$

The pole contribution at $y = 0$ cancels and the only contribution come from poles at $y = n\pi$.

Let $y = n\pi + \delta$, with $n \geq 1$ and small δ then

$$\sin y = \sin(n\pi + \delta) = \delta \cos n\pi,$$

$$\cos y = \cos(n\pi + \delta) = \cos n\pi,$$

$$\tan y = \delta.$$

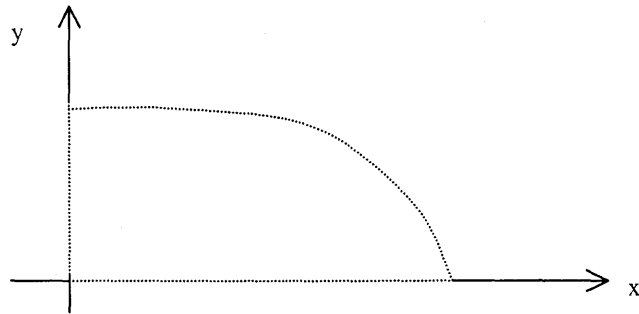


Figure C.1 - Closed contour

Equation C.27 becomes

$$\tilde{I} = -\frac{1}{a} \operatorname{Re} i \sum_{n=1}^{\infty} \int_0^{\infty} d\delta \frac{(e^{-\alpha n\pi} - e^{-\beta n\pi})}{n\pi\delta},$$

$$\tilde{I} = -\frac{1}{a} \operatorname{Re} i \sum_{n=1}^{\infty} \pi i \frac{(e^{-\alpha n\pi} - e^{-\beta n\pi})}{n\pi},$$

$$\tilde{I} = \frac{\pi}{a} \sum_{n=1}^{\infty} \frac{(e^{-\alpha n \pi} - e^{-\beta n \pi})}{n \pi}. \quad (\text{C.28})$$

Substituting equations C.24 and C.28 into Equation C.23 gives

$$I = \frac{\pi x}{a^2} + \frac{\pi}{a} \sum_{n=1}^{\infty} \frac{(e^{-\alpha n \pi} - e^{-\beta n \pi})}{n \pi}. \quad (\text{C.29})$$

This equation only holds for $m = 0$. Similarly, the integral of the Equation C.16 can be evaluated for $m \neq 0$. In this case

$$k_m^2 = k^2 + \frac{m^2 \pi^2}{w^2},$$

and

$$\begin{aligned} I &= \int_{-\infty}^{\infty} dk \frac{\sin(kx) \sin(kl)}{k_m a \tanh k_m a}, \\ I &= 2 \int_0^{\infty} dk \frac{\sin(kx) \sin(kl)}{k_m a \tanh k_m a}, \\ I &= 2 \int_0^{\infty} dk \sin(kx) \sin(kl) \left[\frac{1}{k_m a \tanh k_m a} - \frac{1}{k_m^2 a^2} + \frac{1}{k_m^2 a^2} \right]. \end{aligned} \quad (\text{C.30})$$

Equation C.30 can be separated into two parts:

$$\begin{aligned} I1 &= 2 \int_0^{\infty} dk \frac{\sin(kx) \sin(kl)}{k^2 a^2 + \frac{m^2 \pi^2 a^2}{w^2}}, \\ I1 &= \frac{2}{a^2} \int_0^{\infty} dk \frac{\sin(kx) \sin(kl)}{k^2 + \frac{m^2 \pi^2}{w^2}}, \end{aligned}$$

and from tables (Gradshteyn and Ryzhik, 1994) the integral above can be expressed as

$$I1 = \frac{2}{a^2} \frac{\pi}{4} \frac{w}{m \pi} \left[e^{-\frac{m \pi}{w}(l-x)} - e^{-\frac{m \pi}{w}(l+x)} \right],$$

$$I1 = \frac{\pi w}{2a^2} \left[\frac{e^{-\frac{m\pi}{w}(l-x)} - e^{-\frac{m\pi}{w}(l+x)}}{m\pi} \right]. \quad (\text{C.31})$$

The second integral can be expressed as

$$\begin{aligned} I2 &= 2 \int_0^{\infty} dk \sin(kx) \sin(kl) \left[\frac{1}{k_m a \tanh k_m a} - \frac{1}{k_m^2 a^2} \right], \\ I2 &= \int_0^{\infty} dk [\cos k(l-x) - \cos k(l+x)] \left[\frac{1}{k_m a \tanh k_m a} - \frac{1}{k_m^2 a^2} \right], \\ I2 &= \text{Re} \int_0^{\infty} dk [e^{ik(l-x)} - e^{ik(l+x)}] \left(\frac{1}{k_m a \tanh k_m a} - \frac{1}{k_m^2 a^2} \right). \end{aligned} \quad (\text{C.32})$$

Letting $k = yi$ and evaluating this integral along the dashed path defined in Figure C.1 results in

$$\begin{aligned} I2 &= \text{Re} \int dy (e^{-y(l-x)} - e^{-y(l+x)}) \left(\frac{1}{k_m a \tanh k_m a} - \frac{1}{k_m^2 a^2} \right), \\ I2 &= \text{Re} \int dy [e^{-y(l-x)} - e^{-y(l+x)}] \left(\frac{1}{\sqrt{\frac{m^2 \pi^2 a^2}{w^2} - y^2 a^2} \tanh \sqrt{\frac{m^2 \pi^2 a^2}{w^2} - y^2 a^2}} - \frac{1}{\frac{m^2 \pi^2 a^2}{w^2} - y^2 a^2} \right). \end{aligned} \quad (\text{C.33})$$

The integrand is real only for $0 < y < \frac{m\pi}{w}$ and vanishes for $y \rightarrow \infty$. Thus,

$$I2 = -\text{Re} \int_0^{\frac{m\pi}{w}} dy [e^{-y(l-x)} - e^{-y(l+x)}] \left(\frac{1}{\sqrt{y^2 a^2 - \frac{m^2 \pi^2 a^2}{w^2}} \tan \sqrt{y^2 a^2 - \frac{m^2 \pi^2 a^2}{w^2}}} - \frac{1}{y^2 a^2 - \frac{m^2 \pi^2 a^2}{w^2}} \right). \quad (\text{C.34})$$

Contribution only comes from poles at

$$y^2 a^2 = \frac{m^2 \pi^2 a^2}{w^2} + n^2 \pi^2 \quad \text{with } n \geq 1.$$

$$\text{Let } \sqrt{y^2 a^2 - \frac{m^2 \pi^2 a^2}{w^2}} = n\pi + \delta \quad \text{with } \delta \ll 1,$$

therefore,

$$\tan \sqrt{y^2 a^2 - \frac{m^2 \pi^2 a^2}{w^2}} \approx \delta,$$

$$d\delta = dy \frac{a^2}{n\pi} \sqrt{\frac{n^2 \pi^2}{a^2} + \frac{m^2 \pi^2}{w^2}}.$$

$$\text{Let } y_{mn} = \sqrt{\frac{m^2 \pi^2}{w^2} + \frac{n^2 \pi^2}{a^2}}.$$

Equation C.34 can be expressed as

$$\begin{aligned} I_2 &= -\text{Re} \, i \sum_{n=1}^{\infty} \int_0^{\infty} d\delta \frac{[e^{-y_{mn}(l-x)} - e^{-y_{mn}(l+x)}]}{n\pi\delta} \frac{n\pi}{a^2 \sqrt{\frac{m^2 \pi^2}{w^2} + \frac{n^2 \pi^2}{a^2}}}, \\ I_2 &= -\text{Re} \, i \sum_{n=1}^{\infty} \frac{\pi i}{a^2} \frac{[e^{-y_{mn}(l-x)} - e^{-y_{mn}(l+x)}]}{\sqrt{\frac{m^2 \pi^2}{w^2} + \frac{n^2 \pi^2}{a^2}}}, \\ I_2 &= \frac{\pi}{a^2} \sum_{n=1}^{\infty} \frac{[e^{-y_{mn}(l-x)} - e^{-y_{mn}(l+x)}]}{\sqrt{\frac{m^2 \pi^2}{w^2} + \frac{n^2 \pi^2}{a^2}}}, \\ I_2 &= \frac{\pi}{a^2} \sum_{n=1}^{\infty} \frac{[e^{-y_{mn}(l-x)} - e^{-y_{mn}(l+x)}]}{y_{mn}}. \end{aligned} \tag{C.35}$$

Combining equations C.31 and C.35 gives

$$I = \frac{\pi w}{2a^2} \left[\frac{e^{-\frac{m\pi}{w}(l-x)} - e^{-\frac{m\pi}{w}(l+x)}}{m\pi} \right] + \frac{\pi}{a^2} \sum_{n=1}^{\infty} \frac{[e^{-y_{mn}(l-x)} - e^{-y_{mn}(l+x)}]}{y_{mn}},$$

$$I = \frac{\pi}{2a^2} \left[\frac{e^{-y_{m0}(l-x)} - e^{-y_{m0}(l+x)}}{y_{m0}} \right] + \frac{\pi}{a^2} \sum_{n=1}^{\infty} \frac{[e^{-y_{mn}(l-x)} - e^{-y_{mn}(l+x)}]}{y_{mn}}, \quad (\text{C.36})$$

where $y_{m0} = \frac{m\pi}{w}$.

Equation C.36 is valid only for $m \neq 0$ and can be rewritten as

$$I = \frac{\pi}{a^2} \sum_{n=0}^{\infty} \frac{e^{-y_{mn}(l-x)} - e^{-y_{mn}(l+x)}}{\sigma_n y_{mn}}, \quad (\text{C.37})$$

where $\sigma_n = 1$ if $n \neq 0$ and $\sigma_n = 2$ if $n = 0$.

Returning to Equation C.29 a general formula for any value of m can be built. It was shown that for $m = 0$

$$I = \frac{\pi x}{a^2} + \frac{\pi}{a} \sum_{n=1}^{\infty} \frac{(e^{\frac{l-x}{a}n\pi} - e^{\frac{l+x}{a}n\pi})}{n\pi},$$

$$I = \frac{\pi}{a^2} \left[x + \sum_{n=1}^{\infty} \frac{(e^{\frac{l-x}{a}n\pi} - e^{\frac{l+x}{a}n\pi})}{\frac{n\pi}{a}} \right],$$

$$I = \frac{\pi}{a^2} \left[x + \sum_{n=1}^{\infty} \frac{(e^{-y_{0n}(l-x)} - e^{-y_{0n}(l+x)})}{y_{0n}} \right]. \quad (\text{C.38})$$

However, as $n \rightarrow 0$, $\frac{(e^{-y_{0n}(l-x)} - e^{-y_{0n}(l+x)})}{y_{0n}} \rightarrow 2x$ and, therefore, Equation C.38 can be

written as

$$I = \frac{\pi}{a^2} \sum_{n=0}^{\infty} \frac{(e^{-y_{0n}(l-x)} - e^{-y_{0n}(l+x)})}{\sigma_n y_{0n}}. \quad (\text{C.39})$$

Combining equations C.37 and C.39 a general expression for the integral of the Equation C.16 is derived. So, for any value of m

$$I = \frac{\pi}{a^2} \sum_{n=0}^{\infty} \frac{e^{-y_{mn}(l-x)} - e^{-y_{mn}(l+x)}}{\sigma_n y_{mn}}, \quad (\text{C.40})$$

where $\sigma_n = 1$ if $n \neq 0$ and $\sigma_n = 2$ if $n = 0$.

Returning to Equation C.16 an analytical expression for the voltage difference at

$z = \frac{w}{2}$ is derived:

$$V(x) = \frac{4\rho S_0 a}{\pi w} \sum_{m=0}^{\infty} \sum_{k=1}^{N_w} \frac{\cos\left(\frac{m\pi}{2}\right) \cos\left(\frac{m\pi z_k}{w}\right)}{\sigma_m} \frac{\pi}{a^2} \sum_{n=0}^{\infty} \frac{e^{-y_{mn}(l-x)} - e^{-y_{mn}(l+x)}}{\sigma_n y_{mn}},$$

$$V(x) = \frac{4\rho S_0}{wa} \sum_{m=0}^{\infty} \sum_{k=1}^{N_w} \frac{\cos\left(\frac{m\pi}{2}\right) \cos\left(\frac{m\pi z_k}{w}\right)}{\sigma_m} \sum_{n=0}^{\infty} \frac{e^{-y_{mn}(l-x)} - e^{-y_{mn}(l+x)}}{\sigma_n y_{mn}},$$

which is Equation 4.14.

APPENDIX D

This appendix describes the analytic solution for a semi-infinite plate without defects using Fourier transformation. Consider equations 4.19, 4.20 and 4.21:

$$\frac{\partial^2 \hat{\phi}}{\partial y^2} - k^2 \hat{\phi} = 0, \quad (\text{D.1})$$

$$\left. \frac{\partial \hat{\phi}}{\partial y} \right|_{y=0} = 0, \quad (\text{D.2})$$

$$\left. \frac{\partial \hat{\phi}}{\partial y} \right|_{y=a} = \frac{\rho}{2\pi} \int_{-\infty}^{\infty} e^{-ikx} S(x) dx. \quad (\text{D.3})$$

The general solution to Equation D.1 is

$$\hat{\phi} = A \cosh(ky). \quad (\text{D.4})$$

From the boundary condition at the surface ($y = a$)

$$\left. \frac{\partial \hat{\phi}}{\partial y} \right|_{y=a} = \frac{\rho}{2\pi} \int_{-\infty}^{\infty} e^{-ikx} \frac{S_0}{w} [\delta(x-l) - \delta(x+l)] dx,$$

$$\left. \frac{\partial \hat{\phi}}{\partial y} \right|_{y=a} = \frac{\rho S_0}{2\pi w} \int_{-\infty}^{\infty} e^{-ikx} [\delta(x-l) - \delta(x+l)] dx,$$

$$\left. \frac{\partial \hat{\phi}}{\partial y} \right|_{y=a} = \frac{\rho S_0}{2\pi w} [e^{-ikl} - e^{ikl}],$$

$$\left. \frac{\partial \hat{\phi}}{\partial y} \right|_{y=a} = -\frac{i\rho S_0}{\pi w} \sin kl. \quad (\text{D.5})$$

The derivative of Equation D.4 with respect to y is

$$\left. \frac{\partial \hat{\phi}}{\partial y} \right|_{y=a} = Ak \sinh ka, \quad (\text{D.6})$$

and combining equations D.5 and D.6 determines the constant A . Thus,

$$Ak \sinh ka = -\frac{i\rho S_0}{\pi w} \sin kl,$$

$$A = -\frac{i\rho S_0}{\pi w k} \frac{\sin kl}{\sinh ka}. \quad (\text{D.7})$$

Substituting this constant into Equation D.4 gives

$$\hat{\phi} = -\frac{i\rho S_0}{\pi w k} \frac{\sin kl}{\sinh ka} \cosh(ky). \quad (\text{D.8})$$

Entering this result into Equation 4.17 results in

$$\varphi(x, y) = -\frac{i\rho S_0}{\pi w} \int_{-\infty}^{\infty} e^{ikx} \frac{\sin kl}{k \sinh ka} \cosh(ky) dk, \quad (\text{D.9})$$

which is the expression for Equation 4.22.

This allows the potential difference between two points at the surface to be calculated as

$$V(x) = \varphi(x, a) - \varphi(-x, a). \quad (\text{D.10})$$

Therefore,

$$V(x) = -\frac{i\rho S_0}{\pi w} \int_{-\infty}^{\infty} (e^{ikx} - e^{-ikx}) \frac{\sin kl}{k \sinh ka} \cosh(ka) dk,$$

$$V(x) = \frac{2\rho S_0}{\pi w} \int_{-\infty}^{\infty} \frac{\sin kx \sin kl}{k \tanh ka} dk. \quad (\text{D.11})$$

This integral has been evaluated before using complex analysis. Thus,

$$V(x) = \frac{2\rho S_0}{\pi w} \left[\frac{\pi x}{a} + \pi \sum_{n=1}^{\infty} \frac{e^{-\frac{(l-x)n\pi}{a}} - e^{-\frac{(l+x)n\pi}{a}}}{n\pi} \right],$$

$$V(x) = \frac{2\rho S_0 x}{w a} + \frac{2\rho S_0}{\pi w} \sum_{n=1}^{\infty} \frac{e^{-\frac{(l-x)n\pi}{a}} - e^{-\frac{(l+x)n\pi}{a}}}{n}. \quad (\text{D.12})$$

Consider the series

$$K = \sum_{n=1}^{\infty} e^{-\alpha n}. \quad (\text{D.13})$$

Now consider the following integral

$$J = \int_{\alpha}^{\infty} d\alpha' K. \quad (\text{D.14})$$

Substituting Equation D.13 into Equation D.14 gives

$$J = \sum_{n=1}^{\infty} \int_{\alpha}^{\infty} d\alpha' e^{-\alpha' n},$$

$$J = \sum_{n=1}^{\infty} \left. \frac{e^{-\alpha' n}}{-n} \right|_{\alpha}^{\infty} = \sum_{n=1}^{\infty} \frac{e^{-\alpha n}}{n},$$

which is the series that appears in Equation D.12.

Evaluating the series of the Equation D.13 gives

$$K = \sum_{n=1}^{\infty} e^{-\alpha n} = \sum_{n=0}^{\infty} e^{-\alpha n} - 1 = \frac{1}{1 - e^{-\alpha}} - 1 = \frac{e^{-\alpha}}{1 - e^{-\alpha}}. \quad (\text{D.15})$$

Substituting this result into Equation D.14 results in

$$J = \int_{\alpha}^{\infty} d\alpha' \frac{e^{-\alpha'}}{1 - e^{-\alpha'}}.$$

Let $z = e^{-\alpha}$. Thus,

$$J = \int_{e^{-\alpha}}^0 \frac{dz}{1 - z},$$

$$J = -\ln(1 - e^{-\alpha}).$$

Using this result and Equation D.12 gives

$$V(x) = \frac{2\rho S_0 x}{w a} - \frac{2\rho S_0}{\pi w} \left[\ln \left(1 - e^{\frac{(l-x)\pi}{a}} \right) - \ln \left(1 - e^{\frac{(l+x)\pi}{a}} \right) \right],$$

$$V(x) = \frac{2\rho S_0 x}{w a} - \frac{2\rho S_0}{\pi w} \left[\ln \frac{1 - e^{\frac{(l-x)n\pi}{a}}}{1 - e^{\frac{(l+x)n\pi}{a}}} \right],$$

$$V(x) = \frac{2\rho S_0}{w} \left[\frac{x}{a} - \frac{1}{\pi} \ln \frac{1 - e^{\frac{(l-x)\pi}{a}}}{1 - e^{\frac{(l+x)\pi}{a}}} \right], \quad (\text{D.16})$$

which is Equation 4.24.

Since the potential is an odd function it can be expressed as

$$\varphi(x) = \frac{\rho S_0}{w} \left[\frac{x}{a} - \frac{1}{\pi} \ln \frac{1 - e^{\frac{(l-x)\pi}{a}}}{1 - e^{\frac{(l+x)\pi}{a}}} \right]. \quad (\text{D.17})$$

There is another way to find an analytic expression for the potential function. Consider

Equation D.9:

$$\varphi(x, y) = -\frac{i\rho S_0}{\pi w} \int_{-\infty}^{\infty} e^{ikx} \frac{\sin kl}{k \sinh ka} \cosh(ky) dk .$$

A table of integrals may be used to find a new expression for this function. So, the equation above can be rewritten as

$$\begin{aligned} \varphi(x, y) &= \frac{\rho S_0}{\pi w} \int_{-\infty}^{\infty} \frac{\sin kx \sin kl}{k \sinh ka} \cosh(ky) dk , \\ \varphi(x, y) &= \frac{2\rho S_0}{\pi w} \int_0^{\infty} \frac{\sin kx \sin kl}{k \sinh ka} \cosh(ky) dk . \end{aligned} \quad (\text{D.18})$$

Knowing that

$$\begin{aligned} \sin kx \sin kl &= \frac{1}{2} [\cos k(l-x) - \cos k(l+x)] , \\ \sin kx \sin kl &= \frac{1}{2} \left[1 - 2 \sin^2 \frac{k(l-x)}{2} - 1 + 2 \sin^2 \frac{k(l+x)}{2} \right] , \\ \sin kx \sin kl &= \sin^2 \frac{k(l+x)}{2} - \sin^2 \frac{k(l-x)}{2} , \end{aligned} \quad (\text{D.19})$$

and substituting Equation D.19 into Equation D.18 gives

$$\varphi(x, y) = \frac{2\rho S_0}{\pi w} \int_0^{\infty} \frac{\cosh(ky)}{k \sinh ka} \left[\sin^2 \frac{k(l+x)}{2} - \sin^2 \frac{k(l-x)}{2} \right] dk .$$

Making the following change of variable

$$\xi = ka ,$$

the potential function will be

$$\varphi(x, y) = \frac{2\rho S_0}{\pi w} \int_0^{\infty} \frac{\cosh\left(\frac{y}{a}\xi\right)}{\xi \sinh \xi} \left[\sin^2 \frac{\xi(l+x)}{2a} - \sin^2 \frac{\xi(l-x)}{2a} \right] d\xi .$$

It can be seen from tables (Gradshteyn and Ryzhik, 1994) that

$$\int_0^{\infty} \sin^2 ax \frac{\cosh \beta x}{\sinh x} \frac{dx}{x} = \frac{1}{4} \ln \frac{\cosh 2a\pi + \cos \beta\pi}{1 + \cos \beta\pi}.$$

Therefore,

$$\varphi(x, y) = \frac{2\rho S_0}{\pi w} \frac{1}{4} \left\{ \ln \frac{\cosh \frac{\pi(l+x)}{a} + \cos \frac{\pi y}{a}}{1 + \cos \frac{\pi y}{a}} - \ln \frac{\cosh \frac{\pi(l-x)}{a} + \cos \frac{\pi y}{a}}{1 + \cos \frac{\pi y}{a}} \right\},$$

$$\varphi(x, y) = \frac{\rho S_0}{2\pi w} \ln \frac{\cosh \frac{\pi(l+x)}{a} + \cos \frac{\pi y}{a}}{\cosh \frac{\pi(l-x)}{a} + \cos \frac{\pi y}{a}},$$

which is the expression for Equation 4.26.

APPENDIX E

This appendix describes the steps necessary to get equations 4.32, 4.35 and 4.37 that are part of the analytic solution for a semi-infinite plate with slot defect. Consider Equation 4.31:

$$\left(\frac{\partial \varphi}{\partial y} - \Delta \frac{\partial \varphi}{\partial x} \right)_{s_1} = 0. \quad (\text{E.1})$$

The first term of this equation may be approximated as

$$\frac{\partial \varphi(x, y)}{\partial y} \Big|_{s_1} \approx \frac{\partial \varphi(x, 0)}{\partial y} + \Delta \frac{\partial^2 \varphi(x, 0)}{\partial y^2} + \frac{\Delta^2}{2} \frac{\partial^3 \varphi(x, 0)}{\partial y^3},$$

$$\frac{\partial \varphi(x, y)}{\partial y} \Big|_{s_1} \approx \frac{\partial \varphi_0(x, 0)}{\partial y} + \left(\frac{\partial \varphi_1(x, 0)}{\partial y} + \Delta \frac{\partial^2 \varphi_0(x, 0)}{\partial y^2} \right) + \left(\Delta \frac{\partial^2 \varphi_1(x, 0)}{\partial y^2} + \frac{\Delta^2}{2} \frac{\partial^2 \varphi_0(x, 0)}{\partial y^2} \right) + \frac{\Delta^2}{2} \frac{\partial^2 \varphi_1(x, 0)}{\partial y^2}.$$

The second term of Equation E.1 can be expressed as

$$\Delta \frac{\partial \varphi(x, y)}{\partial x} \Big|_{s_1} \approx \Delta \left[\frac{\partial \varphi_0(x, 0)}{\partial x} + \left(\frac{\partial \varphi_1(x, 0)}{\partial x} + \Delta \frac{\partial^2 \varphi_0}{\partial x \partial y} \right) \right].$$

Substituting these results on the boundary condition of Equation E.1 produces, for each order of magnitude indicated as a superscript index, the following equations:

$$\Delta^{(0)} = \frac{\partial \varphi_0}{\partial y} \Big|_{y=0} = 0;$$

$$\Delta^{(1)} = \left(\frac{\partial \varphi_1}{\partial y} + \Delta \frac{\partial^2 \varphi_0}{\partial y^2} - \Delta \frac{\partial \varphi_0}{\partial x} \right)_{y=0} = 0;$$

$$\Delta^{(2)} = \left(\Delta \frac{\partial^2 \varphi_1}{\partial y^2} + \frac{\Delta^2}{2} \frac{\partial^2 \varphi_0}{\partial y^2} - \Delta \frac{\partial \varphi_1}{\partial x} - \Delta \frac{\partial^2 \varphi_0}{\partial x \partial y} \right)_{y=0} = 0.$$

Considering only the first order approximation ($\Delta^{(1)}$) the boundary condition can be expressed as

$$\left(\frac{\partial \varphi_1}{\partial y} + \Delta \frac{\partial^2 \varphi_0}{\partial y^2} - \Delta \frac{\partial \varphi_0}{\partial x} \right)_{y=0} = 0, \quad (\text{E.2})$$

which is Equation 4.32.

Now consider equations 4.33 and 4.34:

$$\varphi_1(x, y) = \int_{-\infty}^{\infty} e^{ikx} \hat{\varphi}_1(k, y) dk, \quad \text{and} \quad (\text{E.3})$$

$$\hat{\varphi}_1(k, y) = \frac{1}{2\pi} \int_{-\infty}^{\infty} e^{-ikx} \varphi_1(x, y) dx, \quad (\text{E.4})$$

where $\hat{\varphi}_1(k, y)$ is the Fourier transform of $\varphi_1(x, y)$.

The general solution to the Laplace equation with the boundary condition of Equation 4.30 will be

$$\hat{\varphi}_1(k, y) = B \cosh k(y - a). \quad (\text{E.5})$$

Consider the terms of the equation E.2:

$$\begin{aligned} \frac{\partial \varphi_1(x, 0)}{\partial y} &= - \int_{-\infty}^{\infty} dk e^{ikx} B k \sinh ka, \\ \Delta \frac{\partial^2 \varphi_0(x, 0)}{\partial y^2} &= - \frac{i\rho S_0 \Delta}{\pi w} \int_{-\infty}^{\infty} e^{ikx} k \frac{\sin kl}{\sinh ka} dk, \\ - \Delta \frac{\partial \varphi_0(x, 0)}{\partial x} &= - \Delta \frac{\rho S_0}{\pi w} \int_{-\infty}^{\infty} e^{ikx} \frac{\sin kl}{\sinh ka} dk. \end{aligned}$$

Therefore Equation E.2 can be rewritten as

$$- \int_{-\infty}^{\infty} dk e^{ikx} B k \sinh ka - \frac{i\rho S_0 \Delta}{\pi w} \int_{-\infty}^{\infty} e^{ikx} k \frac{\sin kl}{\sinh ka} dk - \Delta \frac{\rho S_0}{\pi w} \int_{-\infty}^{\infty} e^{ikx} \frac{\sin kl}{\sinh ka} dk = 0. \quad (\text{E.6})$$

Multiplying this equation by $\int_{-\infty}^{\infty} e^{-ik'x} dx$ the unknown coefficient can be calculated. The

first term, I_1 , of Equation E.6 may then be reduced as follows:

$$I_1 = - \int_{-\infty}^{\infty} dk e^{ikx} B k \sinh ka \int_{-\infty}^{\infty} e^{-ik'x} dx ,$$

$$I_1 = - \int_{-\infty}^{\infty} \int_{-\infty}^{\infty} e^{i(k-k')x} B k \sinh ka dx dk ,$$

$$I_1 = -2\pi k' B \sinh k'a . \quad (E.7)$$

The second term, I_2 , of Equation E.6 can be reduced as follows:

$$I_2 = - \frac{i\rho S_0}{\pi w} \int_{-\infty}^{\infty} e^{ikx} k \frac{\sin kl}{\sinh ka} dk \int_{-\infty}^{\infty} e^{-ik'x} \Delta dx ,$$

$$I_2 = - \frac{i\rho S_0 h}{\pi w} \int_{-\infty}^{\infty} e^{ikx} k \frac{\sin kl}{\sinh ka} dk \int_{-\infty}^{\infty} e^{-ik'x} [U(x+\lambda) - U(x-\lambda)] dx ,$$

$$I_2 = - \frac{i\rho S_0 h}{\pi w} \int_{-\infty}^{\infty} k \frac{\sin kl}{\sinh ka} dk \int_{-\lambda}^{\lambda} e^{i(k-k')x} dx ,$$

$$I_2 = - \frac{i\rho S_0 h}{\pi w} \int_{-\infty}^{\infty} dk \frac{k \sin kl}{\sinh ka} \frac{e^{i(k-k')\lambda} - e^{-i(k-k')\lambda}}{i(k-k')} ,$$

$$I_2 = - \frac{2i\rho S_0 h}{\pi w} \int_{-\infty}^{\infty} dk \frac{k \sin kl}{\sinh ka} \frac{\sin(k-k')\lambda}{(k-k')} . \quad (E.8)$$

Finally the third term, I_3 , of Equation E.6 may be reduced as follows:

$$I_3 = - \frac{\rho S_0}{\pi w} \int_{-\infty}^{\infty} e^{ikx} \frac{\sin kl}{\sinh ka} dk \int_{-\infty}^{\infty} \Delta' e^{-ik'x} dx ,$$

$$I_3 = - \frac{\rho h S_0}{\pi w} \int_{-\infty}^{\infty} \frac{\sin kl}{\sinh ka} dk \int_{-\infty}^{\infty} [\delta(x+\lambda) - \delta(x-\lambda)] e^{i(k-k')x} dx ,$$

$$I_3 = -\frac{\rho h S_0}{\pi w} \int_{-\infty}^{\infty} \frac{\sin kl}{\sinh ka} [e^{-i(k-k')\lambda} - e^{i(k-k')\lambda}] dk,$$

$$I_3 = \frac{2i\rho h S_0}{\pi w} \int_{-\infty}^{\infty} \frac{\sin kl}{\sinh ka} \sin(k-k')\lambda dk. \quad (\text{E.9})$$

Adding equations E.7, E.8 and E.9 the coefficient B can be calculated.

$$-2\pi k' B \sinh k'a - \frac{2i\rho S_0 h}{\pi w} \int_{-\infty}^{\infty} dk \frac{k \sin kl}{\sinh ka} \frac{\sin(k-k')\lambda}{(k-k')} + \frac{2i\rho h S_0}{\pi w} \int_{-\infty}^{\infty} \frac{\sin kl}{\sinh ka} \sin(k-k')\lambda dk = 0,$$

$$2\pi k' B \sinh k'a = -\frac{2i\rho S_0 h}{\pi w} \int_{-\infty}^{\infty} dk \frac{k \sin kl}{\sinh ka} \frac{\sin(k-k')\lambda}{(k-k')} + \frac{2i\rho h S_0}{\pi w} \int_{-\infty}^{\infty} \frac{\sin kl}{\sinh ka} \sin(k-k')\lambda dk,$$

$$2\pi k' B \sinh k'a = \frac{2i\rho S_0 h}{\pi w} \int_{-\infty}^{\infty} dk \frac{\sin kl \sin(k-k')\lambda}{\sinh ka} \left[1 - \frac{k}{k-k'}\right],$$

$$2\pi B \sinh k'a = -\frac{2i\rho S_0 h}{\pi w} \int_{-\infty}^{\infty} dk \frac{\sin kl \sin(k-k')\lambda}{(k-k') \sinh ka},$$

$$B = -\frac{i\rho S_0 h}{\pi^2 w} \frac{1}{\sinh k'a} \int_{-\infty}^{\infty} dk \frac{\sin kl}{\sinh ka} \frac{\sin(k-k')\lambda}{(k-k')}, \text{ or}$$

switching k' by k results in

$$B(k) = -\frac{i\rho S_0 h}{\pi^2 w} \frac{1}{\sinh ka} \int_{-\infty}^{\infty} dk' \frac{\sin k'l}{\sinh k'a} \frac{\sin(k'-k)\lambda}{(k'-k)}. \quad (\text{E.10})$$

Substituting this result into Equation E.5 gives

$$\hat{\phi}_1(k, y) = -\frac{i\rho S_0 h}{\pi^2 w} \frac{\cosh k(y-a)}{\sinh ka} \int_{-\infty}^{\infty} dk' \frac{\sin k'l}{\sinh k'a} \frac{\sin(k'-k)\lambda}{(k'-k)}. \quad (\text{E.11})$$

An expression for the potential function $\phi_1(x, y)$ can be obtained substituting Equation

E.11 into Equation E.3. Thus,

$$\phi_1(x, y) = -\frac{i\rho S_0 h}{\pi^2 w} \int_{-\infty}^{\infty} \int_{-\infty}^{\infty} dk' dk \frac{\sin k'l}{\sinh k'a} \frac{\sin(k'-k)\lambda}{(k'-k)} \frac{\cosh k(y-a) e^{ikx}}{\sinh ka}, \quad (\text{E.12})$$

which is the expression for Equation 4.35.

The potential difference may be calculated as

$$V_1(x) = \varphi_1(x, a) - \varphi_1(-x, a),$$

$$V_1(x) = \frac{2\rho S_0 h}{\pi^2 w} \int_{-\infty}^{\infty} \int_{-\infty}^{\infty} dk' dk \frac{\sin k'l}{\sinh k'a} \frac{\sin(k'-k)\lambda}{(k'-k)} \frac{\sin kx}{\sinh ka}. \quad (\text{E.13})$$

Consider the integrals

$$J = \int_{-\infty}^{\infty} \int_{-\infty}^{\infty} dk' dk \frac{\sin k'l}{\sinh k'a} \frac{\sin(k'-k)\lambda}{(k'-k)} \frac{\sin kx}{\sinh ka},$$

$$K = \int_{-\infty}^{\infty} \int_{-\infty}^{\infty} dk' dk \frac{\sin k'l}{\sinh k'a} \frac{\sin kx}{\sinh ka} \cos(k'-k)\lambda.$$

It can be seen that

$$J = \int_0^\lambda K d\lambda. \quad (\text{E.14})$$

Evaluating the integral K gives

$$K = \int_{-\infty}^{\infty} \int_{-\infty}^{\infty} dk' dk \frac{\sin k'l}{\sinh k'a} \frac{\sin kx}{\sinh ka} [\cos k\lambda \cos k'\lambda - \sin k\lambda \sin k'\lambda],$$

$$K = \int_{-\infty}^{\infty} \int_{-\infty}^{\infty} dk' dk \frac{\sin k'l}{\sinh k'a} \frac{\sin kx}{\sinh ka} \cos k\lambda \cos k'\lambda,$$

$$K = \int_0^\infty \int_0^\infty dk' dk \frac{\sin k'(l+\lambda) + \sin k'(l-\lambda)}{\sinh k'a} \frac{\sin k(x+\lambda) + \sin k(x-\lambda)}{\sinh ka}.$$

It can be seen from tables (Gradshteyn and Ryzhik, 1994) that

$$K = \left(\frac{\pi}{2a}\right)^2 \left[\tanh \frac{\pi(x+\lambda)}{2a} \tanh \frac{\pi(l+\lambda)}{2a} + \tanh \frac{\pi(x-\lambda)}{2a} \tanh \frac{\pi(l-\lambda)}{2a} + \right. \\ \left. \tanh \frac{\pi(x+\lambda)}{2a} \tanh \frac{\pi(l-\lambda)}{2a} + \tanh \frac{\pi(x-\lambda)}{2a} \tanh \frac{\pi(l+\lambda)}{2a} \right] \quad (\text{E.15})$$

Making the following change of variables

$$\theta = \frac{\pi\lambda}{2a}, \quad \alpha = \frac{\pi x}{2a}, \quad \beta = \frac{\pi l}{2a},$$

Equation E.15 can be rewritten as

$$K = \left(\frac{\pi}{2a}\right)^2 [\tanh(\alpha + \theta) \tanh(\beta + \theta) + \tanh(\alpha - \theta) \tanh(\beta - \theta) + \tanh(\alpha + \theta) \tanh(\beta - \theta) + \tanh(\alpha - \theta) \tanh(\beta + \theta)]$$

Substituting this equation into Equation E.14 gives

$$J = \left(\frac{\pi}{2a}\right) \int_0^{\frac{\pi\lambda}{2a}} d\theta \tanh(\alpha + \theta) \tanh(\beta + \theta) + \left(\frac{\pi}{2a}\right) \int_0^{\frac{\pi\lambda}{2a}} d\theta \tanh(\alpha - \theta) \tanh(\beta - \theta) + \left(\frac{\pi}{2a}\right) \int_0^{\frac{\pi\lambda}{2a}} d\theta \tanh(\alpha + \theta) \tanh(\beta - \theta) + \left(\frac{\pi}{2a}\right) \int_0^{\frac{\pi\lambda}{2a}} d\theta \tanh(\alpha - \theta) \tanh(\beta + \theta) \quad (\text{E.16})$$

Consider the first term of Equation E.16, represented by J_1 :

$$J_1 = \left(\frac{\pi}{2a}\right) \int_0^{\frac{\pi\lambda}{2a}} d\theta \tanh(\alpha + \theta) \tanh(\beta + \theta).$$

Let

$$\phi = \theta + \frac{\beta + \alpha}{2},$$

$$\nu = \frac{\beta - \alpha}{2}.$$

Therefore,

$$J_1 = \left(\frac{\pi}{2a}\right) \int_{\frac{\beta+\alpha}{2}}^{\frac{\pi\lambda}{2a} + \frac{\beta+\alpha}{2}} d\phi \tanh(\phi - \nu) \tanh(\phi + \nu).$$

Knowing that

$$\sinh(\phi - \nu) \sinh(\phi + \nu) = \frac{1}{2} (\cosh 2\phi - \cosh 2\nu), \text{ and}$$

$$\cosh(\phi - \nu) \cosh(\phi + \nu) = \frac{1}{2} (\cosh 2\phi + \cosh 2\nu),$$

gives

$$J_1 = \left(\frac{\pi}{2a}\right) \int_{\frac{\beta+\alpha}{2}}^{\frac{\pi\lambda + \beta + \alpha}{2a} + \frac{\beta+\alpha}{2}} d\phi \frac{\cosh 2\phi + \cosh 2\nu - 2 \cosh 2\nu}{\cosh 2\phi + \cosh 2\nu},$$

$$J_1 = \left(\frac{\pi}{2a}\right) \int_{\frac{\beta+\alpha}{2}}^{\frac{\pi\lambda + \beta + \alpha}{2a} + \frac{\beta+\alpha}{2}} d\phi \left[1 - \frac{2 \cosh 2\nu}{\cosh 2\phi + \cosh 2\nu}\right].$$

Making $\xi = 2\phi$, the previous equation becomes

$$J_1 = \left(\frac{\pi}{2a}\right) \int_{\beta+\alpha}^{\frac{\pi\lambda + \beta + \alpha}{a} + \beta + \alpha} \frac{d\xi}{2} \left[1 - \frac{2 \cosh 2\nu}{\cosh 2\phi + \cosh 2\nu}\right],$$

$$J_1 = \left(\frac{\pi}{2a}\right) \left[\frac{\pi\lambda}{2a} - \int_{\beta+\alpha}^{\frac{\pi\lambda + \beta + \alpha}{a} + \beta + \alpha} d\xi \frac{\cosh 2\nu}{\cosh \xi + \cosh 2\nu}\right],$$

$$J_1 = \left(\frac{\pi}{2a}\right) \left[\frac{\pi\lambda}{2a} - \cosh(\beta - \alpha) \int_{\beta+\alpha}^{\frac{\pi\lambda + \beta + \alpha}{a} + \beta + \alpha} \frac{d\xi}{\cosh \xi + \cosh(\beta - \alpha)}\right].$$

It can be seen from tables (Gradshteyn and Ryzhik, 1994) that

$$\int \frac{dx}{\cosh a + \cosh x} = \operatorname{coth} a \left[\ln \cosh \frac{x+a}{2} - \ln \cosh \frac{x-a}{2} \right],$$

thus,

$$J_1 = \left(\frac{\pi}{2a}\right) \left\{ \frac{\pi\lambda}{2a} - \coth(\beta - \alpha) \left[\ln \frac{\cosh\left(\frac{\pi\lambda}{2a} + \beta\right)}{\cosh\left(\frac{\pi\lambda}{2a} + \alpha\right)} - \ln \frac{\cosh \beta}{\cosh \alpha} \right] \right\},$$

$$J_1 = \left(\frac{\pi}{2a}\right) \left\{ \frac{\pi\lambda}{2a} - \coth(\beta - \alpha) \ln \frac{\cosh\left(\frac{\pi\lambda}{2a} + \beta\right) \cosh \alpha}{\cosh\left(\frac{\pi\lambda}{2a} + \alpha\right) \cosh \beta} \right\},$$

$$J_1 = \left(\frac{\pi}{2a}\right) \left\{ \frac{\pi\lambda}{2a} - \coth \frac{\pi}{2a} (l - x) \ln \frac{\cosh \frac{\pi}{2a} (l + \lambda) \cosh \frac{\pi x}{2a}}{\cosh \frac{\pi}{2a} (x + \lambda) \cosh \frac{\pi l}{2a}} \right\}. \quad (\text{E.17})$$

Now, consider the second term, J_2 , of Equation E.16:

$$J_2 = \left(\frac{\pi}{2a}\right) \int_0^{\frac{\pi\lambda}{2a}} d\theta \tanh(\alpha - \theta) \tanh(\beta - \theta),$$

$$J_2 = \left(\frac{\pi}{2a}\right) \int_0^{\frac{\pi\lambda}{2a}} d\theta \tanh(\theta - \alpha) \tanh(\theta - \beta).$$

Let

$$\phi = \theta - \frac{\beta + \alpha}{2},$$

$$\nu = \frac{\beta - \alpha}{2}.$$

Therefore,

$$J_2 = \left(\frac{\pi}{2a}\right) \int_{-\left(\frac{\beta+\alpha}{2}\right)}^{\frac{\pi\lambda}{2a} - \frac{\beta+\alpha}{2}} d\phi \tanh(\phi - \nu) \tanh(\phi + \nu),$$

$$J_2 = \left(\frac{\pi}{2a}\right) \int_{-\left(\frac{\beta+\alpha}{2}\right)}^{\frac{\pi\lambda}{2a} - \frac{\beta+\alpha}{2}} d\phi \left[1 - \frac{2 \cosh 2\nu}{\cosh 2\phi + \cosh 2\nu} \right].$$

Making $\xi = 2\phi$, gives

$$\begin{aligned}
J_2 &= \left(\frac{\pi}{2a}\right) \left[\frac{\pi\lambda}{2a} - \cosh(\beta - \alpha) \int_{-(\beta+\alpha)}^{\frac{\pi\lambda}{a} - (\beta+\alpha)} \frac{d\xi}{\cosh \xi + \cosh(\beta - \alpha)} \right], \\
J_2 &= \left(\frac{\pi}{2a}\right) \left\{ \frac{\pi\lambda}{2a} - \coth(\beta - \alpha) \ln \frac{\cosh\left(\frac{\pi\lambda}{2a} - \alpha\right) \cosh \beta}{\cosh\left(\frac{\pi\lambda}{2a} - \beta\right) \cosh \alpha} \right\}, \\
J_2 &= \left(\frac{\pi}{2a}\right) \left\{ \frac{\pi\lambda}{2a} - \coth \frac{\pi}{2a} (l - x) \ln \frac{\cosh \frac{\pi}{2a} (\lambda - x) \cosh \frac{\pi l}{2a}}{\cosh \frac{\pi}{2a} (\lambda - l) \cosh \frac{\pi x}{2a}} \right\}. \tag{E.18}
\end{aligned}$$

Consider the third term, J_3 , of Equation E.16:

$$\begin{aligned}
J_3 &= \left(\frac{\pi}{2a}\right) \int_0^{\frac{\pi\lambda}{2a}} d\theta \tanh(\alpha + \theta) \tanh(\beta - \theta), \\
J_3 &= -\left(\frac{\pi}{2a}\right) \int_0^{\frac{\pi\lambda}{2a}} d\theta \tanh(\alpha + \theta) \tanh(\theta - \beta).
\end{aligned}$$

Let

$$\begin{aligned}
\phi &= \theta - \frac{\beta - \alpha}{2}, \\
\nu &= \frac{\beta + \alpha}{2}.
\end{aligned}$$

Therefore,

$$\begin{aligned}
J_3 &= -\left(\frac{\pi}{2a}\right) \int_{-\frac{\beta-\alpha}{2}}^{\frac{\pi\lambda}{2a} - \frac{\beta-\alpha}{2}} d\phi \tanh(\phi - \nu) \tanh(\phi + \nu), \\
J_3 &= -\left(\frac{\pi}{2a}\right) \int_{-\frac{\beta-\alpha}{2}}^{\frac{\pi\lambda}{2a} - \frac{\beta-\alpha}{2}} d\phi \left[1 - \frac{2 \cosh 2\nu}{\cosh 2\phi + \cosh 2\nu} \right].
\end{aligned}$$

Making $\xi = 2\phi$, the previous equation becomes

$$J_3 = -\left(\frac{\pi}{2a}\right)\left[\frac{\pi\lambda}{2a} - \cosh(\beta + \alpha) \int_{-(\beta-\alpha)}^{\frac{\pi\lambda}{a} - (\beta-\alpha)} \frac{d\xi}{\cosh \xi + \cosh(\beta + \alpha)}\right],$$

$$J_3 = -\left(\frac{\pi}{2a}\right)\left\{\frac{\pi\lambda}{2a} - \coth(\beta + \alpha) \ln \frac{\cosh\left(\frac{\pi\lambda}{2a} + \alpha\right) \cosh \beta}{\cosh\left(\frac{\pi\lambda}{2a} - \beta\right) \cosh \alpha}\right\},$$

$$J_3 = -\left(\frac{\pi}{2a}\right)\left\{\frac{\pi\lambda}{2a} - \coth \frac{\pi}{2a}(l + x) \ln \frac{\cosh \frac{\pi}{2a}(\lambda + x) \cosh \frac{\pi l}{2a}}{\cosh \frac{\pi}{2a}(\lambda - l) \cosh \frac{\pi x}{2a}}\right\}. \quad (\text{E.19})$$

Finally, consider the last term, J_4 , of Equation E.16:

$$J_4 = \left(\frac{\pi}{2a}\right) \int_0^{\frac{\pi\lambda}{2a}} d\theta \tanh(\alpha - \theta) \tanh(\beta + \theta),$$

$$J_4 = -\left(\frac{\pi}{2a}\right) \int_0^{\frac{\pi\lambda}{2a}} d\theta \tanh(\theta - \alpha) \tanh(\theta + \beta).$$

Let

$$\phi = \theta + \frac{\beta - \alpha}{2},$$

$$\nu = \frac{\beta + \alpha}{2}.$$

Therefore,

$$J_4 = -\left(\frac{\pi}{2a}\right) \int_{\left(\frac{\beta-\alpha}{2}\right)}^{\frac{\pi\lambda}{2a} + \frac{\beta-\alpha}{2}} d\phi \tanh(\phi - \nu) \tanh(\phi + \nu),$$

$$J_4 = -\left(\frac{\pi}{2a}\right) \int_{\left(\frac{\beta-\alpha}{2}\right)}^{\frac{\pi\lambda + \beta - \alpha}{2a}} d\phi \left[1 - \frac{2 \cosh 2\nu}{\cosh 2\phi + \cosh 2\nu}\right].$$

Making $\xi = 2\phi$, gives

$$J_4 = -\left(\frac{\pi}{2a}\right) \left[\frac{\pi\lambda}{2a} - \cosh(\beta + \alpha) \int_{(\beta-\alpha)}^{\frac{\pi\lambda + (\beta-\alpha)}{a}} \frac{d\xi}{\cosh \xi + \cosh(\beta + \alpha)} \right],$$

$$J_4 = -\left(\frac{\pi}{2a}\right) \left\{ \frac{\pi\lambda}{2a} - \coth(\beta + \alpha) \ln \frac{\cosh\left(\frac{\pi\lambda}{2a} + \beta\right) \cosh \alpha}{\cosh\left(\frac{\pi\lambda}{2a} - \alpha\right) \cosh \beta} \right\},$$

$$J_4 = -\left(\frac{\pi}{2a}\right) \left\{ \frac{\pi\lambda}{2a} - \coth \frac{\pi}{2a} (l+x) \ln \frac{\cosh \frac{\pi}{2a} (\lambda+l) \cosh \frac{\pi x}{2a}}{\cosh \frac{\pi}{2a} (\lambda-x) \cosh \frac{\pi l}{2a}} \right\}. \quad (\text{E.20})$$

An expression for the integral J can be obtained by adding equations E.17 through E.20.

Thus,

$$\begin{aligned} J &= -\left(\frac{\pi}{2a}\right) \coth \frac{\pi}{2a} (l-x) \ln \frac{\cosh \frac{\pi}{2a} (l+\lambda) \cosh \frac{\pi x}{2a}}{\cosh \frac{\pi}{2a} (x+\lambda) \cosh \frac{\pi l}{2a}} - \left(\frac{\pi}{2a}\right) \coth \frac{\pi}{2a} (l-x) \ln \frac{\cosh \frac{\pi}{2a} (\lambda-x) \cosh \frac{\pi l}{2a}}{\cosh \frac{\pi}{2a} (\lambda-l) \cosh \frac{\pi x}{2a}} \\ &\quad + \left(\frac{\pi}{2a}\right) \coth \frac{\pi}{2a} (l+x) \ln \frac{\cosh \frac{\pi}{2a} (\lambda+x) \cosh \frac{\pi l}{2a}}{\cosh \frac{\pi}{2a} (\lambda-l) \cosh \frac{\pi x}{2a}} + \left(\frac{\pi}{2a}\right) \coth \frac{\pi}{2a} (l+x) \ln \frac{\cosh \frac{\pi}{2a} (\lambda+l) \cosh \frac{\pi x}{2a}}{\cosh \frac{\pi}{2a} (\lambda-x) \cosh \frac{\pi l}{2a}} \\ J &= -\left(\frac{\pi}{2a}\right) \coth \frac{\pi}{2a} (l-x) \ln \frac{\cosh \frac{\pi}{2a} (l+\lambda) \cosh \frac{\pi}{2a} (\lambda-x)}{\cosh \frac{\pi}{2a} (x+\lambda) \cosh \frac{\pi}{2a} (\lambda-l)} + \left(\frac{\pi}{2a}\right) \coth \frac{\pi}{2a} (l+x) \ln \frac{\cosh \frac{\pi}{2a} (\lambda+x) \cosh \frac{\pi}{2a} (\lambda+l)}{\cosh \frac{\pi}{2a} (\lambda-l) \cosh \frac{\pi}{2a} (\lambda-x)}. \end{aligned}$$

From Equation E.13

$$V_1(x) = \frac{2\rho S_0 h}{\pi^2 w} J,$$

thus,

$$V_1(x) = -\frac{\rho S_0 h}{\pi a w} \left[\coth \frac{\pi}{2a} (l-x) \ln \frac{\cosh \frac{\pi}{2a} (l+\lambda) \cosh \frac{\pi}{2a} (\lambda-x)}{\cosh \frac{\pi}{2a} (x+\lambda) \cosh \frac{\pi}{2a} (\lambda-l)} - \coth \frac{\pi}{2a} (l+x) \ln \frac{\cosh \frac{\pi}{2a} (\lambda+x) \cosh \frac{\pi}{2a} (\lambda+l)}{\cosh \frac{\pi}{2a} (\lambda-l) \cosh \frac{\pi}{2a} (\lambda-x)} \right] \quad (\text{E.21})$$

which is the expression for equation 4.37.

Now consider equations 4.40 and 4.41:

$$\varphi_0^{new}(x, y) = -\frac{i\rho S_0}{\pi w} \int_{-\infty}^{\infty} e^{ikx} \frac{\sin kl}{k \sinh k(a-\Delta_0)} \cosh k(y-\Delta_0) dk, \quad (\text{E.22})$$

$$\varphi_0^{new}(x, y) = \frac{\rho S_0}{2\pi w} \ln \frac{\cosh \frac{\pi(l+x)}{(a-\Delta_0)} + \cos \frac{\pi(y-\Delta_0)}{(a-\Delta_0)}}{\cosh \frac{\pi(l-x)}{(a-\Delta_0)} + \cos \frac{\pi(y-\Delta_0)}{(a-\Delta_0)}}. \quad (\text{E.23})$$

The potential function may be written as $\varphi = \varphi_0 + \varphi_1$ and, therefore,

$$\varphi_1^{new} = \varphi_0 + \varphi_1 - \varphi_0^{new}.$$

The parameter Δ_0 may be estimated. At large x evaluated at $y = a$ Equation E.23 can be approximated as

$$\varphi_0^{new} \Big|_{y=a} \approx \frac{\rho S_0}{2\pi w} \ln \frac{e^{\frac{\pi(l+x)}{(a-\Delta_0)}}}{e^{\frac{\pi(x-l)}{(a-\Delta_0)}}},$$

$$\varphi_0^{new} \Big|_{y=a} \approx \frac{\rho S_0 l}{w(a-\Delta_0)}. \quad (\text{E.24})$$

Also, the potential function φ_0 in this region can be approximated as

$$\varphi_0|_{y=a} \approx \frac{\rho S_0}{2\pi w} \ln \frac{e^{\frac{\pi(l+x)}{a}}}{e^{\frac{\pi(x-l)}{a}}},$$

$$\varphi_0|_{y=a} \approx \frac{\rho S_0 l}{wa}. \quad (\text{E.25})$$

Analogously, the potential function φ_1 at $y = a$ for large values of x can be approximated as

$$\varphi_1|_{y=a} \approx \frac{\rho S_0 h}{2\pi a w} \left[-\ln \frac{e^{\frac{\pi}{2a}(l+\lambda)} e^{\frac{\pi}{2a}(x-\lambda)}}{e^{\frac{\pi}{2a}(x+\lambda)} e^{\frac{\pi}{2a}(l-\lambda)}} - \ln \frac{e^{\frac{\pi}{2a}(\lambda+x)} e^{\frac{\pi}{2a}(\lambda+l)}}{e^{\frac{\pi}{2a}(l-\lambda)} e^{\frac{\pi}{2a}(x-\lambda)}} \right],$$

$$\varphi_1|_{y=a} \approx \frac{\rho S_0 h \lambda}{a^2 w}. \quad (\text{E.26})$$

The parameter Δ_0 is such that

$$\left(\varphi - \varphi_0^{new} \right)_{\substack{x=\pm\infty \\ y=a}} = 0.$$

Thus,

$$\frac{\rho S_0 l}{wa} + \frac{\rho S_0 h \lambda}{a^2 w} = \frac{\rho S_0 l}{w(a - \Delta_0)},$$

$$\frac{\rho S_0 l}{wa} \left(1 + \frac{h\lambda}{al} \right) = \frac{\rho S_0 l}{w(a - \Delta_0)},$$

$$\frac{1}{a} \left(1 + \frac{h\lambda}{al} \right) = \frac{1}{a - \Delta_0},$$

$$\frac{1}{a} \left(1 + \frac{h\lambda}{al} \right) \approx \frac{1}{a} \left(1 + \frac{\Delta_0}{a} \right),$$

$$\Delta_0 \approx \frac{h\lambda}{l}, \quad (\text{E.27})$$

which is the expression for Equation 4.42.

APPENDIX F

This appendix describes the steps necessary to get the equations that are part of the analytic solution for a semi-infinite plate with smooth defect. Consider equations 4.33 and 4.34:

$$\varphi_1(x, y) = \int_{-\infty}^{\infty} e^{ikx} \hat{\varphi}_1(k, y) dk, \text{ and} \quad (\text{F.1})$$

$$\hat{\varphi}_1(k, y) = \frac{1}{2\pi} \int_{-\infty}^{\infty} e^{-ikx} \varphi_1(x, y) dx. \quad (\text{F.2})$$

Taking the Fourier transformation of equations 4.44, 4.45 and 4.46 gives

$$\frac{\partial^2 \hat{\varphi}_1}{\partial y^2} - k^2 \hat{\varphi}_1 = 0, \quad (\text{F.3})$$

$$\left. \frac{\partial \hat{\varphi}_1}{\partial y} \right|_{y=a} = 0, \quad (\text{F.4})$$

$$\left. \frac{\partial \hat{\varphi}_1}{\partial y} \right|_{y=0} = \frac{1}{2\pi} \int_{-\infty}^{\infty} e^{-ikx} dx \left[\frac{\partial}{\partial x} \left(\Delta \frac{\partial \varphi_0}{\partial x} \right) \right]_{y=0}. \quad (\text{F.5})$$

The solution to the Equation F.3 is

$$\hat{\varphi}_1(k, y) = B \cosh k(y - a). \quad (\text{F.6})$$

The derivative of this equation with respect to y is

$$\frac{\partial \hat{\varphi}_1}{\partial y} = k B \sinh k(y - a).$$

Evaluating this expression at $y = 0$ and replacing it in Equation F.5 results in

$$-k B \sinh ka = \frac{1}{2\pi} \int_{-\infty}^{\infty} e^{-ikx'} dx' \left[\frac{\partial}{\partial x'} (\Delta \frac{\partial \varphi_0}{\partial x'}) \right]_{y=0},$$

$$B = -\frac{1}{2\pi k \sinh ka} \int_{-\infty}^{\infty} e^{-ikx'} dx' \left[\frac{\partial}{\partial x'} (\Delta \frac{\partial \varphi_0}{\partial x'}) \right]_{y=0}. \quad (\text{F.7})$$

Substituting Equation F.7 into Equation F.6 gives

$$\hat{\varphi}_1(k, y) = -\frac{\cosh k(y-a)}{2\pi k \sinh ka} \int_{-\infty}^{\infty} e^{-ikx'} dx' \left[\frac{\partial}{\partial x'} (\Delta \frac{\partial \varphi_0}{\partial x'}) \right]_{y=0}. \quad (\text{F.8})$$

Replacing this equation in Equation F.1 gives

$$\varphi_1(x, y) = -\frac{1}{2\pi} \int_{-\infty}^{\infty} e^{ikx} \frac{\cosh k(y-a)}{k \sinh ka} dk \int_{-\infty}^{\infty} e^{-ikx'} dx' \left[\frac{\partial}{\partial x'} (\Delta \frac{\partial \varphi_0}{\partial x'}) \right]_{y=0},$$

$$\varphi_1(x, y) = -\frac{1}{2\pi} \int_{-\infty}^{\infty} dk \int_{-\infty}^{\infty} dx' e^{ik(x-x')} \frac{\cosh k(y-a)}{k \sinh ka} \left[\frac{\partial}{\partial x'} (\Delta \frac{\partial \varphi_0}{\partial x'}) \right]_{y=0},$$

$$\varphi_1(x, y) = -\frac{2}{\pi} \int_0^{\infty} dk \int_0^{\infty} dx' \sin kx \sin kx' \frac{\cosh k(y-a)}{k \sinh ka} \left[\frac{\partial}{\partial x'} (\Delta \frac{\partial \varphi_0}{\partial x'}) \right]_{y=0},$$

$$\varphi_1(x, y) = -\frac{2}{\pi} \int_0^{\infty} dx' \left[\frac{\partial}{\partial x'} (\Delta \frac{\partial \varphi_0}{\partial x'}) \right]_{y=0} \int_0^{\infty} dk \sin kx \sin kx' \frac{\cosh k(y-a)}{k \sinh ka},$$

$$\varphi_1(x, y) = -\frac{2}{\pi} \int_0^{\infty} dx' \left[\frac{\partial}{\partial x'} (\Delta \frac{\partial \varphi_0}{\partial x'}) \right]_{y=0} \int_0^{\infty} dk \frac{\cosh k(y-a)}{k \sinh ka} \left[\sin^2 \frac{k(x+x')}{2} - \sin^2 \frac{k(x'-x)}{2} \right].$$

Making the following change of variable

$$\xi = ka,$$

the potential function φ_1 becomes

$$\varphi_1(x, y) = -\frac{2}{\pi} \int_0^{\infty} dx' \left[\frac{\partial}{\partial x'} (\Delta \frac{\partial \varphi_0}{\partial x'}) \right]_{y=0} \int_0^{\infty} d\xi \frac{\cosh \xi \left(\frac{y-a}{a} \right)}{\xi \sinh \xi} \left[\sin^2 \frac{\xi(x+x')}{2a} - \sin^2 \frac{\xi(x'-x)}{2a} \right].$$

It can be seen from tables (Gradshteyn and Ryzhik, 1994) that

$$\int_0^{\infty} \sin^2 ax \frac{\cosh \beta x}{\sinh x} \frac{dx}{x} = \frac{1}{4} \ln \frac{\cosh 2a\pi + \cos \beta\pi}{1 + \cos \beta\pi}.$$

Therefore,

$$\varphi_1(x, y) = -\frac{1}{2\pi} \int_0^{\infty} dx' \left[\frac{\partial}{\partial x'} (\Delta \frac{\partial \varphi_0}{\partial x'}) \right]_{y=0} \left[\ln \frac{\cosh \frac{\pi(x+x')}{a} + \cos \frac{\pi(y-a)}{a}}{\cosh \frac{\pi(x'-x)}{a} + \cos \frac{\pi(y-a)}{a}} \right], \quad (\text{F.9})$$

which is the expression for Equation 4.47.

Evaluating this potential function at the surface of the plate ($y = a$) results in

$$\varphi_1(x) \Big|_{y=a} = -\frac{1}{2\pi} \int_0^{\infty} dx' \left[\frac{\partial}{\partial x'} (\Delta \frac{\partial \varphi_0}{\partial x'}) \right]_{y=0} \left[\ln \frac{\cosh \frac{\pi(x+x')}{a} + 1}{\cosh \frac{\pi(x'-x)}{a} + 1} \right],$$

but

$$\cosh(2\alpha) + 1 = 2 \cosh^2 \alpha,$$

therefore,

$$\varphi_1(x) \Big|_{y=a} = -\frac{1}{2\pi} \int_0^{\infty} dx' \left[\frac{\partial}{\partial x'} (\Delta \frac{\partial \varphi_0}{\partial x'}) \right]_{y=0} \ln \frac{\cosh^2 \frac{\pi(x+x')}{2a}}{\cosh^2 \frac{\pi(x'-x)}{2a}},$$

$$\varphi_1(x) \Big|_{y=a} = -\frac{1}{\pi} \int_0^{\infty} dx' \left[\frac{\partial}{\partial x'} (\Delta \frac{\partial \varphi_0}{\partial x'}) \right]_{y=0} \ln \frac{\cosh \frac{\pi(x+x')}{2a}}{\cosh \frac{\pi(x'-x)}{2a}}.$$

Integrating by parts gives

$$\varphi_1(x) \Big|_{y=a} = \frac{1}{2a} \int_0^{\infty} \left[dx' (\Delta \frac{\partial \varphi_0}{\partial x'}) \right]_{y=0} \left[\tanh \frac{\pi(x'+x)}{2a} + \tanh \frac{\pi(x-x')}{2a} \right]. \quad (\text{F.10})$$

Deriving Equation 4.43 with respect to x gives

$$\left. \frac{\partial \varphi_0}{\partial x} \right|_{y=0} = \frac{\rho S_0}{2aw} \left[\tanh \frac{\pi(l+x)}{2a} + \tanh \frac{\pi(l-x)}{2a} \right], \quad (\text{F.11})$$

thus,

$$\varphi_1(x) \Big|_{y=a} = \frac{\rho S_0}{4a^2 w} \int_0^\infty \Delta(x') \left[\tanh \frac{\pi(l+x)}{2a} + \tanh \frac{\pi(l-x)}{2a} \right] \left[\tanh \frac{\pi(x'+x)}{2a} + \tanh \frac{\pi(x-x')}{2a} \right] dx'. \quad (\text{F.12})$$

This is the expression used for Equation 4.48.

Now consider equations 4.49, 4.50 and 4.51:

$$\nabla^2 \varphi_2(x, y) = 0, \quad (\text{F.13})$$

$$\left. \frac{\partial \varphi_2}{\partial y} \right|_{y=a} = 0, \quad (\text{F.14})$$

$$\left(\frac{\partial \varphi}{\partial y} - \Delta \frac{\partial \varphi}{\partial x} \right)_{S_1} = 0. \quad (\text{F.15})$$

Expanding the last boundary condition and considering the second order term gives

$$\left(\frac{\partial \varphi_2}{\partial y} + \Delta \frac{\partial^2 \varphi_1}{\partial y^2} + \frac{\Delta^2}{2} \frac{\partial^3 \varphi_0}{\partial y^3} - \Delta \frac{\partial \varphi_1}{\partial x} - \Delta \Delta \frac{\partial^2 \varphi_0}{\partial x \partial y} \right)_{y=0} = 0,$$

$$\left[\frac{\partial \varphi_2}{\partial y} - \Delta \frac{\partial^2 \varphi_1}{\partial x^2} - \frac{\Delta^2}{2} \frac{\partial}{\partial x^2} \left(\frac{\partial \varphi_0}{\partial y} \right) - \Delta \frac{\partial \varphi_1}{\partial x} - \Delta \Delta \frac{\partial^2 \varphi_0}{\partial x \partial y} \right]_{y=0} = 0,$$

$$\left. \frac{\partial \varphi_2}{\partial y} \right|_{y=0} = \left(\Delta \frac{\partial^2 \varphi_1}{\partial x^2} + \Delta \frac{\partial \varphi_1}{\partial x} \right)_{y=0},$$

$$\left. \frac{\partial \varphi_2}{\partial y} \right|_{y=0} = \left(\frac{\partial}{\partial x} \left(\Delta \frac{\partial \varphi_1}{\partial x} \right) \right)_{y=0}. \quad (\text{F.16})$$

This is the expression for Equation 4.52.

The potential function φ_2 and its Fourier transform $\hat{\varphi}_2$ are given, by definition, as

$$\varphi_2(x, y) = \int_{-\infty}^{\infty} e^{ikx} \hat{\varphi}_2(k, y) dk, \text{ and} \quad (\text{F.17})$$

$$\hat{\varphi}_2(k, y) = \frac{1}{2\pi} \int_{-\infty}^{\infty} e^{-ikx} \varphi_2(x, y) dx. \quad (\text{F.18})$$

The Fourier transformation of equations F.13, F.14 and F.16 are

$$\frac{\partial^2 \hat{\varphi}_2}{\partial y^2} - k^2 \hat{\varphi}_2 = 0, \quad (\text{F.19})$$

$$\left. \frac{\partial \hat{\varphi}_2}{\partial y} \right|_{y=a} = 0, \quad (\text{F.20})$$

$$\left. \frac{\partial \hat{\varphi}_2}{\partial y} \right|_{y=0} = \frac{1}{2\pi} \int_{-\infty}^{\infty} e^{-ikx} dx \left[\frac{\partial}{\partial x'} (\Delta \frac{\partial \varphi_0}{\partial x'}) \right]_{y=0}. \quad (\text{F.21})$$

The solution to Equation F.19 is

$$\hat{\varphi}_2(k, y) = C \cosh k(y - a). \quad (\text{F.22})$$

The derivative of the equation above with respect to y is

$$\frac{\partial \hat{\varphi}_2}{\partial y} = k C \sinh k(y - a).$$

Evaluating this expression at $y = 0$ and replacing it in Equation F.21 gives

$$\begin{aligned} -k C \sinh ka &= \frac{1}{2\pi} \int_{-\infty}^{\infty} e^{-ikx} dx \left[\frac{\partial}{\partial x'} (\Delta \frac{\partial \varphi_0}{\partial x'}) \right]_{y=0}, \\ C &= -\frac{1}{2\pi k \sinh ka} \int_{-\infty}^{\infty} e^{-ikx} dx \left[\frac{\partial}{\partial x'} (\Delta \frac{\partial \varphi_0}{\partial x'}) \right]_{y=0}. \end{aligned} \quad (\text{F.23})$$

Substituting Equation F.23 into Equation F.22 results in

$$\hat{\varphi}_2(k, y) = -\frac{\cosh k(y - a)}{2\pi k \sinh ka} \int_{-\infty}^{\infty} e^{-ikx} dx \left[\frac{\partial}{\partial x'} (\Delta \frac{\partial \varphi_0}{\partial x'}) \right]_{y=0}. \quad (\text{F.24})$$

Replacing this equation in Equation F.17 gives

$$\varphi_2(x, y) = -\frac{1}{2\pi} \int_{-\infty}^{\infty} e^{ikx} \frac{\cosh k(y-a)}{k \sinh ka} dk \int_{-\infty}^{\infty} e^{-ikx'} dx' \left[\frac{\partial}{\partial x'} (\Delta \frac{\partial \varphi_0}{\partial x'}) \right]_{y=0}.$$

Using the same algebra as for φ_1 , the potential function φ_2 is found to be:

$$\varphi_2(x, y) = -\frac{1}{2\pi} \int_0^{\infty} dx' \left[\frac{\partial}{\partial x'} (\Delta \frac{\partial \varphi_0}{\partial x'}) \right]_{y=0} \left[\ln \frac{\cosh \frac{\pi(x+x')}{a} + \cos \frac{\pi(y-a)}{a}}{\cosh \frac{\pi(x'-x)}{a} + \cos \frac{\pi(y-a)}{a}} \right], \quad (\text{F.25})$$

which is the expression for Equation 4.55.

Evaluating this potential function at the surface of the plate ($y = a$) gives

$$\varphi_2(x) \Big|_{y=a} = -\frac{1}{2\pi} \int_0^{\infty} dx' \left[\frac{\partial}{\partial x'} (\Delta \frac{\partial \varphi_0}{\partial x'}) \right]_{y=0} \left[\ln \frac{\cosh \frac{\pi(x+x')}{a} + 1}{\cosh \frac{\pi(x'-x)}{a} + 1} \right],$$

$$\varphi_2(x) \Big|_{y=a} = -\frac{1}{\pi} \int_0^{\infty} dx' \left[\frac{\partial}{\partial x'} (\Delta \frac{\partial \varphi_0}{\partial x'}) \right]_{y=0} \ln \frac{\cosh \frac{\pi(x+x')}{2a}}{\cosh \frac{\pi(x'-x)}{2a}}.$$

Integrating by parts yields

$$\varphi_2(x) \Big|_{y=a} = \frac{1}{2a} \int_0^{\infty} dx' \Delta(x') \frac{\partial \varphi_1}{\partial x'} \Big|_{y=0} \left[\tanh \frac{\pi(x'+x)}{2a} + \tanh \frac{\pi(x-x')}{2a} \right], \quad (\text{F.26})$$

which is the expression for Equation 4.56.

The term $\frac{\partial \varphi_1}{\partial x'} \Big|_{y=0}$ must be evaluated. From Equation F.9

$$\varphi_1(x, y) = -\frac{1}{2\pi} \int_0^{\infty} dx' \left[\frac{\partial}{\partial x'} (\Delta \frac{\partial \varphi_0}{\partial x'}) \right]_{y=0} \left[\ln \frac{\cosh \frac{\pi(x+x')}{a} + \cos \frac{\pi(y-a)}{a}}{\cosh \frac{\pi(x'-x)}{a} + \cos \frac{\pi(y-a)}{a}} \right],$$

and changing the integration variable results in

$$\varphi_1(x', y) = -\frac{1}{2\pi} \int_0^{\infty} dx'' \left[\frac{\partial}{\partial x''} (\Delta \frac{\partial \varphi_0}{\partial x''}) \right]_{y=0} \left[\ln \frac{\cosh \frac{\pi(x' + x'')}{a} + \cos \frac{\pi(y-a)}{a}}{\cosh \frac{\pi(x'' - x')}{a} + \cos \frac{\pi(y-a)}{a}} \right]. \quad (\text{F.27})$$

Evaluating the first derivative of this function with respect to x' gives

$$\frac{\partial \varphi_1(x', y)}{\partial x'} = -\frac{1}{2\pi} \int_0^{\infty} dx'' \left[\frac{\partial}{\partial x''} (\Delta \frac{\partial \varphi_0}{\partial x''}) \right]_{y=0} \frac{\partial}{\partial x'} \left[\ln \frac{\cosh \frac{\pi(x' + x'')}{a} + \cos \frac{\pi(y-a)}{a}}{\cosh \frac{\pi(x'' - x')}{a} + \cos \frac{\pi(y-a)}{a}} \right]. \quad (\text{F.28})$$

It can be observed that

$$\begin{aligned} \frac{\partial}{\partial x'} \left\{ \ln \left[\cosh \frac{\pi(x' + x'')}{a} + \cos \frac{\pi(y-a)}{a} \right] - \ln \left[\cosh \frac{\pi(x'' - x')}{a} + \cos \frac{\pi(y-a)}{a} \right] \right\} = \\ \frac{\partial}{\partial x''} \left\{ \ln \left[\cosh \frac{\pi(x' + x'')}{a} + \cos \frac{\pi(y-a)}{a} \right] + \ln \left[\cosh \frac{\pi(x'' - x')}{a} + \cos \frac{\pi(y-a)}{a} \right] \right\} \end{aligned}$$

Replacing this identity in Equation F.28 gives

$$\frac{\partial \varphi_1}{\partial x'} = -\frac{1}{2\pi} \int_0^{\infty} dx'' \left[\frac{\partial}{\partial x''} (\Delta \frac{\partial \varphi_0}{\partial x''}) \right]_{y=0} \frac{\partial}{\partial x''} \left\{ \ln \left[\cosh \frac{\pi(x' + x'')}{a} + \cos \frac{\pi(y-a)}{a} \right] + \ln \left[\cosh \frac{\pi(x'' - x')}{a} + \cos \frac{\pi(y-a)}{a} \right] \right\}$$

and integrating it by parts

$$\frac{\partial \varphi_1}{\partial x'} = \frac{1}{2\pi} \int_0^{\infty} dx'' \left[\frac{\partial}{\partial x''} (\Delta \frac{\partial \varphi_0}{\partial x''}) \right]_{y=0} \left\{ \ln \left[\cosh \frac{\pi(x' + x'')}{a} + \cos \frac{\pi(y-a)}{a} \right] + \ln \left[\cosh \frac{\pi(x'' - x')}{a} + \cos \frac{\pi(y-a)}{a} \right] \right\}$$

Evaluating the expression above at $y = 0$ gives

$$\frac{\partial \varphi_1}{\partial x'} \Big|_{y=0} = \frac{1}{2\pi} \int_0^{\infty} dx'' \left[\frac{\partial}{\partial x''} (\Delta \frac{\partial \varphi_0}{\partial x''}) \right]_{y=0} \left\{ \ln \left[\cosh \frac{\pi(x' + x'')}{a} - 1 \right] + \ln \left[\cosh \frac{\pi(x'' - x')}{a} - 1 \right] \right\},$$

but

$$\cosh(2\alpha) - 1 = 2 \sinh^2 \alpha,$$

therefore,

$$\frac{\partial \varphi_1}{\partial x'} \Big|_{y=0} = \frac{1}{2\pi} \int_0^\infty dx'' \left[\frac{\partial^2}{\partial x''^2} \left(\Delta \frac{\partial \varphi_0}{\partial x''} \right) \right]_{y=0} \ln \left[4 \sinh^2 \frac{\pi(x' + x'')}{2a} \sinh^2 \frac{\pi(x'' - x')}{2a} \right],$$

$$\frac{\partial \varphi_1}{\partial x'} \Big|_{y=0} = \frac{1}{2\pi} \int_0^\infty dx'' \left[\frac{\partial^2}{\partial x''^2} \left(\Delta \frac{\partial \varphi_0}{\partial x''} \right) \right]_{y=0} \ln \left[2 \sinh \frac{\pi(x' + x'')}{2a} \sinh \frac{\pi(x'' - x')}{2a} \right]^2. \quad (\text{F.29})$$

Knowing that

$$\sinh a \sinh b = \frac{1}{2} [\cosh(a + b) - \cosh(a - b)],$$

Equation F.29 can be rewritten as

$$\frac{\partial \varphi_1}{\partial x'} \Big|_{y=0} = \frac{1}{2\pi} \int_0^\infty dx'' \left[\frac{\partial^2}{\partial x''^2} \left(\Delta \frac{\partial \varphi_0}{\partial x''} \right) \right]_{y=0} \ln \left[\cosh \frac{\pi x''}{a} - \cosh \frac{\pi x'}{a} \right]^2. \quad (\text{F.30})$$

The integrand has a logarithmic singularity when $x' = x''$, but this singularity is integrable if Δ and φ_0 are sufficiently smooth. Figure F.1 shows a schematic view of the singularity.

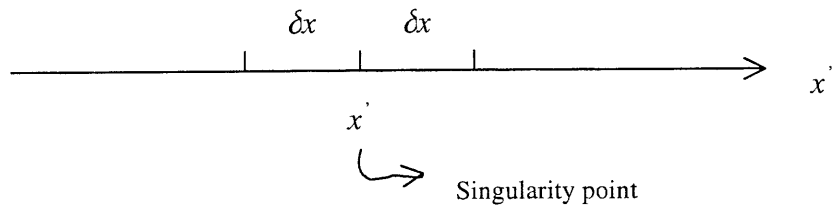


Figure F.1 – Schematic view of the singularity in Equation F.30

Consider Equation F.30 as

$$\left. \frac{\partial \varphi_1}{\partial x'} \right|_{y=0} = \frac{1}{2\pi} \int_{x'-\delta x}^{x'+\delta x} dx'' f(x'') \ln \left[\cosh \frac{\pi x''}{a} - \cosh \frac{\pi x'}{a} \right]^2, \quad (\text{F.31})$$

where $f(x'') = \left[\frac{\partial^2}{\partial x''^2} (\Delta \frac{\partial \varphi_0}{\partial x''}) \right]_{y=0}$ and δx is a small increment about the singularity point.

Expanding near $x'' = x' + \xi$, where ξ is a small term, results in

$$f(x'') \approx f(x'),$$

$$\cosh \frac{\pi x''}{a} = \cosh \frac{\pi(x' + \xi)}{a} \approx \cosh \frac{\pi x'}{a} + \frac{\pi \xi}{a} \sinh \frac{\pi x'}{a}.$$

Substituting these expansions into Equation F.31 gives

$$\left. \frac{\partial \varphi_1}{\partial x'} \right|_{y=0} \approx \frac{1}{2\pi} \int_{-\delta x}^{\delta x} d\xi f(x') \ln \left[\frac{\pi \xi}{a} \sinh \frac{\pi x'}{a} \right]^2,$$

$$\left. \frac{\partial \varphi_1}{\partial x'} \right|_{y=0} \approx \frac{1}{2\pi} \int_{-\delta x}^{\delta x} d\xi f(x') \left[\ln \left(\frac{\pi^2}{a^2} \sinh^2 \frac{\pi x'}{a} \right) + \ln \xi^2 \right],$$

$$\left. \frac{\partial \varphi_1}{\partial x'} \right|_{y=0} \approx \frac{1}{2\pi} f(x') \left[2\delta x \ln \left(\frac{\pi^2}{a^2} \sinh^2 \frac{\pi x'}{a} \right) + 2 \int_0^{\delta x} d\xi \ln \xi^2 \right],$$

$$\left. \frac{\partial \varphi_1}{\partial x'} \right|_{y=0} \approx \frac{1}{2\pi} f(x') \left[2\delta x \ln \left(\frac{\pi}{a} \sinh \frac{\pi x'}{a} \right)^2 + 4 \int_0^{\delta x} d\xi \ln \xi \right],$$

$$\left. \frac{\partial \varphi_1}{\partial x'} \right|_{y=0} \approx \frac{1}{2\pi} f(x') \left[2\delta x \ln \left(\frac{\pi}{a} \sinh \frac{\pi x'}{a} \right)^2 + 4(\delta x \ln \delta x - \delta x) \right],$$

$$\left. \frac{\partial \varphi_1}{\partial x'} \right|_{y=0} \approx \frac{\delta x}{\pi} f(x') \left[\ln \left(\frac{\pi \delta x}{a} \sinh \frac{\pi x'}{a} \right)^2 - 2 \right],$$

$$\left. \frac{\partial \varphi_1}{\partial x'} \right|_{y=0} \approx \frac{\delta x}{\pi} \left[\frac{\partial^2}{\partial x''^2} (\Delta \frac{\partial \varphi_0}{\partial x''}) \right]_{y=0} \left[\ln \left(\frac{\pi \delta x}{a} \sinh \frac{\pi x'}{a} \right)^2 - 2 \right]. \quad (\text{F.32})$$

This equation replaces Equation F.30 at the singularity $x' = x''$.

The term $\left[\frac{\partial^2}{\partial x''^2} (\Delta \frac{\partial \varphi_0}{\partial x''}) \right]_{y=0}$ can be rewritten as

$$\left[\frac{\partial^2}{\partial x''^2} (\Delta \frac{\partial \varphi_0}{\partial x''}) \right]_{y=0} = \frac{\partial}{\partial x''} \left[\frac{\partial}{\partial x''} \Delta \frac{\partial \varphi_0}{\partial x''} \right]_{y=0},$$

$$\left[\frac{\partial^2}{\partial x''^2} (\Delta \frac{\partial \varphi_0}{\partial x''}) \right]_{y=0} = \left[\Delta \frac{\partial^3 \varphi_0}{\partial x''^3} + 2 \frac{d\Delta}{dx''} \frac{\partial^2 \varphi_0}{\partial x''^2} + \frac{d^2 \Delta}{dx''^2} \frac{\partial \varphi_0}{\partial x''} \right]_{y=0}. \quad (\text{F.33})$$

Substituting Equation F.33 into Equation F.30 gives

$$\frac{\partial \varphi_1}{\partial x'} \Big|_{y=0} = \frac{1}{2\pi} \int_0^\infty dx'' \left[\Delta \frac{\partial^3 \varphi_0}{\partial x''^3} + 2 \frac{d\Delta}{dx''} \frac{\partial^2 \varphi_0}{\partial x''^2} + \frac{d^2 \Delta}{dx''^2} \frac{\partial \varphi_0}{\partial x''} \right]_{y=0} \ln \left[\cosh \frac{\pi x''}{a} - \cosh \frac{\pi x'}{a} \right]^2, \quad (\text{F.34})$$

which is the expression for Equation 4.57.

Substituting Equation F.33 into Equation F.32 gives the equation above evaluated at the singularity $x' = x''$. So,

$$\frac{\partial \varphi_1}{\partial x'} \Big|_{y=0} \approx \frac{\delta x}{\pi} \left[\Delta \frac{\partial^3 \varphi_0}{\partial x''^3} + 2 \frac{d\Delta}{dx''} \frac{\partial^2 \varphi_0}{\partial x''^2} + \frac{d^2 \Delta}{dx''^2} \frac{\partial \varphi_0}{\partial x''} \right]_{y=0} \left[\ln \left(\frac{\pi \delta x}{a} \sinh \frac{\pi x'}{a} \right)^2 - 2 \right], \quad (\text{F.35})$$

which is Equation 4.58.

From Equation 4.43 the derivatives of the potential function φ_0 with respect to x'' can be evaluated. Therefore,

$$\frac{\partial \varphi_0}{\partial x''} \Big|_{y=0} = \frac{\rho S_0}{2aw} \left[\tanh \frac{\pi(l+x'')}{2a} + \tanh \frac{\pi(l-x'')}{2a} \right], \quad (\text{F.36})$$

$$\frac{\partial^2 \varphi_0}{\partial x''^2} \Big|_{y=0} = \frac{\rho S_0 \pi}{4a^2 w} \left[\sec^2 h^2 \frac{\pi(l+x'')}{2a} - \sec^2 h^2 \frac{\pi(l-x'')}{2a} \right], \quad (\text{F.37})$$

$$\frac{\partial^3 \varphi_0}{\partial x''^3} \Big|_{y=0} = -\frac{\rho S_0 \pi^2}{4a^3 w} \left[\sec^2 h^2 \frac{\pi(l+x'')}{2a} \tanh \frac{\pi(l+x'')}{2a} + \sec^2 h^2 \frac{\pi(l-x'')}{2a} \tanh \frac{\pi(l-x'')}{2a} \right]. \quad (\text{F.38})$$

Consider the defect given by Equation 4.59.

$$\Delta(x) = h \left[\frac{\tanh \frac{(c+x)}{s} + \tanh \frac{(c-x)}{s}}{2 \tanh(c/s)} \right], \quad (\text{F.39})$$

The first and second derivatives of this function with respect to x must be calculated in order to substituted into equations F.34 and F.35. Thus,

$$\frac{d\Delta}{dx} = \frac{h}{2 s \tanh(c/s)} \left[\sec h^2 \left(\frac{c+x}{s} \right) - \sec h^2 \left(\frac{c-x}{s} \right) \right], \quad (\text{F.40})$$

$$\frac{d^2\Delta}{dx^2} = \frac{h}{2 s^2 \tanh(c/s)} \left[\sec h^2 \left(\frac{c+x}{s} \right) \tanh \left(\frac{c+x}{s} \right) - \sec h^2 \left(\frac{c-x}{s} \right) \tanh \left(\frac{c-x}{s} \right) \right]. \quad (\text{F.41})$$

Equations F.34 through F.41 are used to calculate the potential function φ_2 evaluated at $y = a$, which is given by Equation F.26.

APPENDIX G

This appendix contains a listing of the code “forward_smooth”, which was developed to solve the forward problem for a plate with a “smooth defect”. This code includes the subroutines “calcphone” and “calcphi2”.

```
%  
  
%          PROGRAM FORWARD_SMOOTH  
  
%  
  
function smooth_forward  
  
clear  
  
global lprobe w l a rho curr deltax x  
  
global xp0 numcol numxp deltaxp  
  
global h c s i x2p0 deltax2p numx2p  
  
input('enter with the length of probe in x direction : lprobe (mm)= ');  
  
input('enter with the width : w (mm) =');  
  
input('enter with the defect height : h (mm) =');  
  
input('enter with the defect width : c (mm) =');  
  
input('enter with the length :l (mm) =');
```

```

input('enter with the thickness :a (mm) =');
input('enter with the resistivity :rho (micro_ohm*mm) =');
input('enter with the current : curr (amp) =');
input('enter with the increment in xprime : deltaxp (mm) =');
input('enter with the increment in xdouble_prime : delta2xp (mm) =');
input('enter with the parameter s : s (mm) =');
input('enter with the increment in x : deltax (mm) =');

numcol = lprobe/deltax +1;
numxp = (2*1)/deltaxp+1;
numx2p = (2*1)/deltaxp+1;

for i=1:1:numcol,
    x(i)= (-lprobe/2)+deltax*(i-1);
    num1 = sinh((pi/(2*a))*(1+x(i)));
    den1 = sinh((pi/(2*a))*(1-x(i)));
    phizero(i) = ((rho*curr)/(pi*w))*log(num1/den1)
    [phione] = calcphione(xp0);
    [phi2] = calcphi2(xp0,x2p0);
    phi(i) = phizero(i) + phione(i) + phi2(i);

end

plot(x,phi,'b-',x,phizero,'r--')

```



```
title('Potential functions versus distance: plate with smooth defect')  
xlabel('Distance from the center to the border of the plate (mm)')  
ylabel('Potential (microvolt)')
```



```

var2 = -
(pi*pi*curr*rho)/(4*a*a*a*w)*[((sech(pi*(1+xp)/(2*a)))^2)*tanh((pi/(2*a))*(1+xp))+...
((sech(pi*(1-xp)/(2*a)))^2)*tanh((pi/(2*a))*(1-xp))];
var3 = (h/(2*s*tanh(c/s)))*[(sech((c+xp)/s))^2-(sech((c-xp)/s))^2];
var4 = ((pi*curr*rho)/(4*a*a*a*w)*[(sech((1+xp)*pi/(2*a)))^2-(sech((1-
xp)*pi/(2*a)))^2];
var5 = -(h/(s*s*tanh(c/s)))*[((sech((c+xp)/s))^2)*tanh((c+xp)/s)+((sech((c-
xp)/s))^2)*tanh((c-xp)/s)];
var6 = ((rho*curr)/(2*a*w))*[tanh((pi/(2*a))*(1+xp))+tanh((pi/(2*a))*(1-xp))];
deriv2xp = var1*var2+2*var3*var4+var5*var6;
excessao = (1/pi)*incremxp*deriv2xp*[(log((pi/a)*incremxp*sinh(pi*xp/a)))^2-2];
x2p = x2p + deltax2p;

end

if (aux~=0)
var7 = (h/(2*tanh(c/s)))*(tanh((c+x2p)/s)+tanh((c-x2p)/s));
var8 = -
((pi*pi*curr*rho)/(4*a*a*a*w)*[((sech(pi*(1+x2p)/(2*a)))^2)*tanh((pi/(2*a))*(1+x2p))+
((sech(pi*(1-x2p)/(2*a)))^2)*tanh((pi/(2*a))*(1-x2p))];
var9 = (h/(2*s*tanh(c/s)))*[(sech((c+x2p)/s))^2-(sech((c-x2p)/s))^2];
var10 = ((pi*curr*rho)/(4*a*a*a*w)*[(sech((1+x2p)*pi/(2*a)))^2-(sech((1-
x2p)*pi/(2*a)))^2];

```

```
var11 = -(h/(s*s*tanh(c/s)))*[((sech((c+x2p)/s))^2)*tanh((c+x2p)/s)+((sech((c-x2p)/s))^2)*tanh((c-x2p)/s)];
```

```
var12 = ((rho*curr)/(2*a*w))*[tanh((pi/(2*a))*(1+x2p))+tanh((pi/(2*a))*(1-x2p))];
```

```
deriv2x2p = var7*var8 + 2*var9*var10 + var11*var12;
```

```
prod1 = deriv2x2p*log((cosh((pi/a)*xp)-cosh((pi/a)*x2p))^2);
```

```
sumx2p = sumx2p + prod1;
```

```
x2p = x2p + deltax2p;
```

```
end
```

```
end
```

```
dphi1dxi = (1/pi)*deltax2p*sumx2p + excessao;
```

```
var13 = (h/(2*tanh(c/s)))*(tanh((c+xp)/s)+tanh((c-xp)/s));
```

```
var14 = tanh((pi/2*a)*(x(i)+xp))+ tanh((pi/2*a)*(x(i)-xp));
```

```
prod2 = dphi1dxi*var13*var14;
```

```
sumxp = sumxp + prod2;
```

```
xp = xp + deltaxp;
```

```
end
```

```
phi2(i) = (1/(2*a))*deltaxp*sumxp;
```

APPENDIX H

This appendix describes the derivation of Equation 4.63, which is the cylindrical correction for the potential function. Consider the equations below:

$$\frac{\partial^2 \varphi_c}{\partial x^2} + \frac{\partial^2 \varphi_c}{\partial y^2} = -\frac{1}{r_0} \frac{\partial \varphi_0}{\partial y},$$

$$\left. \frac{\partial \varphi_c}{\partial y} \right|_{y=a} = 0,$$

$$\left. \frac{\partial \varphi_c}{\partial y} \right|_{y=\Delta_0} = 0.$$

$$\text{Let } \varphi_c(x, y) = K(y - a)\varphi_0(x, y) + \Psi_c. \quad (\text{H.1})$$

Thus,

$$\nabla^2 \varphi_c = K[(y - a)\nabla^2 \varphi_0 + 2\nabla(y - a) \cdot \nabla \varphi_0 + \varphi_0 \nabla^2(y - a)] + \nabla^2 \Psi_c,$$

$$\nabla^2 \varphi_c = 2K \frac{\partial \varphi_0}{\partial y} + \nabla^2 \Psi_c.$$

Choosing $K = -\frac{1}{2r_0}$, Equation H.1 can be written as

$$\varphi_c(x, y) = -\frac{(y - a)}{2r_0} \varphi_0(x, y) + \Psi_c(x, y). \quad (\text{H.2})$$

The function $\Psi_c(x, y)$ satisfies the Laplace equation, therefore

$$\nabla^2 \Psi_c(x, y) = 0,$$

$$\frac{\partial \varphi_c}{\partial y} = \frac{\partial \Psi_c}{\partial y} - \frac{\varphi_0}{2r_0} - \frac{y - a}{2r_0} \frac{\partial \varphi_0}{\partial y}.$$

The boundary conditions are

$$\text{at } y = \Delta_0: \quad \left(\frac{\partial \Psi_c}{\partial y} - \frac{\varphi_0}{2r_0} \right)_{y=\Delta_0} = 0, \quad (\text{H.3})$$

$$\text{at } y = a: \quad \left(\frac{\partial \Psi_c}{\partial y} - \frac{\partial \varphi_0}{2r_0} \right)_{y=a} = 0. \quad (\text{H.4})$$

Consider

$$\Psi_c(x, y) = \int_{-\infty}^{\infty} e^{ikx} \hat{\Psi}_c(k, y) dk,$$

$$\hat{\Psi}_c(k, y) = \frac{1}{2\pi} \int_{-\infty}^{\infty} e^{-ikx} \Psi_c(x, y) dx.$$

The Laplace equation changes to

$$\frac{\partial^2 \hat{\Psi}_c}{\partial^2 y} - k^2 \hat{\Psi}_c = 0.$$

The general solution for this equation is

$$\hat{\Psi}_c(k, y) = A \cosh k(y - a) + B \cosh k(y - \Delta_0). \quad (\text{H.5})$$

Thus,

$$\frac{\partial \hat{\Psi}_c}{\partial y} = kA \sinh k(y - a) + kB \sinh k(y - \Delta_0).$$

From Equation H.3

$$-kA \sinh k(a - \Delta_0) = \frac{1}{2r_0} \hat{\varphi}_0(\Delta_0),$$

$$A = -\frac{1}{2r_0 k \sinh k(a - \Delta_0)} \hat{\varphi}_0(\Delta_0).$$

From Equation H.4

$$kB \sinh k(a - \Delta_0) = \frac{1}{2r_0} \hat{\phi}_0(a),$$

$$B = \frac{1}{2r_0 k \sinh k(a - \Delta_0)} \hat{\phi}_0(a).$$

Substituting these results into Equation H.5 gives

$$\hat{\Psi}_c(k, y) = \frac{1}{2r_0 k \sinh k(a - \Delta_0)} [\hat{\phi}_0(a) \cosh k(y - \Delta_0) - \hat{\phi}_0(\Delta_0) \cosh k(y - a)]. \quad (\text{H.6})$$

From Equation 4.40

$$\hat{\phi}_0(k, y) = -\frac{i\rho S_0}{\pi w} \frac{\sin kl}{k \sinh k(a - \Delta_0)} \cosh k(y - \Delta_0).$$

Thus,

$$\hat{\phi}_0(a) = -\frac{i\rho S_0}{\pi w} \frac{\cosh k(a - \Delta_0) \sinh kl}{k \sinh k(a - \Delta_0)},$$

$$\hat{\phi}_0(\Delta_0) = -\frac{i\rho S_0}{\pi w} \frac{\sinh kl}{k \sinh k(a - \Delta_0)}.$$

Substituting the equations above into Equation H.6 results in

$$\hat{\Psi}_c(k, y) = -\frac{i\rho S_0 \sin kl}{2\pi w r_0 k^2 \sinh^2 k(a - \Delta_0)} [\cosh k(a - \Delta_0) \cosh k(y - \Delta_0) - \cosh k(y - a)]. \quad (\text{H.7})$$

Evaluating this equation at the surface ($y = a$) gives

$$\hat{\Psi}_c(k, a) = -\frac{i\rho S_0}{2\pi w r_0} \frac{\sin kl}{k^2}. \quad (\text{H.8})$$

By definition

$$\Psi_c(x, y) = \int_{-\infty}^{\infty} e^{ikx} \hat{\Psi}_c(k, y) dk,$$

$$\Psi_c(x, a) = \int_{-\infty}^{\infty} e^{ikx} \hat{\Psi}_c(k, a) dk,$$

and substituting Equation H.8 into this equation results in

$$\Psi_c(x, a) = -\frac{i\rho S_0}{2\pi w r_0} \int_{-\infty}^{\infty} e^{ikx} \frac{\sin kl}{k^2} dk,$$

$$\Psi_c(x, a) = \frac{\rho S_0}{2\pi w r_0} \int_{-\infty}^{\infty} \frac{\sin kx \sin kl}{k^2} dk.$$

It can be seen from tables (Gradshteyn and Ryzhik, 1994) that

$$\int_{-\infty}^{\infty} \frac{\sin ka \sin kb}{k^2} dk = \begin{cases} \pi a & \text{if } a < b \\ \pi b & \text{if } a > b \end{cases}$$

or
$$\int_{-\infty}^{\infty} \frac{\sin ka \sin kb}{k^2} dk = \frac{\pi}{2} [|b+a| - |b-a|].$$

Therefore,

$$\Psi_c(x, a) = \frac{\rho S_0}{4 w r_0} [|l+x| - |l-x|]. \quad (\text{H.9})$$

From Equation H.2

$$\varphi_c(x, a) = \Psi_c(x, a),$$

therefore,

$$\varphi(x, a) = \varphi_0(x, a) + \varphi_c(x, a),$$

$$\varphi(x, a) = \frac{\rho S_0}{4 w} \left\{ \frac{1}{r_0} [|l+x| - |l-x|] + \frac{2}{\pi} \ln \frac{\cosh \frac{\pi(l+x)}{(a-\Delta_0)} + \cos \frac{\pi(a-\Delta_0)}{(a-\Delta_0)}}{\cosh \frac{\pi(l-x)}{(a-\Delta_0)} + \cos \frac{\pi(a-\Delta_0)}{(a-\Delta_0)}} \right\},$$

which is the expression for Equation 4.63.

APPENDIX I

This appendix describes the derivation of equations 4.72 through 4.75, 4.81 and 4.82, which are parts of the forward 3D solution for a pipe with a non-symmetric defect.

Consider Equation 4.71:

$$\left[\frac{\partial \varphi}{\partial y} - \frac{r_0^2}{(r_0 + y - \frac{a}{2})^2} \frac{\partial \varphi}{\partial z} \frac{\partial \Delta}{\partial z} - \frac{\partial \varphi}{\partial x} \frac{\partial \Delta}{\partial x} \right]_{\Delta} = 0. \quad (\text{I.1})$$

Expanding this equation about $\Delta = 0$ gives

$$\left[\frac{\partial \varphi}{\partial y} + \Delta \frac{\partial^2 \varphi}{\partial y^2} + \frac{\Delta^2}{2} \frac{\partial^3 \varphi}{\partial y^3} - \frac{r_0^2}{(r_0 + y - \frac{a}{2})^2} \frac{\partial \Delta}{\partial z} \left(\frac{\partial \varphi}{\partial z} + \Delta \frac{\partial^2 \varphi}{\partial y \partial z} \right) - \frac{\partial \Delta}{\partial x} \left(\frac{\partial \varphi}{\partial x} + \Delta \frac{\partial^2 \varphi}{\partial x \partial y} \right) \right]_{\Delta} = 0. \quad (\text{I.2})$$

Knowing that

$$\varphi(x, y, z) \approx \varphi_0(x, y) + \varphi_1(x, y, z) + \varphi_2(x, y, z) + \varphi_c(x, y, z)$$

and substituting it into Equation I.2 produces, for each order of magnitude indicated as a superscript, the following equations:

$$\Delta^{(0)} : \left. \frac{\partial \varphi_0}{\partial y} \right|_{y=0} = 0; \quad (\text{I.3})$$

$$\Delta^{(1)} : \left[\frac{\partial \varphi_1}{\partial y} + \Delta \frac{\partial^2 \varphi_0}{\partial y^2} - \frac{\partial \Delta}{\partial x} \frac{\partial \varphi_0}{\partial x} \right]_{y=0} = 0,$$

$$\Delta^{(1)} : \left[\frac{\partial \varphi_1}{\partial y} - \Delta \frac{\partial^2 \varphi_0}{\partial x^2} - \frac{\partial \Delta}{\partial x} \frac{\partial \varphi_0}{\partial x} \right]_{y=0} = 0,$$

$$\Delta^{(1)} : \left[\frac{\partial \varphi_1}{\partial y} - \frac{\partial}{\partial x} \left(\Delta \frac{\partial \varphi_0}{\partial x} \right) \right]_{y=0} = 0; \quad (\text{I.4})$$

$$\Delta^{(2)} : \left[\frac{\partial}{\partial y} (\varphi_2 + \varphi_c) + \Delta \frac{\partial^2 \varphi_1}{\partial y^2} + \frac{\Delta^2}{2} \frac{\partial^3 \varphi_0}{\partial y^3} - \frac{\partial \Delta}{\partial z} \frac{\partial \varphi_1}{\partial z} - \frac{\partial \Delta}{\partial x} \frac{\partial \varphi_1}{\partial x} - \Delta \frac{\partial \Delta}{\partial x} \frac{\partial^2 \varphi_0}{\partial x \partial y} \right]_{y=0} = 0,$$

$$\Delta^{(2)} : \left. \frac{\partial \varphi_c}{\partial y} \right|_{y=0} = 0, \quad (\text{I.5})$$

$$\Delta^{(2)} : \left[\frac{\partial \varphi_2}{\partial y} - \Delta \frac{\partial^2 \varphi_1}{\partial x^2} - \Delta \frac{\partial^2 \varphi_1}{\partial z^2} - \frac{\partial \Delta}{\partial z} \frac{\partial \varphi_1}{\partial z} - \frac{\partial \Delta}{\partial x} \frac{\partial \varphi_1}{\partial x} \right]_{y=0} = 0,$$

$$\Delta^{(2)} : \left[\frac{\partial \varphi_2}{\partial y} - \frac{\partial}{\partial x} \left(\Delta \frac{\partial \varphi_1}{\partial x} \right) - \frac{\partial}{\partial z} \left(\Delta \frac{\partial \varphi_1}{\partial z} \right) \right]_{y=0} = 0. \quad (\text{I.6})$$

These are equations 4.72 through 4.75.

Now consider the equations:

$$\frac{\partial^2 \varphi_1}{\partial x^2} + \frac{\partial^2 \varphi_1}{\partial y^2} + \frac{\partial^2 \varphi_1}{\partial z^2} = 0,$$

$$\left[\frac{\partial \varphi_1}{\partial y} - \frac{\partial}{\partial x} \left(\Delta \frac{\partial \varphi_0}{\partial x} \right) \right]_{y=0} = 0,$$

$$\left. \frac{\partial \varphi_1}{\partial y} \right|_{y=a} = 0. \quad (\text{I.7})$$

By definition,

$$\varphi_1(x, y, z) = \sum_{n=-\infty}^{\infty} e^{i \frac{2\pi n z}{w}} \varphi_{1n}(x, y), \quad (\text{I.8})$$

$$\varphi_1(x, y, z) = \sum_{n=-\infty}^{\infty} e^{i \frac{2\pi n z}{w}} \int_{-\infty}^{\infty} e^{ikx} \hat{\varphi}_{1n}(k, y) dk, \quad (\text{I.9})$$

$$\varphi_{1n}(x, y) = \int_{-\infty}^{\infty} dk e^{ikx} \hat{\varphi}_{1n}(k, y), \quad (\text{I.10})$$

where $\hat{\varphi}_{1n}(k, y)$ is the Fourier transform of $\varphi_{1n}(x, y)$.

Fourier analysis may solve Equation I.9 after multiplying both sides by

$$\int_{-\infty}^{\infty} e^{-ikx} dx \int_0^w e^{-i\frac{2m\pi z}{w}} dz. \quad (\text{I.11})$$

The right hand side becomes

$$\begin{aligned} RHS &= \int_{-\infty}^{\infty} e^{-ikx} dx \int_0^w e^{-i\frac{2m\pi z}{w}} dz \sum_{n=-\infty}^{\infty} e^{i\frac{2\pi n z}{w}} \int_{-\infty}^{\infty} e^{ikx} \hat{\varphi}_{1n}(k, y) dk, \\ RHS &= \sum_{n=-\infty}^{\infty} \int_{-\infty}^{\infty} e^{-ikx} e^{ikx} dx \int_0^w e^{-i\frac{2m\pi z}{w}} e^{i\frac{2\pi n z}{w}} dz \int_{-\infty}^{\infty} \hat{\varphi}_{1n}(k, y) dk, \\ RHS &= \sum_{n=-\infty}^{\infty} \int_{-\infty}^{\infty} e^{i(k-k')x} dx \int_0^w e^{i\frac{2\pi}{w}(n-m)z} dz \int_{-\infty}^{\infty} \hat{\varphi}_{1n}(k, y) dk. \end{aligned} \quad (\text{I.12})$$

We know that

$$\begin{aligned} \int_{-\infty}^{\infty} e^{i(k-k')x} dx &= 2\pi \delta(k - k'), \text{ and} \\ \int_0^w e^{i\frac{2\pi}{w}(n-m)z} dz &= w \delta_{nm}, \end{aligned}$$

therefore, Equation I.12 will be

$$RHS = 2\pi w \hat{\varphi}_{1m}(k'). \quad (\text{I.13})$$

The left-hand side of Equation I.9 becomes

$$\begin{aligned} LHS &= \int_{-\infty}^{\infty} e^{-ikx} dx \int_0^w e^{-i\frac{2m\pi z}{w}} dz \varphi_1(x, y, z). \\ LHS &= \int_{-\infty}^{\infty} e^{-ikx} dx \int_0^w e^{-i\frac{2m\pi z}{w}} dz \sum_{n=-\infty}^{\infty} e^{i\frac{2\pi n z}{w}} \varphi_{1n}(x, y), \end{aligned}$$

$$LHS = \sum_{n=-\infty}^{\infty} \int_{-\infty}^{\infty} e^{-ik'x} dx \int_0^w e^{-i\frac{2m\pi z}{w}} e^{i\frac{2\pi nz}{w}} dz \varphi_{1n}(x, y),$$

$$LHS = \sum_{n=-\infty}^{\infty} \int_{-\infty}^{\infty} e^{-ik'x} dx \int_0^w e^{i\frac{2\pi}{w}(n-m)z} dz \varphi_{1n}(x, y),$$

$$LHS = w \int_{-\infty}^{\infty} e^{-ik'x} dx \varphi_{1m}(x, y). \quad (I.14)$$

Recombining equations I.13 and I.14 gives

$$2\pi w \hat{\varphi}_{1m}(k') = w \int_{-\infty}^{\infty} e^{-ik'x} dx \varphi_{1m}(x, y),$$

$$\hat{\varphi}_{1m}(k') = \frac{1}{2\pi} \int_{-\infty}^{\infty} dx e^{-ik'x} \varphi_{1m}(x, y). \quad (I.15)$$

Can also apply Fourier analysis to the boundary condition of Equation I.4 after multiplying both sides by

$$\int_{-\infty}^{\infty} e^{-ikx} dx \int_0^w e^{-i\frac{2m\pi z}{w}} dz. \quad (I.16)$$

Therefore, the left-hand side becomes

$$LHS = \frac{\partial}{\partial y} \sum_{n=-\infty}^{\infty} \int_{-\infty}^{\infty} e^{-ikx} dx \int_0^w e^{-i\frac{2m\pi z}{w}} e^{i\frac{2\pi nz}{w}} \varphi_{1n}(x) \Big|_{y=0} dz,$$

$$LHS = \frac{\partial}{\partial y} \sum_{n=-\infty}^{\infty} \int_{-\infty}^{\infty} e^{-ikx} dx \int_0^w e^{i\frac{2\pi}{w}(n-m)z} dz \varphi_{1n}(x) \Big|_{y=0} dz,$$

$$LHS = \frac{\partial}{\partial y} w \int_{-\infty}^{\infty} e^{-ikx} dx \varphi_{1m}(x) \Big|_{y=0},$$

$$LHS = 2\pi w \frac{\partial \hat{\varphi}_{1m}}{\partial y} \Big|_{y=0}. \quad (I.17)$$

Assume

$$\Delta(x, z) = \sum_{n=-\infty}^{\infty} \Delta_n(x) e^{i \frac{2\pi n z}{w}}. \quad (\text{I.18})$$

The right hand side of Equation I.4 will be

$$\begin{aligned} RHS &= \int_{-\infty}^{\infty} e^{-ikx} dx \int_0^w e^{-i \frac{2m\pi z}{w}} dz \left(\frac{\partial}{\partial x} (\Delta \frac{\partial \phi_0}{\partial x}) \right)_{y=0}, \\ RHS &= \sum_{n=-\infty}^{\infty} \int_{-\infty}^{\infty} e^{-ikx} dx \int_0^w e^{-i \frac{2m\pi z}{w}} dz \left[\frac{\partial}{\partial x} (\Delta_n(x) e^{i \frac{2\pi n z}{w}} \frac{\partial \phi_0}{\partial x}) \right]_{y=0}, \\ RHS &= \sum_{n=-\infty}^{\infty} \int_{-\infty}^{\infty} e^{-ikx} dx \int_0^w e^{i \frac{2\pi}{w}(n-m)z} dz \left[\frac{\partial}{\partial x} (\Delta_n(x) \frac{\partial \phi_0}{\partial x}) \right]_{y=0}, \\ RHS &= w \int_{-\infty}^{\infty} dx e^{-ikx} \left[\frac{\partial}{\partial x} (\Delta_m(x) \frac{\partial \phi_0}{\partial x}) \right]_{y=0}, \end{aligned}$$

and integrating by parts

$$RHS = w i \int_{-\infty}^{\infty} dx k e^{-ikx} \Delta_m(x) \frac{\partial \phi_0}{\partial x} \Big|_{y=0}. \quad (\text{I.19})$$

Recombining equations I.17 and I.19 gives

$$\begin{aligned} 2\pi w \frac{\partial \hat{\phi}_{1m}}{\partial y} \Big|_{y=0} &= w i \int_{-\infty}^{\infty} dx k e^{-ikx} \Delta_m(x) \frac{\partial \phi_0}{\partial x} \Big|_{y=0}, \\ \frac{\partial \hat{\phi}_{1m}}{\partial y} \Big|_{y=0} &= \frac{i}{2\pi} \int_{-\infty}^{\infty} dx k e^{-ikx} \Delta_m(x) \frac{\partial \phi_0}{\partial x} \Big|_{y=0}. \end{aligned} \quad (\text{I.20})$$

Applying the Fourier transformation to the Laplace equation gives

$$\frac{\partial^2 \hat{\phi}_{1m}}{\partial y^2} - \left(k^2 + \frac{4m^2 \pi^2}{w^2} \right) \hat{\phi}_{1m} = 0 \quad (\text{I.21})$$

and calling $k_m^2 = k^2 + \frac{4m^2 \pi^2}{w^2}$, the Laplace equation can be expressed as

$$\frac{\partial^2 \hat{\phi}_{1m}}{\partial y^2} - k_m^2 \hat{\phi}_{1m} = 0. \quad (\text{I.22})$$

The boundary condition at the surface changes to

$$\left. \frac{\partial \hat{\phi}_{1m}}{\partial y} \right|_{y=a} = 0. \quad (\text{I.23})$$

The general solution to this equation is

$$\hat{\phi}_{1m}(k, y) = A_m \cosh k_m (y - a). \quad (\text{I.24})$$

Thus,

$$\begin{aligned} \frac{\partial \hat{\phi}_{1m}}{\partial y} &= k_m A_m \sinh k_m (y - a), \\ \left. \frac{\partial \hat{\phi}_{1m}}{\partial y} \right|_{y=0} &= -k_m A_m \sinh k_m a. \end{aligned} \quad (\text{I.25})$$

Substituting Equation I.25 into Equation I.20 determines the coefficient A_m . So,

$$\begin{aligned} -k_m A_m \sinh k_m a &= \frac{i}{2\pi} \int_{-\infty}^{\infty} dx k e^{-ikx} \Delta_m(x) \left. \frac{\partial \varphi_0}{\partial x} \right|_{y=0}, \\ A_m &= -\frac{i}{2\pi} \frac{1}{k_m \sinh k_m a} \int_{-\infty}^{\infty} dx k e^{-ikx} \Delta_m(x) \left. \frac{\partial \varphi_0}{\partial x} \right|_{y=0}. \end{aligned} \quad (\text{I.26})$$

Substituting this result into Equation I.24 produces

$$\hat{\phi}_{1m}(k, y) = -\frac{i}{2\pi} \frac{1}{k_m \sinh k_m a} \int_{-\infty}^{\infty} dx k e^{-ikx} \Delta_m(x) \left. \frac{\partial \varphi_0}{\partial x} \right|_{y=0} \cosh k_m (y - a). \quad (\text{I.27})$$

Finally, substituting this equation into Equation I.10 gives

$$\varphi_{1m}(x, y) = -\frac{i}{2\pi} \int_{-\infty}^{\infty} dk e^{ikx} \frac{1}{k_m \sinh k_m a} \int_{-\infty}^{\infty} dx' k e^{-ikx'} \Delta_m(x') \left. \frac{\partial \varphi_0}{\partial x'} \right|_{y=0} \cosh k_m (y - a),$$

$$\varphi_{1m}(x, y) = -\frac{i}{2\pi} \int_{-\infty}^{\infty} dk \int_{-\infty}^{\infty} dx' \frac{\cosh k_m (y-a)}{k_m \sinh k_m a} k e^{ik(x-x')} \Delta_m(x') \frac{\partial \varphi_0}{\partial x'} \Big|_{y=0},$$

$$\varphi_{1m}(x, y) = \frac{1}{2\pi} \int_{-\infty}^{\infty} dk \int_{-\infty}^{\infty} dx' \frac{\cosh k_m (y-a)}{k_m \sinh k_m a} k \sin k(x-x') \Delta_m(x') \frac{\partial \varphi_0}{\partial x'} \Big|_{y=0}. \quad (\text{I.28})$$

Evaluating this equation at $y = a$ gives

$$\varphi_{1m}(x) \Big|_{y=a} = \frac{1}{2\pi} \int_{-\infty}^{\infty} dk \int_{-\infty}^{\infty} dx' \frac{k \sin k(x-x')}{k_m \sinh k_m a} \Delta_m(x') \frac{\partial \varphi_0}{\partial x'} \Big|_{y=0},$$

which is the expression for Equation 4.81.

Now consider the equations:

$$\frac{\partial^2 \varphi_2}{\partial x^2} + \frac{\partial^2 \varphi_2}{\partial y^2} + \frac{\partial^2 \varphi_2}{\partial z^2} = 0,$$

$$\left[\frac{\partial \varphi_2}{\partial y} - \frac{\partial}{\partial x} \left(\Delta \frac{\partial \varphi_1}{\partial x} \right) - \frac{\partial}{\partial z} \left(\Delta \frac{\partial \varphi_1}{\partial z} \right) \right]_{y=0} = 0,$$

$$\frac{\partial \varphi_2}{\partial y} \Big|_{y=a} = 0. \quad (\text{I.29})$$

By definition,

$$\varphi_2(x, y, z) = \sum_{n=-\infty}^{\infty} e^{i \frac{2\pi n z}{w}} \varphi_{2n}(x, y), \quad (\text{I.30})$$

$$\varphi_2(x, y, z) = \sum_{n=-\infty}^{\infty} e^{i \frac{2\pi n z}{w}} \int_{-\infty}^{\infty} e^{ikx} \hat{\varphi}_{2n}(k, y) dk, \quad (\text{I.31})$$

$$\varphi_{2n}(x, y) = \int_{-\infty}^{\infty} dk e^{ikx} \hat{\varphi}_{2n}(k, y), \quad (\text{I.32})$$

where $\hat{\varphi}_{2n}(k, y)$ is the Fourier transform of $\varphi_{2n}(x, y)$.

A Fourier analysis of the boundary condition of Equation I.6 can be performed after multiplying both sides of the equation by

$$\int_{-\infty}^{\infty} e^{-ik'x} dx \int_0^w e^{-i\frac{2m\pi z}{w}} dz. \quad (\text{I.33})$$

Therefore, the left-hand side of Equation I.6 becomes

$$\begin{aligned} LHS &= \int_{-\infty}^{\infty} e^{-ik'x} dx \int_0^w e^{-i\frac{2m\pi z}{w}} dz \left. \frac{\partial \varphi_2}{\partial y} \right|_{y=0}, \\ LHS &= \frac{\partial}{\partial y} \sum_{n=-\infty}^{\infty} \int_{-\infty}^{\infty} e^{-ik'x} dx \int_0^w e^{-i\frac{2m\pi z}{w}} e^{i\frac{2\pi nz}{w}} \varphi_{2n}(x) \Big|_{y=0} dz, \\ LHS &= \frac{\partial}{\partial y} w \int_{-\infty}^{\infty} e^{-ik'x} dx \varphi_{2m}(x) \Big|_{y=0}, \\ LHS &= 2\pi w \left. \frac{\partial \hat{\varphi}_{2m}(k')}{\partial y} \right|_{y=0}. \end{aligned} \quad (\text{I.34})$$

The right hand side of Equation I.6 will be

$$RHS = \int_{-\infty}^{\infty} e^{-ik'x} dx \int_0^w e^{-i\frac{2m\pi z}{w}} dz \left[\frac{\partial}{\partial x} \left(\Delta \frac{\partial \varphi_1}{\partial x} \right) + \frac{\partial}{\partial z} \left(\Delta \frac{\partial \varphi_1}{\partial z} \right) \right]_{y=0}. \quad (\text{I.35})$$

Consider the first term of the equation above as

$$RHS_1 = \int_{-\infty}^{\infty} e^{-ik'x} dx \int_0^w e^{-i\frac{2m\pi z}{w}} dz \left[\frac{\partial}{\partial x} \left(\Delta \frac{\partial \varphi_1}{\partial x} \right) \right]_{y=0}. \quad (\text{I.36})$$

Assuming

$$\Delta(x, z) = \sum_{p=-\infty}^{\infty} \Delta_p(x) e^{i\frac{2\pi p z}{w}}$$

and replacing Equation I.8 in the Equation I.36 gives

$$RHS_1 = \sum_{p=-\infty}^{\infty} \sum_{n=-\infty}^{\infty} \int_{-\infty}^{\infty} e^{-ik'x} dx \int_0^w e^{-i\frac{2m\pi z}{w}} dz \left[\frac{\partial}{\partial x} \left(\Delta_p(x) e^{i\frac{2\pi pz}{w}} \frac{\partial}{\partial x} e^{i\frac{2\pi nz}{w}} \varphi_{1n}(x) \right) \right]_{y=0},$$

$$RHS_1 = \sum_{p=-\infty}^{\infty} \sum_{n=-\infty}^{\infty} \int_{-\infty}^{\infty} e^{-ik'x} dx \int_0^w dz \left[\frac{\partial}{\partial x} \left(\Delta_p(x) e^{i\frac{2\pi}{w}(p-m+n)z} \frac{\partial}{\partial x} \varphi_{1n}(x) \right) \right]_{y=0},$$

$$RHS_1 = w \sum_{n=-\infty}^{\infty} \int_{-\infty}^{\infty} dx e^{-ik'x} \left[\frac{\partial}{\partial x} \left(\Delta_{m-n}(x) \frac{\partial}{\partial x} \varphi_{1n}(x) \right) \right]_{y=0}, \text{ and}$$

integrating by parts results in

$$RHS_1 = w i \sum_{n=-\infty}^{\infty} \int_{-\infty}^{\infty} dx k' e^{-ik'x} \Delta_{m-n}(x) \frac{\partial \varphi_{1n}}{\partial x} \Big|_{y=0}. \quad (I.37)$$

Now consider the second term of Equation I.35 as

$$RHS_2 = \int_{-\infty}^{\infty} e^{-ik'x} dx \int_0^w e^{-i\frac{2m\pi z}{w}} dz \left[\frac{\partial}{\partial z} \left(\Delta \frac{\partial \varphi_1}{\partial z} \right) \right]_{y=0}. \quad (I.38)$$

Using the same approach as was done before gives

$$RHS_2 = \sum_{p=-\infty}^{\infty} \sum_{n=-\infty}^{\infty} \int_{-\infty}^{\infty} e^{-ik'x} dx \int_0^w e^{-i\frac{2m\pi z}{w}} dz \left[\frac{\partial}{\partial z} \left(\Delta_p(x) e^{i\frac{2\pi pz}{w}} \frac{\partial}{\partial z} e^{i\frac{2\pi nz}{w}} \varphi_{1n}(x) \right) \right]_{y=0},$$

$$RHS_2 = \sum_{p=-\infty}^{\infty} \sum_{n=-\infty}^{\infty} \int_{-\infty}^{\infty} e^{-ik'x} dx \int_0^w e^{-i\frac{2m\pi z}{w}} dz \varphi_{1n}(x) \Big|_{y=0} \Delta_p(x) \frac{\partial}{\partial z} \left[e^{i\frac{2\pi pz}{w}} \frac{\partial}{\partial z} e^{i\frac{2\pi nz}{w}} \right],$$

$$RHS_2 = \sum_{p=-\infty}^{\infty} \sum_{n=-\infty}^{\infty} \int_{-\infty}^{\infty} e^{-ik'x} dx \int_0^w e^{-i\frac{2m\pi z}{w}} dz \varphi_{1n}(x) \Big|_{y=0} \Delta_p(x) \frac{\partial}{\partial z} \left[e^{i\frac{2\pi pz}{w}} \frac{2\pi ni}{w} e^{i\frac{2\pi nz}{w}} \right],$$

$$RHS_2 = \sum_{p=-\infty}^{\infty} \sum_{n=-\infty}^{\infty} \int_{-\infty}^{\infty} e^{-ik'x} dx \int_0^w e^{-i\frac{2m\pi z}{w}} dz \varphi_{1n}(x) \Big|_{y=0} \Delta_p(x) \frac{2\pi ni}{w} \frac{\partial}{\partial z} \left[e^{i\frac{2\pi}{w}(p+n)z} \right],$$

$$RHS_2 = \sum_{p=-\infty}^{\infty} \sum_{n=-\infty}^{\infty} \int_{-\infty}^{\infty} e^{-ik'x} dx \int_0^w e^{-i\frac{2m\pi z}{w}} dz \varphi_{1n}(x) \Big|_{y=0} \Delta_p(x) \frac{2\pi ni}{w} \frac{2\pi (n+p)i}{w} e^{i\frac{2\pi}{w}(p+n)z},$$

$$RHS_2 = \sum_{p=-\infty}^{\infty} \sum_{n=-\infty}^{\infty} \int_{-\infty}^{\infty} e^{-ik'x} dx \int_0^w dz \varphi_{1n}(x)|_{y=0} \Delta_p(x) \frac{2\pi ni}{w} \frac{2\pi(n+p)i}{w} e^{i\frac{2\pi}{w}(p+n-m)z},$$

$$RHS_2 = -w \sum_{n=-\infty}^{\infty} \frac{2\pi n}{w} \frac{2\pi m}{w} \int_{-\infty}^{\infty} dx e^{-ik'x} \Delta_{m-n}(x) \varphi_{1n}(x)|_{y=0}. \quad (I.39)$$

Adding equations I.37 and I.39 gives

$$RHS = w i \sum_{n=-\infty}^{\infty} \int_{-\infty}^{\infty} dx k' e^{-ik'x} \Delta_{m-n}(x) \frac{\partial \varphi_{1n}}{\partial x} \Big|_{y=0} - w \sum_{n=-\infty}^{\infty} \frac{2\pi n}{w} \frac{2\pi m}{w} \int_{-\infty}^{\infty} dx e^{-ik'x} \Delta_{m-n}(x) \varphi_{1n}(x)|_{y=0},$$

$$RHS = w \sum_{n=-\infty}^{\infty} \left[\int_{-\infty}^{\infty} dx ik' e^{-ik'x} \Delta_{m-n}(x) \frac{\partial \varphi_{1n}}{\partial x} \Big|_{y=0} - \frac{2\pi m}{w} \frac{2\pi n}{w} \int_{-\infty}^{\infty} dx e^{-ik'x} \Delta_{m-n}(x) \varphi_{1n}(x)|_{y=0} \right],$$

$$RHS = w \int_{-\infty}^{\infty} dx e^{-ik'x} \sum_{n=-\infty}^{\infty} \left[ik' \Delta_{m-n}(x) \frac{\partial \varphi_{1n}}{\partial x} \Big|_{y=0} - \frac{2\pi m}{w} \frac{2\pi n}{w} \Delta_{m-n}(x) \varphi_{1n}(x)|_{y=0} \right]. \quad (I.40)$$

Equating equations I.34 and I.40 produces

$$2\pi w \frac{\partial \hat{\varphi}_{2m}}{\partial y} \Big|_{y=0} = w \int_{-\infty}^{\infty} dx e^{-ik'x} \sum_{n=-\infty}^{\infty} \left[ik' \Delta_{m-n}(x) \frac{\partial \varphi_{1n}}{\partial x} \Big|_{y=0} - \frac{2\pi m}{w} \frac{2\pi n}{w} \Delta_{m-n}(x) \varphi_{1n}(x)|_{y=0} \right],$$

$$\frac{\partial \hat{\varphi}_{2m}}{\partial y} \Big|_{y=0} = \frac{1}{2\pi} \int_{-\infty}^{\infty} dx e^{-ik'x} \sum_{n=-\infty}^{\infty} \left[ik' \Delta_{m-n}(x) \frac{\partial \varphi_{1n}}{\partial x} \Big|_{y=0} - \frac{2\pi m}{w} \frac{2\pi n}{w} \Delta_{m-n}(x) \varphi_{1n}(x)|_{y=0} \right]. \quad (I.41)$$

Analogous to Equation I.22 the Laplace equation will be

$$\frac{\partial^2 \hat{\varphi}_{2m}}{\partial y^2} - k_m^2 \hat{\varphi}_{2m} = 0. \quad (I.42)$$

The boundary condition at the surface changes to

$$\frac{\partial \hat{\varphi}_{2m}}{\partial y} \Big|_{y=a} = 0. \quad (I.43)$$

The general solution to this equation is

$$\hat{\varphi}_{2m}(k, y) = B_m \cosh k_m (y - a). \quad (I.44)$$

Thus,

$$\frac{\partial \hat{\phi}_{2m}}{\partial y} = k_m B_m \sinh k_m (y - a),$$

$$\left. \frac{\partial \hat{\phi}_{2m}}{\partial y} \right|_{y=0} = -k_m B_m \sinh k_m a. \quad (\text{I.45})$$

Equating equations I.45 and I.41 gives the coefficient B_m . So,

$$-k_m B_m \sinh k_m a = \frac{1}{2\pi} \int_{-\infty}^{\infty} dx e^{-ikx} \sum_{n=-\infty}^{\infty} \left[ik \Delta_{m-n}(x) \frac{\partial \varphi_{1n}}{\partial x} \Big|_{y=0} - \frac{2\pi m}{w} \frac{2\pi n}{w} \Delta_{m-n}(x) \varphi_{1n}(x) \Big|_{y=0} \right],$$

$$B_m = -\frac{1}{2\pi k_m \sinh k_m a} \int_{-\infty}^{\infty} dx e^{-ikx} \sum_{n=-\infty}^{\infty} \left[ik \Delta_{m-n}(x) \frac{\partial \varphi_{1n}}{\partial x} \Big|_{y=0} - \frac{2\pi m}{w} \frac{2\pi n}{w} \Delta_{m-n}(x) \varphi_{1n}(x) \Big|_{y=0} \right], \text{ or}$$

switching k by k gives

$$B_m = -\frac{1}{2\pi k_m \sinh k_m a} \int_{-\infty}^{\infty} dx e^{-ikx} \sum_{n=-\infty}^{\infty} \left[ik \Delta_{m-n}(x) \frac{\partial \varphi_{1n}}{\partial x} \Big|_{y=0} - \frac{2\pi m}{w} \frac{2\pi n}{w} \Delta_{m-n}(x) \varphi_{1n}(x) \Big|_{y=0} \right].$$

Substituting this result into Equation I.44 we have

$$\hat{\phi}_{2m} = -\frac{1}{2\pi k_m \sinh k_m a} \int_{-\infty}^{\infty} dx e^{-ikx} \sum_{n=-\infty}^{\infty} \left[ik \Delta_{m-n}(x) \frac{\partial \varphi_{1n}}{\partial x} \Big|_{y=0} - \frac{2\pi m}{w} \frac{2\pi n}{w} \Delta_{m-n}(x) \varphi_{1n}(x) \Big|_{y=0} \right] \cosh k_m (y - a).$$

Finally, substituting this equation into Equation I.32 results in

$$\varphi_{2m} = -\frac{1}{2\pi} \int_{-\infty}^{\infty} dk e^{ikx} \frac{\cosh k_m (y - a)}{k_m \sinh k_m a} \int_{-\infty}^{\infty} dx' e^{-ikx'} \sum_{n=-\infty}^{\infty} \left[ik \Delta_{m-n}(x') \frac{\partial \varphi_{1n}}{\partial x'} \Big|_0 - \left(\frac{2\pi}{w}\right)^2 mn \Delta_{m-n}(x') \varphi_{1n}(x') \Big|_0 \right]$$

$$\varphi_{2m} = -\frac{1}{2\pi} \int_{-\infty}^{\infty} dk \int_{-\infty}^{\infty} dx' e^{ik(x-x')} \frac{\cosh k_m (y - a)}{k_m \sinh k_m a} \sum_{n=-\infty}^{\infty} \left[ik \Delta_{m-n}(x') \frac{\partial \varphi_{1n}}{\partial x'} \Big|_0 - \left(\frac{2\pi}{w}\right)^2 mn \Delta_{m-n}(x') \varphi_{1n}(x') \Big|_0 \right]$$

$$\varphi_{2m} = \frac{1}{2\pi} \int_{-\infty}^{\infty} dk \int_{-\infty}^{\infty} dx' \frac{\cosh k_m (y - a)}{k_m \sinh k_m a} \sum_{n=-\infty}^{\infty} \left[k \sin k(x-x') \Delta_{m-n} \frac{\partial \varphi_{1n}}{\partial x'} \Big|_0 + \left(\frac{2\pi}{w}\right)^2 mn \cos k(x-x') \Delta_{m-n} \varphi_{1n} \Big|_0 \right]$$

Evaluating the expression above at $y = a$ gives

$$\varphi_{2m}(x)|_{y=a} = \frac{1}{2\pi} \sum_{n=-\infty}^{\infty} \int_{-\infty}^{\infty} dk \int_{-\infty}^{\infty} dx' \frac{\Delta_{m-n}(x')}{k_m \sinh k_m a} \left[k \sin k(x-x') \frac{\partial \varphi_{1n}}{\partial x'} + \left(\frac{2\pi}{w}\right)^2 m n \cos k(x-x') \varphi_{1n} \right]_{y=0},$$

which is the expression for Equation 4.82.

APPENDIX J

This appendix shows how equations 4.81 and 4.82 can be written in a more convenient form. Consider Equation 4.81:

$$\varphi_{1m}(x)|_{y=a} = \frac{1}{2\pi} \int_{-\infty}^{\infty} dk \int_{-\infty}^{\infty} dx' \frac{k \sin k(x-x')}{k_m \sinh k_m a} \Delta_m(x') \frac{\partial \varphi_0}{\partial x'} \Big|_{y=0}, \quad (\text{J.1})$$

where $k_m^2 = k^2 + \frac{4m^2 \pi^2}{w^2}$.

Consider

$$T_{1m}(x, x') = \frac{1}{2\pi} \int_{-\infty}^{\infty} dk \frac{k \sin k(x-x')}{k_m \sinh k_m a}. \quad (\text{J.2})$$

So,

$$\varphi_{1m}(x)|_{y=a} = \int_{-\infty}^{\infty} dx' \Delta_m(x') \frac{\partial \varphi_0}{\partial x'} \Big|_{y=0} T_{1m}(x, x'). \quad (\text{J.3})$$

Equation J.2 can be written, for $m \neq 0$, as

$$T_{1m}(x, x') = \frac{1}{\pi} \int_0^{\infty} dk \frac{k \sin k(x-x')}{k_m \sinh k_m a}. \quad (\text{J.4})$$

In addition, for $m = 0$ Equation J.2 can be evaluated as

$$T_{10}(x, x') = \frac{1}{2\pi} \int_{-\infty}^{\infty} dk \frac{\sin k(x-x')}{\sinh ka},$$

$$T_{10}(x, x') = \frac{1}{\pi} \int_0^{\infty} dk \frac{\sin k(x-x')}{\sinh ka}.$$

It can be seen from tables (Gradshteyn and Ryzhik, 1994) that

$$\int_0^{\infty} \frac{\sin ax}{\sinh bx} dx = \frac{\pi}{2b} \tanh \frac{\pi a}{2b},$$

therefore,

$$T_{10}(x, x') = \frac{1}{\pi} \frac{\pi}{2a} \tanh \frac{\pi(x-x')}{2a},$$

$$T_{10}(x, x') = \frac{1}{2a} \tanh \frac{\pi(x-x')}{2a}. \quad (\text{J.5})$$

Equations J.3 through J.5 represent an alternative form of expressing Equation 4.81.

Now recall Equation 4.82:

$$\varphi_{2m}(x)|_{y=a} = \frac{1}{2\pi} \sum_{n=-\infty}^{\infty} \int_{-\infty}^{\infty} dk \int_{-\infty}^{\infty} dx' \frac{\Delta_{m-n}(x')}{k_m \sinh k_m a} \left[k \sin k(x-x') \frac{\partial \varphi_{1n}}{\partial x'} + \left(\frac{2\pi}{w}\right)^2 m n \cos k(x-x') \varphi_{1n} \right]_{y=0}.$$

Consider the terms that appear in this equation. Assume

$$S_{2n} = \frac{2\pi n}{w} \varphi_{1n}|_{y=0}. \quad (\text{J.6})$$

Thus,

$$\varphi_{2m}(x)|_{y=a} = \frac{1}{2\pi} \sum_{n=-\infty}^{\infty} \int_{-\infty}^{\infty} dk \int_{-\infty}^{\infty} dx' \frac{\Delta_{m-n}(x')}{k_m \sinh k_m a} \left[k \sin k(x-x') \frac{\partial \varphi_{1n}}{\partial x'} \Big|_0 + \left(\frac{2\pi}{w}\right) m \cos k(x-x') S_{2n} \right]. \quad (\text{J.7})$$

From Equation I.28

$$\varphi_{1n}(x, y) = \frac{1}{2\pi} \int_{-\infty}^{\infty} dk \int_{-\infty}^{\infty} dx' \frac{\cosh k_n(y-a)}{k_n \sinh k_n a} k \sin k(x-x') \Delta_n(x') \frac{\partial \varphi_0}{\partial x'} \Big|_{y=0}, \quad (\text{J.8})$$

thus,

$$\varphi_{1n}(x)|_{y=0} = \frac{1}{2\pi} \int_{-\infty}^{\infty} dk \int_{-\infty}^{\infty} dx' \frac{\cosh k_n a}{k_n \sinh k_n a} k \sin k(x-x') \Delta_n(x') \frac{\partial \varphi_0}{\partial x'} \Big|_{y=0}. \quad (\text{J.9})$$

Substituting Equation J.9 into Equation J.6 results in

$$S_{2n} = \frac{2\pi n}{w} \frac{1}{2\pi} \int_{-\infty}^{\infty} dk' \int_{-\infty}^{\infty} dx'' \frac{\cosh k'_n a}{k'_n \sinh k'_n a} k' \sin k'(x' - x'') \Delta_n(x'') \left. \frac{\partial \varphi_0}{\partial x''} \right|_{y=0}. \quad (\text{J.10})$$

So, if $n = 0$ then $S_{2n} = 0$.

Observe that

$$\begin{aligned} k' \sin k'(x' - x'') \Delta_n(x'') \left. \frac{\partial \varphi_0}{\partial x''} \right|_{y=0} &= \Delta_n(x'') \left. \frac{\partial \varphi_0}{\partial x''} \right|_{y=0} \frac{\partial}{\partial x''} \cos k'(x' - x''), \\ k' \sin k'(x' - x'') \Delta_n(x'') \left. \frac{\partial \varphi_0}{\partial x''} \right|_{y=0} &= \frac{\partial}{\partial x''} \left[\Delta_n(x'') \left. \frac{\partial \varphi_0}{\partial x''} \right|_{y=0} \cos k'(x' - x'') \right] - \\ &\quad \cos k'(x' - x'') \left[\frac{\partial}{\partial x''} \Delta_n(x'') \left. \frac{\partial \varphi_0}{\partial x''} \right|_{y=0} \right] \end{aligned} \quad (\text{J.11})$$

Substituting this result into Equation J.10 gives

$$S_{2n} = -\frac{n}{w} \int_{-\infty}^{\infty} dk' \int_{-\infty}^{\infty} dx'' \frac{\cosh k'_n a}{k'_n \sinh k'_n a} \cos k'(x' - x'') \left[\frac{\partial}{\partial x''} \Delta_n(x'') \left. \frac{\partial \varphi_0}{\partial x''} \right|_{y=0} \right]. \quad (\text{J.12})$$

Observing that

$$\cosh k'_n a = \cosh k'_n a - \sinh k'_n a + \sinh k'_n a = e^{-k'_n a} + \sinh k'_n a,$$

and that the integral above is even in k' , Equation J.12 may be rewritten as

$$S_{2n} = -\frac{2n}{w} \int_0^{\infty} dk' \int_{-\infty}^{\infty} dx'' \left[\frac{\partial}{\partial x''} \Delta_n(x'') \left. \frac{\partial \varphi_0}{\partial x''} \right|_{y=0} \right] \left[\frac{e^{-k'_n a} \cos k'(x' - x'')}{k'_n \sinh k'_n a} + \frac{\cos k'(x' - x'')}{k'_n} \right]. \quad (\text{J.13})$$

It can be seen from tables (Gradshteyn and Ryzhik, 1994) that

$$\int_0^{\infty} \frac{\cos ax}{\sqrt{x^2 + b^2}} dx = K_0(ab),$$

therefore, in Equation J.13

$$\int_0^{\infty} dk \frac{\cos k'(x' - x'')}{k_n'} = \int_0^{\infty} dk \frac{\cos k'(x' - x'')}{\sqrt{k'^2 + \left(\frac{2n\pi}{w}\right)^2}} = K_0 \left[\frac{2\pi(x' - x'')n}{w} \right]. \quad (\text{J.14})$$

Using the result above in Equation J.13 for $n \neq 0$ gives

$$S_{2n} = -\frac{2n}{w} \int_{-\infty}^{\infty} dx'' \left[\frac{\partial}{\partial x''} \Delta_n(x'') \frac{\partial \varphi_0}{\partial x''} \Big|_{y=0} \right] \left[K_0 \left(\frac{2\pi(x' - x'')n}{w} \right) \right] + \int_0^{\infty} dk \frac{e^{-k_n a} \cos k'(x' - x'')}{k_n' \sinh k_n' a}. \quad (\text{J.15})$$

Consider the second term of Equation J.7, represented by $\varphi_{2m}^{(2)}(x) \Big|_{y=a}$. Thus,

$$\varphi_{2m}^{(2)}(x) \Big|_{y=a} = \frac{1}{2\pi} \sum_{n=-\infty}^{\infty} \int_{-\infty}^{\infty} dk \int_{-\infty}^{\infty} dx' \frac{\Delta_{m-n}(x')}{k_m \sinh k_m a} \left(\frac{2\pi}{w} \right) m \cos k(x - x') S_{2n}. \quad (\text{J.16})$$

Substituting Equation J.15 into Equation J.16 results in

$$\varphi_{2m}^{(2)}(x) \Big|_{y=a} = -\frac{4}{w^2} \sum_{n=-\infty}^{\infty} \int_0^{\infty} dk \int_{-\infty}^{\infty} dx'' \int_{-\infty}^{\infty} dx' mn \frac{\Delta_{m-n}(x')}{k_m \sinh k_m a} \left[G_n \frac{\partial}{\partial x''} \Delta_n(x'') \frac{\partial \varphi_0}{\partial x''} \Big|_{y=0} \right] \cos k(x - x'), \quad (\text{J.17})$$

where

$$G_n(x', x'') = K_0 \left(\frac{2\pi(x' - x'')n}{w} \right) + \int_0^{\infty} dk \frac{e^{-k_n a} \cos k'(x' - x'')}{k_n' \sinh k_n' a}. \quad (\text{J.18})$$

Calling

$$C_m(x, x') = \frac{2\pi m}{w} \int_0^{\infty} dk \frac{\cos k(x - x')}{k_m \sinh k_m a} \quad (\text{J.19})$$

Equation J.17 can be rewritten as

$$\varphi_{2m}^{(2)}(x) \Big|_{y=a} = -\frac{1}{\pi^2} \sum_{n=-\infty}^{\infty} \int_{-\infty}^{\infty} dx' \int_{-\infty}^{\infty} dx'' \Delta_{m-n}(x') G_n \frac{2\pi n}{w} C_m \left[\frac{\partial}{\partial x''} \Delta_n(x'') \frac{\partial \varphi_0}{\partial x''} \Big|_{y=0} \right]. \quad (\text{J.20})$$

Recall Equation J.8:

$$\varphi_{1n}(x, y) = \frac{1}{2\pi} \int_{-\infty}^{\infty} dk \int_{-\infty}^{\infty} dx' \frac{\cosh k_n(y-a)}{k_n \sinh k_n a} k \sin k(x-x') \Delta_n(x') \frac{\partial \varphi_0}{\partial x'} \Big|_{y=0},$$

thus

$$\frac{\partial \varphi_{1n}}{\partial x} = \frac{1}{2\pi} \int_{-\infty}^{\infty} dk \int_{-\infty}^{\infty} dx' \frac{\cosh k_n(y-a)}{k_n \sinh k_n a} k^2 \cos k(x-x') \Delta_n(x') \frac{\partial \varphi_0}{\partial x'} \Big|_{y=0}. \quad (\text{J.21})$$

Evaluating the equation above at $y = 0$ gives

$$\frac{\partial \varphi_{1n}}{\partial x} \Big|_{y=0} = \frac{1}{2\pi} \int_{-\infty}^{\infty} dk \int_{-\infty}^{\infty} dx' \frac{\cosh k_n a}{k_n \sinh k_n a} k^2 \cos k(x-x') \Delta_n(x') \frac{\partial \varphi_0}{\partial x'} \Big|_{y=0}. \quad (\text{J.22})$$

Consider $n = 0$. In this case,

$$\frac{\partial \varphi_{10}}{\partial x} \Big|_{y=0} = \frac{1}{2\pi} \int_{-\infty}^{\infty} dk \int_{-\infty}^{\infty} dx' \frac{\cosh ka}{\sinh ka} k \cos k(x-x') \Delta_0(x') \frac{\partial \varphi_0}{\partial x'} \Big|_{y=0}. \quad (\text{J.23})$$

Observe that the integrand of Equation J.23 will be

$$I1 = k \coth ka \cos k(x-x') \Delta_0(x') \frac{\partial \varphi_0}{\partial x'} \Big|_{y=0},$$

$$I1 = \coth ka \left[-\frac{\partial}{\partial x'} (\sin k(x-x') \Delta_0(x') \frac{\partial \varphi_0}{\partial x'} \Big|_{y=0}) + \sin k(x-x') \frac{\partial}{\partial x'} \Delta_0(x') \frac{\partial \varphi_0}{\partial x'} \Big|_{y=0} \right].$$

Substituting this result into Equation J.23 gives

$$\frac{\partial \varphi_{10}}{\partial x} \Big|_{y=0} = \frac{1}{2\pi} \int_{-\infty}^{\infty} dk \int_{-\infty}^{\infty} dx' \coth ka \sin k(x-x') \frac{\partial}{\partial x'} \Delta_0(x') \frac{\partial \varphi_0}{\partial x'} \Big|_{y=0}. \quad (\text{J.24})$$

The new integrand can be rewritten as

$$I2 = \coth ka \sin k(x-x') \frac{\partial}{\partial x'} \Delta_0(x') \frac{\partial \varphi_0}{\partial x'} \Big|_{y=0},$$

$$I2 = \coth ka \left\{ \frac{1}{k} \frac{\partial}{\partial x} [(\cos k(x-x') - \cos kx) \frac{\partial}{\partial x} \Delta_0(x') \frac{\partial \varphi_0}{\partial x'} \Big|_{y=0}] - \left[\frac{\cos k(x-x') - \cos kx}{k} \right] \frac{\partial^2}{\partial x'^2} \Delta_0(x') \frac{\partial \varphi_0}{\partial x'} \Big|_{y=0} \right\}$$

Entering this result into Equation J.24 gives

$$\begin{aligned} \frac{\partial \varphi_{10}}{\partial x} \Big|_{y=0} &= -\frac{1}{2\pi} \int_{-\infty}^{\infty} dk \int_{-\infty}^{\infty} dx' \coth ka \left[\frac{\cos k(x-x') - \cos kx}{k} \right] \frac{\partial^2}{\partial x'^2} \Delta_0(x') \frac{\partial \varphi_0}{\partial x'} \Big|_{y=0}, \\ \frac{\partial \varphi_{10}}{\partial x} \Big|_{y=0} &= \frac{1}{2\pi} \int_0^{\infty} dk \int_{-\infty}^{\infty} dx' \coth ka \left[\frac{\cos kx - \cos k(x-x')}{k} \right] \frac{\partial^2}{\partial x'^2} \Delta_0(x') \frac{\partial \varphi_0}{\partial x'} \Big|_{y=0}. \end{aligned} \quad (J.25)$$

Now consider the integral

$$F = \int_0^{\infty} dk \frac{\cos kx - \cos k(x-x')}{k} \coth ka.$$

Recalling that

$$\cos kx - \cos k(x-x') = -2 \sin^2 \frac{kx}{2} + 2 \sin^2 \frac{k(x-x')}{2}$$

gives

$$F = 2 \int_0^{\infty} dk \left[\sin^2 \frac{k(x-x')}{2} - \sin^2 \frac{kx}{2} \right] \frac{\coth ka}{k}.$$

Let $\xi = ka$. Thus,

$$F = 2 \int_0^{\infty} d\xi \left[\sin^2 \frac{\xi(x-x')}{2a} - \sin^2 \frac{\xi x}{2a} \right] \frac{\coth \xi}{\xi}.$$

It can be seen from tables (Gradshteyn and Ryzhik, 1994) that

$$\int_0^{\infty} \sin^2 ax \frac{\cosh bx}{\sinh x} \frac{dx}{x} = \frac{1}{4} \ln \frac{\cosh 2\pi a + \cos b\pi}{1 + \cos b\pi}$$

therefore,

$$F = \frac{1}{2} \left[\ln \frac{\cosh \frac{\pi(x-x')}{a} + \cos \pi}{1 + \cos \pi} - \ln \frac{\cosh \frac{\pi x}{a} + \cos \pi}{1 + \cos \pi} \right],$$

$$F = \frac{1}{2} \ln \frac{\cosh \frac{\pi(x-x')}{a} - 1}{\cosh \frac{\pi x}{a} - 1},$$

$$F = \frac{1}{2} \ln \left(\frac{\sinh \frac{\pi(x-x')}{2a}}{\sinh \frac{\pi x}{2a}} \right)^2. \quad (\text{J.26})$$

Substituting this result into Equation J.25 results in

$$\frac{\partial \varphi_{10}}{\partial x} \Big|_{y=0} = \frac{1}{4\pi} \int_{-\infty}^{\infty} dx' \frac{\partial^2}{\partial x'^2} \Delta_0(x') \frac{\partial \varphi_0}{\partial x'} \Big|_{y=0} \ln \left(\frac{\sinh \frac{\pi(x-x')}{2a}}{\sinh \frac{\pi x'}{2a}} \right)^2$$

$$\frac{\partial \varphi_{10}}{\partial x} \Big|_{y=0} = \frac{1}{4\pi} \int_{-\infty}^{\infty} dx' \frac{\partial^2}{\partial x'^2} \Delta_0(x') \frac{\partial \varphi_0}{\partial x'} \Big|_{y=0} \ln \left(\sinh \frac{\pi(x-x')}{2a} \right)^2. \quad (\text{J.27})$$

Consider $n \neq 0$ in Equation J.22. The integrand of this equation can be written as

$$I3 = \frac{\cosh k_n a}{k_n \sinh k_n a} k^2 \cos k(x-x') \Delta_n(x') \frac{\partial \varphi_0}{\partial x'} \Big|_{y=0},$$

$$I3 = \frac{\coth k_n a}{k_n} k^2 \cos k(x-x') \Delta_n(x') \frac{\partial \varphi_0}{\partial x'} \Big|_{y=0},$$

$$I3 = \frac{\coth k_n a}{k_n} \left\{ -\frac{\partial}{\partial x'} \left[k \sin k(x-x') \Delta_n(x') \frac{\partial \varphi_0}{\partial x'} \Big|_{y=0} \right] + k \sin k(x-x') \frac{\partial}{\partial x'} \Delta_n(x') \frac{\partial \varphi_0}{\partial x'} \Big|_{y=0} \right\}$$

Entering this result into Equation J.22 gives

$$\left. \frac{\partial \varphi_{1n}}{\partial x} \right|_{y=0} = \frac{1}{2\pi} \int_{-\infty}^{\infty} dk \int_{-\infty}^{\infty} dx' \frac{\coth k_n a}{k_n} k \sin k(x-x') \frac{\partial}{\partial x'} \Delta_n(x') \left. \frac{\partial \varphi_0}{\partial x'} \right|_{y=0}. \quad (\text{J.28})$$

This new integrand can be written as

$$I4 = \frac{\coth k_n a}{k_n} k \sin k(x-x') \frac{\partial}{\partial x'} \Delta_n(x') \left. \frac{\partial \varphi_0}{\partial x'} \right|_{y=0},$$

$$I4 = \frac{\coth k_n a}{k_n} \left\{ \frac{\partial}{\partial x'} \left[\cos k(x-x') \frac{\partial}{\partial x'} \Delta_n(x') \left. \frac{\partial \varphi_0}{\partial x'} \right|_{y=0} \right] - \cos k(x-x') \frac{\partial^2}{\partial x'^2} \Delta_n(x') \left. \frac{\partial \varphi_0}{\partial x'} \right|_{y=0} \right\}.$$

Substituting this result into Equation J.28 produces

$$\left. \frac{\partial \varphi_{1n}}{\partial x} \right|_{y=0} = -\frac{1}{2\pi} \int_{-\infty}^{\infty} dk \int_{-\infty}^{\infty} dx' \frac{\coth k_n a}{k_n} \cos k(x-x') \frac{\partial^2}{\partial x'^2} \Delta_n(x') \left. \frac{\partial \varphi_0}{\partial x'} \right|_{y=0},$$

but

$$\frac{\coth k_n a}{k_n} \cos k(x-x') = \frac{\cos k(x-x')}{k_n} \left[\frac{e^{-k_n a} + \sinh k_n a}{\sinh k_n a} \right],$$

$$\frac{\coth k_n a}{k_n} \cos k(x-x') = \frac{\cos k(x-x')}{k_n} + \frac{\cos k(x-x')}{k_n} \left[\frac{e^{-k_n a}}{\sinh k_n a} \right].$$

Thus,

$$\left. \frac{\partial \varphi_{1n}}{\partial x} \right|_{y=0} = -\frac{1}{\pi} \int_{-\infty}^{\infty} dx' \int_0^{\infty} dk \left[\frac{\cos k(x-x')}{k_n} + \frac{\cos k(x-x')}{k_n} \frac{e^{-k_n a}}{\sinh k_n a} \right] \frac{\partial^2}{\partial x'^2} \Delta_n(x') \left. \frac{\partial \varphi_0}{\partial x'} \right|_{y=0}. \quad (\text{J.29})$$

From the result of Equation J.14

$$\left. \frac{\partial \varphi_{1n}}{\partial x} \right|_{y=0} = -\frac{1}{\pi} \int_{-\infty}^{\infty} dx' \frac{\partial^2}{\partial x'^2} \Delta_n(x') \left. \frac{\partial \varphi_0}{\partial x'} \right|_{y=0} \left[K_0 \left(\left| \frac{2\pi(x'-x'')n}{w} \right| \right) + \int_0^{\infty} dk \frac{\cos k(x-x')}{k_n} \frac{e^{-k_n a}}{\sinh k_n a} \right],$$

$$\left. \frac{\partial \varphi_{1n}}{\partial x} \right|_{y=0} = -\frac{1}{\pi} \int_{-\infty}^{\infty} dx' \frac{\partial^2}{\partial x'^2} \Delta_n(x') \left. \frac{\partial \varphi_0}{\partial x'} \right|_{y=0} G_n(x, x'). \quad (\text{J.30})$$

Consider the first term of Equation J.7, represented by $\varphi_{2m}^{(1)}(x)|_{y=a}$. Thus,

$$\varphi_{2m}^{(1)}(x)|_{y=a} = \frac{1}{2\pi} \sum_{n=-\infty}^{\infty} \int_{-\infty}^{\infty} dk \int_{-\infty}^{\infty} dx' \frac{\Delta_{m-n}(x')}{k_m \sinh k_m a} \left[k \sin k(x-x') \frac{\partial \varphi_{1n}}{\partial x'} \Big|_{y=0} \right]. \quad (\text{J.31})$$

Entering Equation J.30 into equation above results in

$$\begin{aligned} \varphi_{2m}^{(1)}(x)|_{y=a} &= -\frac{1}{2\pi^2} \sum_{n=-\infty}^{\infty} \int_{-\infty}^{\infty} dk \int_{-\infty}^{\infty} dx' \frac{\Delta_{m-n}(x')}{k_m \sinh k_m a} \left[k \sin k(x-x') \int_{-\infty}^{\infty} dx'' \frac{\partial^2}{\partial x''^2} \Delta_n(x'') \frac{\partial \varphi_0}{\partial x''} \Big|_{y=0} G_n(x', x'') \right] \\ \varphi_{2m}^{(1)}(x)|_{y=a} &= -\frac{1}{\pi^2} \sum_{n=-\infty}^{\infty} \int_{-\infty}^{\infty} dx' \int_{-\infty}^{\infty} dx'' \int_0^{\infty} dk \frac{\Delta_{m-n}(x')}{k_m \sinh k_m a} k \sin k(x-x') \frac{\partial^2}{\partial x''^2} \Delta_n(x'') \frac{\partial \varphi_0}{\partial x''} \Big|_{y=0} G_n(x', x'') \quad (\text{J.32}) \end{aligned}$$

Calling

$$S_m(x, x') = \int_0^{\infty} dk \frac{k \sin k(x-x')}{k_m \sinh k_m a}, \quad (\text{J.33})$$

the Equation J.32 can be rewritten as

$$\varphi_{2m}^{(1)}(x)|_{y=a} = -\frac{1}{\pi^2} \sum_{n=-\infty}^{\infty} \int_{-\infty}^{\infty} dx' \int_{-\infty}^{\infty} dx'' \frac{\partial^2}{\partial x''^2} \Delta_n(x'') \frac{\partial \varphi_0}{\partial x''} \Big|_{y=0} \Delta_{m-n}(x') G_n(x', x'') S_m(x, x'). \quad (\text{J.34})$$

Note that for $m = 0$

$$S_0(x, x') = \int_0^{\infty} dk \frac{\sin k(x-x')}{\sinh ka} = \frac{\pi}{2a} \tanh \frac{\pi}{2a} (x-x'). \quad (\text{J.35})$$

Adding equations J.20 and J.34 gives

$$\begin{aligned} \varphi_{2m}(x)|_{y=a} &= -\frac{1}{\pi^2} \sum_{n=-\infty}^{\infty} \int_{-\infty}^{\infty} dx' \int_{-\infty}^{\infty} dx'' \frac{\partial^2}{\partial x''^2} \Delta_n(x'') \frac{\partial \varphi_0}{\partial x''} \Big|_{y=0} \Delta_{m-n}(x') G_n(x', x'') S_m(x, x') - \\ &\quad \frac{1}{\pi^2} \sum_{n=-\infty}^{\infty} \int_{-\infty}^{\infty} dx' \int_{-\infty}^{\infty} dx'' \Delta_{m-n}(x') G_n \frac{2\pi n}{w} C_m \left[\frac{\partial}{\partial x''} \Delta_n(x'') \frac{\partial \varphi_0}{\partial x''} \Big|_{y=0} \right] \\ \varphi_{2m}(x)|_{y=a} &= -\frac{1}{\pi^2} \sum_{n=-\infty}^{\infty} \int_{-\infty}^{\infty} dx' \int_{-\infty}^{\infty} dx'' \Delta_{m-n}(x') G_n \left[S_m \left(\frac{\partial^2}{\partial x''^2} \Delta_n(x'') \frac{\partial \varphi_0}{\partial x''} \Big|_{y=0} \right) + \frac{2\pi n}{w} C_m \left(\frac{\partial}{\partial x''} \Delta_n(x'') \frac{\partial \varphi_0}{\partial x''} \Big|_{y=0} \right) \right] \end{aligned}$$

where S_m , C_m and G_n are given by equations J.33, J.19 and J.18, respectively.

APPENDIX K

This appendix describes the derivation of equations 4.93 and 4.94, which are the solution for a 2D symmetric defect considering the first and second order approximation, respectively. Consider the equations below:

$$\varphi(x, y) = \varphi_0(x, y) + \varphi_1(x, y), \quad (\text{K.1})$$

$$\Delta(x) \approx \Delta_1(x) + \Delta_2(x), \text{ and} \quad (\text{K.2})$$

$$\left(\frac{\partial \varphi}{\partial y} - \frac{\partial \Delta}{\partial x} \frac{\partial \varphi}{\partial x} \right) \Big|_{S_2} = 0. \quad (\text{K.3})$$

After expansion of Equation K.3 as a Taylor series about $y = \Delta_0$, the first term is

$$\begin{aligned} \frac{\partial \varphi}{\partial y} \Big|_{y=\Delta(x)} &\approx \frac{\partial \varphi}{\partial y} \Big|_{y=\Delta_0} + (\Delta - \Delta_0) \frac{\partial^2 \varphi}{\partial y^2} \Big|_{y=\Delta_0} + \frac{(\Delta - \Delta_0)^2}{2} \frac{\partial^3 \varphi}{\partial y^3} \Big|_{y=\Delta_0}, \\ \frac{\partial \varphi}{\partial y} \Big|_{y=\Delta(x)} &\approx \frac{\partial \varphi_0}{\partial y} \Big|_{y=\Delta_0} + \left[\frac{\partial \varphi_1}{\partial y} + (\Delta_1 - \Delta_0) \frac{\partial^2 \varphi_0}{\partial y^2} \right] \Big|_{y=\Delta_0} + \left[\Delta_2 \frac{\partial^2 \varphi_0}{\partial y^2} + (\Delta_1 - \Delta_0) \frac{\partial^2 \varphi_1}{\partial y^2} + \frac{(\Delta - \Delta_0)^2}{2} \frac{\partial^3 \varphi_0}{\partial y^3} \right] \Big|_{y=\Delta_0}, \\ \frac{\partial \varphi}{\partial y} \Big|_{y=\Delta(x)} &\approx \frac{\partial \varphi_0}{\partial y} \Big|_{y=\Delta_0} + \left[\frac{\partial \varphi_1}{\partial y} + (\Delta_1 - \Delta_0) \frac{\partial^2 \varphi_0}{\partial y^2} \right] \Big|_{y=\Delta_0} + \left[\Delta_2 \frac{\partial^2 \varphi_0}{\partial y^2} + (\Delta_1 - \Delta_0) \frac{\partial^2 \varphi_1}{\partial y^2} \right] \Big|_{y=\Delta_0}. \end{aligned} \quad (\text{K.4})$$

And the second term is

$$\begin{aligned} \frac{\partial \Delta}{\partial x} \frac{\partial \varphi}{\partial x} \Big|_{y=\Delta(x)} &\approx \frac{\partial(\Delta_1 + \Delta_2)}{\partial x} \left[\frac{\partial \varphi}{\partial x} + (\Delta - \Delta_0) \frac{\partial^2 \varphi}{\partial x \partial y} \right] \Big|_{y=\Delta_0}, \\ \frac{\partial \Delta}{\partial x} \frac{\partial \varphi}{\partial x} \Big|_{y=\Delta(x)} &\approx \frac{\partial \Delta_1}{\partial x} \frac{\partial \varphi_0}{\partial x} \Big|_{y=\Delta_0} + \left[\frac{\partial \Delta_2}{\partial x} \frac{\partial \varphi_0}{\partial x} + \frac{\partial \Delta_1}{\partial x} \frac{\partial \varphi_1}{\partial x} + \frac{\partial \Delta_1}{\partial x} (\Delta_1 - \Delta_0) \frac{\partial^2 \varphi_0}{\partial x \partial y} \right] \Big|_{y=\Delta_0}, \\ \frac{\partial \Delta}{\partial x} \frac{\partial \varphi}{\partial x} \Big|_{y=\Delta(x)} &\approx \frac{\partial \Delta_1}{\partial x} \frac{\partial \varphi_0}{\partial x} \Big|_{y=\Delta_0} + \left[\frac{\partial \Delta_2}{\partial x} \frac{\partial \varphi_0}{\partial x} + \frac{\partial \Delta_1}{\partial x} \frac{\partial \varphi_1}{\partial x} \right] \Big|_{y=\Delta_0}. \end{aligned} \quad (\text{K.5})$$

Substituting the results obtained from equations K.4 and K.5 and into Equation K.3 produces, for each order of magnitude indicated as a superscript index, the following equations:

$$\Delta^{(0)} : \left. \frac{\partial \varphi_0}{\partial y} \right|_{y=\Delta_0} = 0 ;$$

$$\Delta^{(1)} : \left[\frac{\partial \varphi_1}{\partial y} + (\Delta_1 - \Delta_0) \frac{\partial^2 \varphi_0}{\partial y^2} \right]_{y=\Delta_0} - \left. \frac{\partial \Delta_1}{\partial x} \frac{\partial \varphi_0}{\partial x} \right|_{y=\Delta_0} = 0 ,$$

$$\Delta^{(1)} : \left. \frac{\partial \varphi_1}{\partial y} \right|_{\Delta_0} = \frac{\partial}{\partial x} \left[(\Delta_1 - \Delta_0) \frac{\partial \varphi_0}{\partial x} \right]_{y=\Delta_0} ; \quad (\text{K.6})$$

$$\Delta^{(2)} : \left[\Delta_2 \frac{\partial^2 \varphi_0}{\partial y^2} + (\Delta_1 - \Delta_0) \frac{\partial^2 \varphi_1}{\partial y^2} \right]_{y=\Delta_0} - \left[\frac{\partial \Delta_2}{\partial x} \frac{\partial \varphi_0}{\partial x} + \frac{\partial \Delta_1}{\partial x} \frac{\partial \varphi_1}{\partial x} \right]_{y=\Delta_0} = 0 ,$$

$$\Delta^{(2)} : \left[-\Delta_2 \frac{\partial^2 \varphi_0}{\partial x^2} - (\Delta_1 - \Delta_0) \frac{\partial^2 \varphi_1}{\partial x^2} \right]_{y=\Delta_0} - \left[\frac{\partial \Delta_2}{\partial x} \frac{\partial \varphi_0}{\partial x} + \frac{\partial \Delta_1}{\partial x} \frac{\partial \varphi_1}{\partial x} \right]_{y=\Delta_0} = 0 ,$$

$$\Delta^{(2)} : \frac{\partial}{\partial x} \left[\Delta_2 \frac{\partial \varphi_0}{\partial x} + (\Delta_1 - \Delta_0) \frac{\partial \varphi_1}{\partial x} \right]_{y=\Delta_0} = 0 . \quad (\text{K.7})$$

From Equation K.6 the first order defect $\Delta_1(x)$ can be calculated. Thus,

$$\Delta_1(x) = \Delta_0 + \frac{\int_{-\infty}^x \left. \frac{\partial \varphi_1}{\partial y} \right|_{y=\Delta_0} dx}{\left. \frac{\partial \varphi_0}{\partial x} \right|_{y=\Delta_0}} , \quad (\text{K.8})$$

which is the expression for Equation 4.93.

From Equation K.7 the second order defect $\Delta_2(x)$ can be calculated. Therefore,

$$\Delta_2(x) = -(\Delta_1 - \Delta_0) \frac{\left. \frac{\partial \varphi_1}{\partial x} \right|_{y=\Delta_0}}{\left. \frac{\partial \varphi_0}{\partial x} \right|_{y=\Delta_0}}, \quad (\text{K.9})$$

which is the expression for Equation 4.94.

APPENDIX L

This appendix describes the code developed in MATLAB to solve the inverse problem in two-dimensions considering only the first order term of the defect, that is, $\Delta_1(x)$. The code, called “inverse_first_data”, includes a subroutine called “calcphis2d” that calculates the experimental potential data $\varphi_s(x)$ that accounts for the defect region.

The experimental potential data $\varphi_s(x)$ is calculated as

$$\varphi_s(x) = \varphi_m(x) - \varphi_0(x), \quad (\text{L.1})$$

where $\varphi_m(x)$ is the measurement potential data at the surface and $\varphi_0(x)$ is the known analytical potential function for a non-defect region. This function is given by Equation 4.69

$$\varphi_0(x, y) = \frac{\rho S_0}{2\pi w} \ln \frac{\cosh \frac{\pi(l+x)}{(a-\Delta_0)} + \cos \frac{\pi y}{(a-\Delta_0)}}{\cosh \frac{\pi(l-x)}{(a-\Delta_0)} + \cos \frac{\pi y}{(a-\Delta_0)}}. \quad (\text{L.2})$$

The defect in two-dimensions is given by Equation 4.93

$$\Delta_1(x) = \Delta_0 + \frac{\int_{x_{ini}}^x \left. \frac{\partial \varphi_1}{\partial y} \right|_{y=\Delta_0} dx}{\left. \frac{\partial \varphi_0}{\partial x} \right|_{y=\Delta_0}}, \quad (\text{L.3})$$

where x_{ini} is an initial position chosen such that we do not have negative values of

$\Delta_1(x)$. The numerator in Equation L.3 is given by Equation 4.100

$$\left. \frac{\partial \varphi_1}{\partial y} \right|_{y=\Delta_0} = \int_{-\infty}^{\infty} e^{ikx} B(k) k \sinh k(\Delta_0 - a) dk. \quad (\text{L.4})$$

The coefficient $B(k)$ is given by Equation 4.101

$$B(k) = \frac{1}{2\pi} \int_{-\infty}^{\infty} e^{-ikx} \varphi_s(x) dx.$$

This expression can be discretized as

$$B(k_l) = \frac{\Delta x}{2\pi} \sum_j \varphi_s(x_j) e^{-ik_l x_j}, \quad (\text{L.5})$$

where x_j are the positions where we have data measurements and $\varphi_s(x_j)$ are the corresponding potential measurements calculated using the subroutine “calcphis2d”.

Substituting Equation L.5 into Equation L.4 results in

$$\left. \frac{\partial \varphi_1}{\partial y} \right|_{y=\Delta_0} = -\frac{\Delta x}{2\pi} \sum_j \int_{-\infty}^{\infty} dk \varphi_s(x_j) e^{ik(x-x_j)} k \sinh k(a - \Delta_0). \quad (\text{L.6})$$

The numerator of Equation L.3, represented by $Num(x)$, is given by

$$\begin{aligned} Num(x) &= \int_{x_{min}}^x \left. \frac{\partial \varphi_1}{\partial y} \right|_{y=\Delta_0} dx, \\ Num(x) &= -\frac{\Delta x}{2\pi i} \sum_j \int_{-k_{max}}^{k_{max}} dk \varphi_s(x_j) [e^{ik(x-x_j)} - e^{ik(x_{min}-x_j)}] \sinh k(a - \Delta_0), \\ Num(x) &= -\frac{\Delta x}{4\pi i} \sum_j \varphi_s(x_j) \int_{-k_{max}}^{k_{max}} dk [e^{ik(x-x_j)} - e^{ik(x_{min}-x_j)}] [e^{k(a-\Delta_0)} - e^{-k(a-\Delta_0)}]. \quad (\text{L.7}) \end{aligned}$$

It can be observed that a maximum value to the parameter k , called k_{max} , was chosen in order to solve the integral. This parameter will be responsible for the stability of the final solution. Factoring Equation L.7 results in

$$\begin{aligned}
Num(x) &= -\frac{\Delta x}{4\pi i} \sum_j \varphi_s(x_j) \int_{-k_{\max}}^{k_{\max}} dk [e^{k[a-\Delta_0+i(x-x_j)]} - e^{k[a-\Delta_0+i(x_{init}-x_j)]} - e^{-k[a-\Delta_0-i(x-x_j)]} + e^{-k[a-\Delta_0-i(x_{init}-x_j)]}] , \\
Num(x) &= -\frac{\Delta x}{4\pi i} \sum_j \varphi_s(x_j) \left\{ \frac{e^{k_{\max}(a-\Delta_0+i(x-x_j))} - e^{-k_{\max}(a-\Delta_0+i(x-x_j))}}{a-\Delta_0+i(x-x_j)} - \frac{e^{k_{\max}(a-\Delta_0+i(x_{init}-x_j))} - e^{-k_{\max}(a-\Delta_0+i(x_{init}-x_j))}}{a-\Delta_0+i(x_{init}-x_j)} \right. \\
&\quad \left. + \frac{e^{-k_{\max}(a-\Delta_0-i(x-x_j))} - e^{k_{\max}(a-\Delta_0-i(x-x_j))}}{a-\Delta_0-i(x-x_j)} - \frac{e^{-k_{\max}(a-\Delta_0-i(x_{init}-x_j))} - e^{k_{\max}(a-\Delta_0-i(x_{init}-x_j))}}{a-\Delta_0-i(x_{init}-x_j)} \right\} \quad (L.8)
\end{aligned}$$

Rearranging the terms of Equation L.8 and after some algebra gives

$$\begin{aligned}
Num(x) &= -\frac{\Delta x}{\pi} \sum_j \left\{ \frac{\varphi_s(x_j)}{[(a-\Delta_0)^2 + (x-x_j)^2]} [(a-\Delta_0) \cosh k_{\max}(a-\Delta_0) \sin k_{\max}(x-x_j) - (x-x_j) \sinh k_{\max}(a-\Delta_0) \cos k_{\max}(x-x_j)] - \right. \\
&\quad \left. \frac{\varphi_s(x_j)}{[(a-\Delta_0)^2 + (x_{init}-x_j)^2]} [(a-\Delta_0) \cosh k_{\max}(a-\Delta_0) \sin k_{\max}(x_{init}-x_j) - (x_{init}-x_j) \sinh k_{\max}(a-\Delta_0) \cos k_{\max}(x_{init}-x_j)] \right\} \quad (L.9)
\end{aligned}$$

The denominator of Equation L.3, represented by $Den(x)$, can be easily calculated as

$$Den(x) = \frac{\partial \varphi_0}{\partial x} \Big|_{y=\Delta_0} = \frac{\rho S_0}{2wa} \left[\frac{\sinh \left[\frac{\pi(l+x)}{(a-\Delta_0)} \right]}{\cosh \left[\frac{\pi(l+x)}{(a-\Delta_0)} \right] + 1} + \frac{\sinh \left[\frac{\pi(l-x)}{(a-\Delta_0)} \right]}{\cosh \left[\frac{\pi(l-x)}{(a-\Delta_0)} \right] + 1} \right]. \quad (L.10)$$

Now the defect $\Delta_1(x)$ can be calculated substituting equations L.9 and L.10 into the following expression:

$$\Delta_1(x) = \Delta_0 + \frac{Num(x)}{Den(x)}.$$

The code “inverse_first_data” is listed below.

```

%
%           PROGRAM INVERSE_FIRST_DATA
%
function inverse_first_data

clear

global lprobe w l a rho curr deltax x

global x0 nimag numcol kmax new_x

global xinit new_x delta0

input('enter with the length of probe in x direction : lprobe (mm)= ');

input('enter with the width of the plate: w (mm) =');

input('enter with the length of the plate: l (mm) =');

input('enter with the thickness of the plate :a (mm) =');

input('enter with the resistivity of the material: rho (micro_ohm*mm) =');

input('enter with the current : curr (amp) =');

input('enter with the potential measurements matrix: phim (microvolt) =');

input('enter with the increment in x : deltax (mm) =');

input('enter with the initial position in x : x0 (mm) =');

input('enter with the maximum value of k : kmax (1/mm) =');

input('enter with the parameter delta0 : delta0 (mm) =');

xinit= input('enter with the inferior limit of the integral: xinit (mm) =');

```

```

nimag= sqrt(-1);

numcol = lprobe/deltax +1;

[phis2d] = calcphis2d(phim,x0);

for j=1:1:numcol,

    x(j)= (-lprobe/2)+deltax*(j-1);

end

new_x=-x0:2.54:x0;

size_new_x=length(new_x);

for i=1:size_new_x,

    sum = 0;

    sum1 = 0;

    for j=1:numcol,

        var1 = (delta0-a)*cosh(kmax*(delta0-a))*sin(kmax*(new_x(i)-x(j)));
        var2 = (new_x(i)-x(j))*sinh(kmax*(delta0-a))*cos(kmax*(new_x(i)-x(j)));
        var3 = (delta0-a)*cosh(kmax*(delta0-a))*sin(kmax*(xinit-x(j)));
        var4 = (xinit-x(j))*sinh(kmax*(delta0-a))*cos(kmax*(xinit-x(j)));
        var5 = (phis2d(j)/(((delta0-a)^2)+(new_x(i)-x(j))^2))*(var1-var2);
        var6 = (phis2d(j)/(((delta0-a)^2)+(xinit-x(j))^2))*(var3-var4);
        var7 = var5 - var6;

        sum = sum + var7;
    end
end

```

```

end

num1(i) = (deltax/(pi))*sum;

den(i) = ((rho*curr)/(2*(a-delta0)*w))* ( sinh((pi/(a-
delta0))*(1+new_x(i)))/(cosh((pi/(a-
delta0))*(1+new_x(i)))+cos(pi*delta0/(a-delta0))) + (sinh((pi/(a-delta0))*(1-
new_x(i)))/(cosh((pi/(a-delta0))*(1-new_x(i)))+cos(pi*delta0/(a-delta0))));

delta1(i)= (delta0+num1(i)/den(i));

end

defect1 = delta1

plot(new_x,defect1,'b-')

title('Defect Mapping using the experimental data - kmax = /mm')

xlabel('distance from the center to the border of the plate (mm)')

ylabel('defect (mm)')

```

```

%
%
% SUBROUTINE CALCPHIS2D
%
% This subroutine calculates phis(x,y=a) using phim(x,y=a), which
% is the measurement potential at (x,y=a), and phizero(x,y=a)
% that is the potential function for a non-defect region on the
% surface (y=a).All the potential are in microvolts.
% The position of the first value of x is defined as x0, which is
% the closest point to the current wires in the negative direction of
% x. The unit for x0 is mm.

function [phis2d]= calcphis2d(phim,x0)
global w l a rho curr deltax
global x0 numcol phim delta0

% numcol is the number of columns in the grid of measurements, which is
% the number of points in the x direction.

x=x0;

for j=1:numcol,

    num1= cosh((pi/(a-delta0))*(1+x))+cos(pi*a/(a-delta0));
    den1= cosh((pi/(a-delta0))*(1-x))+cos(pi*a/(a-delta0));
    var1= log(num1/den1);
    var2=((rho*curr)/(2*pi*w))*var1;
    phizero(j)= var2;
    newphis2d(j)= phim(j)-phizero(j);
    x = x + deltax;

end

```


APPENDIX M

This appendix describes the derivation of equations 4.109, 4.112 and 4.113, which are part of the alternative solution for a 2D symmetric defect considering the first and the second order approximation. Consider the equations below:

$$\frac{\partial^2 \hat{\varphi}_1}{\partial y^2} - k^2 \hat{\varphi}_1 = -\frac{\varphi_\infty}{2\pi} \int_{-\infty}^{\infty} e^{-ikx} \nabla^2 \tanh \frac{\pi x}{2a} dx, \quad (\text{M.1})$$

$$\left. \frac{\partial \hat{\varphi}_1}{\partial y} \right|_{y=a} = 0, \quad (\text{M.2})$$

$$\hat{\varphi}_1 \Big|_{y=a} = \frac{1}{2\pi} \int_{-\infty}^{\infty} e^{-ikx} \left[\varphi_m - \varphi_0 \Big|_{y=a} - \varphi_\infty \tanh \frac{\pi x}{2a} \right] dx. \quad (\text{M.3})$$

Defining

$$\delta\hat{\varphi} = -\frac{1}{\pi} \int_0^{\infty} \sin kx \left[\varphi_m - \varphi_0 \Big|_{y=a} - \varphi_\infty \tanh \frac{\pi x}{2a} \right] dx, \quad (\text{M.4})$$

Equation M.3 may be written as

$$\hat{\varphi}_1 \Big|_{y=a} = i \delta\hat{\varphi}. \quad (\text{M.5})$$

Observe that

$$\nabla^2 \tanh \frac{\pi x}{2a} = \frac{\partial^2}{\partial x^2} \tanh \frac{\pi x}{2a},$$

$$\nabla^2 \tanh \frac{\pi x}{2a} = \frac{\pi}{2a} \frac{\partial}{\partial x} \operatorname{sech}^2 \frac{\pi x}{2a},$$

$$\nabla^2 \tanh \frac{\pi x}{2a} = -\frac{\pi^2}{2a^2} \operatorname{sech}^2 \frac{\pi x}{2a} \tanh \frac{\pi x}{2a}.$$

Therefore Equation M.1 can be rewritten as

$$\frac{\partial^2 \hat{\varphi}_1}{\partial y^2} - k^2 \hat{\varphi}_1 = \frac{\varphi_\infty \pi}{4a^2} \int_{-\infty}^{\infty} e^{-ikx} \sec h^2 \frac{\pi x}{2a} \tanh \frac{\pi x}{2a} dx. \quad (\text{M.6})$$

The right hand side of the equation above can be solved. Thus

$$RHS = \frac{\varphi_\infty \pi}{4a^2} \int_{-\infty}^{\infty} e^{-ikx} \sec h^2 \frac{\pi x}{2a} \tanh \frac{\pi x}{2a} dx,$$

$$RHS = -i \frac{\varphi_\infty \pi}{2a^2} \int_0^{\infty} \sin kx \frac{\sinh \frac{\pi x}{2a}}{\cosh^3 \frac{\pi x}{2a}} dx.$$

Let $y = \frac{\pi x}{2a}$, so

$$RHS = -i \frac{\varphi_\infty}{a} \int_0^{\infty} \sin(ky \frac{2a}{\pi}) \frac{\sinh y}{\cosh^3 y} dy.$$

Solving this integral by parts yields

$$RHS = -i \frac{\varphi_\infty}{\pi} \int_0^{\infty} \cos(\frac{2ka}{\pi} y) \frac{k}{\cosh^2 y} dy.$$

It can be seen from tables (Gradshteyn and Ryzhik, 1994) that

$$\int_0^{\infty} \frac{\cos ax}{\cosh^2 bx} dx = \frac{a\pi}{2b^2 \sinh \frac{a\pi}{2b}},$$

therefore,

$$RHS = -i \frac{\varphi_\infty}{\pi} \frac{k^2 a}{\sinh ka}. \quad (\text{M.7})$$

Substituting this result into Equation M.6 gives

$$\frac{\partial^2 \hat{\varphi}_1}{\partial y^2} - k^2 \hat{\varphi}_1 = -i \frac{\varphi_\infty}{\pi} \frac{k^2 a}{\sinh ka}. \quad (\text{M.8})$$

The general solution to the equation above is

$$\hat{\phi}_1 = i \frac{\varphi_\infty a}{\pi} \frac{1}{\sinh ka} + A_1 \cosh k(y-a). \quad (\text{M.9})$$

From the boundary condition of Equation M.5 the constant A_1 can be calculated. Thus

$$A_1(k) = i\delta\hat{\phi} - i \frac{\varphi_\infty a}{\pi} \frac{1}{\sinh ka}.$$

Replacing this result into Equation M.9 gives

$$\hat{\phi}_1 = i \left\{ \frac{\varphi_\infty a}{\pi} \frac{1}{\sinh ka} + \left[\delta\hat{\phi} - \frac{\varphi_\infty a}{\pi} \frac{1}{\sinh ka} \right] \cosh k(y-a) \right\}, \quad (\text{M.10})$$

which is the expression for Equation 4.109.

Now consider Equation 4.111:

$$\hat{\phi}_1 = i \left\{ \frac{\varphi_\infty a}{\pi} \frac{1}{\sinh ka} + \left[\delta\hat{\phi} - \frac{\varphi_\infty a}{\pi} \frac{1}{\sinh ka} \right] \cosh k(y-a) e^{\frac{k^2}{k_m^2}} \right\}. \quad (\text{M.11})$$

The numerator of Equation 4.102 can be represented by $Num(x)$. Thus,

$$Num(x) = \int_{-\infty}^x \frac{\partial \phi_1}{\partial y} \Big|_{y=0} dx',$$

$$Num(x) = \int_{-\infty}^x dx' \int_{-\infty}^{\infty} dk e^{ikx'} \frac{\partial \hat{\phi}_1}{\partial y} \Big|_{y=0}. \quad (\text{M.12})$$

The term $\frac{\partial \hat{\phi}_1}{\partial y} \Big|_{y=0}$ can be evaluated as

$$\frac{\partial \hat{\phi}_1}{\partial y} \Big|_{y=0} = \frac{\partial \hat{\phi}_1}{\partial y} \Big|_{y=0} = -i \left[\left(\delta\hat{\phi} - \frac{\varphi_\infty a}{\pi} \frac{1}{\sinh ka} \right) k \sinh ka \right] e^{\frac{k^2}{k_m^2}},$$

$$\frac{\partial \hat{\phi}_1}{\partial y} \Big|_{y=0} = \frac{\partial \hat{\phi}_1}{\partial y} \Big|_{y=0} = -i \left(\delta\hat{\phi} k \sinh ka - \frac{k\varphi_\infty a}{\pi} \right) e^{\frac{k^2}{k_m^2}}. \quad (\text{M.13})$$

Substituting Equation M.13 into Equation M.14 results in

$$\begin{aligned}
 Num(x) &= -i \int_{-\infty}^x dx' \int_{-\infty}^{\infty} dk e^{ikx'} \left(\delta\hat{\varphi} k \sinh ka - \frac{k\varphi_{\infty} a}{\pi} \right) e^{-\frac{k^2}{k_m^2}}, \\
 Num(x) &= -i \int_{-\infty}^x dx' \frac{\partial}{\partial x'} \int_{-\infty}^{\infty} dk \frac{e^{ikx'}}{i} \left(\delta\hat{\varphi} \sinh ka - \frac{\varphi_{\infty} a}{\pi} \right) e^{-\frac{k^2}{k_m^2}}, \\
 Num(x) &= - \int_{-\infty}^{\infty} dk e^{ikx} \left(\delta\hat{\varphi} \sinh ka - \frac{\varphi_{\infty} a}{\pi} \right) e^{-\frac{k^2}{k_m^2}}, \\
 Num(x) &= - \int_{-\infty}^{\infty} dk e^{ikx} (\delta\hat{\varphi} \sinh ka) e^{-\frac{k^2}{k_m^2}} + \int_{-\infty}^{\infty} dk e^{ikx} \frac{\varphi_{\infty} a}{\pi} e^{-\frac{k^2}{k_m^2}}. \tag{M.14}
 \end{aligned}$$

Calling the second integral of Equation M.14 $Num1(x)$ results in

$$\begin{aligned}
 Num1(x) &= \int_{-\infty}^{\infty} dk e^{ikx} \frac{\varphi_{\infty} a}{\pi} e^{-\frac{k^2}{k_m^2}}, \\
 Num1(x) &= \frac{\varphi_{\infty} a}{\pi} \int_{-\infty}^{\infty} dk e^{\left(ikx - \frac{k^2}{k_m^2} \right)}.
 \end{aligned}$$

Let $k = k_m \zeta$, thus

$$\begin{aligned}
 Num1(x) &= \frac{\varphi_{\infty} a k_m}{\pi} \int_{-\infty}^{\infty} d\zeta e^{(ik_m x \zeta - \zeta^2)}, \\
 Num1(x) &= \frac{\varphi_{\infty} a k_m}{\pi} \int_{-\infty}^{\infty} d\zeta e^{-\left(\zeta - i \frac{k_m x}{2} \right)^2} e^{-\frac{k_m^2 x^2}{4}}, \\
 Num1(x) &= \frac{\varphi_{\infty} a k_m}{\sqrt{\pi}} e^{-\frac{k_m^2 x^2}{4}}. \tag{M.15}
 \end{aligned}$$

Substituting this equation into Equation M.14 gives

$$Num(x) = - \int_{-\infty}^{\infty} dk e^{ikx} (\delta\hat{\varphi} \sinh ka) e^{-\frac{k^2}{k_m^2}} + \frac{\varphi_{\infty} a k_m}{\sqrt{\pi}} e^{-\frac{k_m^2 x^2}{4}},$$

$$Num(x) = \frac{\varphi_\infty a k_m}{\sqrt{\pi}} e^{-\frac{k_m^2 x^2}{4}} - 2 \int_0^\infty dk \cos kx (\delta\hat{\varphi} \sinh ka) e^{-\frac{k^2}{k_m^2}}, \quad (M.16)$$

which is the expression for Equation 4.112.

From Equation 4.105

$$\frac{\partial \varphi_1}{\partial x} = \frac{\partial \tilde{\varphi}_1}{\partial x} + \frac{\pi \varphi_\infty}{2a} \operatorname{sech}^2 \frac{\pi x}{2a}, \quad (M.17)$$

and by definition

$$\tilde{\varphi}_1(x, y) = \int_{-\infty}^{\infty} e^{ikx} \hat{\varphi}_1(k, y) dk,$$

$$\tilde{\varphi}_1(x, y) = 2i \int_0^\infty dk \hat{\varphi}_1(k, y) \sin kx.$$

Thus,

$$\frac{\partial \tilde{\varphi}_1}{\partial x} = 2i \int_0^\infty dk \hat{\varphi}_1(k, y) k \cos kx. \quad (M.18)$$

Substituting Equation M.11 into Equation M.18 results in

$$\frac{\partial \tilde{\varphi}_1}{\partial x} = -2 \int_0^\infty dk k \cos kx \left\{ \frac{\varphi_\infty a}{\pi} \frac{1}{\sinh ka} + \left[\delta\hat{\varphi} - \frac{\varphi_\infty a}{\pi} \frac{1}{\sinh ka} \right] \cosh k(y-a) e^{-\frac{k^2}{k_m^2}} \right\}. \quad (M.19)$$

It can be seen from tables (Gradshteyn and Ryzhik, 1994) that

$$\int_0^\infty \frac{x \cos ax}{\sinh bx} dx = \frac{\pi^2}{4b^2} \operatorname{sech}^2 \frac{\pi a}{2b},$$

therefore,

$$\frac{\partial \tilde{\varphi}_1}{\partial x} = -\frac{\pi \varphi_\infty}{2a} \operatorname{sech}^2 \frac{\pi x}{2a} - 2 \int_0^\infty dk k \cos kx \left[\delta\hat{\varphi} - \frac{\varphi_\infty a}{\pi \sinh ka} \right] \cosh k(y-a) e^{-\frac{k^2}{k_m^2}}. \quad (M.20)$$

From Equation M.17

$$\left. \frac{\partial \varphi_1}{\partial x} \right|_{y=0} = \left. \frac{\partial \tilde{\varphi}_1}{\partial x} \right|_{y=0} + \frac{\pi \varphi_\infty}{2a} \sinh^2 \frac{\pi x}{2a}, \text{ and}$$

evaluating Equation M.20 at $y = 0$ and substituting into the result above gives

$$\left. \frac{\partial \varphi_1}{\partial x} \right|_{y=0} = -2 \int_0^\infty dk k \cos kx \left[\delta \hat{\varphi} - \frac{\varphi_\infty a}{\pi \sinh ka} \right] \cosh ka e^{-\frac{k^2}{k_m^2}}, \quad (\text{M.21})$$

which is the expression for Equation 4.113.

APPENDIX N

This appendix contains a listing of the code “inverse_second” developed in MATLAB to solve the inverse problem in two-dimensions considering the second order term of the defect, that is, $\Delta_2(x)$. The code includes the subroutines “calcdeltaphihat”, “calcintnum” and “calcdphidx”.

```
%  
  
%          PROGRAM INVERSE_SECOND  
  
%  
  
function inverse_second  
  
clear  
  
global lprobe w l a rho curr deltax x  
  
global xp0 numcol numxp deltaxp  
  
global i phim phi_inf kmax deltak km k  
  
input('enter with the length of probe in x direction : lprobe (mm)= ');  
  
input('enter with the width : w (mm) =');  
  
input('enter with the length :l (mm) =');  
  
input('enter with the thickness :a (mm) =');
```

```
input('enter with the resistivity :rho (micro_ohm*mm) =?');  
input('enter with the current : curr (amp) =?');  
input('enter with the potential measurements matrix: phim (microvolt) =?');  
input('enter with the increment in xprime : deltaxp (mm) =?');  
input('enter with the increment in k : deltak (1/mm) =?');  
input('enter with the maximum value of k : kmax (1/mm) =?');  
input('enter with the increment in x : deltax (mm) =?');  
input('enter with the parameter phi_infinite : phi_inf (microvolt) =?');  
input('enter with the parameter km : km (1/mm) =?');
```

```
xp0= 0;
```

```
numcol = lprobe/deltax +1;
```

```
numxp = 5*l/deltaxp+1;
```

```
cont =1;
```

```
for k=0.01:deltak:kmax,
```

```
    [deltaphihat] = calcdeltaphihat(xp0);
```

```
    vec_deltaphihat(cont) = deltaphihat;
```

```
    vec_k(cont)= k;
```

```
    cont= cont + 1;
```

```
end
```



```

for i=1:1:numcol,

    x= (-lprobe/2)+deltax*(i-1);

    [intnum] = calcintnum(vec_k,vec_deltaphihat,x);

    num= (phi_inf/sqrt(pi))*km*a*exp(-(km*x/2)^2)-intnum;

    den= (rho*curr/(2*w*a))*(tanh(pi*(1+x)/(2*a))+tanh(pi*(1-x)/(2*a)));

    delta1 = num/den;

    [dphi1dx] = calcdphi1dx(vec_k,vec_deltaphihat,x);

    delta2 = -delta1*dphi1dx/den;

    defect1(i) = delta1;

    defect2(i) = delta1 + delta2

    new_x(i) = x;

end

plot(new_x,defect2,'b-')

title('Inverse Problem with 2nd order approximation - km =/mm')

xlabel('Distance from the center to the border of the plate (mm)')

ylabel('Defect (mm)')

```

```

%
%
%           SUBROUTINE CALCDELTAPHIHAT
%
%           This subroutine calculates the Equation 4.110.
%
%
```

```

function [deltaphihat]= calcdeltaphihat(xp0)
global w a numxp deltaxp phim
global xp0 k rho curr l phi_inf

xp = xp0;
sum1xp = 0;
sum2xp = 0;

for j=1:numxp,
    if (xp<=140)

        n = 24 + j;
        num1 = sinh(pi*(1+xp)/(2*a));
        den1 = sinh(pi*(1-xp)/(2*a));
        var1 = (rho*curr/(2*pi*w))*log((num1/den1)^2);
        var2 = phi_inf*tanh(pi*xp/(2*a));
        var3 = phim(n) - var1 - var2;
    end
end
```

```
prod1 = sin(k*xp)*var3;
```

```
sum1xp = sum1xp + prod1;
```

```
xp = xp + deltaxp;
```

```
end
```

```
if (xp>140)
```

```
var1 = phi_inf*tanh(pi*xp/(2*a));
```

```
var2 = phi_inf - var1;
```

```
prod2 = sin(k*xp)*var2;
```

```
sum2xp = sum2xp +prod2;
```

```
xp = xp + deltaxp;
```

```
end
```

```
end
```

```
deltaphihat = -(1/pi)*deltaxp*(sum1xp+sum2xp);
```

```

%                SUBROUTINE CALCINTNUM

%

%   This subroutine calculates the second term of the Equation 4.112.

%

function [intnum]= calcintnum(vec_k,vec_deltaphihat,x)

global a vec_k vec_deltaphihat km x

size_k = length(vec_k);

for ind=1:size_k,

    var1 = cos(vec_k(ind)*x)*sinh(vec_k(ind)*a);
    var2 = exp(-(vec_k(ind)/km)^2);
    interf(ind) = vec_deltaphihat(ind)*var1*var2;

end

intnum = 2*trapz(vec_k,interf);

```

```

%           SUBROUTINE CALCDPHI1DX

%

%           This subroutine calculates the Equation 4.113.

%

function [dphi1dx]= calcdphi1dx(vec_k,vec_deltaphihat,x)

global a vec_k vec_deltaphihat km x phi_inf i

size_k = length(vec_k);

for ind=1:size_k,

    vara = (phi_inf*a)/(pi*sinh(vec_k(ind)*a));

    varb = vec_deltaphihat(ind) - vara;

    varc = exp(-(vec_k(ind)/km)^2);

    interf(ind) = vec_k(ind)*cos(vec_k(ind)*x)*cosh(vec_k(ind)*a)*varb*varc;

end

dphi1dx = -2*trapz(vec_k,interf);

```

APPENDIX O

This appendix describes the derivation of equations 4.122, 4.123, 4.137, 4.144 and 4.146 which are parts of the solution for a 3D cylindrical non-symmetric defect.

Consider the equations below:

$$\varphi(x, y, z) \approx \varphi_0(x, y) + \varphi_1(x, y, z) + \frac{\rho S_0}{4 w r_0} [|l + x| - |l - x|], \quad (\text{O.1})$$

$$\Delta(x, z) \approx \Delta_1(x, z) + \Delta_2(x, z), \quad (\text{O.2})$$

$$\left[\frac{\partial \varphi}{\partial y} - \frac{r_0^2}{(r_0 + y - \frac{a}{2})^2} \frac{\partial \varphi}{\partial z} \frac{\partial \Delta}{\partial z} - \frac{\partial \varphi}{\partial x} \frac{\partial \Delta}{\partial x} \right]_{\Delta} = 0. \quad (\text{O.3})$$

Expanding the first term of Equation O.3 about $\Delta = 0$ gives

$$\frac{\partial \varphi}{\partial y} \Big|_{\Delta} = \left[\frac{\partial \varphi_0}{\partial y} + \frac{\partial \varphi_1}{\partial y} + \Delta_1 \frac{\partial^2 \varphi_0}{\partial y^2} + \Delta_1 \frac{\partial^2 \varphi_1}{\partial y^2} + \Delta_2 \frac{\partial^2 \varphi_0}{\partial y^2} + \frac{\Delta_1^2}{2} \frac{\partial^3 \varphi_0}{\partial y^3} \right]_{y=0}. \quad (\text{O.4})$$

Expanding the second term of Equation O.3 about $\Delta = 0$ gives

$$\left[-\frac{r_0^2}{(r_0 + y - \frac{a}{2})^2} \frac{\partial \varphi}{\partial z} \frac{\partial \Delta}{\partial z} \right]_{\Delta} = \frac{\partial \varphi_1}{\partial z} \frac{\partial \Delta_1}{\partial z} \Big|_{y=0}. \quad (\text{O.5})$$

Finally, expanding the last term of Equation O.3 about $\Delta = 0$ gives

$$\left[-\frac{\partial \varphi}{\partial x} \frac{\partial \Delta}{\partial x} \right]_{\Delta} = \left[-\frac{\partial \varphi}{\partial x} \frac{\partial \Delta}{\partial x} - \Delta \frac{\partial^2 \Delta}{\partial x \partial y} \frac{\partial \varphi}{\partial y} \right]_{y=0},$$

$$\left[-\frac{\partial \varphi}{\partial x} \frac{\partial \Delta}{\partial x} \right]_{\Delta} = \left[-\frac{\partial \varphi_0}{\partial x} \frac{\partial \Delta_1}{\partial x} - \frac{\partial \varphi_1}{\partial x} \frac{\partial \Delta_1}{\partial x} - \frac{\partial \varphi_0}{\partial x} \frac{\partial \Delta_2}{\partial x} - \Delta_1 \frac{\partial^2 \Delta_1}{\partial x \partial y} \frac{\partial \varphi_0}{\partial y} \right]_{y=0}. \quad (\text{O.6})$$

Substituting equations O.4 through O.6 into Equation O.3 produces, for each order of magnitude indicated as a superscript, the following equations:

$$\Delta^{(0)} : \left. \frac{\partial \varphi_0}{\partial y} \right|_{y=0} = 0; \quad (\text{O.7})$$

$$\Delta^{(1)} : \left[\frac{\partial \varphi_1}{\partial y} + \Delta_1 \frac{\partial^2 \varphi_0}{\partial y^2} - \frac{\partial \Delta_1}{\partial x} \frac{\partial \varphi_0}{\partial x} \right]_{y=0} = 0,$$

$$\Delta^{(1)} : \left[\frac{\partial \varphi_1}{\partial y} - \Delta_1 \frac{\partial^2 \varphi_0}{\partial x^2} - \frac{\partial \Delta_1}{\partial x} \frac{\partial \varphi_0}{\partial x} \right]_{y=0} = 0,$$

$$\Delta^{(1)} : \left[\frac{\partial \varphi_1}{\partial y} - \frac{\partial}{\partial x} \left(\Delta_1 \frac{\partial \varphi_0}{\partial x} \right) \right]_{y=0} = 0; \quad (\text{O.8})$$

$$\Delta^{(2)} : \left[\Delta_1 \frac{\partial^2 \varphi_1}{\partial y^2} + \Delta_2 \frac{\partial^2 \varphi_0}{\partial y^2} + \frac{\Delta_1^2}{2} \frac{\partial^3 \varphi_0}{\partial y^3} - \frac{\partial \Delta_1}{\partial x} \frac{\partial \varphi_1}{\partial x} - \frac{\partial \Delta_2}{\partial x} \frac{\partial \varphi_0}{\partial x} - \Delta_1 \frac{\partial^2 \Delta_1}{\partial x \partial y} \frac{\partial \varphi_0}{\partial y} - \frac{\partial \Delta_1}{\partial z} \frac{\partial \varphi_1}{\partial z} \right]_{y=0} = 0,$$

$$\Delta^{(2)} : \left[-\Delta_1 \frac{\partial^2 \varphi_1}{\partial x^2} - \Delta_1 \frac{\partial^2 \varphi_1}{\partial z^2} - \Delta_2 \frac{\partial^2 \varphi_0}{\partial x^2} - \frac{\partial \Delta_1}{\partial x} \frac{\partial \varphi_1}{\partial x} - \frac{\partial \Delta_2}{\partial x} \frac{\partial \varphi_0}{\partial x} - \frac{\partial \Delta_1}{\partial z} \frac{\partial \varphi_1}{\partial z} \right]_{y=0} = 0,$$

$$\Delta^{(2)} : \left[\frac{\partial}{\partial x} \left(\Delta_2 \frac{\partial \varphi_0}{\partial x} + \Delta_1 \frac{\partial \varphi_1}{\partial x} \right) + \frac{\partial}{\partial z} \left(\Delta_1 \frac{\partial \varphi_1}{\partial z} \right) \right]_{y=0} = 0. \quad (\text{O.9})$$

Equations O.8 and O.9 correspond to equations 4.122 and 4.123.

Now consider the equations:

$$\varphi_1(x, y, z) = \tilde{\varphi}_1(x, y, z) + \frac{\varphi(\infty) + \varphi(-\infty)}{2} + \left[\frac{\varphi(\infty) - \varphi(-\infty)}{2} \right] \tanh \frac{\pi x}{2a}, \quad (\text{O.10})$$

$$\varphi(\infty) = \left[\varphi_m - \varphi_0 \right]_a - \frac{\rho S_0 l}{2r_0 w} \Bigg|_{x \rightarrow \infty},$$

$$\varphi(\infty) = \left[\varphi_m - \frac{\rho S_0 l}{wa} - \frac{\rho S_0 l}{2r_0 w} \right]_{x \rightarrow \infty}, \quad (\text{O.11})$$

$$\varphi(-\infty) = \left[\varphi_m - \varphi_0|_a + \frac{\rho S_0 l}{2r_0 w} \right]_{x \rightarrow -\infty},$$

$$\varphi(-\infty) = \left[\varphi_m + \frac{\rho S_0 l}{wa} + \frac{\rho S_0 l}{2r_0 w} \right]_{x \rightarrow -\infty}. \quad (\text{O.12})$$

Thus,

$$\varphi_1(x, y, z) = \tilde{\varphi}_1(x, y, z) + \sigma + \delta \tanh \frac{\pi x}{2a}, \quad (\text{O.13})$$

where

$$\sigma = \frac{1}{2} [\varphi(\infty) + \varphi(-\infty)], \text{ and} \quad (\text{O.14})$$

$$\delta = \frac{1}{2} [\varphi(\infty) - \varphi(-\infty)]. \quad (\text{O.15})$$

Observe that $\tilde{\varphi}_1|_{y=a} = 0$ as $|x| \rightarrow \infty$.

The function $\tilde{\varphi}_1(x, y, z)$ satisfies

$$\nabla^2 \tilde{\varphi}_1 = -\delta \nabla^2 \tanh \frac{\pi x}{2a}, \quad (\text{O.16})$$

$$\frac{\partial \tilde{\varphi}_1}{\partial y} \Big|_{y=a} = 0, \quad (\text{O.17})$$

$$\tilde{\varphi}_1|_{y=a} = \varphi_m - \varphi_0|_a - \frac{\rho S_0}{4 w r_0} [|l+x| - |l-x|] - \sigma - \delta \tanh \frac{\pi x}{2a}. \quad (\text{O.18})$$

By definition,

$$\tilde{\varphi}_1(x, y, z) = \sum_{n=-\infty}^{\infty} e^{i \frac{2\pi n z}{w}} \varphi_{1n}(x, y), \quad (\text{O.19})$$

$$\varphi_{1n}(x, y) = \int_{-\infty}^{\infty} dk e^{ikx} \hat{\varphi}_{1n}(k, y), \quad (\text{O.20})$$

$$\hat{\varphi}_{1n}(k, y) = \frac{1}{2\pi} \int_{-\infty}^{\infty} e^{-ikx} \varphi_{1n}(x, y) dx, \quad (\text{O.21})$$

where $\hat{\varphi}_{1n}(k, y)$ is the Fourier transform of $\varphi_{1n}(x, y)$.

Equation O.16 gives

$$\frac{\partial^2 \tilde{\varphi}_1}{\partial x^2} + \frac{\partial^2 \tilde{\varphi}_1}{\partial y^2} + \frac{\partial^2 \tilde{\varphi}_1}{\partial z^2} + \delta \nabla^2 \tanh \frac{\pi x}{2a} = 0.$$

Substituting Equation O.19 into the equation above results in

$$\sum_n \left[\frac{\partial^2}{\partial x^2} + \frac{\partial^2}{\partial y^2} - \left(\frac{2\pi n}{w} \right)^2 \right] \varphi_{1n} e^{i \frac{2\pi n z}{w}} + \delta \nabla^2 \tanh \frac{\pi x}{2a} = 0. \quad (\text{O.22})$$

A Fourier analysis of the equation above can be performed after multiplying both

sides of the equation by $\frac{1}{w} \int_0^w dz e^{-i \frac{2\pi m z}{w}}$. Therefore, Equation O.22 becomes

$$\left[\frac{\partial^2}{\partial x^2} + \frac{\partial^2}{\partial y^2} - \left(\frac{2\pi m}{w} \right)^2 \right] \varphi_{1m} + \delta_m \delta \nabla^2 \tanh \frac{\pi x}{2a} = 0, \quad (\text{O.23})$$

where

$$\delta_m = \frac{1}{w} \int_0^w dz e^{-i \frac{2\pi m z}{w}} = \begin{cases} 1, & \text{if } m = 0 \\ 0, & \text{if } m \neq 0 \end{cases}.$$

Can also apply Fourier analysis to Equation O.23 after multiplying both sides by

$\frac{1}{2\pi} \int_{-\infty}^{\infty} dx e^{-ikx}$. Therefore, equation O.23 becomes

$$\left[\frac{\partial^2}{\partial y^2} - k_m^2 \right] \hat{\varphi}_{1m} + \delta_m \frac{\delta}{2\pi} \int_{-\infty}^{\infty} dx e^{-ikx} \nabla^2 \tanh \frac{\pi x}{2a} = 0, \quad (\text{O.24})$$

where $k_m = \sqrt{k^2 + \left(\frac{2\pi m}{w}\right)^2}$.

Observe that

$$\begin{aligned}\nabla^2 \tanh \frac{\pi x}{2a} &= \frac{\partial^2}{\partial x^2} \tanh \frac{\pi x}{2a}, \\ \nabla^2 \tanh \frac{\pi x}{2a} &= \frac{\pi}{2a} \frac{\partial}{\partial x} \operatorname{sech}^2 \frac{\pi x}{2a}, \\ \nabla^2 \tanh \frac{\pi x}{2a} &= -\frac{\pi^2}{2a^2} \operatorname{sech}^2 \frac{\pi x}{2a} \tanh \frac{\pi x}{2a}.\end{aligned}$$

Therefore Equation O.24 can be rewritten as

$$\frac{\partial^2 \hat{\phi}_{1m}}{\partial y^2} - k_m^2 \hat{\phi}_{1m} = \delta_m \frac{\delta \pi}{4a^2} \int_{-\infty}^{\infty} e^{-ikx} \operatorname{sech}^2 \frac{\pi x}{2a} \tanh \frac{\pi x}{2a} dx. \quad (\text{O.25})$$

The right hand side of the equation above can be solved. Thus

$$\begin{aligned}RHS &= \delta_m \frac{\delta \pi}{4a^2} \int_{-\infty}^{\infty} e^{-ikx} \operatorname{sech}^2 \frac{\pi x}{2a} \tanh \frac{\pi x}{2a} dx, \\ RHS &= -i\delta_m \frac{\delta \pi}{2a^2} \int_0^{\infty} \sin kx \frac{\sinh \frac{\pi x}{2a}}{\cosh^3 \frac{\pi x}{2a}} dx.\end{aligned}$$

Let $y = \frac{\pi x}{2a}$, so

$$RHS = -i\delta_m \frac{\delta}{a} \int_0^{\infty} \sin\left(ky \frac{2a}{\pi}\right) \frac{\sinh y}{\cosh^3 y} dy.$$

Solving this integral by parts yields

$$RHS = -i\delta_m \frac{\delta}{\pi} \int_0^{\infty} \cos\left(\frac{2ka}{\pi} y\right) \frac{k}{\cosh^2 y} dy.$$

It can be seen from tables (Gradshteyn and Ryzhik, 1994) that

$$\int_0^{\infty} \frac{\cos ax}{\cosh^2 bx} dx = \frac{a\pi}{2b^2 \sinh \frac{a\pi}{2b}},$$

therefore,

$$RHS = -i\delta_m \frac{\delta}{\pi} \frac{k^2 a}{\sinh ka}. \quad (O.26)$$

Substituting this result into Equation O.25 gives

$$\frac{\partial^2 \hat{\phi}_{1m}}{\partial y^2} - k_m^2 \hat{\phi}_{1m} = -i\delta_m \frac{\delta}{\pi} \frac{k^2 a}{\sinh ka}. \quad (O.27)$$

Taking the Fourier transformation of equations O.17 and O.18 gives

$$\left. \frac{\partial \hat{\phi}_{1m}}{\partial y} \right|_{y=a} = 0, \quad (O.28)$$

$$\hat{\phi}_{1m}|_{y=a} = \frac{1}{2\pi w} \int_{-\infty}^{\infty} dx \int_0^w dz e^{-i\frac{2\pi m}{w}z} e^{-ikx} \left\{ \varphi_m - \varphi_0|_a - \frac{\rho S_0}{4 wr_0} [|l+x| - |l-x|] - \sigma - \delta \tanh \frac{\pi x}{2a} \right\}. \quad (O.29)$$

Defining

$$\hat{\Psi}_m(k) = \frac{1}{2\pi i w} \int_{-\infty}^{\infty} dx \int_0^w dz e^{-i\frac{2\pi m}{w}z} e^{-ikx} \left\{ \varphi_m - \varphi_0|_a - \frac{\rho S_0}{4 wr_0} [|l+x| - |l-x|] - \sigma - \delta \tanh \frac{\pi x}{2a} \right\}, \quad (O.30)$$

Equation O.29 may be written as

$$\hat{\phi}_{1m}|_{y=a} = i \hat{\Psi}_m(k). \quad (O.31)$$

The general solution to Equation O.27 is

$$\hat{\phi}_{1m} = i\delta_m \frac{\delta a}{\pi k_m^2} \frac{k^2}{\sinh ka} + A_1 \cosh k_m(y-a). \quad (O.32)$$

From the boundary condition of Equation O.31 the constant A_1 can be calculated. Thus

$$A_1(k) = i \hat{\Psi}_m(k) - i\delta_m \frac{\delta a}{\pi k_m^2} \frac{k^2}{\sinh ka}. \quad (O.33)$$

Replacing this result into Equation O.32 gives

$$\hat{\phi}_{1m} = i\delta_m \frac{\delta a}{\pi k_m^2} \frac{k^2}{\sinh ka} + \left[i\hat{\Psi}_m(k) - i\delta_m \frac{\delta a}{\pi k_m^2} \frac{k^2}{\sinh ka} \right] \cosh k_m(y-a),$$

$$\hat{\phi}_{1m} = i \left\{ \delta_m \frac{\delta a}{\pi k_m^2} \frac{k^2}{\sinh ka} + \left[\hat{\Psi}_m(k) - \delta_m \frac{\delta a}{\pi k_m^2} \frac{k^2}{\sinh ka} \right] \cosh k_m(y-a) \right\},$$

which is the expression for Equation 4.137.

In order to avoid the ill-conditioned part of this solution the short wavelengths must be suppressed. This can be done introducing a damping factor to the solution above.

Consider

$$\hat{\phi}_{1m} = i \left\{ \delta_m \frac{\delta a}{\pi k_m^2} \frac{k^2}{\sinh ka} + \left[\hat{\Psi}_m - \delta_m \frac{\delta a}{\pi k_m^2} \frac{k^2}{\sinh ka} \right] \cosh k_m(y-a) e^{-\frac{k_m^2}{k_{\max}^2}} \right\},$$

$$\hat{\phi}_{1m} = i \left\{ \frac{\delta_m}{\pi} \frac{\delta a}{\sinh ka} + \left[\hat{\Psi}_m - \frac{\delta_m}{\pi} \frac{\delta a}{\sinh ka} \right] \cosh k_m(y-a) e^{-\frac{k_m^2}{k_{\max}^2}} \right\}, \quad (\text{O.34})$$

where k_{\max} is a damping parameter.

Assume

$$\Delta_1(x, z) = \sum_m \Delta_{1m}(x) e^{i\frac{2\pi m}{w}z}, \text{ and} \quad (\text{O.35})$$

$$\Delta_{1m}(x) = \frac{\int_{-\infty}^x \frac{\partial \phi_{1m}}{\partial y} \Big|_{y=0} dx'}{\frac{\partial \phi_0}{\partial x} \Big|_{y=0}}. \quad (\text{O.36})$$

The numerator of the equation above, $N(x)$, can be calculated as

$$N(x) = \int_{-\infty}^x \frac{\partial \phi_{1m}}{\partial y} \Big|_{y=0} dx',$$

$$\begin{aligned}
N(x) &= \int_{-\infty}^x dx' \int_{-\infty}^{\infty} dk e^{ikx'} \frac{\partial \hat{\phi}_{1m}}{\partial y} \Big|_{y=0}, \\
N(x) &= \int_{-\infty}^x dx' \frac{\partial}{\partial x'} \left(\int_{-\infty}^{\infty} dk \frac{e^{ikx'}}{ik} \frac{\partial \hat{\phi}_{1m}}{\partial y} \Big|_{y=0} \right), \\
N(x) &= \int_{-\infty}^{\infty} dk \frac{e^{ikx}}{ik} \frac{\partial \hat{\phi}_{1m}}{\partial y} \Big|_{y=0}. \tag{O.37}
\end{aligned}$$

From Equation O.34

$$\begin{aligned}
\frac{\partial \hat{\phi}_{1m}}{\partial y} &= i \left[\hat{\Psi}_m - \frac{\delta_m}{\pi} \frac{\delta a}{\sinh ka} \right] k_m \sinh k_m (y-a) e^{-\frac{k_m^2}{k_{\max}^2}}, \\
\frac{\partial \hat{\phi}_{1m}}{\partial y} \Big|_{y=0} &= -i \left[\hat{\Psi}_m - \frac{\delta_m}{\pi} \frac{\delta a}{\sinh ka} \right] k_m \sinh k_m a e^{-\frac{k_m^2}{k_{\max}^2}}. \tag{O.38}
\end{aligned}$$

Substituting Equation O.38 into Equation O.37 results in

$$\begin{aligned}
N(x) &= - \int_{-\infty}^{\infty} dk \frac{e^{ikx}}{k} \left[\hat{\Psi}_m - \frac{\delta_m}{\pi} \frac{\delta a}{\sinh ka} \right] k_m \sinh k_m a e^{-\frac{k_m^2}{k_{\max}^2}}, \\
N(x) &= - \int_{-\infty}^{\infty} dk e^{\left(ikx - \frac{k_m^2}{k_{\max}^2} \right)} \left[\hat{\Psi}_m - \frac{\delta_m}{\pi} \frac{\delta a}{\sinh ka} \right] \frac{k_m \sinh k_m a}{k}, \\
N(x) &= - \int_{-\infty}^{\infty} dk e^{\left(ikx - \frac{k_m^2}{k_{\max}^2} \right)} \hat{\Psi}_m \frac{k_m \sinh k_m a}{k} + \delta_m \frac{\delta a}{\pi} \int_{-\infty}^{\infty} dk e^{\left(ikx - \frac{k_m^2}{k_{\max}^2} \right)}. \tag{O.39}
\end{aligned}$$

Consider the second term of the integral above:

$$I = \delta_m \frac{\delta a}{\pi} \int_{-\infty}^{\infty} dk e^{\left(ikx - \frac{k_m^2}{k_{\max}^2} \right)}.$$

Let $k = k_{\max} \xi$. Thus,

$$I = \delta_m \frac{\delta a}{\pi} k_{\max} \int_{-\infty}^{\infty} d\xi e^{(ik_{\max}\xi x - \xi^2)},$$

$$I = \delta_m \frac{\delta a}{\pi} k_{\max} e^{\left(\frac{k_{\max}^2 x^2}{4}\right)} \int_{-\infty}^{\infty} d\xi e^{-\left(\xi - \frac{ik_{\max} x}{2}\right)^2},$$

$$I = \delta_m \frac{\delta a}{\pi} k_{\max} e^{\left(\frac{k_{\max}^2 x^2}{4}\right)} \sqrt{\pi},$$

$$I = \delta_m \frac{\delta a}{\sqrt{\pi}} k_{\max} e^{\left(\frac{k_{\max}^2 x^2}{4}\right)}.$$

Substituting this result into Equation O.39 gives

$$N(x) = - \int_{-\infty}^{\infty} dk e^{\left(ikx - \frac{k^2}{k_{\max}^2}\right)} \hat{\Psi}_m \frac{k_m \sinh k_m a}{k} + \delta_m \frac{\delta a}{\sqrt{\pi}} k_{\max} e^{\left(\frac{k_{\max}^2 x^2}{4}\right)},$$

which is the expression for Equation 4.144.

Consider Equation 4.125:

$$\left[\Delta_2 \frac{\partial \varphi_0}{\partial x} + \Delta_1 \frac{\partial \varphi_1}{\partial x} + \int_{-\infty}^x dx' \frac{\partial}{\partial z} \left(\Delta_1 \frac{\partial \varphi_1}{\partial z} \right) \right]_{y=0} = 0 \quad (\text{O.40})$$

Assume

$$\Delta_2(x, z) = \sum_p \Delta_{2p}(x) e^{i \frac{2\pi p}{w} z}. \quad (\text{O.41})$$

A Fourier analysis of Equation O.40 can be performed after multiplying both sides of the

equation by $\frac{1}{w} \int_0^w dz e^{-i \frac{2\pi p}{w} z}$.

The first term of Equation O.40, represented by $I1$, becomes

$$I1 = \frac{1}{w} \int_0^w dz \Delta_2 \frac{\partial \varphi_0}{\partial x} \Big|_{y=0} e^{-i \frac{2\pi p}{w} z},$$

$$\begin{aligned}
I1 &= \frac{1}{w} \frac{\partial \varphi_0}{\partial x} \Big|_{y=0} \sum_p \Delta_{2p}(x) \int_0^w dz e^{i \frac{2\pi p}{w} z} e^{-i \frac{2\pi p}{w} z}, \\
I1 &= \frac{1}{w} \frac{\partial \varphi_0}{\partial x} \Big|_{y=0} \sum_p \Delta_{2p}(x) \int_0^w dz e^{i \frac{2\pi(p-p)}{w} z}, \\
I1 &= \frac{\partial \varphi_0}{\partial x} \Big|_{y=0} \Delta_{2p}(x). \tag{O.42}
\end{aligned}$$

The second term of Equation O.40, represented by $I2$, becomes

$$\begin{aligned}
I2 &= \frac{1}{w} \int_0^w dz \Delta_1 \frac{\partial \varphi_1}{\partial x} \Big|_{y=0} e^{-i \frac{2\pi p}{w} z}, \\
I2 &= \frac{1}{w} \sum_m \Delta_{1m}(x) \int_0^w dz \frac{\partial \varphi_1}{\partial x} \Big|_{y=0} e^{-i \frac{2\pi p}{w} z} e^{i \frac{2\pi m}{w} z}, \\
I2 &= \frac{1}{w} \sum_m \Delta_{1m}(x) \int_0^w dz \frac{\partial \varphi_1}{\partial x} \Big|_{y=0} e^{i \frac{2\pi(m-p)}{w} z}. \tag{O.43}
\end{aligned}$$

From Equation O.13

$$\begin{aligned}
\frac{\partial \varphi_1}{\partial x} &= \frac{\partial \tilde{\varphi}_1}{\partial x} + \delta \frac{\pi}{2a} \operatorname{sech}^2 \frac{\pi x}{2a}, \\
\frac{\partial \varphi_1}{\partial x} &= \sum_{n=-\infty}^{\infty} e^{i \frac{2\pi n z}{w}} \frac{\partial \varphi_{1n}}{\partial x} + \delta \frac{\pi}{2a} \operatorname{sech}^2 \frac{\pi x}{2a}, \\
\frac{\partial \varphi_1}{\partial x} \Big|_{y=0} &= \sum_{n=-\infty}^{\infty} e^{i \frac{2\pi n z}{w}} \frac{\partial \varphi_{1n}}{\partial x} \Big|_{y=0} + \delta \frac{\pi}{2a} \operatorname{sech}^2 \frac{\pi x}{2a}. \tag{O.44}
\end{aligned}$$

Substituting Equation O.44 into Equation O.43 gives

$$\begin{aligned}
I2 &= \frac{1}{w} \sum_m \Delta_{1m}(x) \int_0^w dz e^{i \frac{2\pi(m-p)}{w} z} \left[\sum_{n=-\infty}^{\infty} e^{i \frac{2\pi n z}{w}} \frac{\partial \varphi_{1n}}{\partial x} \Big|_{y=0} + \delta \frac{\pi}{2a} \operatorname{sech}^2 \frac{\pi x}{2a} \right], \\
I2 &= \Delta_{1p}(x) \delta \frac{\pi}{2a} \operatorname{sech}^2 \frac{\pi x}{2a} + \sum_{n=-\infty}^{\infty} \Delta_{1(p-n)}(x) \frac{\partial \varphi_{1n}}{\partial x} \Big|_{y=0},
\end{aligned}$$

$$I2 = \Delta_{1p}(x) \delta \frac{\pi}{2a} \sec h^2 \frac{\pi x}{2a} + \sum_{n=-\infty}^{\infty} \Delta_{1(p-n)}(x) \int_{-\infty}^{\infty} dk e^{ikx} ik \hat{\phi}_{1n} \Big|_{y=0},$$

$$I2 = \Delta_{1p}(x) \delta \frac{\pi}{2a} \sec h^2 \frac{\pi x}{2a} - \sum_{n=-\infty}^{\infty} \Delta_{1(p-n)}(x) \int_{-\infty}^{\infty} dk e^{ikx} k \left\{ \frac{\delta_n}{\pi} \frac{\delta a}{\sinh ka} + \left[\hat{\Psi}_n - \frac{\delta_n}{\pi} \frac{\delta a}{\sinh ka} \right] \cosh k_n a e^{-\frac{k_n^2}{k_{\max}^2}} \right\}$$

$$I2 = \Delta_{1p}(x) \delta \frac{\pi}{2a} \sec h^2 \frac{\pi x}{2a} - \sum_{n=-\infty}^{\infty} \Delta_{1(p-n)}(x) \int_{-\infty}^{\infty} dk e^{ikx} k \left[\hat{\Psi}_n - \frac{\delta_n}{\pi} \frac{\delta a}{\sinh ka} \right] \cosh k_n a e^{-\frac{k_n^2}{k_{\max}^2}} - \Delta_{1p}(x) \int_{-\infty}^{\infty} dk e^{ikx} \frac{\delta ka}{\pi \sinh ka}$$

Observe that

$$-\Delta_{1p}(x) \int_{-\infty}^{\infty} dk e^{ikx} \frac{\delta ka}{\pi \sinh ka} = -\Delta_{1p}(x) \frac{2\delta a}{\pi} \int_0^{\infty} dk \frac{k \cos kx}{\sinh ka} = -\Delta_{1p}(x) \delta \frac{\pi}{2a} \sec h^2 \frac{\pi x}{2a}.$$

Thus,

$$I2 = - \sum_{n=-\infty}^{\infty} \Delta_{1(p-n)}(x) \int_{-\infty}^{\infty} dk e^{ikx} k \left[\hat{\Psi}_n - \frac{\delta_n}{\pi} \frac{\delta a}{\sinh ka} \right] \cosh k_n a e^{-\frac{k_n^2}{k_{\max}^2}},$$

$$I2 = - \sum_{n=-\infty}^{\infty} \Delta_{1(p-n)}(x) \int_{-\infty}^{\infty} dk k e^{ikx} \hat{\Psi}_n e^{-\frac{k_n^2}{k_{\max}^2}} \cosh k_n a + \Delta_{1p}(x) \frac{\delta a}{\pi} \int_{-\infty}^{\infty} dk e^{ikx} k \left[\frac{\cosh ka}{\sinh ka} \right] e^{-\frac{k^2}{k_{\max}^2}}$$

$$I2 = \int_{-\infty}^{\infty} dk k e^{ikx} \left[- \sum_{n=-\infty}^{\infty} \Delta_{1(p-n)}(x) \hat{\Psi}_n e^{-\frac{k_n^2}{k_{\max}^2}} \cosh k_n a + \Delta_{1p}(x) \frac{\delta a}{\pi} \frac{\cosh ka}{\sinh ka} e^{-\frac{k^2}{k_{\max}^2}} \right]. \quad (O.45)$$

The third term of Equation O.40, represented by $I3$, becomes

$$I3 = \frac{1}{w} \int_{-\infty}^x \int_{-\infty}^w dz e^{-i \frac{2\pi p z}{w}} dx \frac{\partial}{\partial z} \left(\Delta_1 \frac{\partial \phi_1}{\partial z} \right) \Big|_{y=0},$$

$$\begin{aligned}
I3 &= \frac{1}{w} \int_{-\infty}^x \int_0^w dz e^{-i\frac{2\pi pz}{w}} dx' \frac{\partial}{\partial z} \left(\sum_m \Delta_{1m}(x) e^{i\frac{2\pi m z}{w}} \frac{\partial \varphi_1}{\partial z} \right) \Big|_{y=0}, \\
I3 &= \frac{1}{w} \int_{-\infty}^x \int_0^w dz dx' e^{-i\frac{2\pi pz}{w}} \frac{\partial}{\partial z} \left(\sum_m \Delta_{1m}(x) e^{i\frac{2\pi m z}{w}} \frac{\partial}{\partial z} \sum_{n=-\infty}^{\infty} e^{i\frac{2\pi n z}{w}} \varphi_{1n} \right) \Big|_{y=0}, \\
I3 &= \frac{1}{w} \int_{-\infty}^x \int_0^w dz dx' e^{-i\frac{2\pi pz}{w}} \frac{\partial}{\partial z} \left(\sum_m \Delta_{1m}(x) e^{i\frac{2\pi m z}{w}} i \sum_{n=-\infty}^{\infty} \frac{2\pi n}{w} e^{i\frac{2\pi n z}{w}} \varphi_{1n} \Big|_{y=0} \right), \\
I3 &= -\frac{1}{w} \int_{-\infty}^x \int_0^w dz dx' e^{-i\frac{2\pi pz}{w}} \left(\sum_m \sum_n \frac{2\pi(m+n)}{w} \frac{2\pi n}{w} \Delta_{1m}(x) e^{i\frac{2\pi(m+n)z}{w}} \varphi_{1n} \Big|_{y=0} \right), \\
I3 &= -\frac{1}{w} \int_{-\infty}^x \int_0^w dz dx' \left(\sum_m \sum_n \frac{2\pi(m+n)}{w} \frac{2\pi n}{w} \Delta_{1m}(x) e^{i\frac{2\pi(m+n-p)z}{w}} \varphi_{1n} \Big|_{y=0} \right), \\
I3 &= -\int_{-\infty}^x dx' \left(\sum_n \frac{2\pi p}{w} \frac{2\pi n}{w} \Delta_{1(p-n)}(x) \varphi_{1n} \Big|_{y=0} \right), \\
I3 &= -i \int_{-\infty}^x \int_{-\infty}^{\infty} dk e^{ikx'} dx' \left(\sum_n \frac{2\pi p}{w} \frac{2\pi n}{w} \Delta_{1(p-n)}(x) \left\{ \frac{\delta_n}{\pi} \frac{\delta a}{\sinh ka} + \left[\hat{\Psi}_n - \frac{\delta_n}{\pi} \frac{\delta a}{\sinh ka} \right] \cosh k_n a e^{\frac{k_n^2}{k_{\max}^2}} \right\} \right), \\
I3 &= -i \sum_n \frac{2\pi p}{w} \frac{2\pi n}{w} \int_{-\infty}^x dx' \int_{-\infty}^{\infty} dk e^{ikx'} \Delta_{1(p-n)}(x) \left\{ \frac{\delta_n}{\pi} \frac{\delta a}{\sinh ka} + \left[\hat{\Psi}_n - \frac{\delta_n}{\pi} \frac{\delta a}{\sinh ka} \right] \cosh k_n a e^{\frac{k_n^2}{k_{\max}^2}} \right\}, \\
I3 &= -i \sum_n \frac{2\pi p}{w} \frac{2\pi n}{w} \int_{-\infty}^x dx' \int_{-\infty}^{\infty} dk \left(\Delta_{1(p-n)}(x) \hat{\Psi}_n e^{ikx' - \frac{k_n^2}{k_{\max}^2}} \cosh k_n a \right). \tag{O.46}
\end{aligned}$$

Substituting equations O.42, O.45 and O.46 into Equation O.40 and solving for $\Delta_{2p}(x)$

gives

$$\Delta_{2p}(x) = \frac{1}{\left. \frac{\partial \varphi_0}{\partial x} \right|_{y=0}} \left\{ \begin{aligned} & \sum_n \int_{-\infty}^{\infty} dk k e^{ikx} \Delta_{1(p-n)} \hat{\Psi}_n \cosh k_n a e^{-\left(\frac{k_n^2}{k_{\max}^2}\right)} \\ & - \frac{\delta a}{\pi} \Delta_{1p} \int_{-\infty}^{\infty} dk k \cos kx \frac{\cosh ka}{\sinh ka} e^{-\left(\frac{k^2}{k_{\max}^2}\right)} \\ & - i \sum_n \frac{2\pi n}{w} \frac{2\pi p}{w} \int_{-\infty}^x dx' \int_{-\infty}^{\infty} dk e^{ikx'} \Delta_{1(p-n)} \hat{\Psi}_n \cosh k_n a e^{-\left(\frac{k_n^2}{k_{\max}^2}\right)} \end{aligned} \right\},$$

which is the expression for Equation 4.146.


```

input('enter with the defect width : c (mm) =');
input('enter with the length :l (mm) =');
input('enter with the thickness :a (mm) =');
input('enter with the resistivity :rho (micro_ohm*mm) =');
input('enter with the current : curr (amp) =');
input('enter with the increment in x : deltax (mm) =');
input('enter with the initial position in x : x0 (mm) =');
input('enter with the parameter delta0: delta0 (mm) =');
input('enter with the maximum value of k : kmax (1/mm) =');
xinic= input('enter with the inferior limit of the integral: x1 =');

nimag= sqrt(-1);
numcol = lprobe/deltax +1;
[newphi1] = calcnewphi1(x0);

for j=1:1:numcol,
    x(j)= (-lprobe/2)+deltax*(j-1);

end

new_x=-x0:12.7:x0;
size_new_x=length(new_x);

```

```

for i=1:size_new_x,

    sum = 0;

    for j=1:numcol,

        var1 = (delta0-a)*cosh(kmax*(delta0-a))*sin(kmax*(new_x(i)-x(j)));
        var2 = (new_x(i)-x(j))*sinh(kmax*(delta0-a))*cos(kmax*(new_x(i)-x(j)));
        var3 = (delta0-a)*cosh(kmax*(delta0-a))*sin(kmax*(xinic-x(j)));
        var4 = (xinic-x(j))*sinh(kmax*(delta0-a))*cos(kmax*(xinic-x(j)));
        var5 = (newphi1(j)/(((delta0-a)^2)+(new_x(i)-x(j))^2))*(var1-var2);
        var6 = (newphi1(j)/(((delta0-a)^2)+(xinic-x(j))^2))*(var3-var4);
        var7 = var5 - var6;

        sum = sum + var7;

    end

    num1(i) = (deltax/(pi))*sum;

    den(i) = ((rho*curr)/(2*(a-delta0)*w))* (sinh((pi/(a-
delta0))*(1+new_x(i)))/(cosh((pi/(a-delta0))*(1+new_x(i)))+cos(pi*delta0/(a-delta0))) +
(sinh((pi/(a-delta0))*(1-new_x(i)))/(cosh((pi/(a-delta0))*(1-new_x(i)))+cos(pi*delta0/(a-
delta0))));

    delta1(i)= (delta0+num1(i)/den(i));

```

```
end
```

```
defect1 = delta1
```

```
plot(new_x,defect1,'b')
```

```
title('Defect using the "analytical data" : kmax = /mm')
```

```
xlabel('distance from the center to the border of the plate (mm)')
```

```
ylabel('defect (mm)')
```

%

% SUBROUTINE CALCNEWPHI1

%

function [newphi1]= calcnewphi1(x0)

global w l a rho curr deltax h c

global x0 numcol x delta0

% numcol is the number of columns in the grid of measurements, which is

% the number of points in the x direction.

x=x0;

for j=1:numcol,

num1= cosh((pi/(a-delta0))*(1+x)-1);

den1= cosh((pi/(a-delta0))*(1-x)-1);

var1= log(num1/den1);

var2 = ((rho*curr)/(2*pi*w))*var1;

newphizero = var2;

num2 = cosh((pi/a)*(1+x))-1;

den2 = cosh((pi/a)*(1-x))-1;

var3 = log(num2/den2);

```

phizero = ((rho*curr)/(2*pi*w))*var3;
num3= cosh((pi/(2*a))*(1+c))*cosh((pi/(2*a))*(c-x));
den3= cosh((pi/(2*a))*(x+c))*cosh((pi/(2*a))*(c-1));
var4= coth((pi/(2*a))*(1-x))*log(num3/den3);
var5= -((rho*curr*h)/(2*pi*a*w))*var4;
num4= cosh((pi/(2*a))*(x+c))*cosh((pi/(2*a))*(c+1));
den4= cosh((pi/(2*a))*(c-1))*cosh((pi/(2*a))*(c-x));
var6= coth((pi/(2*a))*(1+x))*log(num4/den4);
var7= ((rho*curr*h)/(2*pi*a*w))*var6;
phi1 = var5 + var7;
newphi1(j) = phizero + phi1 - newphizero;
x=x+deltax;

```

end